

**The role of Fission Yeast
Microtubule Associated Protein, Alp14, in
Microtubule Stabilisation and
Spindle Assembly Checkpoint Maintenance**

Nirada Koonrugsa

Thesis submitted towards the degree of Doctor of Philosophy

University of London



**University College London
Department of Biology
London, WC1E 6BT.**



**London Research Institute
Cancer Research UK
Laboratory of Cell Regulation
London WC2A 3PX**

UMI Number: U592959

All rights reserved

INFORMATION TO ALL USERS

The quality of this reproduction is dependent upon the quality of the copy submitted.

In the unlikely event that the author did not send a complete manuscript and there are missing pages, these will be noted. Also, if material had to be removed, a note will indicate the deletion.



UMI U592959

Published by ProQuest LLC 2013. Copyright in the Dissertation held by the Author.
Microform Edition © ProQuest LLC.

All rights reserved. This work is protected against
unauthorized copying under Title 17, United States Code.



ProQuest LLC
789 East Eisenhower Parkway
P.O. Box 1346
Ann Arbor, MI 48106-1346

Abstract

Accurate and timely chromosome segregation of replicated DNA during cell division is crucial to cell integrity. This process requires mitotic spindles to physically interact with sister kinetochores located at the centromeres. Proteins that function to facilitate this crucial interaction include regulators of microtubule dynamics such as microtubule associated proteins. This thesis primarily describes the study of fission yeast microtubule associated protein, Alp14 by domain analysis. We report the surprising finding that despite high structural conservation, the two TOG domains in Alp14 are required for distinct mechanisms. From our consistent data, the first TOG domain (TOG1 - resides at the N-terminus) is shown to be required for the spindle assembly checkpoint. Its deletion results in failure to maintain the spindle checkpoint in spindle damaged conditions, while its overproduction causes hyper-activation of the checkpoint without spindle damage. The second TOG domain (TOG2 - resides near the centre of the proteins), on the other hand, is required for microtubule stabilisation. Further analysis of the role of TOG1 in the spindle assembly checkpoint suggests that Alp14 may maintain the checkpoint via the outer kinetochore Nuf2/Ndc80 complex. Alp14 is found to bind to Nuf2, while deletion of TOG1 causes Nuf2 and Ndc80 to be delocalised from kinetochore in spindle damaged conditions.

In this thesis, we have also studied the interaction of Alp14 with kinesins Klp5 and Klp6. Our results show that Klp5 and Klp6 are essential for accurate chromosome segregation, promote microtubule depolymerisation and suggest that the kinesins are required for tension-generation at the kinetochore in metaphase. Surprisingly, although the function of Klp5/Klp6 in microtubule regulation is opposed to that of Alp14/Dis1, the proteins collaborate to ensure accurate chromosome segregation.

Acknowledgements

Firstly, I would like to thank my supervisor Takashi Toda for his many advices throughout my PhD course. Takashi's opinions and suggestions have been of great value to my development and experience in the lab. I would also like to thank Miguel Angel and Masa for their help and discussions, and simply for being fine examples of hard working scientists!

I thank members of the lab for making my time here most enjoyable, with special thanks to past members Clare and Aki for their support and interesting discussions, both scientific and otherwise.

Finally, many thanks to friends and family for never failing to listen, understand and support me throughout these years. A special thanks to my husband Anders, who among many things, sacrificed his time to keep me company at the lab during many late nights and weekends.

Table of Contents

Abstract.....	2
Acknowledgements	3
Table of Contents	4
Abbreviations	10
List of figures	12
CHAPTER 1: Introduction	16
1.1 The fission yeast	16
1.2 The Cytoskeletal systems	17
1.2.1 Microtubules	18
1.2.2 Fission yeast microtubules.....	19
1.3 Microtubule associated proteins	21
1.3.1 The TOG family	21
Fission yeast TOG proteins.....	22
TOG family structures and partner proteins	23
1.3.2 The Kinesin-13 family.....	24
1.4 Mitosis.....	27
1.4.1 Kinetochores attachment and tension	28
1.5 Mitotic Checkpoints: delaying anaphase onset	30
1.5.1 Mad2-independent checkpoint.....	33
1.5.2 Turning off the checkpoint	34
1.6 The kinetochore	34
1.6.1 Site of kinetochore formation	34
1.6.2 Kinetochore proteins	36
1.6.3 Kinetochore stability and spindle assembly checkpoint.....	40

1.7 This thesis.....	41
Figures 1.1 to 1.7	43-49
CHAPTER 2: Characterisation of <i>alp14</i> deletion mutant	50
Introduction.....	51
2.1 Identification of Alp14.....	52
Fission yeast TOGs, Alp14 and Dis1, have overlapping functions	53
2.2 Characterisation of <i>alp14</i> deletion mutant	54
Defects in microtubule function of Alp14 cause temperature-sensitivity.....	54
Defects in spindle assembly checkpoint function of Alp14 results in TBZ- hypersensitivity.	55
Alp14-GFP localisation.....	56
2.3 Summary and Concluding Remarks	56
Figures 2.1.1 to 2.2.5	59-66
CHAPTER 3: Analysis of <i>alp14</i> partial deletions.....	67
Introduction	68
3.1 Systematic deletion of <i>alp14</i> ⁺ from the C-terminus	69
3.1.1 Construction of <i>alp14</i> C-terminus-deletion mutants.....	69
3.1.2 Deletion of the C-terminal region of Alp14 results in the loss of microtubule function and localisation.....	70
3.2 Systematic deletion of <i>alp14</i> ⁺ from the N-terminus	71
3.2.1 Construction of <i>alp14</i> N-terminus-deletion mutants.....	71
3.2.2 The C-terminal tail of Alp14 is required for localisation.	72
3.2.3 The second TOG domain, together with the C-terminus is required for microtubule stabilisation.....	73
Temperature-sensitivity and microtubule defects of <i>alp14</i> N-terminal deletion mutants.....	73
TBZ-sensitivity of <i>alp14</i> N-terminal deletion mutants.....	74
3.3. The Requirement of Alp14 TOG1 in the spindle assembly checkpoint	75
3.3.1 TOG1 is required to maintain the spindle assembly checkpoint	75

Cells loose viability and become cut in $\Delta TOG1$ in presence of TBZ.....	76
Cyclin B is degraded prematurely in $\Delta TOG1$ in presence of TBZ.....	76
Spindle assembly checkpoint maintenance in <i>cut7-446</i> mutant requires the first TOG domain of Alp14.....	77
TOG1 and the spindle assembly checkpoint cascade.	78
Simultaneous deletions of spindle checkpoint proteins and TOG1.....	79
Overproduction of Mph1 and Mad2 is toxic in $\Delta TOG1$	79
Mad2 and Mad3 hyper-accumulate transiently at the kinetochore when spindle is damaged in the absence of TOG1.	80
3.4 Requirement of Alp14 TOG1 in kinetochore stability.	82
Nuf2 and Ndc80 are delocalised in $\Delta TOG1$ in presence of CBZ.....	82
Alp14 binds to Nuf2.....	83
3.5 Summary and Concluding Remarks 84	84
The microtubule function of Alp14 85	85
The spindle checkpoint function of Alp14..... 87	87
Separate functions of the two TOG domains..... 89	89
Figures 3.1.1 to 3.5.2 91-123	91-123
CHAPTER 4: Domain analysis of Alp14 by overexpression.....	124
Introduction.....	125
4.1 Overproduction of full-length Alp14.....	126
Overexpression of <i>alp14</i> ⁺ results in microtubule defects, chromosome missegregation and cell cycle arrest.	126
4.2. Overexpression of <i>pTOG</i>⁺.....	128
4.2.1 Overexpression of <i>pTOG</i>⁺ activates the spindle assembly checkpoint..	129
The lethality of <i>pTOG</i> ⁺ overexpression is rescued by deletion of any components of the spindle assembly checkpoint.	129
Overexpression of <i>pTOG</i> ⁺ results in Bub1 but not Mad2 localisation to the kinetochore.....	131
4.2.2 Overexpression of <i>pTOG</i>⁺ results in long astral microtubules.	132
4.3. Overproduction of Alp14 domains from the N-terminus.....	133
Cells overexpressing of <i>alp14</i> ^N -terminal regions display microtubule defects.	134

Overexpression of <i>alp14</i> N-terminal activates the spindle assembly checkpoint.....	135
4.4. Overproduction of Alp14 domains from the C-terminus.....	136
Overexpression of Alp14 C-terminus is toxic and results in microtubule defects and spindle assembly checkpoint activation.....	137
4.5. Summary and Concluding Remarks	138
The role of Alp14 in microtubule stabilisation.....	138
The role of Alp14 in the spindle assembly checkpoint	140
Figures 4.1.1 to 4.5.1	143-170
CHAPTER 5: Analysis of fission yeast kinesins, Klp5 and Klp6.....	171
Introduction.....	172
5.1 Identification of Klp5 and Klp6.....	173
5.2 Analysis of <i>klp5</i> ⁺ and <i>klp6</i> ⁺ gene products	174
5.3 Analysis of <i>klp5</i> and <i>klp6</i> deletion mutants.....	175
Klp5 and Klp6 destabilise microtubules in vivo.....	175
Klp5 and Klp6 are involved in the fidelity of chromosome segregation	176
5.4 Analysis of <i>klp5</i> and <i>klp6</i> overexpression mutants.....	178
Klp5 and Klp6 are required for microtubule function and accurate chromosome segregation.	178
5.5. <i>klp5</i> and <i>klp6</i> mutants activate the spindle assembly checkpoint.....	179
5.6. Genetic interaction between <i>klp5</i> ⁺ / <i>klp6</i> ⁺ and <i>alp14</i> ⁺ / <i>dis1</i> ⁺	180
Fission yeast Kinesin-8 and TOG proteins play a collaborative role.	180
Klp5/6 and Alp14/Dis1 play a common role in mitotic progression.....	181
<i>alp14klp5</i> and <i>dis1klp5</i> activate the spindle assembly checkpoint.....	181
Proper mitotic localisation of Klp5 is dependent on <i>alp14</i>	182
5.7 Summary and Discussion.....	183
Klp5 and Klp6 promote microtubule depolymerisation and ensures accurate chromosome segregation.	183
The Klp5/Klp6 and Alp14/Dis1 collaborate to ensure stable bipolar attachment in mitosis.....	185
Figures 5.1.1 to 5.7.1	186-207

CHAPTER 6: Discussion	208
Introduction.....	208
6.1 The C-terminal tail of Alp14 is required for localisation.....	209
6.1.1 The Conservation of the C-terminus in the localisation function.	210
6.2.The second TOG domain (TOG2) and the C-terminus of Alp14 stabilise microtubules.	211
6.2.1 How does Alp14 stabilise microtubules?	213
6.2.2 The Conservation of the TOG2 and the C-terminus in microtubule stabilisation... ..	214
6.3. The first TOG domain of Alp14 (TOG1) is required to maintain the spindle checkpoint in spindle damage.....	216
6.3.1 Involvement of TOG1 in the spindle checkpoint through kinetochore proteins	217
6.3.2 The importance of kinetochore stability in spindle assembly checkpoint and maintenance.....	221
6.3.3 The conservation of the TOG1 in spindle assembly checkpoint maintenance. ..	222
6.4 Alp14 and Dis1	222
6.5 Concluding Remarks.....	223
 CHAPTER 7: Materials and Methods	 225
7.1 Laboratory stocks and solutions	227
7.2 Yeast physiology	227
7.2.1 Fission yeast nomenclature	227
Strain growth and maintenance	227
7.2.2 Transformation of DNA into fission yeast cells	228
7.2.3 Tetrad dissection and random spore analysis.....	228
7.2.4 Production of synchronous culture.....	228
7.2.5 Microtubule drug treatment	230
7.2.6 Chromosome loss assay	230
7.2.7 Two hybrid assay	230
7.2.8 Plasmids	232
7.2.9 Oligomers.....	234
7.2.10 Strain list.....	238

7.3 Molecular Biological techniques	245
Nucleic Acid preparation and manipulation.....	245
Polymerase Chain Reaction.....	246
Deletion, overexpression and C-terminal epitope tagging of genes by chromosomal integration	246
Sub-cloning genes and partially deleted genes into plasmids	247
Isolation of plasmid DNA from <i>E. coli</i>	248
Transformation of <i>E.coli</i>	248
7.4 Protein biochemistry	248
Fission yeast cell extract and Western blotting	248
Immunoprecipitations	248
7.5 Microscopic analysis.....	249
Analysis of DNA and septa	249
Indirect immunoflorescent microscopy.....	249
Florescent microscopy imaging of fixed and live cells.....	250
References.....	251-265

Abbreviations

alp	altered polarity
APC	anaphase promoting complex
bp	base pair(s)
BSA	bovine serum albumin
CBZ	carbendazole
CDK	cyclin-dependent kinase
CDKI	cyclin-dependent kinase inhibitor
CFP	cyan florescent protein
DAPI	4', 6-diamidino-2-phenylindole dihydrochloride
dis	defect in sister chromatid disjoining
DNA	deoxyribonucleic acid
dNTP	deoxynucleotide triphosphate(s)
EDTA	ethylene diamine tetra-acetic acid
EM	electron microscopy
GDP	guanosine diphosphate
GFP	green fluorescent protein
GTP	guanosine tri-phosphate
g	gram(s)
GDP	guanosine diphosphate
h	hour(s)
HA	hemagglutinin A
HU	hydroxy-urea
MTOC	microtubule organising centre
IP	immunoprecipitation
kb	kilo base(s)
kDa	kilo Dalton(s)
klp	kinesin-like protein
L	litre(s)
M	molar
m	metre(s)
MAPs	microtubule associated proteins
mg	milligram(s)

min	minute(s)
ml	millilitre(s)
mm	millimetre(s)
mM	millimolar(s)
MTOC	microtubule organising centre
Myc	myelocytomatosis
ng	nanogram
ORF	open reading frame
PAA	post anaphase array
PAGE	polyacrylamide gel electrophoresis
PBS	phosphate buffered saline
PCR	polymerase chain reaction
pH	puissance hydrogene
RNAi	ribonucleic acid – interference
rpm	revolutions per minute
s	second(s)
SDS	sodium dodecyl phosphate
SPB	spindle pole body
TAE	Tris acetate/EDTA
TBE	Tris borate/EDTA
TBZ	thiabendazole
TE	tris/EDTA
TOG	tumour overexpressed gene
WT	wild type
µg	microgram(s)
µl	microlitre(s)
µM	micromolar(s)
µm	micrometre(s)
Δ	deletion
°C	degree(s) centigrade
%	percentage

List of Figures

Chapter1

- ❖ Fig. 1.1 The fission yeast cell cycle.
- ❖ Fig. 1.2 Microtubule dynamics in fission yeast.
- ❖ Fig. 1.3 Chromosome-attachment by spindles.
- ❖ Fig. 1.4 A Summary of structural domains and known functions of spindle checkpoint components.
- ❖ Fig. 1.5 A summary of known complex formations between spindle checkpoint proteins.
- ❖ Fig. 1.6 Activation of the spindle assembly checkpoint.
- ❖ Fig. 1.7 Known components of the kinetochore.

Chapter2

- ❖ Fig.2.1.1.Comparison between Alp14 and Dis1 and their homologues.
- ❖ Fig. 2.1.2 Evolutionary relationship between Alp14 and its homologues.
- ❖ Fig. 2.1.3 Functional redundancy between Alp14 and Dis1.
- ❖ ^{Fig.} 2.2.1 $\Delta alp14$ shows retarded growth and growth polarity defects at the restrictive temperature.
- ❖ Fig. 2.2.2 Deletion of $alp14^+$ results in short and broken microtubules.
- ❖ Fig. 2.2.3 Deletion of $alp14^+$ results in chromosome missegregation.
- ❖ Fig. 2.2.4 Deletion of $alp14^+$ causes in sensitivity to microtubule drug, TBZ.
- ❖ Fig. 2.2.5 Localisation of Alp14-GFP.

Chapter3

- ❖ Fig. 3.1.1 Systematic deletion of $alp14^+$ from the C-terminal.
- ❖ Fig. 3.1.2 Deletion of the C-terminal region of Alp14 results in cell polarity defects.
- ❖ Fig. 3.1.3 The C-terminal region of Alp14 is required for localisation and microtubule function.
- ❖ Fig. 3.2.1 Systematic deletion of $alp14^+$ from the N-terminal.
- ❖ Fig. 3.2.2 Localisation and microtubule morphology of $alp14$ N-terminal deletions.

- ❖ Fig. 3.2.3 Temperature-sensitivity and microtubule function of *alp14* N-terminal deletions.
- ❖ Fig. 3.2.4 TBZ-sensitivity of *alp14* N-terminal deletions.
- ❖ Fig. 3.2.5 Introduction of *palp14⁺* abolishes the temperature- and TBZ-sensitivity of *alp14* N-terminal deletions.
- ❖ Fig. 3.3.1 $\Delta TOG1$ does not exhibit microtubule defects.
- ❖ Fig. 3.3.2 The first TOG domain of Alp14 is required for the spindle assembly checkpoint pathway.
- ❖ Fig. 3.3.3 Cyclin B is degraded prematurely in $\Delta TOG1$ in presence of TBZ.
- ❖ Fig. 3.3.4 The first TOG domain of Alp14 is required for the spindle assembly checkpoint pathway.
- ❖ Fig. 3.3.5 Simultaneous deletions of spindle checkpoint proteins and TOG1 display non-additive phenotype in
- ❖ Fig. 3.3.6 Overproduction is toxic in $\Delta TOG1$.
- ❖ Fig. 3.3.7 Mad2 accumulates at $\Delta TOG1$ kinetochores when spindle is damaged
- ❖ Fig. 3.3.8 Mad3 accumulates at $\Delta TOG1$ kinetochores when spindle is damaged.
- ❖ Fig. 3.3.9 Bub1 localises normally at $\Delta TOG1$ kinetochores when spindle is damaged.
- ❖ Fig. 3.4.1 Ndc80 is delocalised in $\Delta TOG1$ in presence of spindle damage.
- ❖ Fig. 3.4.2 Nuf2 is delocalised in $\Delta TOG1$ in presence of spindle damage.
- ❖ Fig 3.4.3 Nuf2 co-immunoprecipitates with Alp14.
- ❖ Fig. 3.4.4 Two-hybrid binding assays failed to show binding between Alp14 and Mad2 or Slp1.
- ❖ Fig. 3.5.1 Schematic diagram showing a summary of specific domain functions in Alp14.
- ❖ Fig. 3.5.2 Model showing TOG1 in spindle assembly checkpoint maintenance by stabilisation of outer kinetochore protein, Nuf2.

Chapter4

- ❖ Fig. 4.1.1 Overexpression of *alp14⁺* is toxic.
- ❖ Fig. 4.1.2 Overexpression of *alp14⁺* results in chromosome missegregation and microtubule defects.
- ❖ Fig. 4.1.3 Overexpression of *alp14⁺* results in chromosome missegregation.

- ❖ Fig. 4.1.4 Overexpression of *alp14*⁺ results in accumulation of cells in interphase.
- ❖ Fig. 4.2.1 Overexpression of *pTOG*⁺ results is toxic.
- ❖ Fig. 4.2.2 Toxicity of *pTOG*⁺ overexpression is dependent on the presence of Mad2 and Bub1.
- ❖ Table. 4.2.3 Toxic-dependency of overproduction of *TOG* or spindle checkpoint proteins.
- ❖ Fig. 4.2.4 Overexpression of *pTOG*⁺ results Mad2-dependent metaphase arrest
- ❖ Fig. 4.2.5 Overexpression of *pTOG*⁺ results localisation of Bub1 but not Mad2.
- ❖ Fig. 4.2.6 Overexpression of *pTOG*⁺ results in long astral microtubules.
- ❖ Fig. 4.3 Systematic overexpression of *alp14*⁺ N-terminal.
- ❖ Fig. 4.3.1 Overexpression of *alp14* N-terminal results in cell polarity defects.
- ❖ Fig. 4.3.2 Overexpression of *alp14* N-terminal results in microtubule defects.
- ❖ Fig. 4.3.3 Overexpression of *alp14* N-terminal results in chromosome missegregation.
- ❖ Fig. 4.3.4 Overexpression of *alp14* N-terminal results in dispersed kinetochores.
- ❖ Fig. 4.3.5 The toxicity of *alp14* N-terminal overexpression is alleviated in presence of *palp14*⁺.
- ❖ Fig. 4.3.6 The toxicity of *alp14* N-terminal overexpression is dependent on the presence of Mad2 and Bub1.
- ❖ Fig. 4.3.7 Overexpression of *alp14* N-terminal activates the spindle assembly checkpoint.
- ❖ Fig. 4.4 Systematic overexpression of *alp14*⁺ C-terminal.
- ❖ Fig. 4.4.1 The absence of the C-terminus results in temperature-sensitivity.
- ❖ Fig. 4.4.2 Overexpression of *alp14* C-terminal results in lost of viability.
- ❖ Fig. 4.4.3 Overexpression of *alp14* C-terminal results in microtubule defects.
- ❖ Fig. 4.4.4 Overexpression *alp14* C-terminal results in microtubule defects and chromosome missegregation.
- ❖ Fig. 4.4.5 Overexpression of *alp14* C-terminal activates the spindle assembly checkpoint.
- ❖ Fig. 4.5.1 Summary figure.

Chapter5

- ❖ Fig.5.1.1 Comparison between Klp5, Klp6 and their closest kinesin homologues.

- ❖ Fig.5.1.2 Evolutionary relationship between yeast Klp5, Klp6 and Kip3 with their closest homologues in frog and human.
- ❖ Fig.5.1.3 Structural comparison between Klp5 and Klp6 and their homologues in frog and budding yeast.
- ❖ Fig.5.2.1 Estimation of Klp5 and Klp6 protein expression level.
- ❖ Fig. 5.3.1. Deletion of *klp5*⁺ and *klp6*⁺ results in resistance to microtubule drug, TBZ.
- ❖ Fig.5.3.2 Deletion of *klp5*⁺ and *klp6*⁺ shows elongated and curved microtubules.
- ❖ Fig.5.3.3 Deletion of *klp5*⁺ and *klp6*⁺ causes mini-chromosome loss.
- ❖ Fig.5.3.4. Deletion of *klp5*⁺ and *klp6*⁺ causes chromosome missegregation.
- ❖ Fig.5.3.5. Deletion of *klp5*⁺ and *klp6*⁺ causes delay in mitotic progression.
- ❖ Fig.5.4.1. Overexpression of *klp5*⁺ and *klp6*⁺ is toxic.
- ❖ Fig.5.4.2. Overexpression of *klp5*⁺ and *klp6*⁺ results in defective cell shape.
- ❖ Fig.5.4.3. Overexpression of *klp5*⁺ and *klp6*⁺ results in mitotic spindle defects and chromosome missegregation.
- ❖ Fig.5.4.4. Overexpression of *klp5*⁺ and *klp6*⁺ shows defects in septation.
- ❖ Fig.5.5.1. Deletion of *mad2*⁺ in Δ *klp5* mutant exacerbates chromosome loss.
- ❖ Fig.5.5.2. Deletion of *mad2*⁺ in *klp5* and *klp6* overexpression mutant exacerbates toxicity.
- ❖ Fig.5.5.3. Deletion of *mad2*⁺ in *klp5* and *klp6* overexpression mutant results in cut cells.
- ❖ Table 5.6.1 Genetic interaction between *klp5*⁺, *klp6*⁺, *alp14*⁺ and *dis1*⁺.
- ❖ Fig. 5.6.2. Klp5/Klp6 and Dis1/Alp14 share an essential function in mitotic progression.
- ❖ Fig. 5.6.3. Simultaneous deletion of *klp5*⁺/*klp6*⁺ and *dis1*⁺/*alp14*⁺ or *alp14*⁺ and *dis1*⁺ results in condensed chromosomes.
- ❖ Fig. 5.6.4. Mutations in *mad2*⁺, *dis1*⁺/*alp14*⁺ and *klp5*⁺/*klp6*⁺ cause stretched chromosome phenotype.
- ❖ Fig. 5.6.5. Deletion of *alp14*⁺ causes the kinetochore localisation of Klp5 to be reduced.
- ❖ Fig. 5.7.1 A role for Klp5/Klp6 and Alp14/Dis1 in the formation of bipolar mitotic spindles.

CHAPTER 1

Introduction

Timely and accurate chromosome segregation is crucial to the integrity and stability of cells in all organisms. Unequal chromosome segregation leads to genome instability, with the resulting aneuploidy commonly found in various cancers. The mechanism of accurate chromosome segregation is highly conserved and requires precise interaction between spindles and centromeric regions of the DNA, known as kinetochores. Proteins that function to ensure proper interaction include regulators of spindle dynamics. Cells also have checkpoints during cell division to monitor inaccurate processes and delay the next stage until the error has been corrected.

This thesis presents a study of conserved microtubule-associated proteins in regulating interphase microtubules, mitotic spindles, spindle-kinetochore attachment and spindle assembly checkpoint in fission yeast. Included in the thesis are projects performed independently and as a team. The introduction focuses on the regulation of microtubule dynamics, mitosis, spindle assembly checkpoint and the kinetochore structure.

1.1 Fission Yeast

The fission yeast, *Schizosaccharomyces pombe*, is a unicellular eukaryote that is rod-shaped and grows by medial division. Its genome is relatively small with three chromosomes of sizes 5.6, 4.7 and 3.5 Mb (Moreno *et al.* 1991). The fission yeast spends most of its life in the haploid state, with cells growing asexually by repeatedly going through rounds of mitotic cell cycle. Cells start the mitotic cell cycle by entering at a gap phase known as G₁, where they prepare for DNA synthesis. After the DNA is replicated in S phase, cells pass through another gap phase G₂ in preparation for mitosis (M phase - fig1.1). During M phase, precise mechanisms ensure that pairs of sister chromatids are aligned and equally segregated towards opposite poles prior to cytokinesis. To ensure orderly and timely cell cycle progression, regulators of the cell

cycle monitor the cell state and exert control of transitions from one stage to the next (Hartwell and Weinert 1989; Nurse 1990). Cells also have additional checkpoints for monitoring and correcting DNA damage, DNA replication and spindle assembly during chromosome segregation (Enoch and Nurse 1991; D'Urso and Nurse 1995; Murray 1994).

When starved of nitrogen, cells exit the mitotic cell cycle at G_1 . In lack of mating partners they remain arrested in the gap phase, and in presence of a mating partner they undergo meiotic cell division (fig.1.1). On the other hand, when glucose is lacking, cells exit the mitotic cell cycle at G_2 and enter stationary gap phase G_0 , where growth is ceased. If favourable growing conditions once again become available, these cells re-enter the mitotic cycle not at start/ G_1 , but at G_2 where they have left off. In the absence of nitrogen but presence of mating partners, fission yeast cells of opposite mating types conjugate to form a diploid zygote before DNA replication in meiotic S phase. Note that haploid fission yeast cells have two mating types, h^+ and h^- . Homothallic cells are able to switch mating types and are able to mate their h^+ and h^- cells growing within the same colony (Forsburg SL. 1994). After DNA replication in meiotic S phase, the zygote then undergoes meiotic prophase where oscillation of DNA, known as horsetail movement, facilitates recombination. Chromosome segregation in meiosis I and II then ensues, resulting in four haploid spores (Forsburg SL. 1994; Davis and Smith 2001).

Because the fission yeast can be easily manipulated using different nutrient and stress conditions, it makes for an excellent and powerful tool to study cell biology. Its unicellular and haploid states also allow it to be genetically amenable, and its three chromosomes facilitate visualisation of individual DNA when arrested at mid mitosis.

1.2 Cytoskeletal systems

The cytoskeleton is required for various cellular processes in all eukaryotes, including protein and organelle transport, cell migration, cell polarity organisation and chromosome segregation. The cytoskeleton is organised into three systems of primary protein filaments, namely intermediate filaments, actin and microtubules. Though related, these systems play distinct roles (Alberts *et al.* 1994). Intermediate filaments,

which made up of durable long monomers, are formed at the nuclear membrane as nuclear lamina and across the cytoplasm. These are often found in cells undergoing mechanical stress such as epithelial tissues (Alberts *et al.* 1994). Actin, on the other hand, is found in most cells and form large networks of filaments. These filaments, known as F-actin, are made up of globular actin subunits called G actin. Actin filaments are varied in stability and flexibility to contribute to their diverse functions, including cell growth, migration, and cell cleavage (Alberts *et al.* 1994). In addition, the functions of actin filaments are further regulated by proteins bound to them.

1.2.1 Microtubules

Similar to actin, the functions of microtubules are varied, including protein and organelle transport, cell polarity organisation and chromosome segregation. Microtubules are made up of α , β , γ and ϵ tubulin subunits. α and β tubulins are formed into cylindrical microtubule filaments by GTP hydrolysis (Alberts *et al.* 1994). On the other hand, γ and ϵ tubulins are part of the structures that are thought to act as platforms for microtubule nucleation, known as microtubule organising centres (MTOCs – Pickett-Heaps 1969; Stearns *et al.* 1991). In vertebrates, MTOCs are known as centrosomes. These are made up of ϵ tubulin-rich centrioles arranged at right angles to form a cylindrical structure, which in turn is surrounded by pericentriolar material (PCM). PCMs function to anchor microtubule filaments (Alberts *et al.* 1994). In yeast, several forms of MTOCs are known, including interphase MTOC (iMTOC), equatorial MTOC (eMTOC) and spindle pole bodies (SPBs – Snyder 1994). Like vertebrate centrosomes, yeast SPBs function as nucleation sites for cytoplasmic microtubules in interphase and for spindles during cell division. However, unlike centrosomes, SPBs are formed by a layered structure (Knop *et al.* 1999). In yeast, microtubules filaments are nucleated from the outermost layer in interphase, while in mitosis they are nucleated from innermost layer (Knop *et al.* 1999; Jaspersen and Winey 2004). Even though centrosomes and SPBs are different in their structures, they have conserved roles in organising microtubules and acting as platforms for microtubule growth (Jaspersen and Winey 2004).

Anchored to an MTOC is the γ tubulin complex, containing highly conserved subunits. Fission yeast microtubules grow in the cytoplasm in interphase, and in mitosis they capture replicated sister chromatids and segregate them towards opposite poles. Because

chromosome segregation occurs without nuclear breakdown in fission yeast, the site of tubulin nucleation must reside in the SPB that is within the nucleus during mitosis. In interphase, SPBs are localised in the cytoplasm at the surface of the nuclear envelope, where the γ tubulin complex is also assembled. Upon mitotic onset, SPBs enter the nucleus and become embedded in the nuclear envelope for intra-nuclear spindle nucleation (Jaspersen and Winey 2004).

α and β tubulin exist as heterodimers that form microtubule filaments growing from an anchored complex of γ tubulin. α/β heterodimers form a wall around a central core, with α or β subunits facing each end, creating a polar structure. The anchored and growing ends are known as minus- and plus-ends, respectively. Addition of α/β heterodimers at the plus-end causes the microtubule to grow, which is dependent on the GTP-binding activities of α and β tubulin (Alberts *et al.* 1994). A α subunit containing GTP is stable and considered part of the molecule. A GTP-bound β tubulin is also stable. However, it is less secure and can be hydrolysed into GDP (Alberts *et al.* 1994). When a microtubule protofilament carries a GTP-bound β tubulin at its plus-end, its stability allows more α/β heterodimers to be added on, which in turn causes polymerisation. However, when it is GDP-bound, β tubulin undergoes a conformational change which prevents heterodimers from being maintained in the filament, causing rapid depolymerisation (fig. 1.2 A).

Microtubule polymerisation and depolymerisation occurs continuously, creating “dynamic instability” (Mitchison and Kirschner 1984). The change in the state of microtubule polymerisation from growth to shrinkage is known as catastrophe and from shrinkage to regrowth is known as rescue. The continual change that creates dynamic instability is crucial to allow microtubule filaments to carry out diverse functions in a timely manner. Microtubule binding proteins have been identified to alter microtubule dynamics at both plus and minus ends, to organise microtubule positioning and function within the cell at different cell cycle and developmental stages.

1.2.2 Fission yeast microtubules

There are many isoforms of α and β tubulins, each encoded by different genes. Even though the diversity of tubulin often determines the localisation and specific functions of microtubules, all α and β tubulins form microtubules *in vitro* when added to each other.

In fission yeast, genes that encode tubulins are *atb2*⁺ and *nda2*⁺ for α tubulin and *nda3*⁺ for β tubulin (Yanagida 1987). Although there are two α tubulin proteins, their functions do not overlap completely as Nda2 is essential for viability while Atb2 is dispensable. Nonetheless, high dosage Atb2 is capable of rescuing lethality of *nda2* mutants, indicating that these two genes are partially redundant.

In fission yeast interphase, microtubules grow along the length of the cell in the cytoplasm, maintaining its shape and growth polarity. It has been shown that cytoplasmic microtubules nucleate from SPBs at the nuclear envelope and are subsequently released (McNally *et al.* 1996; Verde *et al.* 1995). Cytoplasmic microtubules are organised so that microtubule plus ends are facing the cell ends where elongation occurs, and minus ends are overlapped with each other at the cell centre (Drummond and Cross 2000; Brunner and Nurse 2000; Tran *et al.* 2001). As cells enter mitosis, cytoplasmic microtubules disappear and spindles nucleate from SPBs. There are a number of types of mitotic spindles; these include pole-to-kinetochore, pole-to-pole and astral microtubules. Pole-to-kinetochore spindles are attached to SPBs at minus ends and functions to capture and attach DNA at their plus ends. Pole-to-pole spindles also grow towards the direction of the DNA but overlap at the centre of the cell. Astral spindles, on the other hand, grow away from the DNA in an array of short spindles. The dynamics of these spindles are specifically regulated to their functions at different stages of mitosis.

In early mitosis, duplicated SPBs position themselves at opposite poles of the nucleus. Pole-to-kinetochore spindles are then nucleated and polymerised to capture sister chromatids aligned at the metaphase plate. It is thought that in fission yeast, there are around three pole-to-kinetochore spindles per sister chromatid (Ding *et al.* 1993). Once correctly and stably captured, anaphase A onset induces spindle depolymerisation to pull sister chromatids to opposite poles, until they reach the SPBs. In anaphase B, pole-to-pole spindles are polymerised to further push segregated chromosomes apart towards the opposite ends of the cell. It has been shown that astral microtubules may also orient pole-to-pole spindles, aligning them to ensure that separation of sister chromatids occurs along the axis of the cell (Gachet *et al.* 2001; Tournier *et al.* 2004; Zimmerman *et al.* 2004). Once chromosome segregation has been completed, post anaphase array of microtubules nucleates from another MTOC, known as equatorial MTOC, at the site of

cell division (Pardo and Nurse 2003). A contractile ring formed by microtubules nucleated at the same site facilitates cytokinesis. The microtubule dynamics in fission yeast is displayed in fig. 1.2 B.

1.3 Microtubule-associated proteins

Microtubule growth is spatially and temporally controlled to ensure appropriate cell polarity and equal chromosome segregation during the cell cycle and development. Assembled microtubules undergo posttranslational modification including acetylation and detyrosination to modify filaments that have not recently been polymerised (Alberts *et al.* 1994). Additionally, a class of proteins known as microtubule-associated proteins (MAPs) further regulate microtubule dynamics. Conventional MAPs were initially identified biochemically from isolation of brain microtubules. These include TAU proteins whose mutant form aggregates in Alzheimer brains. These proteins were shown to regulate the stability and orientation of neuronal microtubules (Cairns *et al.* 2004). Without this function, aggregates form, causing tangles in the neuron fibres that interfere with nerve function and axonal transport (Binder *et al.* 2005). Although conventional MAPs have been shown to be expressed mainly in neuronal cells, the importance of microtubule dynamics in all cells means that forms of MAPs other than those in the neurons also exist. One highly conserved family of MAPs is the TOG family.

1.3.1 TOG family

The TOG family was independently isolated by various approaches from a variety of organisms. The human TOG protein was first isolated from an expression library of human tumoral brain (Charrasse *et al.* 1995). As its name suggests, ch-TOG (for colonic and hepatic tumour over-expressed gene) was subsequently found to be highly expressed in colonic and hepatic tumours (Charrasse *et al.* 1995 and 1996). Biochemical methods have identified frog XMAP215 as a microtubule polymerising and stabilising factor (Gard and Kirschner 1987; Vasques *et al.* 1994). Other members of the TOG family, identified through genetic screens, were fly Msps (for mini-spindles - Cullen *et al.* 1999), worm Zyg-9 (for zygote defective – Hirsh and Vanderslice 1976), plant Mor-1 (for microtubule organization gene 1 – Whittington *et al.* 2001), budding yeast Stu2 (for

suppressors of a tubulin mutation – Wang and Huffaker 1997), and fission yeast *Dis1* (for defect in sister chromatid disjoining – Okura *et al.* 1988) and *Mtc1/Alp14* (for altered polarity 14 – Nakaseko *et al.* 2001; Garcia *et al.* 2001). As most of their names indicate, homologues of conserved TOG proteins were shown to stabilise microtubules and to be required for functional spindles in accurate chromosome segregation.

XMAP215 was the first found to regulate intrinsic microtubule polymerising activity *in vitro*. When purified XMAP215 was added to pure microtubules, an increase in the growth rate was observed at both plus and minus ends, with the plus end growing five times faster than the minus end (Gard and Kirschner 1987; Vasquez *et al.* 1994). Increase in rates of shrinkage and rescue were also noted, indicating that XMAP215 not only polymerises microtubules but also promotes microtubule dynamics primarily at the plus-end. *In vivo* studies of mutants in various organisms showed that the microtubule polymerising activity of TOG family members is required for intact spindles in accurate chromosome segregation. The fly *msps* mutant displays short spindles that are unable to segregate chromosome equally (Cullen *et al.* 1999). In the worm *zyg-9* mutant, defective spindle formation occurs in both meiosis and the first mitosis, leading to arrest in further rounds of cell division and subsequently to embryonic lethality (Albertson 1984; Kemphues *et al.* 1986). In budding yeast, *Stu2* is required for spindle elongation in anaphase and activates a checkpoint that monitors spindle attachment to the kinetochore (Severin *et al.* 2001).

Fission yeast TOG proteins

In fission yeast, the only eukaryote to harbour more than one member of the TOG family, both *Dis1* and *Alp14* are required for accurate chromosome segregation. Mutants of *dis1*⁺ and *alp14*⁺ are conditional mutants, where *dis1* is defective at low temperatures (cold sensitive – Okura *et al.* 1988; Nabeshima *et al.* 1995 and 1998; Nakaseko *et al.* 1996) and *alp14* is defective at high temperatures (temperature sensitive – Garcia *et al.* 2001). When a single homologue is mutated, the activity of the other is able to compensate for the loss of function. The loss of functions of both homologues, however, leads to lethality at any temperature (Garcia *et al.* 2001). A study of *alp14-1270* point mutant, which causes frame-shift resulting in a stop codon, shows that in the absence of functional *Alp14*, cells become bent and branched-shaped at 36°C. This morphology defect is caused by anomalies in interphase microtubules that normally maintain the cell

shape. In mitosis, *alp14-1270* spindles are short and chromosome missegregation is observed (Garcia *et al.* 2001). As in wild type cells, when the function of mitotic spindles is compromised in the *alp14-1270* mutant, the spindle assembly checkpoint is activated to delay anaphase until the error has been corrected. It is thought that upon detection of unattached kinetochores, spindle checkpoint activation leads to recruitment of checkpoint protein Mad2 to the kinetochores (Rieder *et al.* 1994; Chen *et al.* 1996; Li and Benezra 1996; Waters *et al.* 1998). In *alp14* mutants, kinetochore dots of Mad2-GFP can clearly be observed, suggesting that sister chromatids may be unattached in this condition. However, unlike other mitotic mutants such as *nda3-311* (defective in β -tubulin – Hiraoka *et al.* 1984), the spindle assembly checkpoint could not be maintained in *alp14* mutants (Garcia *et al.* 2001). This suggests that as well as its microtubule stabilising role, Alp14 itself is a component of the spindle checkpoint cascade.

Unlike *alp14*, at 20°C *dis1* mutants do not show morphology defects or weak spindles. Although there are no observable microtubule defects, chromosomes are mis-segregated and mitotic progression is delayed in *dis1* cells (Nakaseko *et al.* 1996). Further investigation led to findings that cell division defects in *dis1* may be due to the protein's role at the kinetochore (Nakaseko *et al.* 2001). Localisation and chromatin immunoprecipitation experiments of Dis1, Alp14 and Stu2 showed that in yeast, TOG proteins bind to the kinetochore and are required for proper microtubule-kinetochore attachment in mitosis (Nakaseko *et al.* 2001; Garcia *et al.* 2001; He *et al.* 2001). Consistent with the TOG proteins' roles in regulating microtubule dynamics, members of the TOG family were also found to be recruited to mitotic spindles, interphase microtubules and centrosomes/SPBs (Nabeshima *et al.* 1995; Wang and Huffaker 1997; Charrasse *et al.* 1998; Matthews *et al.* 1998; Cullen *et al.* 1999; Graf *et al.* 2000; Tournebize *et al.* 2000; Garcia *et al.* 2001; Popov *et al.* 2001).

TOG family structure and partner proteins

The TOG family is conserved at the N-terminal region, with a divergent C-terminal. The conserved N-terminal region consists of units of 'TOG' domains, within which are HEAT repeats. Motifs of HEAT repeats are postulated to act as protein-protein interaction domains. Because HEAT repeats are found in a number of proteins with varying functions such as phosphatase, condensin, cohesin and coatomers, they are thought as protein-interaction adaptors (Neuwald and Hirano 2000). However, so far no member of

the TOG family has been found to bind to other proteins via the HEAT repeats and the function of the conserved TOG domains in the N-terminal region remains unclear and highly debated.

It is intriguing that the diverse C-terminal has been shown to have microtubule polymerising and stabilising activity in various organisms (Nabeshima *et al.* 1995; Wang and Huffaker 1997; Nakaseko *et al.* 2001; Spittle *et al.* 2000). In addition, the C-terminal region has also been shown to act as a binding site for a partner protein from the conserved coiled-coil TACC family (Sato *et al.* 2004). In fly and worm, members of the TACC family of proteins bind to TOG proteins to act as recruitment factors (Cullen and Ohkura 2001; Lee *et al.* 2001; Bellanger and Gonczy 2003; Srayko *et al.* 2003). This is absolutely required for TOG proteins to localise to centrosomes and microtubules in order to exert their microtubule-regulating activity. So far, TACC does not appear to have activities other than regulating TOG localisation. Recent progress has shown that fission yeast Alp14, but not Dis1, also requires TACC member, Alp7 (for altered polarity 7) as a recruitment factor. *alp7* mutants displace Alp14 from the SPB and spindles, and show identical chromosome segregation phenotypes as *alp14* mutants (Sato *et al.* 2004). In *alp14* mutants, on the other hand, only Alp7 recruitment to spindles is lost. Taken together, the report suggests that Alp14 and Alp7 localise in mitosis as a complex. In this model, Alp7 recruits Alp14 to SPBs. Once on SPBs, Alp14 can then be recruited to spindles in an Alp7-independent manner. Alp7, on the other hand, requires Alp14 to localise to spindles (Sato *et al.* 2004).

Studies in various organisms have shown that TOG proteins may also interact with another MAP from the KinI / Kinesin-13 family to regulate microtubule dynamics. Defects in spindle elongation in budding yeast Stu2 mutants were found to be rescued by deletion of Kip3 kinesin protein, which is the closest homologue to the KinI / Kinesin-13 family in this organism and a close structural homologue of fission yeast Klp5 and Klp6 (Severin *et al.* 2001). In fact, one of the first discoveries of frog XMAP215 function was that it opposes the destabilising activity of XKCM1 kinesin (Tournebize *et al.* 2001).

1.3.2 Kinesin-13 family

Kinesins are a super-family of diverse motor proteins that bind to microtubules to perform a variety of functions including transport of proteins, organelles, vesicles and

chromosomes, and regulation of microtubule dynamics. Conventional kinesins were first identified in squid axons as factors that utilise energy from ATP-hydrolysis to move organelles and vesicles along microtubules (Vale *et al.* 1985; for review, see Hirokawa and Takemura 2004). The conventional kinesin consists of two heavy chains and two light chains. The heavy chains contain motor domains, coiled-coil domains and a tail that are required for microtubule binding and ATP-hydrolysis, while the light chains are postulated to bind to the organelles and vesicles cargo (Hirokawa and Takemura 2004). Recent findings have shown that in addition to their role in transport, some kinesins are also required for accurate chromosome segregation. These motors bind spindles and move directionally in an ATP-dependent fashion to facilitate chromosome segregation. KinN kinesins, with conserved motor domain positioned at the N-terminal, move towards microtubule plus-ends to establish and maintain spindle integrity. These kinesins include CENP-E, required for kinetochore-microtubule interactions; Kid, chromosome-passenger proteins that generate polar ejection force; and Eg5, essential for establishment of spindle bipolarity (Schaar *et al.* 1997; Levesque and Compton 2001; Shiroguchi *et al.* 2003; Sawin *et al.* 1992). KinC kinesins, whose motor domain resides at the C-terminal, move towards the microtubule minus-ends to facilitate the focus of spindles at the spindle pole. Note that another group of motors, known as dynein, also transport cargo towards the minus-end direction.

A sub-family of kinesins, with its motor domain in the middle of the protein, has been found to lack motility but surprisingly functions to regulate microtubule dynamics. This sub-family of kinesins was originally known as KinI, but a recent large effort to clarify the nomenclature of the kinesin family has led this subfamily to be renamed Kinesin-13 (Lawrence *et al.* 2004). Initial attempts to isolate members of the Kinesin-13 family in mammalian cells found that there are two Kinesin-13 members in animals: MCAK (for mitotic centromere-associated kinesin) and KIF2 (for kinesin family protein 2). The two proteins have a 60-70% similarity and both were found to function to destabilise microtubules in interphase and mitosis. Despite fairly high homology between the two Kinesin-13 members, only homologues of MCAK have been found to oppose microtubule-polymerising activity of TOG homologues (Tournebize *et al.* 2000; Kinoshita *et al.* 2001; Severin *et al.* 2001), leading to various studies into MCAK function.

Despite the lack of directionality in its motor domain, motor-less MCAK depolymerise microtubules and disrupts spindle elongation in anaphase (Wordeman *et al.* 1999; Ovechkina *et al.* 2002). In addition to spindle localisation and function, MCAK is also recruited to centromeric regions in mitosis. When MCAK localisation to the centromere is lost, anaphase onset is delayed, suggesting that MCAK may work at the region where spindle-kinetochore interacts prior to sister chromatid separation (Kline-Smith *et al.* 2004). In vivo and in vitro studies show that, like mammalian MCAK, frog homologue XKCM1 (for *Xenopus* kinesin catastrophe modulator-1) is also required for accurate chromosome segregation (Walczak *et al.* 1996; Desai *et al.* 1999; Kline-Smith and Walczak 2002; Walczak *et al.* 2002). Over-expression of XKCM1 causes long and monopolar spindles, resulting in mitotic delay. In vitro spindle assembly experiments, XKCM1-depletion caused the rate of catastrophe to decrease by four times, leading to abnormally long microtubule filaments (Walczak *et al.* 1996). Further work into MCAK and XKCM1 determined that these proteins depolymerise microtubule ends in a motor-dependent manner. The motor domain uses energy from ATP-hydrolysis to bend microtubule at the end of the filaments, causing them to destabilise (Moores *et al.* 2002; Ogawa *et al.* 2004). Microtubule protofilaments depolymerised by Kinesin-13 are observed to be split and bent only at the ends.

Although structurally unlike Kinesin-13 (no motor domain in the middle of the protein) budding yeast Kip3 and fission yeast Klp5 and Klp6 are considered functional homologues of MCAK and XKCM1. Kip3 (for kinesin-related protein 3) was found to also localise to spindles and function to ensure equal chromosome segregation (DeZwaan *et al.* 1997). However, subsequent findings suggest that Kip3 acts together with dynein and motors at the cell cortex to orient spindle in moving the nucleus to the bud neck, a mechanism that is specific to budding yeast (DeZwaan *et al.* 1997; Straight *et al.* 1997). Unlike budding yeast, mitotic cell division in fission yeast does not require specific nuclear movement prior to anaphase and its mechanism may be more conserved to higher eukaryotes. A study of fission yeast Klp5 and Klp6 (for kinesin-like proteins 5 and 6) and their interactions with a member of the TOG family, Alp14, is described in further in the results and discussion chapters of the thesis.

1.4 Mitosis

Accurate cell division is essential for cell stability and integrity. In mitosis, the transition from one stage to the next is tightly controlled to ensure equal segregation of DNA at precise timing. Mitosis is classified into phases known as prophase, prometaphase, metaphase, anaphase and telophase. In prophase, cytoplasmic microtubules are disassembled and DNA is condensed in preparation for DNA segregation (Alberts *et al.* 1994). Unlike mammalian cells, nuclear envelope does not break down in yeast as it undergoes closed mitosis, where sister chromatid separation occurs within the nucleus (Egel *et al.* 1980).

Events in metaphase occur with the highest precision and control. Sister chromatids congress to align at the metaphase plate ~~before~~^{after} spindles search and capture sister chromatids. The site of spindle capture on DNA is known as the kinetochore, a proteinous structure that appears to specifically sit on the centromere region of chromosomes. It is essential that kinetochores of all sister chromatids are stably attached to spindles from appropriate poles before anaphase onset to prevent unequal chromosome segregation. Checkpoint controls detect proper kinetochore attachment and delay anaphase until kinetochores are appropriately attached (Wang and Burke 1995; Chen *et al.* 1996; Waters *et al.* 1998; Hardwick *et al.* 1999).

Sister chromatids are held together by ring-like complexes, known as cohesin. At anaphase A onset, cleavage of cohesin, in combination with a pole-ward pulling force provide by depolymerisation of pole-to-kinetochore spindles, segregates sister chromatids to opposite SPBs (Barton and Goldstein 1996). Cohesin is cleaved by a protein known as separase, which activated when its N-terminal and C-terminal interact (Hornig *et al.* 2002). Prior to anaphase onset, a protein known as securin inhibits separase activity by binding to it (Ciosk *et al.* 1998). Anaphase promoting complex (APC), an E3 ubiquitin ligase, degrades securin at anaphase onset, thereby releasing separase, allowing it to activate and cleave cohesin (Uhlmann *et al.* 2000; Uhlmann 2001). APC activity at metaphase to anaphase transition is thought to be dependent on the binding of its activator, Slp1 (Fang *et al.* 1998). Anaphase B sees sister chromatids separating further to opposite ends of the resulting daughter cells by pole-to-pole spindle dynamics. Telophase follows with post-anaphase array microtubules and septation.

Because spindle dynamics is central to chromosome segregation, mitosis can also be classified into phases characterised by spindle dynamics. Under a fluorescent microscope, only pole-to-pole spindles can be visualised throughout mitosis, hence the classification into Phases I, II and III are based only on the dynamics of these spindles. In phase I spindle growth is initiated (prophase), in phase II spindle length remains almost constant (prometaphase to anaphase A) and in phase III spindle elongation occurs (anaphase B). Spindle length corresponds to 0 to 2.5 μm in phase I, and 2.5 to 12-15 μm in phase III (Nabeshima *et al.* 1998). Mitotic mutants affecting microtubule dynamics or regulation of mitotic timing often shows variation in the length of these phases.

1.4.1 Kinetochores attachment and tension

In metaphase/phase II, each of the six kinetochores of sister chromatids must be properly and stably attached. Kinetochores search and capture by spindles is thought to be a random process and would frequently result in unequal or mono-polar attachment (Ghosh and Paweletz N 1987). The proper and accurate attachment of both kinetochores to spindles emanating from opposite poles is known as amphitelic attachment, and results in both bi-polar spindles and chromosome bi-orientation. When one kinetochore is attached, it may be so by spindles from one pole (monotelic attachment) or from both poles (merotelic attachment – fig.1.3 - Nasmyth 2002). The lack of attachment on the free kinetochore signals to mitotic regulators to activate checkpoint control attached (Wang and Burke 1995; Chen *et al.* 1996; Waters *et al.* 1998; Hardwick *et al.* 1999). This delays anaphase onset until all kinetochores are properly attached, preventing unequal chromosome segregation. (Salmon *et al.* 2005; Hardwick 2005)

Detection of attachment, however, is not sufficient in a situation where both kinetochores are attached by spindles emanating from only one pole (syntelic attachment). In this case, detection of lack of tension is thought to also signal to checkpoint control for anaphase onset delay. When amphitelic attachment is established, it is thought that the balance between the inward force provided by cohesin and the pole-ward force provided by spindle depolymerisation generates tension (Garcia *et al.* 2002; Maddox *et al.* 2003). Not only is tension generation an important “test” for correct kinetochore attachment, but it is also crucial for stabilising the attachment.

Astral microtubules may also have a role in tension generation. Prior to onset of anaphase B, where DNA is separated along the length of the cell, astral spindles orient the position of pole-to-kinetochore spindles so that they are aligned to the cell length (Oliferenko and Balasubramanian 2002; Gachet *et al.* 2002 and 2004; Zimmerman *et al.* 2004). Until recently, it has been thought that astral spindles grow into the cytoplasm to anchor themselves to the cell cortex and generate force for orientation. Addition of Latrunculin A and B, drugs that were believed to specifically destroy the ability of astral microtubule to contact the cell cortex by inhibiting actin polymerisation, results in misorientated spindles leading to aberrant chromosome segregation (Gachet *et al.* 2001 and 2004). Although it has now been shown that early mitotic astral microtubules actually grow within the nucleus instead of into the cytoplasm to anchor to the cell cortex, it is likely that they contact the nuclear envelope to create tension required for progression of anaphase (Zimmerman *et al.* 2004). This is because specific checkpoint control proteins required for mitotic progression are activated in lack of astral spindles (Tounier *et al.* 2004).

Another major evidence for the tension-sensing is from the study of aurora kinase Ipl1 in budding yeast. Budding yeast INCENP-aurora complex, sli15-ipl1, required for spindle elongation and cytokinesis, has been shown to promote biorientation (Tanaka *et al.* 2002; Boyrsan and Rancati *et al.* 2005; Tanaka 2005; Indjeian *et al.* 2005; Dewar *et al.* 2004). Because attachment alone is insufficient for equal chromosome segregation, tension must be sensed before anaphase onset can be initiated. When kinetochores are syntelically attached, tension is not detected. In this case, microtubules must be able to detach and reattach to kinetochores to correct the error until equal balance of forces is achieved. In wild type cells, detachment and reattachment occur in equal frequencies. However, when aurora kinase Ipl1 function is lost, kinetochores remain attached, suggesting that Sli15-Ipl1 promotes the turnover of kinetochore-spindle attachment until tension is achieved (Tanaka *et al.* 2001). A study that manipulates the direction in which the kinetochores face further supports Ipl1 promotes kinetochore-spindle turnover in a tension-dependent manner (Dewar *et al.* 2004). Similar work done in fission yeast aurora kinase Ark1, however, suggests that it is required for both attachment and tension (Petersen and Hagan 2003). The requirement for both attachment and tension makes it difficult to experimentally exclude each process for further elucidation in fission yeast.

1.5 Mitotic checkpoints: delaying anaphase onset

The spindle assembly checkpoint delays anaphase onset by blocking ubiquitin ligase activity of APC/C^{cdc20}. The checkpoint proteins were first identified in budding yeast. They include Mad1, Mad2, Mad3 (for mitotic arrest-deficient 1, 2 and 3), Bub1, Bub3 (for budding inhibited by benzimidazole) and Mps1 (synonymous to regulators of cell proliferation kinase 1 - Li and Murray 1991; Hoyt *et al.*, 1991; Weiss and Winey 1996). Homologues of these proteins are found in all eukaryotes and are known by identical names, with exceptions of Mad3 and Mps1, which are BubR1 (for bub1-related 1) in higher eukaryotes and Mph1 (mps1-like pombe homologue) in fission yeast, respectively (He *et al.* 1997 and 1998; Bernard *et al.* 1998; Chan *et al.* 1999; Ikui *et al.* 2002; Millband and Hardwick 2002). The proteins are well conserved from yeast to human both structurally and functionally. However, yeast Mad3 and BubR1 in higher eukaryotes differ slightly in their structures. BubR1, like Bub1, contain two highly conserved regions at the N-terminus and a kinase domain at the C-terminus (Chan *et al.* 1999). In addition, BubR1 carries an extension at the N-terminus, containing a putative KEN box, which is lacking in Bub1. While yeast Mad3 also carries the N-terminal extension, the C-terminal kinase domain is absent (Millband and Hardwick 2002). Fig. 1.4 shows a comparison between yeast Mad3 and human BubR1, as well as conserved domains of checkpoint proteins. Protein complex formations are also summarised in fig.1.5. Studies in a range of organisms have shown that mutants of the checkpoint component lead to failure to arrest the cell cycle in presence of spindle damage.

Although various studies have been carried out to elucidate the checkpoint-signalling cascade, it is still unsure what requirements and events lead to APC inhibition *in vivo*. Functions of all checkpoint proteins are specific to activating and maintaining anaphase delay, apart from Mps1 and Bub1, which have been implicated in SPB duplication and kinetochore stability, respectively (Winey *et al.* 1991; Weiss and Winey 1996; Kinagawa *et al.* 2003). Despite this, the levels of all checkpoint proteins, except that of Bub1, are not cell cycle regulated. It is rather the regulation of checkpoint protein localisation and complex formation in mitosis that leads to anaphase delay when unattached and/or tensionless kinetochores are detected. Upon checkpoint activation, all checkpoint proteins are recruited to the kinetochore. A complex of Mad1-Mad2 tetramer is

postulated to form for Mad2 to be recruited to the kinetochore (Ikui *et al.* 2002; Sironi *et al.* 2002; Vigneron *et al.* 2004). Complexes of Bub1-Bub3 and Bub3-Mad3/BubR1 may also lead to kinetochore-recruitment of these proteins (Chen *et al.* 1999; Hardwick *et al.* 2000; Millband and Hardwick 2002).

Kinetochore-localisation of all checkpoint proteins is not sufficient for checkpoint activation. A complex of Mad2, Mad3/BubR1, Bub3 and Slp1/Cdc20, known as mitotic checkpoint complex (MCC), is thought to inhibit APC by binding to its activator, Slp1/Cdc20 (Sudakin *et al.* 2001; Fang 2002; Hardwick *et al.* 2000; Millband and Hardwick 2002). The formation of this complex is dependent on all checkpoint proteins, but not an intact kinetochore (Fraschini *et al.* 2001). Independent interaction to Cdc20 by Mad2 and Mad3/BubR1 have also been reported (Sironi *et al.* 2001; Zhang and Lees 2001; Luo *et al.* 2002). In vitro, Mad2-Cdc20 binding does not require other checkpoint proteins, but studies in budding yeast show that Mad1 is required for this complex formation in vivo (Hwang *et al.* 98; Fraschini *et al.* 2001). A *cdc20* mutant that lacks Mad2-binding motif is unable to arrest in mitosis when Mad2 or Mph1 is over-expressed (Hwang *et al.* 1998; Kimet 1998). Interaction between Mad2 and Cdc20, as the independent Mad2-Cdc20 complex or as a part of the MCC complex, is absolutely required for APC inhibition (Li *et al.* 1997; Fang *et al.* 1998; Hwang *et al.* 1998; Kalleo *et al.* 1998, Kimet *et al.* 1998; Wassmann and Benezra 1998).

Mad1 and Cdc20 share the same 10-residue Mad2-binding motif (Sironi *et al.* 2002). Binding of Mad2 to either Mad1 or Cdc20 results in the same conformational change at the C-terminal tail of Mad2. When Mad2 is unbound, its C-terminal is predicted to be have an “open” conformation (Luo *et al.* 2000). When bound to Mad1 or Cdc20, Mad2 C-terminal forms a “safety-belt” to stabilise the complexes (Sironi *et al.* 2002). Mad2 release from the Mad2-Mad1 complex requires energy-consuming unfolding of the Mad2 C-terminal tail. In fact, Mad1 will not release Mad2 unless the tetramer is perturbed. These results led to the postulation that in vivo, Mad1 binds Mad2 to allow it to bind to Cdc20 downstream of the checkpoint, suggesting that there is a cycle of Mad2 (Fraschini *et al.* 2001; Sironi *et al.* 2001 and 2002; De Antoni *et al.* 2005). Indeed, Mad2-Mad1 complex has been shown to decrease the rate of Cdc20-Mad2 formation relative to free Mad2 (Sironi *et al.* 2002; De Antoni *et al.* 2005).

Mad2 localisation to the kinetochore in the form of Mad1-Mad2 complex is transient and requires intact and stable kinetochore structure (Chung and Chen 2002; Liu *et al.* 2003; McClelland *et al.* 2003; Howell *et al.* 2004). The MCC complex formation, however, is not dependent upon an intact kinetochore but requires Mad2 recruitment to the kinetochore as the Mad1-Mad2 complex (Fraschini *et al.* 2001; Sironi *et al.* 2002; Howell *et al.* 2004; De Antoni *et al.* 2005). This suggests that the kinetochore acts as a catalytic site for Mad2 release from Mad1, leading to Mad2 binding to Cdc20 in the MCC complex to inhibit APC/C. A model of the spindle assembly checkpoint based on these results is shown in fig.1.6. Note that this model is supported by genetic, biochemical and structural studies of the spindle checkpoint proteins.

Apart from inhibition of APC by protein-protein interaction, little else is known about requirements and events leading to anaphase delay. Phosphorylation of checkpoint proteins have also been reported (see fig.1.4), though it remains unclear if these modifications are required for mitotic arrest. Phosphorylation of Cdc20 by Cdk1 has been shown by various groups, with conflicting reports as to the requirement of this modification in regulation of APC. Suggestions that Cdc20 phosphorylation by Cdk1 activates, inhibits or has no effect on APC activity have been noted (Fang *et al.* 1998; Shteinberg *et al.* 1999; Kotani *et al.* 1999; Kramer *et al.* 2000; Yudkovsky *et al.* 2002; D'Angiolella *et al.* 2003). Another group reports that Cdc20 is also phosphorylated by Bub1 (at different phosphorylation sites to Cdk1) to inhibit APC activity and is required for proper spindle checkpoint signalling (Tang *et al.* 2004). Studies in human show that Mad1 is phosphorylated by both Bub1 and Mph1 upon checkpoint activation (Seeley *et al.* 1999; Hardwick *et al.* 1996). Although this modification is dependent on Mad2, Bub1 and Bub3 activity, again there are conflicting reports as to whether these modifications are actually essential for mitotic delay (Hardwick and Murray 1995; Warren *et al.* 2002; Roberts *et al.* 1994; Farr and Hoyt 1998). Phosphorylation of Bub1 by Cdc2 has also been reported to be required for its spindle checkpoint activity (Yamaguchi *et al.* 2003; Vanoosthuyse and Hardwick 2003). Moreover, phosphorylation of Mad2 has also been found to be required for its binding to Mad1 (Wassmann *et al.* 2003).

1.5.1 **Mad2 –independent checkpoint**

It has been previously thought that Mad2 is absolutely required for anaphase delay. However, recent reports have suggested that a Mad2-independent pathway may also exist. Various studies of factors leading to mitotic arrest have independently shown that anaphase onset may be delayed without Mad2 kinetochore-localisation or binding to Cdc20 in some conditions (Tang *et al.* 2004; DeLuca *et al.* 2003; McClelland *et al.* 2003). A complex of Bub3-BubR1-Cdc20 was found to exist without Mad2 and was surprisingly shown to be capable of mitotic arrest (Tang *et al.* 2004). In higher eukaryotes, only Bub1, BubR1 and Bub3 are found at kinetochores during chromosome congression, suggesting that these checkpoint proteins may have additional Mad2-independent roles (Waters *et al.* 1998; Hoffman *et al.* 2001). In addition, chromosome alignment defect in fission yeast *pcp1* mutant was reported to be detected at the SPBs by Bub1 and Mph1 but not Mad1 and Mad2 (Rajagopalan *et al.* 2004; Tournier *et al.* 2004). It is thought that when anaphase delay occurs in a Mad2-independent manner, the cell is detecting tensionless kinetochores as opposed to unattached kinetochores (Skoufias *et al.* 2001; Garcia *et al.* EMBO 2002; Rajagopalan *et al.* 2004; Tournier *et al.* 2004; Logarinho *et al.* 2004). However, the opposite scenario that Mad2 functions together with BubR1 in the same pathway to sense tension-less kinetochore has also been reported (Shannon *et al.* 2002). In budding yeast, a tension-dependent mechanism that corrects syntelic attachment has been discovered (Ipl1 - discussed in chapter 1.4.1) further supports the idea of a tension checkpoint. It would be interesting to see which of the checkpoint proteins, if any, are required for mitotic delay in this mechanism.

Another support for a Mad2-independent checkpoint is the discovery of the spindle orientation checkpoint in fission yeast (Gachet *et al.* 2001 and 2004; Tournier *et al.* 2004; Zimmerman *et al.* 2004). Orientation of spindle along the length of the cell is important to ensure that segregated sister chromatids are properly separated to the daughter cells. It was believed that astral microtubules anchor to the cell cortex to exert forces that orient the spindle before anaphase B. As mentioned earlier, it has now been shown that astrals grow within the nuclear envelope and therefore cannot contact the cell cortex. However, it remains true that when spindles cannot rotate properly to orient along the cell length, a delay in securin degradation and sister chromatid separation occurs. Intriguingly, the delay requires Bub1, Bub3 and Mad3 but not Mad1 and Mad2.

Moreover, in cells with mis-orientated spindles, Bub1 remains associated with the kinetochores (Tournier *et al.* 2004). It is proposed that the Bub1, Bub3 and Mad3 have additional roles in monitoring the position of the spindle in the spindle orientation checkpoint.

1.5.2 Turning off the checkpoint

Once stable kinetochore-spindle attachments and tension have been sensed, the checkpoint must be turned off in order for the cell to continue to segregate sister chromatids in anaphase. Unfortunately, little is known about how the spindle checkpoint silenced. Two independent groups have reported the identification of p31^{comet}/CMT2 (for comet tail-like mitotic localisation / Caught by Mad2 – Xia *et al.* 2004; Habu *et al.* 2002). In both studies, p31^{comet}/CMT2 was found to bind to Mad2, which did not appear to hinder Mad2-Cdc20 interaction. Intriguingly, p31^{comet}/CMT2 selectively interacts with Cdc20-bound Mad2. Moreover, in vitro studies show that purified p31^{comet}/CMT2 enhances APC activity, suggesting that p31^{comet}/CMT2 binds to Cdc20-bound Mad2 to turn off the spindle assembly checkpoint (Xia *et al.* 2004).

1.6 Kinetochores

Accurate chromosome segregation largely depends on stable and functional kinetochores. In addition to their role as sites for spindle capture and attachment, kinetochores are also required for signalling of mitotic checkpoints and generation of poleward force for chromosomes. Kinetochores are non-DNA structures at the centromeric region of the DNA, consisting of various protein subunits and complexes. In budding yeast, at least 65 kinetochore proteins have been identified (McAinsh *et al.* 2003). Although far fewer kinetochore proteins have been discovered in higher eukaryotes, studies have shown that the overall structure and assembly of the kinetochore is conserved, if not identical.

1.6.1 Site of kinetochore formation

It is attractive to postulate that the site at which the kinetochore is formed may be

determined by DNA sequence. Indeed, when centromeres were first cloned and sequenced in budding yeast, a 125bp centromeric (*CEN*) sequence was found to be necessary and sufficient for accurate chromosome segregation (Gaudet and Fitzgerald-Hayes 1987). The *CEN* region consists of three conserved elements known as *CDEI*, *CDEII* and *CDEIII*. DNA strand containing AT-rich *CDEII* sequence varies in length and is thought to wrap around the nucleosome, while *CDEI* and *CDEIII* interact with protein complexes that constitute the inner kinetochore (McAinsh *et al.* 2003). The *CDEI* element binds Cbf1, a non-essential budding yeast homologue of human CENP-B. In the absence of Cbf1, the rate of chromosome loss is elevated, suggesting that though non-essential, it is important for chromosome stability (Stoyan *et al.* 2001). *CDEIII* interacts with the CBF3 complex, made up of essential proteins Ndc10, Ctf13, Cep3 and Skp1. Kinetochore assembly is completely dependent on CBF3 complex in budding yeast. In the absence of any CBF3 complex component, all other known kinetochore proteins are no longer able to associate to centromeric DNA.

Centromeres in fission yeast and higher eukaryotes, however, are organised differently from that of budding yeast, and are instead made up of tandem sequence repeats (McAinsh *et al.* 2003). In fission yeast, the centromere consists of a central core (*cnt*) flanked by inner and outer inverted repeats (*imr* and *otr*). Similarly, human centromeres are made up of repeats of α -satellite DNA, which are varied in sequence and arrangement in a chromosome-specific manner. Intriguingly, α -satellite DNA sequences can be deleted without affecting normal chromosome segregation and a fully functional neocentromere can be formed in regions of the DNA lacking of α -satellites (Yamamoto and Miklos 1978; Wandall *et al.* 1998). It appears that in fission yeast and higher eukaryotes, DNA sequence itself cannot recruit proteins for kinetochore assembly. Instead, epigenetics may be one determining factor for the site of kinetochore assembly.

Apart from the core region, parts of the centromere and pericentromere are epigenetically modified to become specialised condensed chromatin, known as heterochromatin. Although heterochromatin is predominant at centromeres, it is also found at various parts of the chromosome, including transcriptionally silenced regions and telomeres. The function of heterochromatic regions depends on where they reside, but in general the higher order structures may serve to “protect” or provide a barrier for the DNA sequence from biochemical modifications and DNA-binding proteins (Grewal and Moazed 2003;

Noma *et al.* 2004). Centromeric heterochromatin is crucial for accurate cell division as depletion of components of heterochromatin results in a rate of chromosome missegregation. Proposed roles of heterochromatin at centromeres and pericentromeres include transcription silencing and suppression of meiotic recombination (West and Fraser 2005). In addition, centromeric heterochromatin has been reported to be crucial for cohesin enrichment and retention at centromeres until anaphase onset (Bernard *et al.* 2001; Bernard and Allshire 2002; Pidoux and Allshire 2004).

1.6.2 Kinetochores Proteins

It is postulated that the kinetochore is formed in layers, involving proteins and complexes that bind to the centromere (inner-kinetochore proteins), microtubules (outer-kinetochore proteins) and those that link centromere-binding proteins to microtubule-binding proteins (central-kinetochore proteins). Observation of the kinetochore structure by electron microscopy and hierarchical assembly of kinetochore proteins support the layered organisation (Brinkley and Stubblefield 1966; Ris and Witt 1981). However, recently many proteins within individual complexes have been found to interact with members of other complexes, providing a challenge to the classical classification as their boundaries are becoming blurred (Kops *et al.* 2005; Asakawa *et al.* 2005; He *et al.* Personal communication – submitted at time of writing). Fig.1.7 summarises kinetochore proteins and complexes in budding yeast, fission yeast and metazoans known to date. Note that this area has seen tremendous progress in recent days, which may affect the current knowledge presented in this introduction.

At the inner kinetochore, a conserved histone H3 variant, known as CENP-A in metazoans, interacts with all known centromeric regions, including neocentromeres and centromeres of artificial chromosomes. CENP-A is component of the nucleosome found only in active centromeres and is required for kinetochore assembly (Meluh *et al.* 1998; Howman *et al.* 2000; Takahashi *et al.* 2000; Blower *et al.* 2001). However, the presence of CENP-A is not sufficient to initiate assembly of functional kinetochores (Van Hooser *et al.* 2001). Another core inner kinetochore protein is CENP-B. CENP-B binds to α -satellite in a sequence-specific manner and although α -satellite sequence and CENP-B are both found at centromere, neither is essential for assembly of functional kinetochores (Kouprina *et al.* 2003). Mammalian cells lacking CENP-B do not display any sign of

chromosome missegregation or mitotic arrest (Hudson *et al.* 1998; Perez-Castro *et al.* 1998; Kapoor *et al.* 1998). In fission yeast CENP-B, on the other hand, have been found to assist accurate chromosome segregation (Baum and Clarke 2000). Like CENP-A, conserved protein CENP-C is only found at active centromeres and is required for kinetochore assembly. In chicken DT40 cells, CENP-C loading was shown to be dependent on CENP-I and CENP-H (Fukagawa *et al.* 2001; Nishihashi *et al.* 2002), and its depletion in chicken and human causes mitotic arrest and may be involved in determining kinetochore size (Tomkiel *et al.* 1994; Fukagawa and Brown 1997). Mutation in the budding yeast homologue, Mif2, results in missegregated chromosomes (Meeks-Wagner 1986).

At the central kinetochore, protein complexes have largely been identified in budding yeast. These include MIND, Ctf3, and COMA. MIND consists of at least four protein subunits: Mtw1, Nnf1, Nsl1 and Dsn1 (Euskirchen 2002; De Wulf *et al.* 2003). Mtw1 was originally identified in fission yeast as Mis12 (Takahashi *et al.* 1994). Cells lacking functional Mis12 show abnormal spindle length, speculated to be due to centromere or tension defects (Goshima *et al.* 1999). Further studies in budding yeast indicate that mutants in the budding yeast homologue cause kinetochore tension to be lost, resulting in missegregated chromosomes (Goshima and Yanagida 2000; Pinsky *et al.* 2003). Depletion of human Mis12 results in chromosome missegregation and loss of other central kinetochore proteins, CENP-H and CENP-I, but not CENP-A. In addition to Mis12, the fission yeast MIND/Mis12 complex also contains Mis13, Mis14 and Nnf1 (known as CENP-H in a human).

A homologue of human CENP-I and budding yeast Ctf3, fission yeast Mis6 belongs to a large complex with Mal2 and Sim4 (Jin *et al.* 2002; Pidoux *et al.* 2003). Recent developments in the field have shown that at least seven other proteins, known as Sma-1 to 7, bind to members of this complex (He *et al.* - personal communication – submitted at time of writing). Importantly, fission yeast Mis6 and Sim4 are required for Cnp1 recruitment to the centromere (Takahashi *et al.* 2000; Pidoux *et al.* 2003). However, the reciprocal requirement is found in budding yeast and vertebrates that Cse4/CENP-A is necessary for ctf3/CENP-I kinetochore localisation (Meluh *et al.* 1998; Howman *et al.* 2000; Blower *et al.* 2001; Nishihashi *et al.* 2002). Although fission yeast Mis6 is required for Cnp-1 loading and was found to co-precipitate with Nnf1, no member of the

MIND/Mis12 complex has yet been shown to localise Cnp-1. In fact, Mis14 (of the MIND/Mis12 complex) is recruited to the kinetochore independently of Cnp1, as well as not being required for Cnp-1 recruitment (Takeshi *et al.* 2004). On the other hand, recently identified centromere proteins, Mis16 and Mis18, act as Cnp-1 loading factors most upstream of the kinetochore assembly cascade (Takeshi *et al.* 2004).

An additional central kinetochore complex, known as COMA, has been discovered in budding yeast. COMA consists of Ctf19, Mcm21, Okp1 and Ame1 (De Wulf *et al.* 2003). Although Ctf19 and Mcm21 are essential and the complex is thought to act as a crucial linker, no homologues have been found in fission yeast or metazoans.

Outer kinetochore proteins and complexes can be classed into two categories: one being stable core kinetochore proteins and the other more transient, less stable kinetochore proteins. Subunits of the Ndc80 complex are considered to be core proteins, while transient kinetochore proteins include a sub-class of MAPs, kinesins and yeast DASH complex. The roles of MAPs and kinesins at the outer kinetochore will be further elucidated and discussed in chapter 5. The DASH complex was first identified in budding yeast and contains at least ten subunits: Dam1, Duo1, Dad1, Dad2, Dad3, Dad4/Hsk3, Ask1, Spc19, Spc34, and Hsk3. All members of the complex are essential and localise to spindles and kinetochore foci (Jones *et al.* 1999; Nagasaki *et al.* 1999; Cheeseman *et al.* 2001; Enquist-Newman *et al.* 2001; Janke *et al.* 2002; Li *et al.* 2002; Ikeuchi *et al.* 2003). The homologues of all these proteins have been identified in fission yeast, but surprisingly none are essential (Sanchez-Perez *et al.* – personal communication – submitted at time of writing). Although the kinetochore-localisation of MAPs, kinesins and DASH may be transient and only occur during mitosis, their association is essential for accurate chromosome segregation.

Core-kinetochore protein, Ndc80, was first identified in budding yeast and shown to bind to Nuf2, Spc24 and Spc25 to form a complex (Rout and Kilmartin 1990; Osborne *et al.* 1994; Wigge *et al.* 1998; Wigge and Kilmartin 2001). The complex is relatively well conserved from yeast to humans. Reports of complex localisation showing the lost of kinetochore recruitment in *mis12* mutant and localisation to SPB led to the postulation that the complex is first recruited to centrosomes/SPBs in interphase before transferring onto the kinetochore in mitosis (Asakawa *et al.* 2005). Because of its mitosis-specific

recruitment to the kinetochore, it may be questioned if Ndc80 is really a core kinetochore complex. Budding yeast cells with defective or absent Ndc80 subunit show kinetochore-spindle attachment defects without disruption of the kinetochore structure (Wigge and Kilmartin 2001; De Wulf *et al.* 2003). Similar studies in vertebrate cells using both electron microscopy and live immunofluorescent imaging reports that depletion of human Ndc80, hHec1 and hNuf2 causes structural disruption of outer kinetochore but leave inner and central kinetochore intact (DeLuca *et al.* 2003; McClelland *et al.* 2003). In addition, the study shows that unlike transient kinetochore proteins, hHec1 and hNuf2 recruitment and function are unaffected by microtubule drugs, such as nocodazole (DeLuca *et al.* 2003).

Investigation of homologues of Ndc80 subunits in frog, chicken and human agrees that mutation in the complex leads to elimination of poleward pulling force, observed as unstretched kinetochores (Hori *et al.* 2003; DeLuca *et al.* 2003; McClelland *et al.* 2003 and 2004). However, there have been contradicting reports in regards to kinetochore-spindle attachment defects. Some groups report that Mad1 and Mad2 are recruited to the kinetochores in some *ndc80/hec1* and *nuf2* mutants, and that their recruitment is argued to be evidence for loss of kinetochore-spindle attachment (Martin-Lluesma *et al.* 2002; Cleveland *et al.* 2003; Cheeseman *et al.* 2004). Other studies show that Mad1 and Mad2 kinetochore-recruitment is lost when Hec1 or Nuf2 is depleted, even though the spindle assembly checkpoint is activated in this condition, suggesting that the Ndc80/Nuf2 complex may have a direct role in the spindle checkpoint (Nabetani *et al.* 2001; DeLuca *et al.* 2003; McClelland *et al.* 2003 and 2004; Meraldi *et al.* 2004; Gillett *et al.* 2004). Evidence implicating the Ndc80 complex as a component of the spindle assembly checkpoint is discussed in the next section.

It is important to note that in fission yeast, proteins within individual complexes have recently been found to bind to others. For example, members of the MIND/Mis12^S complex are required for loading of the Nuf2/Ndc80 complex (Asakawa *et al.* 2005; Kops *et al.* 2005). The MIND/Mis12 complex has also been pulled down in a co-immunoprecipitation assay with members of the DASH complex. In the same study, a tagged Mis12 protein also pulled down Dad1 (He *et al.* – personal communication – submitted at time of writing). Results from these studies suggest that kinetochore

complexes may be highly linked together. Alternately, these complexes may form super-complexes.

1.6.3 Kinetochores stability and spindle assembly checkpoint

Kinetochores structure acts as a platform for both microtubule attachment and landing sites for spindle assembly checkpoint proteins. Therefore, it makes sense that the physical state of the kinetochores is crucial to withstand forces on the kinetochores-spindle interaction site and the dynamic turnover of spindle assembly checkpoint proteins. When inner or central kinetochores is disrupted, for example in *mis6* and *mis12* mutants in fission yeast, loss of tension at kinetochores is observed (Goshima *et al.* 1999; Appelgren *et al.* 2003). In *mis6* mutant, the inner centromere structure is somehow disrupted, observed by lack of smeared nucleosome ladder (Goshima *et al.* 1999). In both *mis6* and *mis12* mutants, the spindle assembly checkpoint remains inactive despite lack of attached kinetochores (Goshima *et al.* 1999). A similar study of human Mis6, CENP-I, reports that the loss of CENP-F and checkpoint proteins Mad1 and Mad2 when CENP-I is depleted (Liu *et al.* 2003). These findings suggested that Mis6, Mis12 and their homologues are required for the structure of the kinetochores.

Mutants of the Ndc80 complex, though similar to *mis6* and *mis12*, do not disrupt inner or central kinetochores structure (Nabetani *et al.* 2001; Wigge and Kilmartin 2001; DeLuca *et al.* 2003; De Wulf *et al.* 2003; McClelland *et al.* 2003 and 2004; Meraldi *et al.* 2004; Gillett *et al.* 2004). In these mutants, phenotypes concerning spindle assembly checkpoint activation show allele-specificity, which has led to some controversy. In fission yeast, *nuf2-2* and *nuf2-3* mutants exhibit chromosome segregation defects and spindle checkpoint activation despite the presence of intact spindles (Nabetani *et al.* 2001; Asakawa *et al.* 2005). *nuf2* deletion and *nuf2-1* mutants, however, do not exhibit spindle assembly checkpoint activation, indicating that Nuf2 also functions as a component of the spindle checkpoint (Nabetani *et al.* 2001; Asakawa *et al.* 2005). Similarly in budding yeast, when either *ndc80*⁺ or *nuf2*⁺ are deleted mitotic delay occurs. However, when both Ndc80 and Nuf2 are lost, the spindle checkpoint fails to be activated.

In higher eukaryotes, various studies indicate that the Ndc80 complex may be required for localisation of only some of the spindle checkpoint proteins (Martin-Lluesma *et al.* 2002; DeLuca *et al.* 2003; Gillett *et al.* 2004; Meraldi *et al.* 2004; Bharadwaj *et al.* 2004). In frogs, depletion of xNdc80 or xNuf2 by antibody does not activate the spindle checkpoint. Moreover, no mitotic delay was observed even in the presence of microtubule drug. Upon observation of protein localisation, it appears that xNdc80 and xNuf2 are required for recruiting Mad1, Mad2, Bub1 and Bub3 to the kinetochore (McClelland *et al.* 2003 and 2004). In chicken DT40 cell, Hec1 or Nuf2 depletion causes mitotic arrest with only BubR1 but not Mad2 at the kinetochore (Hori *et al.* 2003). In this study, the group also confirmed that loss of Hec1/Nuf2 does not disrupted inner and central kinetochore by observing intact CENP-A, CENP-C and CENP-H. Depletion of the Ndc80 complex in human HeLa cells using RNAi or antibody injection methods have been carried out by various groups. When hHec1 is depleted, Mad2 is unable to localise to kinetochores while Bub1 recruitment is reduced by approximately 50% during spindle checkpoint activation (Martin-Lluesma *et al.* 2002). Another group reported a similar finding that the kinetochore-localisation of Mps1, Mad2, and Mad3 but not BubR1 or Bub1 is lost when either hHec1 or hNuf2 is depleted (Meraldi *et al.* 2004). Similarly, when hSpc25 is absent, which in turn leads to loss of Hec1, Mad1 was no longer recruited to the kinetochore, whereas the localisation of Bub1 and BubR1 remain largely unaffected (Bharadwaj *et al.* 2004).

1.7 **This Thesis**

A variety of processes in fission yeast and other eukaryotes have been discussed in the introduction, including the regulation of microtubule dynamics, the mitotic cycle, the role of spindle assembly checkpoint and the importance of kinetochore structure. The work described in the following chapters stems from the finding that Alp14 functions in two highly linked, but distinct mechanisms. These are the regulation of microtubule dynamics and the spindle assembly checkpoint. The aim of this thesis is to dissect these distinct roles of Alp14 by domain analysis.

Our study begins with the characterisation of *alp14* (complete) deletion mutant, followed by analyses of mutants that delete or overexpress specific domains of Alp14. In this

thesis, we report the surprising finding that despite high structural conservation, the two TOG domains in Alp14 are required for distinct mechanisms. From our consistent data, the first TOG domain (TOG1 - resides at the N-terminus) is shown to be required for the spindle assembly checkpoint. Its deletion results in failure to maintain the spindle checkpoint in spindle damaged conditions, while its overproduction causes hyperactivation of the checkpoint without spindle damage. The second TOG domain (TOG2 - resides near the centre of the proteins), on the other hand, functions to stabilise microtubules. Lastly, our studies determine that the C-terminus of Alp14 is essential for the localisation of the protein throughout the cell cycle.

Further analysis of the role of TOG1 in the spindle assembly checkpoint suggests that Alp14 may maintain the checkpoint via the outer kinetochore Nuf2/Ndc80 complex. Alp14 is found to bind to Nuf2, while deletion of TOG1 causes Nuf2 and Ndc80 to be delocalised from kinetochore in spindle damaged conditions.

In this thesis, we have also studied the interaction of Alp14 with kinesins Klp5 and Klp6. At the outset of this particular study, the role of Klp5 and Klp6 was analysed as part of team. Our results show that Klp5 and Klp6 are essential for accurate chromosome segregation, promote microtubule depolymerisation and suggest that the kinesins are required for tension-generation at the kinetochore in metaphase. Surprisingly, although the function of Klp5/Klp6 in microtubule regulation is opposed to that of Alp14/Dis1, the proteins collaborate to ensure accurate chromosome segregation.

Vegetative / Mitotic cycle

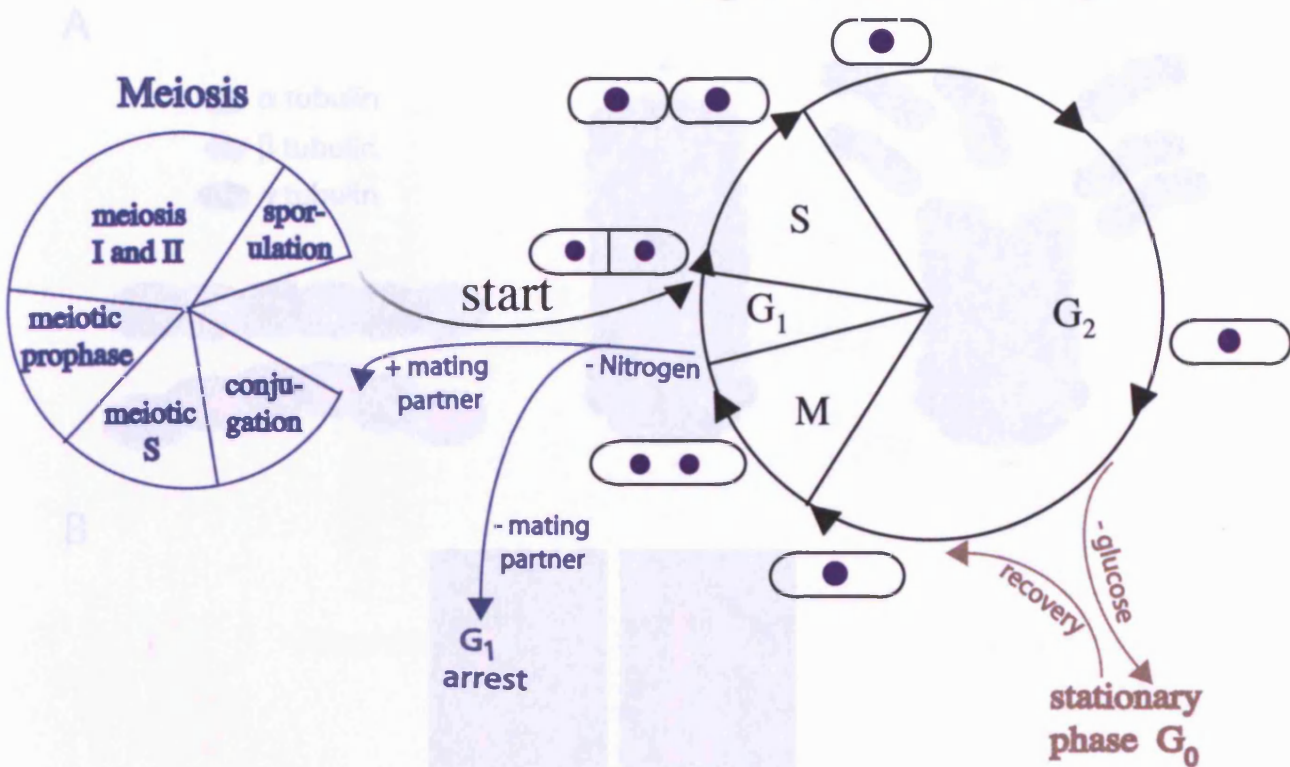


Fig. 1.1. The fission yeast cell cycle.

Fission yeast cells go through rounds of mitotic cell cycle, by entering at G₁ gap phase to prepare for DNA synthesis in S phase. Cells pass through another gap phase G₂ in preparation for chromosome segregation in M phase. When starved of nitrogen, cells exit the mitotic cycle at G₁ and remain in the gap phase in absence of mating partner. In presence of mating partner cells undergo meiotic cell division. When glucose is lacking, cells exit the mitotic cycle at G₂ and enter stationary gap phase G₀, where growth is ceased.

Fig. 1.2. Microtubule dynamics in fission yeast.

A) Addition of $\alpha\beta$ heterodimers at the plus end causes the microtubule to grow, which is dependent on the GTP-binding activities of α and β tubulin (Alberts et al. 1994). α subunit contains GTP is stable and considered part of the molecule. On the other hand, GTP-bound β tubulin is unstable and can be hydrolysed into GDP (Alberts et al. 1994). When a microtubule catastrophe is GTP-bound at its plus end, its stability allows more $\alpha\beta$ heterodimers to be added on, which in turn causes polymerisation. However, when it is GDP-bound β tubulin undergoes a conformational change which prevents heterodimers from being maintained in the filament, causing rapid depolymerisation. B) Microtubule dynamics in fission yeast cell cycle. Interphase microtubules (top panels) grow along the length of the cell in the cytoplasm, maintaining its shape. In mitosis (bottom panels), pole-to-kinetochore spindles nucleated from SPBs grow to capture sister chromatids aligned at the metaphase plate. Once stably captured anaphase onset induces spindle depolymerisation to pull sister chromatids to opposite poles. Acentriolar microtubules may also orient pole-to-pole spindles. Post-anaphase array of microtubules and a contractile ring nucleates from cMTDC to facilitate cytokinesis. Red shows staining of microtubules, green represents SPBs and blue is GAP1-stained DNA. Arrow heads point to asters/spindles and arrow indicates cMTDC.

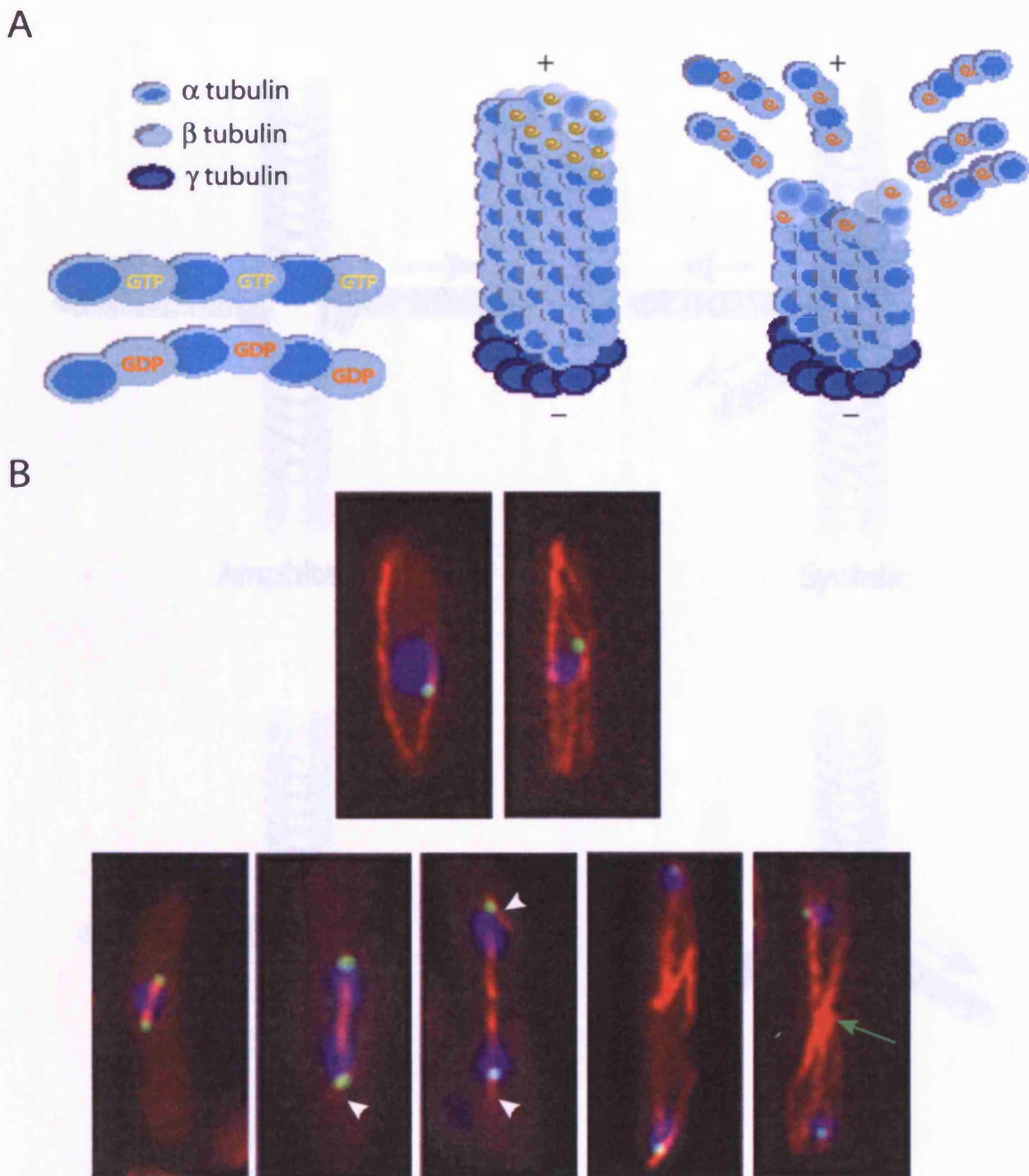


Fig. 1.2. Microtubule dynamics in fission yeast.

A) Addition of α/β heterodimers at the plus-end causes the microtubule to grow, which is dependent on the GTP-binding activities of α and β tubulin (Alberts et al. 1994). A α subunit containing GTP is stable and considered part of the molecule. On the other hand, GTP-bound β tubulin is unstable and can be hydrolysed into GDP (Alberts et al. 1994). When a microtubule protofilament is GTP-bound at its plus-end, its stability allows more α/β heterodimers to be added on, which in turn causes polymerisation. However, when it is GDP-bound, β tubulin undergoes a conformational change which prevents heterodimers from being maintained in the filament, causing rapid depolymerisation. **B)** Microtubule dynamics in fission yeast cell cycle. Interphase microtubules (top panels) grow along the length of the cell in the cytoplasm, maintaining its shape. In mitosis (bottom panels), pole-to-kinetochore spindles nucleated from SPBs grow to capture sister chromatids aligned at the metaphase plate. Once stably captured, anaphase onset induces spindle depolymerisation to pull sister chromatids to opposite poles. Astral microtubules may also orient pole-to-pole spindles. Post anaphase array of microtubules and a contractile ring nucleates from eMTOC to facilitate cytokinesis. Red shows staining of microtubules, green represents SPBs and blue is DAPI-stained DNA. Arrow heads point to astral spindles and arrow indicates eMTOC.

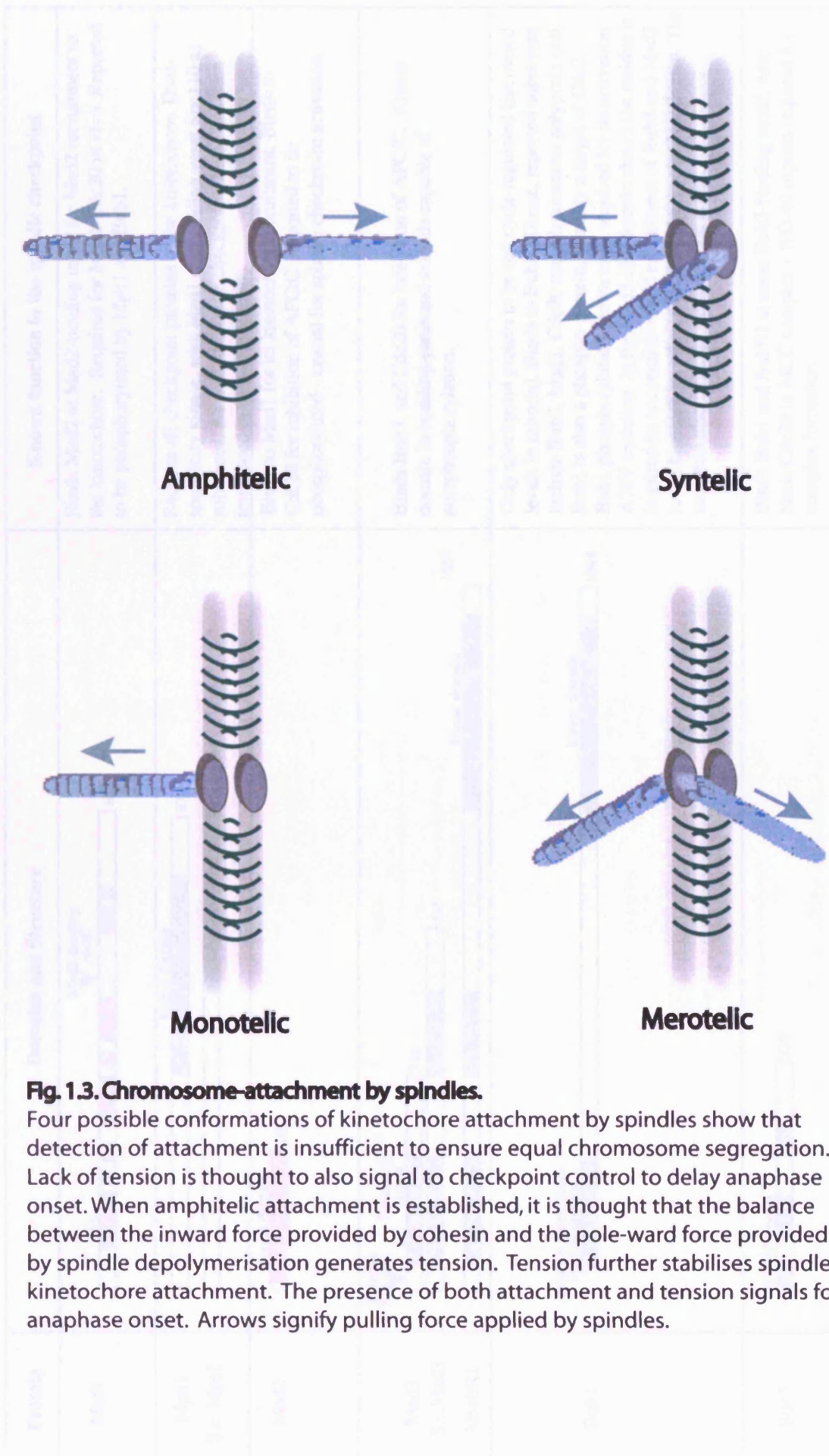


Fig. 1.3. Chromosome-attachment by spindles.

Four possible conformations of kinetochore attachment by spindles show that detection of attachment is insufficient to ensure equal chromosome segregation. Lack of tension is thought to also signal to checkpoint control to delay anaphase onset. When amphitelic attachment is established, it is thought that the balance between the inward force provided by cohesin and the pole-ward force provided by spindle depolymerisation generates tension. Tension further stabilises spindle-kinetochore attachment. The presence of both attachment and tension signals for anaphase onset. Arrows signify pulling force applied by spindles.

Fig. 1.3. Chromosome-attachment by spindles; kinetochore attachment

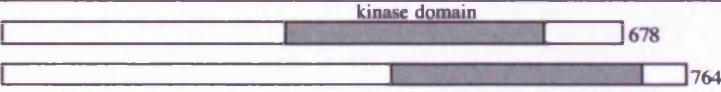
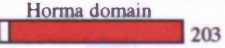
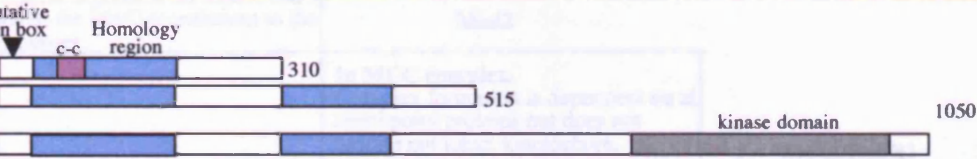
Protein	Domains and Structure	Known function in the spindle checkpoint
Mad1		Binds Mad2 at Mad2-binding motif for Mad2 recruitment to the kinetochore. Required for Mad2-Cdc20 in vivo. Reported to be phosphorylated by Mph1 and Bub1.
Mph1 S.c. Mps1		Recruits all checkpoint proteins to the kinetochore. Dual-specificity kinase, with Mad1 and budding yeast Spc110 as substrates. As well as spindle checkpoint, Mps1 has been implicated in SPB-duplication.
Mad2		Binds to Mad1 for its kinetochore recruitment. Binds to Cdc20 for inhibition of APC/C. Reported to be phosphorylated - crucial for spindle checkpoint activation.
Mad3 S.c. Mad3 hBubR1		Binds Bub3, and Cdc20 for inhibition of APC/C. Kinase domain in budding yeast and animals capable of autophosphorylation.
Bub1		Only checkpoint protein to be cell cycle regulated (increased levels in mitosis). Binds to Bub3. Kinase, reported substrates include Bub3, Mad1, Cdc20 and adenomatous polyposis coli. Bub1 is also a phospho-protein, possibly a target of Cdc2. Bub1 phosphorylation shown to be required for its activation. A78V mutation in the Mad3-like domain shows the residue is required its accumulation and recruitment of Bub3 and Mad3 to the kinetochore when the spindle checkpoint is activated. The mutation also failed to cause mitotic arrest.
Bub3		Binds Bub1 and BubR1 at same Bub3-binding motif. Also binds Cdc20 in MCC complex - WD-40 repeats required for complex formation.

Fig. 1.4. A Summary of structural domains and known functions of spindle checkpoint components.

	Mph1				
Mad1	-	Mad1			
Mad2	-	Tetramer of Mad1-Mad2. Bind throughout cellcycle. Complex formation dependent on mph1, and is required for Mad2 recruitment to the kinetochore.	Mad2		
Mad3/ BubR1	-	-	In MCC complex. Complex formation is dependent on all checkpoint proteins but does not require not intact kinetochore.	Mad3/BubR1	
Bub1	-	-	-	Independent Mad3-Bub1.	Bub1
Bub3	-	-	In MCC complex.	In MCC complex. Independent BubR1-Bub3 also bind throughout the cell cycle, not dependent other checkpoint proteins.	Bub1-Bub3 bind throughout the cell cycle. Bub1-Bub3 interacts with Mad1 in nocodazole.
Slp1/ Cdc20	-	-	In MCC complex. Independent Mad2-Slp1 also forms - dependent on Mad1 in vivo.	In MCC complex. Independent BubR1-Slp1 also forms - dependent on Mad1 and Mad2.	Bub3 In MCC complex.

Fig. 1.5 A summary of known complex formations between spindle checkpoint proteins.

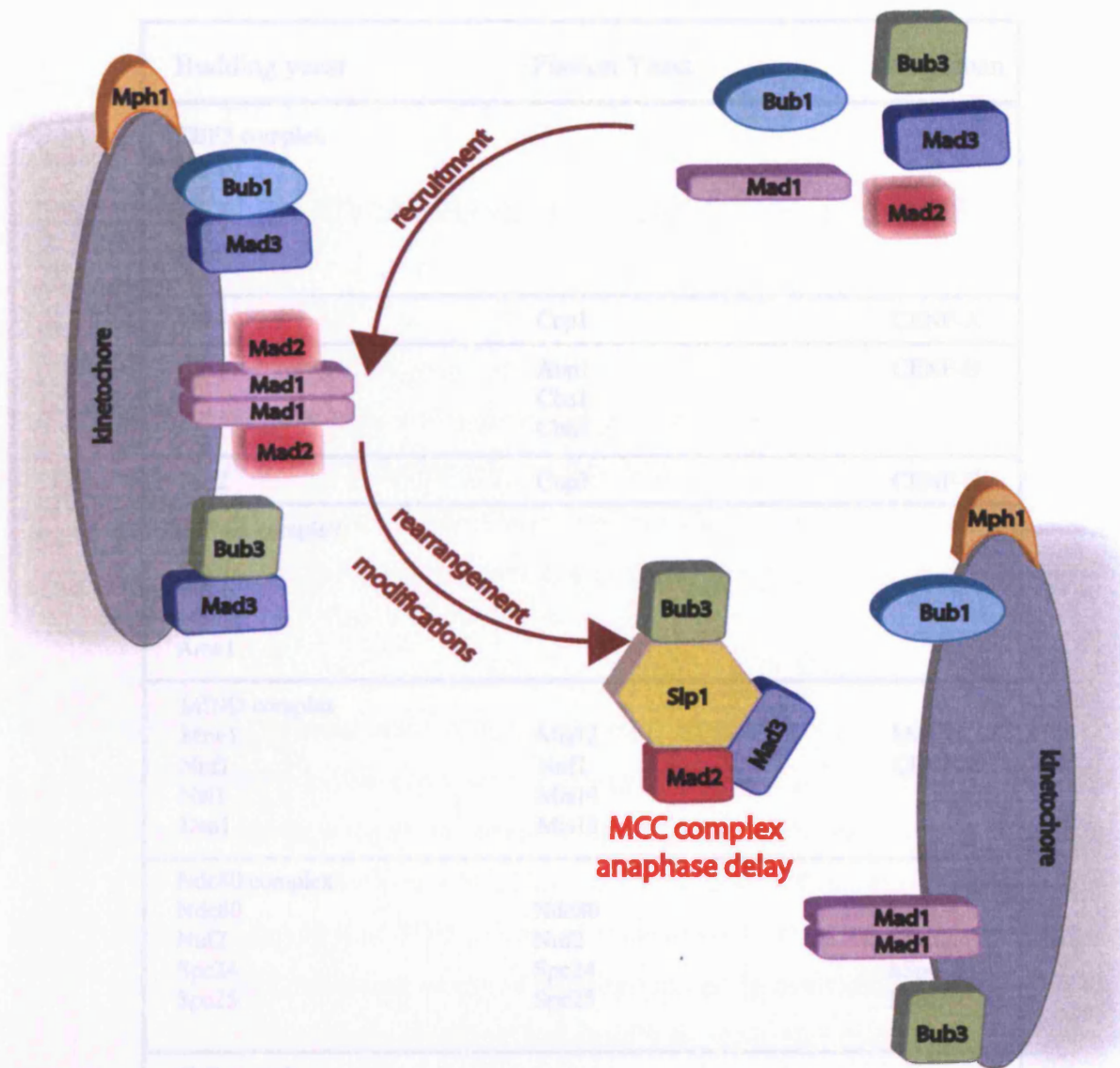


Fig.1.6. Activation of spindle assembly checkpoint.

Genetic, biochemical and structural data suggest that the kinetochore acts as a catalytic site for the turnover of spindle assembly checkpoint proteins. First, checkpoint proteins are recruited to the kinetochore. It is believed that Mad3 kinetochore-recruitment is through its binding with Bub1. Similarly, Bub3 is localised to the kinetochore as a complex with Mad3. Mad2 is transiently recruited to the kinetochore in the form of Mad1-Mad2 complex. Rearrangement then occurs to create the MCC complex that inhibits activator of APC, Slp1. Structural studies indicate that Mad2 recruited to the kinetochore is different from Mad2 in the MCC complex in its conformation.

Budding yeast	Fission Yeast	Metazoan
CBF3 complex Ndc10 Ctf13 Cep3 Skp1		
Cse4	Cnp1	CENP-A
Cbf1	Abp1 Cbn1 Cbn2	CENP-B
Mif2	Cnp3	CENP-C
COMA complex Ctf19 Okp1 Mcm21 Amel		
MIND complex Mtw1 Nnf1 Nsl1 Dsn1	Mis12 Nnf1 Mis14 Mis13	hMis12 CENP-H
Ndc80 complex Ndc80 Nuf2 Spc24 Spc25	Ndc80 Nuf2 Spc24 Spc25	Hec1 hNuf2 hSpc24 hSpc25
Ctf3 complex Ctf3 Mcm16 Mcm22	Mis6 Sim4 Mal2 Sma1-7	CENP-I
DASH complex Dam1 Dad1 Dad2 Dad3 Dad4/Hsk3 Ask1 Duo1 Spc19 Spc34	Dam1 Dad1 Dad2/Hos2 Dad3 Dad4/Hsk3 Ask1 Duo1 Spc19 Spc34	Ask1

Fig. 1.7 Known components of the kinetochore. Thick lines separates known complexes. Dashed-lines represent complexes that have been found to interact in fission yeast, suggesting the existence of super-complexes.

CHAPTER 2

Characterisation of *alp14* deletion mutant

The TOG family of microtubule-associated proteins are functionally highly conserved, with homologues shown to regulate microtubule dynamics and accurate cell division in various organisms. Consistently, studies of fission yeast TOG Alp14 indicate that it is essential for microtubule stabilisation and chromosome segregation. In addition, Alp14 is also involved in the maintenance of the spindle assembly checkpoint.

The TOG family of proteins consists of a conserved N-terminal region, with highly divergent C-terminal tails. Although the microtubule-stabilising function is speculated to be an attribute of the conserved N-terminal domains, several studies have shown the diverse C-terminal region to possess a microtubule-stabilising activity (Nabeshima *et al.* 1995; Wang and Huffaker 1997; Nakaseko *et al.* 2001). The main aim of this thesis is to dissect the function of TOG protein by domain analysis of fission yeast Alp14. In this chapter, characterisation of *alp14* deletion mutant is described. Complete deletion of *alp14*⁺ is temperature-sensitive and results in short and broken microtubules at the restrictive temperature. The absence of Alp14 leads to cell polarity defects in interphase and chromosome missegregation in mitosis. Hallmark phenotypes of the *alp14* deletion mutant are noted for future characterisation of partial deletion mutants in domain analysis.

Microtubules are essential for various cellular processes in all eukaryotes, including transport, cell migration, cell polarity organisation and chromosome segregation. Regulation of microtubule growth is fundamental for accurate and timely chromosome segregation. When regulators of microtubule dynamics such as members of the TOG family are compromised, unequal chromosome segregation occurs leading to genome instability, a hallmark of cancer. In fact studies of human TOG, which was first isolated from an expression library of human brain, showed that it is over-expressed in colonic and hepatic tumours (Charrasse *et al.* 1995 and 1996). Moreover, various members of the TOG family were initially identified as mutants that caused chromosome instability. These include frog *mmps* (Cullen *et al.* 1999), worm *zyg-9* (Hirsh and Vanderslice 1976), plant *mor-1* (Whittington *et al.* 2001), budding yeast *stu2* (Wang and Huffaker 1997), and fission yeast *dis1* and *alp14* (Ohkura *et al.* 1988 and Garcia *et al.* 2001).

XMAP215, a frog member of the TOG family, which was isolated biochemically, was reported to regulate intrinsic microtubule polymerising activity in vitro (Gard and Kirschner 1987; Vasquez *et al.* 1994). When purified XMAP215 was added to pure microtubules, the rate of microtubule growth was substantially increased. Following this breakthrough, in vivo microtubule-regulating activities of other TOG members were investigated. These studies found that when the function of TOG homologues were compromised microtubules became short and/or mitotic spindles defective, suggesting that the microtubule-stabilising function of TOG proteins is highly conserved (Wang and Huffaker 1997; Nabeshima *et al.* 1998; Cullen *et al.* 1999; Gonczy *et al.* 1999; Nakasheko *et al.* 2001; Garcia *et al.* 2001).

Previous studies of a TOG homologue in fission yeast, Alp14, determined that it is essential to promote growth at microtubule plus-ends. Alp14 localises to mitotic spindles and kinetochores in metaphase. Importantly, Alp14 is proposed to act as a bridge between kinetochores and mitotic spindles, which facilitate spindle-kinetochore attachment during mitotic chromosome segregation (Garcia *et al.* 2001). As in wild type cells, when the function of mitotic spindles is compromised in *alp14* mutants, the spindle assembly checkpoint is activated to delay anaphase until the error has been corrected. It is thought that upon detection of unattached kinetochores, spindle checkpoint activation leads to recruitment of checkpoint protein Mad2 to the kinetochores (Rieder *et al.* 1994; Chen *et al.* 1996; Li and Benezra 1996; Waters *et al.* 1998). In *alp14* mutants,

kinetochore dots of Mad2-GFP can clearly be observed, suggesting that sister chromatids may be unattached in this condition. However, unlike other mitotic mutants such as *nda3-311* (defective in β -tubulin – Hiraoka *et al.* 1984), the spindle assembly checkpoint could not be maintained in *alp14* mutants (Garcia *et al.* 2001). This suggests that as well as its microtubule stabilising role, Alp14 itself is a component of the spindle checkpoint cascade.

Although the dual functions of Alp14 are highly linked, they are separate mechanisms. In this thesis, we aim to dissect these distinct roles of Alp14 by domain analysis. Our study would also clarify the function of the conserved TOG domains, which despite high sequence conservation, is yet to be elucidated. To facilitate domain analysis of Alp14, characterisation of complete *alp14*⁺ deletion must first be carried out to find hallmark phenotypes that could be easily detected, which is described in this chapter.

2.1. Identification of Alp14

Microtubules are essential to maintain cell shape and polarity. In fission yeast, defects in microtubule regulation cause cells to take irregular shapes such as bent or branched (Toda *et al.* 1983; Sawin and Nurse 1998). To identify novel genes involved in microtubule function, a screen was undertaken to isolate temperature sensitive mutants defective in cell shape. From this screen *altered polarity (alp)* mutants were isolated, one of which was named *alp14-1270* (Hirata *et al.* 1998; Radcliffe *et al.* 1998). The fission yeast *alp14*⁺ gene was subsequently cloned by complementation from a fission yeast genomic library. Analysis of the *alp14*⁺ sequence showed that it encodes a protein belonging to the TOG family of microtubule-associated proteins (Garcia *et al.* 2001).

A genome-wide search at the Sanger database shows that other members of the TOG family include human ch-TOG, frog XMAP215, fly msps, worm zyg-9 and budding yeast Stu2. In addition to Alp14, another member of the TOG family known as Dis1 was also found in fission yeast (Nabashima *et al.* 1995 and 1998; Nakaseko *et al.* 1996). A sequence alignment between Alp14 and Dis1 and their human ch-TOG, frog XMAP215 and budding yeast Stu2 homologues is shown in fig. 2.1.1. Phylogenetic trees and structural comparison of TOG proteins indicate that TOG members in higher eukaryotes

diverged at the C-terminal while maintaining the conserved 'TOG' domains at the N-terminal region (fig. 2.1.2). The highly conserved TOG domains consist of HEAT repeats, which are representative of protein-protein interaction domain. Note that the general nomenclature for this family of proteins is yet to be established. Although this family of proteins is referred to as the TOG family in this thesis, it is also known as the XMAP215/TOG, Dis1/TOG and XMAP215/Dis1 family (Ohkura *et al.* 2001; Kinoshita *et al.* 2002; Gard *et al.* 2004).

Homologues in yeast possess two TOG domains, whereas in higher eukaryotes five TOG domains are found, which could be a reflection of gene duplication (Gard *et al.* 2004). Another possibility, which is not mutually exclusive, is that several TOG domains are required for complete protein function. Higher eukaryotes may have evolved to use a single protein that carries several TOG domains in contrast to fission yeast, where two homologous proteins containing fewer TOG domains are functional. Domain searches at the diverse C-terminal region of the homologues yielded no obvious known domains. However, in yeast coil-coiled regions have been predicted at the C-terminal tail (Garcia *et al.* 2001), which suggests possible protein-protein interaction in this region.

Fission yeast TOGs, Alp14 and Dis1, have overlapping functions.

The two fission yeast TOG homologues, Alp14 and Dis1, show high conservation. This suggests that the proteins may have overlapping roles. To test this, deletions of each gene were carried out. $\Delta alp14$ and $\Delta dis1$ show temperature-dependent growth defects. At a high temperature (36°C) Alp14 is required for cell growth and at a low temperature (22°C) Dis1 is essential. Growth defects at respective restrictive temperatures were rescued by introduction of multicopy plasmids containing either gene, showing functional redundancy at least at the level of cell growth (fig.2.1.3). However, incomplete suppression of $\Delta dis1$ by the $palp14^+$ raises the possibility that the two proteins may not show a complete overlap in their roles. In support of overlapping functions, deletion of both $alp14^+$ and $dis1^+$ leads to lethality at any temperature, indicating that $alp14$ or $dis1$ mutants were kept viable only by the other's functions (also see chapter 5.6). Indeed, studies of $dis1$ and $alp14$ mutants show that both proteins promote microtubule stabilisation and are required for the formation of bipolar spindle in mitosis (Nabeshima *et al.* 1995 and 1998; Nakaseko *et al.* 1996 and 2001; Garcia *et al.* 2001).

2.2 Characterisation of *alp14* deletion mutant.

To determine the functions of conserved and diverged domains of Alp14 by analysis of *alp14* partial deletion mutants, characterisation of complete *alp14*⁺ deletion is first carried out. Studies to date indicate that at the restrictive temperature, phenotypes of Δ *alp14* have are indistinguishable from that of *alp14-1270*, a point mutant resulting in frameshift and a stop codon (Garcia *et al.* 2001). Because the results of *alp14-1270* are well established, they can be used to find hallmark phenotypes of Δ *alp14* mutant. Results from the study of *alp14-1270* are summarised below.

Similar to other *alp* mutants isolated from the screen, *alp14-1270* is temperature-sensitive and displays cell polarity defects at 36°C. Studies of *alp14-1270* in mitosis at 36°C showed that it failed to form bipolar spindles, leading to gross chromosome missegregation. The spindle assembly checkpoint was activated in response to the mitotic defect, but could not be maintained (Garcia *et al.* 2001). This suggests that as well as its microtubule regulating function, Alp14 itself is a component of the spindle checkpoint cascade. Analysis of Alp14 localisation showed that Alp14-GFP associates with cytoplasmic microtubules during interphase and is then recruited to SPBs and mitotic spindles upon mitotic entry. Chromatin immunoprecipitation analysis showed that Alp14 also localises to mitotic kinetochores in a microtubule-dependent manner (Garcia *et al.* 2001). This dependency suggests that Alp14 may act as a bridge to link kinetochores to mitotic spindles (Garcia *et al.* 2001). Moreover, given the localisation of Alp14 and its role in stabilising microtubules, Alp14 may also facilitate spindle-kinetochore attachment during mitotic chromosome segregation.

Defects in microtubule function of Alp14 cause temperature-sensitivity.

In wild type cells, cytoplasmic microtubules emanate from microtubule organising centres at the middle of the cell towards the cell ends. By growing along the length of the cell and rapidly undergoing catastrophe once they have reached the cell ends, microtubules are able regulate cell's size, shape and polarity. In conditions where microtubules are compromised, for example when microtubule drugs are added or in mutants of tubulin or regulators of microtubule dynamics, cells exhibit bent or branched phenotypes and often show retarded growth (Toda *et al.* 1983; Sawin and Nurse 1998).

To address the role of Alp14 in regulation of microtubule dynamics, $\Delta alp14$ cells were spotted onto rich plates at both permissive (26°C) and restrictive (36°C) temperatures. As fig. 2.2.1 A shows, the $\Delta alp14$ mutant displays retarded growth at the 36°C, and like *alp14-1270* and other *alp* mutants isolated from the screen, $\Delta alp14$ cells are bent and branched at the restrictive temperature (fig. 2.2.1 B). To visualise microtubules in the absence of Alp14, an immuno-staining of α -tubulin of $\Delta alp14$ cells was carried out at 36°C. Results show $\Delta alp14$ cells to exhibit short cytoplasmic microtubules in comparison to wild type at the restrictive temperature (fig. 2.2.2), which suggests that Alp14 is required for microtubule polymerisation and/or stability, at least in interphase cells. In mitosis, the $\Delta alp14$ mutant also shows broken spindles (fig. 2.2.2). The lack of stable spindles in the absence of Alp14 is expected to lead to defects in chromosome segregation. Indeed, missegregated chromosomes are found in $\Delta alp14$ at 36°C (fig. 2.2.3). In the study of *alp4-1270* (Garcia *et al.* 2001) and $\Delta alp14$ (this study, published in Garcia *et al.* 2001), microtubule defects are predominantly found at the restrictive temperature, which suggests that microtubule defects are represented by temperature-sensitivity in *alp14* mutants.

Defects in spindle assembly checkpoint function of Alp14 results in TBZ-hypersensitivity.

Many mutants affecting microtubule stability show sensitivity or resistance to microtubule destabilising drugs. Thiabendazole (TBZ) is a microtubule drug that destabilises microtubules by inhibiting the addition of $\alpha\beta$ tubulin subunits to microtubule protofilaments. Cytoplasmic microtubules and spindles are destroyed in these drugs, causing wild type cells to show retarded growth. Cells with hyper-stabilised microtubules such as $\Delta klp5/klp6$ (see chapter 5) are less affected by the drugs and show growth resistance in comparison to wild type. On the other hand, cells that lack microtubule-stabilising function, the sensitivity to the drugs is increased. Because TBZ destroys mitotic spindles, which leads to unattached kinetochores, the spindle assembly checkpoint is activated to delay anaphase until the error has been corrected. When the checkpoint is defective, untimely mitotic progression leads to premature cytokinesis without chromosome segregation, resulting in 'cut' cells. When the microtubule stability or the spindle assembly checkpoint is compromised, defects are exhibited as retarded growth in presence of microtubule drugs in comparison to wild type. Fig 2.2.4 shows that like α -tubulin mutant $\Delta atb2$ (Adachi *et al.* 1986) and spindle checkpoint mutant

Δmad2 (Li and Murray 1991; Kim *et al.* 1998; Ikui *et al.* 2002; Millband and Hardwick 2002), *Δalp14* is hyper-sensitive to TBZ even at the permissive temperature.

Because Alp14 is involved in both microtubule stabilisation and maintenance of the spindle assembly checkpoint, we reason that these two functions could be executed via distinct structural domains in Alp14. Accordingly, we aim to dissect Alp14 domains for these separate functions by systematic partial truncations of the protein. In our study, both temperature-sensitivity and TBZ-sensitivity will be tested at both permissive and restrictive temperatures. We reason that an *alp14* partial deletion mutant that specifically shows TBZ-sensitivity without microtubule defects may contain defects specific for the spindle checkpoint, while the microtubule function remains intact.

Alp14-GFP localisation.

Before analysing *alp14* partial deletion mutants, the localisation of full length Alp14-GFP has to be confirmed. This is because the loss of localisation in *alp14* partial deletion mutants may render mutant proteins non-functional, which would result in temperature- and TBZ- sensitivity. These phenotypes could then be mistaken for the loss of a specific domain required for microtubule or spindle checkpoint function. To confirm published results (Garcia *et al.* 2001), localisation of wild type Alp14-GFP is analysed in live microscopy as a control. As fig. 2.2.5 shows, Alp14-GFP is localised to cytoplasmic microtubules and spindles in a punctuated pattern (two top panels and two bottom panels), which is identical to published results. Alp14-GFP was also observed as intense dots (middle panel), which may be representative of its SPBs or kinetochore localisation. Overall, from our brief observation of Alp14-GFP as a control, we confirm that Alp14-GFP is recruited to cytoplasmic microtubules in interphase cells, and to SPBs, spindles and kinetochore dots during mitosis, as previously published.

2.3 Summary and Concluding Remarks

This thesis aims to determine the function of conserved and diverged domains of the TOG family of proteins by domain analysis of fission yeast Alp14. To facilitate the characterisation of partial deletion mutants, we have determined and characterised phenotypes of *alp14* deletion mutant that can be easily detected. The temperature-

sensitivity of $\Delta alp14$ is linked to compromised microtubule function, with cells showing cell polarity defects, short microtubules and chromosome missegregation. $\Delta alp14$ also shows hypersensitivity to microtubule drug, TBZ, at any temperature. Sensitivity to microtubule drugs could be a result of compromised spindle checkpoint function or defects in microtubule-stability. Because Alp14 has been shown to play a role in both of these distinct mechanisms (Garcia *et al.* 2001), we aim to create an *alp14* partial deletion mutant that specifically shows TBZ-sensitivity without microtubule defects.

From this study, we have confirmed that $\Delta alp14$ and *alp14-1270* show identical phenotypes, at least at the restrictive temperatures in terms of microtubule-stabilising activity. One of the most obvious phenotypes is short and weak cytoplasmic microtubules, which lead to cell polarity defects displayed as bent and branched cells. Like Alp14, the function of TOG homologues in stabilising microtubules has been observed in various organisms. In frog, microtubule growth is prevented upon depletion of XMAP215 (Charrasse *et al.* 1998; Tournebize *et al.* 2000). Similarly, non-functional mutations in worm *zyg-9* and fly *msps* lead to formation of abnormally short spindles (Gonczy *et al.* 1999; Cullen *et al.* 1999).

Like *alp14-1270*, $\Delta alp14$ shows abnormally short and broken spindles, which lead to chromosome missegregation. When the function of TOG homologues are compromised chromosome missegregation defects are observed in various organisms, suggesting that role of TOG proteins in cell division is also highly conserved (Wang and Huffaker 1997; Nabeshima *et al.* 1998; Gonczy *et al.* 1999). In support for this is the localisation pattern of TOG homologues in mitosis. Like Alp14, fission yeast Dis1, budding yeast Stu2, fly *Msp*s, worm *Zyg-9* and human ch-TOG localise to microtubules and SPBs/centrosomes (Wang and Huffaker 1997; Nabeshima *et al.* 1998; Charrasse *et al.* 1998; Cullen *et al.* 1999; Graf *et al.* 2003; Tournebize *et al.* 2000; Popov *et al.* 2001). To date, only yeast Stu2, Dis1 and Alp14 and dictyostelium DdCP224 have been found to bind to kinetochores, which suggest that the localisation to this region may be specific to yeast and amoeba (Graf *et al.* 2003; Garcia *et al.* 2001; Nakaseko *et al.* 2001; Gard *et al.* 2004). Another possibility is that kinetochore localisation may be too transient to be detected. It is important to note that kinetochores and SPBs/centrosomes reside in close proximity, which has led to some kinetochore components, such as members of the Nuf2/Ndc80 complex, to be initially isolated as centrosomal proteins. In our study,

Alp14-GFP analysed in this chapter was shown to localise to cytoplasmic microtubules and mitotic spindles as previously reported (Garcia *et al.* 2001). In addition, dot-like localisation of Alp14 was observed, which may be representative of Alp14 recruitment to SPBs and kinetochores.

Alp14 has been determined to be essential for spindle assembly checkpoint maintenance (Garcia *et al.* 2001). Although this function is yet to be found in other organisms, it is of note that this role of Alp14 can be easily masked. This is because spindle defects in *alp14* mutants activate the spindle assembly checkpoint while the checkpoint is unable to be maintained in this condition. It had been observed that the spindle checkpoint defects are most obvious in *alp14-1270* at the permissive temperature where spindles are less severely damaged (Garcia *et al.* 2001). The next effort would be to elucidate the role of Alp14 in maintaining the spindle assembly checkpoint. By domain analysis of Alp14, we aim to determine the protein's role in the spindle assembly checkpoint as well as in the microtubule-stabilisation.


```

alp14 .....
dis1 .....
stu2 .....
XMAP215 1201 KAKFTPAKQTLPKKAPSPFVDESDKSGPIYIVPDKQRYKDKAKLVKWPFT
ch-TOG 1201 SCVAKWLQDEHPSDFQENKRLAVMVDLESEKKEGVICLDLILKWLSPFFDPLFV
consensus 1201 s k a v l m v d l e s e k k e g v i c l d l i l k w l s p f f d p l f v

alp14 .....
dis1 .....
stu2 .....
XMAP215 1261 PRRIYFTEIQDQKQDCIANNLQDQLFNADPQKQQLAVLMTHELESEEGISCLDEV
ch-TOG 1261 LMKALETELPLDLSESELTEKASSPIFYLVDVCGSPREVRREDVRAIENEMCLVY
consensus 1261 i l t m s r e a s s p i f y l v d v c g s p r e v r e d v r a i e n e m c l v y

alp14 .....
dis1 .....
stu2 .....
XMAP215 1321 LRFPLVTFRFFDSESVLNKCLVDELVYINLQSQSIESEEMSGTFFPYEMHSGSPKQ
ch-TOG 1321 PASKMPPFTMGGKCHNSHQRAKCHKSGCLNLSYGMHSCGPTFGKLSKASHSKSDS
consensus 1321 t t e a l i m l i c g p t f g k l s k a s h s k s d s

alp14 .....
dis1 .....
stu2 .....
XMAP215 1381 IVKEDVFPALLKMCQVIPASDFPFFMGTGKSKQRAACLEELGCLVSEYGMVVCQ
ch-TOG 1381 AVSAAALSLVTVIEVHGQVFLIGHESKDDKLNLEERIKRSAAKPSAAPIKQVEKFPQ
consensus 1381 v r t i k m v e s a a p i k q v e k f p q

alp14 .....
dis1 .....
stu2 .....
XMAP215 1441 FEPKALEPTEIAISIGRDETVKALSLIYIVYIVVGGQVFLIGLSEEDMSHLEER
ch-TOG 1441 RAQYISSAAEMKAKGKRSVDMKELKALAGSSGHPFAAQHVRRFPQLDLDETDGTVRC
consensus 1441 i g d t t a a i

alp14 .....
dis1 .....
stu2 .....
XMAP215 1501 IKRACKKQAPATAAPAKQVNEKPKQVQANASILEKAPFEDMSKLLQARMHGGGDFPSR
ch-TOG 1501 EMPFLVQKRLDDIFEPVFLDPKIKIADVSPFDDMSMTASTINFIKQVAVAGDIEKIQA
consensus 1501 v e r a l r m i q t

alp14 .....
dis1 .....
stu2 .....
XMAP215 1561 SVPRFPQLDFTTEIENDSGTERCENFPAKQKELDIFPVLIPKPKIRAVSPFDMMS
ch-TOG 1561 LTQLFQIEKARRASTGVLEKDMHGLITSLERRIQLREGQVIRSVMLLVVFLKSD
consensus 1561 i d v m l v e e o l e g q v i r s v m l l v v f l k s d

alp14 .....
dis1 .....
stu2 .....
XMAP215 1621 EIAETTFPFSFQVAVSDVMAKIQALAQSDVLSQDKKAAKMSGIDQPLATFMGERL
ch-TOG 1621 QGILSALLVLLQDSSLATASSPKFSELVKCLMGMVRLLPDTINHSILDRDILLDEIMK
consensus 1621 n t v i i v r i i m i

alp14 .....
dis1 .....
stu2 .....
XMAP215 1681 AINTEMADERLDFTKDDIVELYSCIXGNMISLPQMSKARRASTGVLEKDLMLGLISEMLD
ch-TOG 1681 VFPKERLQCKSEFPFIRTEKTLLETLCCKLGGPKILSDHMTMIDMKNESELAALCRMMKNS
consensus 1681 y v r i m e l m i d m k n e s e l a a l c r m m k n s

alp14 .....
dis1 .....
stu2 .....
XMAP215 1741 ARKEDLEKGGQVVFTEKSLVWVLEKSPQTHIQALESLLQDELLKASPSHSELVLM
ch-TOG 1741 MDQTGSKSDKETAKGASRIDAKSSKAVKPLAKPFRKIGSRHHKESLALYSEKYS
consensus 1741

```

```

alp14 .....
dis1 .....
stu2 .....
XMAP215 1801 KCLSNMILLPFAKQSEHLELDRIDREHFFSEVLPEERLKGKEMFMRKTLLELTC
ch-TOG 1801 DADIEFFLENNKQFQSTYERGLSEIHHHHHHHHHHHISTSTGISFQMEVTCVPTSTVSS
consensus 1801 f i l l d i r

alp14 .....
dis1 .....
stu2 .....
XMAP215 1861 ELKSPKIMDELQIEFTSEHELEHLELVKESIDRLOSRODKRETEKQANCIEDKVGK
ch-TOG 1861 IGTNHESEVGFQYLERELKILQKCHLDRTEKQDDRFPFLKLLSKPAVPTVAKSTDMLESK
consensus 1861 s m k a a t n s e k

alp14 .....
dis1 .....
stu2 .....
XMAP215 1921 ANVSDPLDQPKKIQSFEHEKSKELALSLIYKKYSDADYKQVQKQVVEVGL
ch-TOG 1921 LKQLRESKQKQSSLDLDRTHSEVTVSSSESTANISLKKLELEKIEKREK
consensus 1921 e k t g d k e s

alp14 .....
dis1 .....
stu2 .....
XMAP215 1981 RLIEMRREGKARIAPHTPTGNSTVTEMTFLPTVYHTAAPVSTHGERVQPSVILERLKI
ch-TOG 1981
consensus 1981

alp14 .....
dis1 .....
stu2 .....
XMAP215 2041 LKQRGGLDRAKQDSEFFPTEKLLFAVVESETEKGLKESSEQFQVELDS
ch-TOG 2041
consensus 2041

alp14 .....
dis1 .....
stu2 .....
XMAP215 2101 HQTYPSTTSSASSTMIDFTDLKRLERIKSRK
ch-TOG 2101
consensus 2101

```

Fig.2.1.1. Continued

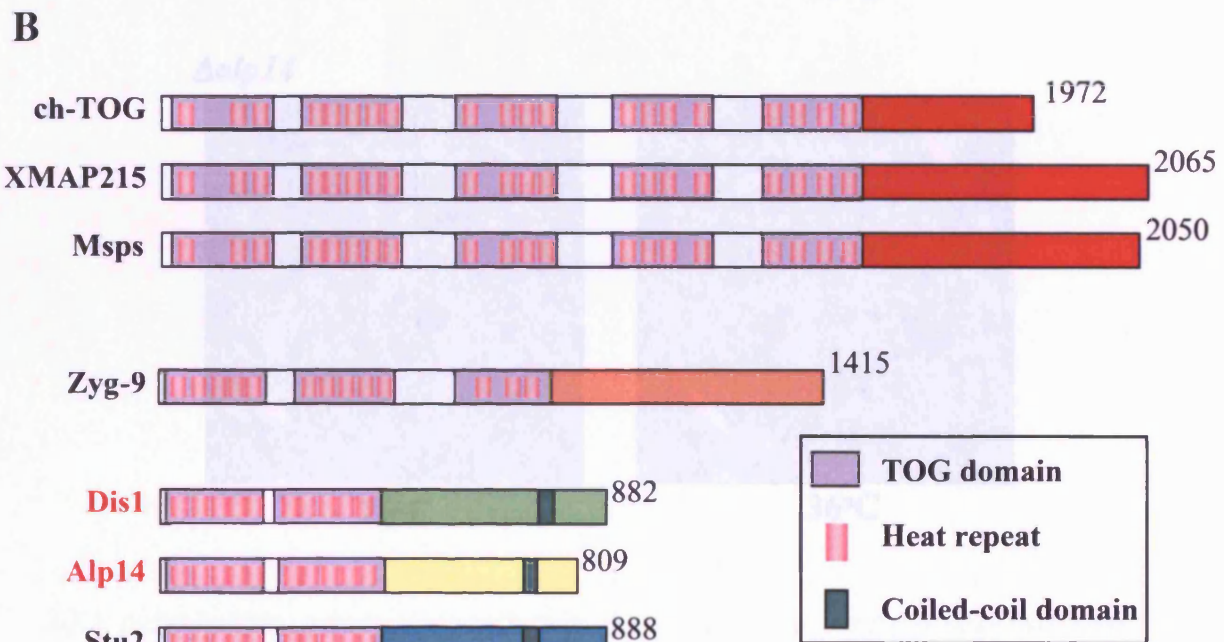
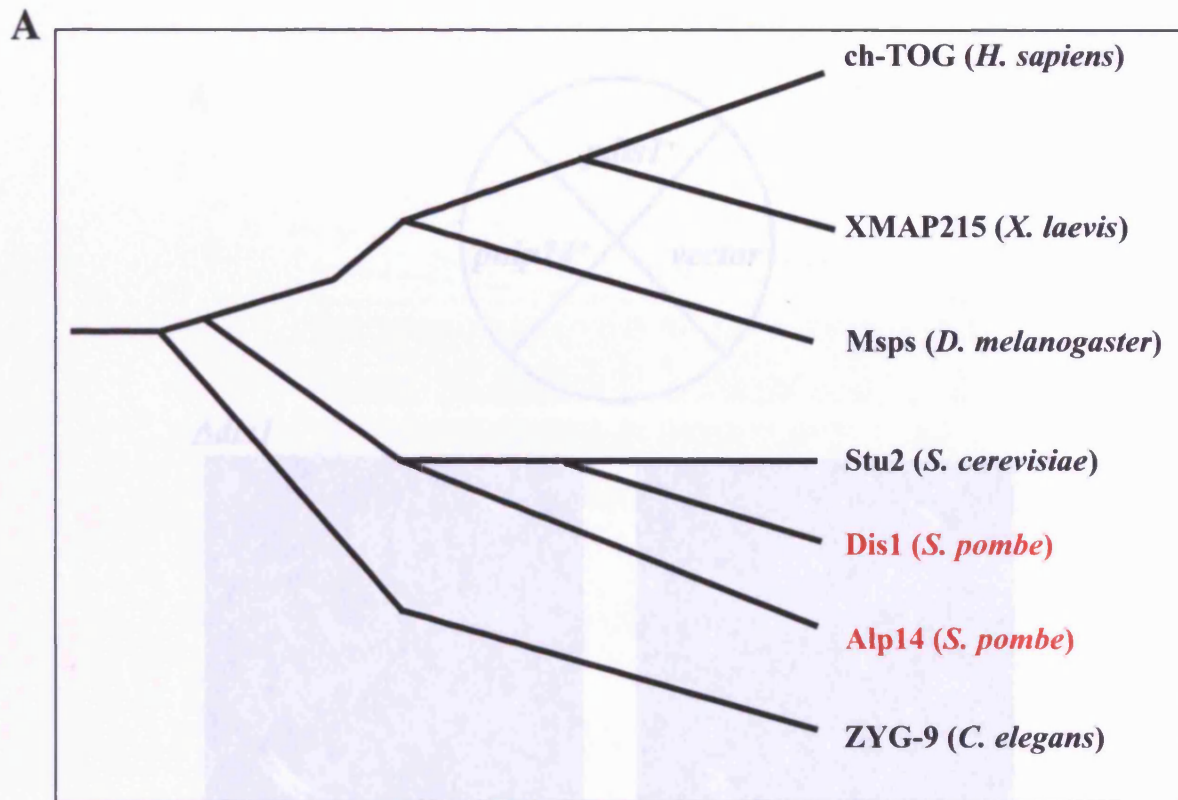


Fig. 2.1.2 Evolutionary relationship between Alp14 and its homologues. **A)** A phylogenetic tree showing evolutionary relationship between Alp14 and its homologues in yeast and metazoans, **B)** Structural comparison between Alp14 and its homologues in yeast and metazoans. Conserved regions are at the N-terminal containing 'TOG' domains, consisting of HEAT repeats. C-terminal is diverse, and contains predicted coiled-coil regions in yeast homologues. Not drawn to scale.

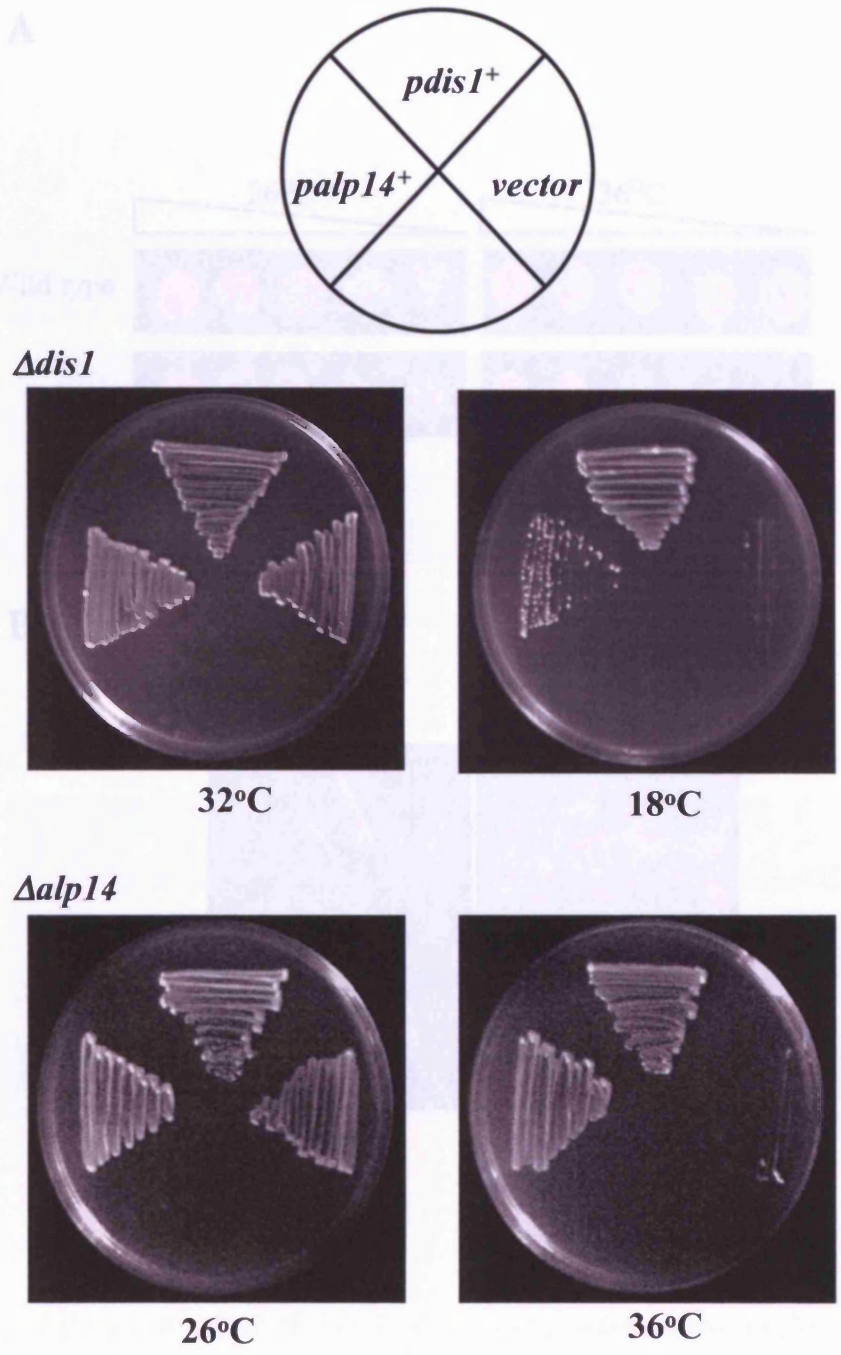
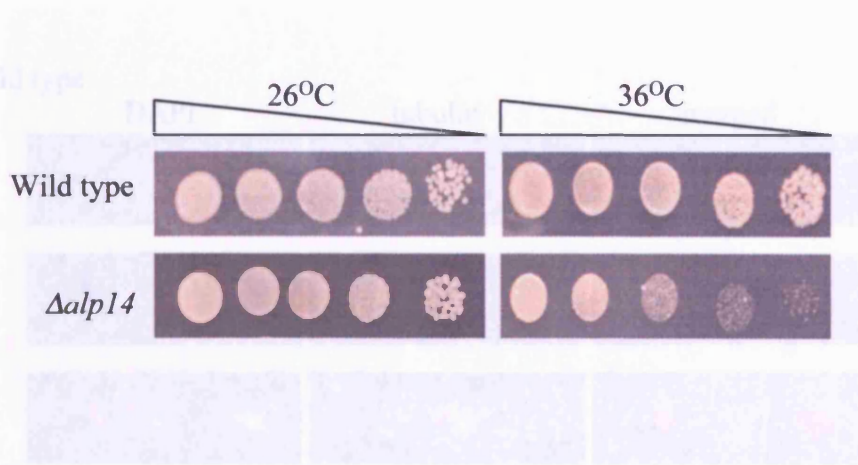


Fig. 2.1.3 Functional redundancy between Alp14 and Dis1. *dis1* and *alp14* deletion mutants carrying an empty vector or multicopy plasmids containing *dis1+* or *alp14+* were streaked on selective media and incubated for four days at permissive and restrictive temperatures for $\Delta alp14$ and $\Delta dis1$. Note that $\Delta alp14$ and $\Delta dis1$ are temperature- and cold-sensitive, respectively.

A



B

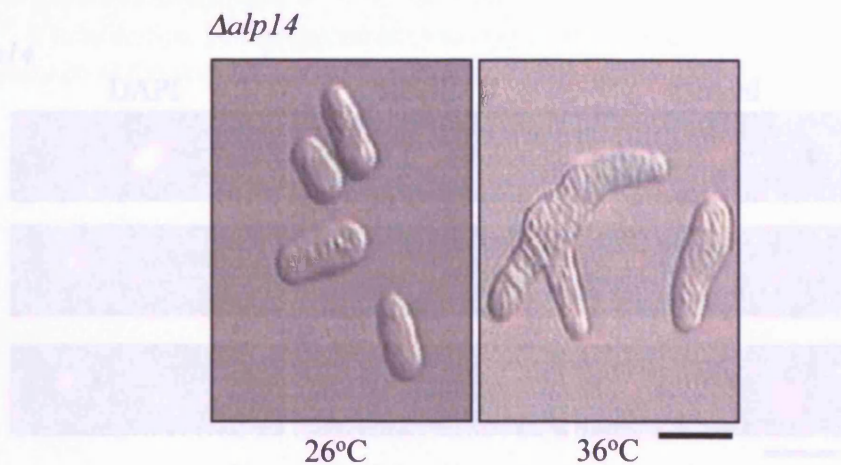


Fig. 2.2.2 Deletion of *alp14* results in short and broken microtubules. Wild type and $\Delta alp14$ cells grown to rich medium at 36°C were fixed with acetone and processed for immunostaining with anti- α -tubulin antibody. Visualization by fluorescence microscopy.

2.2.1 $\Delta alp14$ shows retarded growth and growth polarity defects at the restrictive temperature. A) Wild type and $\Delta alp14$ were spotted after serial dilution (10^6 to 10^2 cells) on rich plates and incubated for 4 days at permissive (26°C) and restrictive (36°C) temperatures. B) $\Delta alp14$ cells grown on rich plates for 4 days at 26°C and 36°C shows branched cells at the restrictive temperature. Scale bar represents 10 μ m.

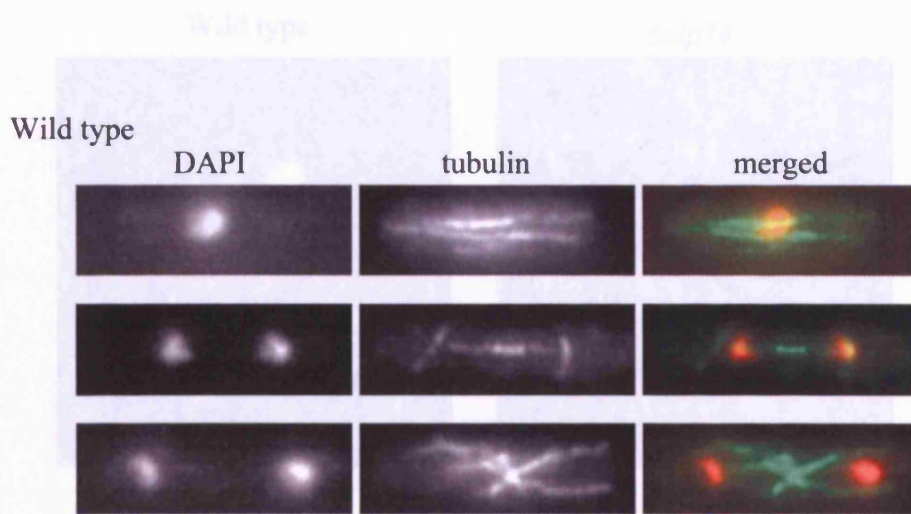


Fig. 2.2.2 Deletion of *alp14⁺* results in chromosome missegregation. Wild type and $\Delta alp14$ cells grown in rich media at 36°C were fixed with 2-propanol and stained with DAPI. Visualisation by fluorescent microscopy shows chromosome missegregation defects in $\Delta alp14$. The restrictive temperature for the *alp14* gene is represented by μ ts.

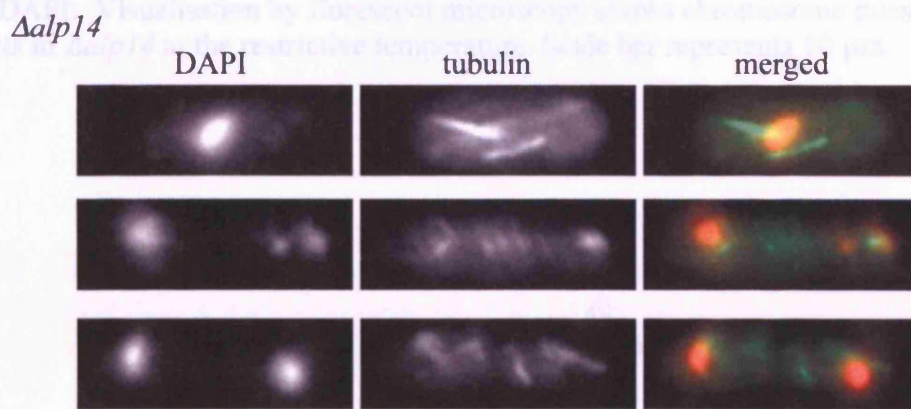


Fig. 2.2.2 Deletion of *alp14⁺* results in short and broken microtubules. Wild type and $\Delta alp14$ cells grown in rich media at 36°C were fixed with methanol and processed for immunostaining with anti- α -tubulin antibody. Visualisation by fluorescent microscopy shows short and broken microtubules in $\Delta alp14$ at the restrictive temperature. Scale bar represents 10 μ m.

Fig. 3.2.4 Deletion of *alp14⁺* causes increased sensitivity to microtubule drug, TBZ. Wild type, $\Delta alp14$, $\Delta alp14$, *alp14-1270* and $\Delta alp14$ cells were spotted at the concentrations of 10^7 and 10^8 cells on rich plates in the absence or presence of 30 μ g/ml TBZ for five days at 36°C.

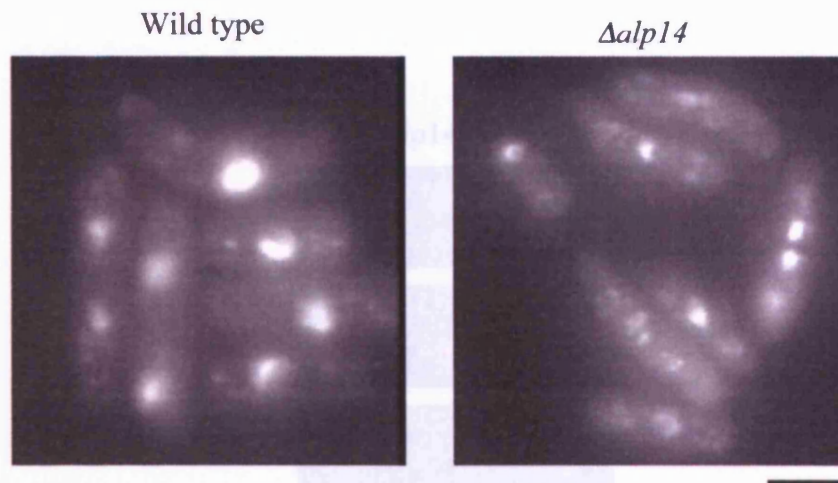


Fig. 2.2.3 Deletion of *alp14*⁺ results in chromosome missegregation. Wild type and *Δalp14* cells grown in rich media at 36°C were fixed with formaldehyde and stained with DAPI. Visualisation by florescent microscopy shows chromosome missegregation defects in *Δalp14* at the restrictive temperature. Scale bar represents 10 μm.

Fig. 2.2.5 Localisation of Alp14-GFP. Cells containing *alp14*⁺-GFP grown in rich media culture were visualised under live fluorescence microscope, showing Alp14 localisation in interphase. Scale bar represents 10 μm.

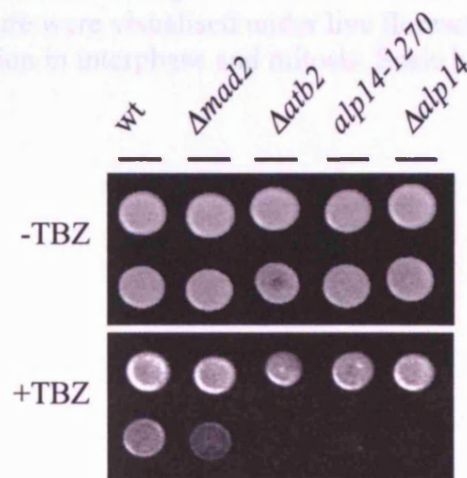


Fig. 2.2.4 Deletion of *alp14*⁺ causes in sensitivity to microtubule drug, TBZ. Wild type, *Δmad2*, *Δatb2*, *alp14-1270* and *Δalp14* cells were spotted at the concentration of 10⁵ and 10⁴ cells on rich plates in the absence or presence of 30μg/ml TBZ for five days at 26°C.

CHAPTER 3

Analysis of *alp14* partial deletions

Alp14-GFP

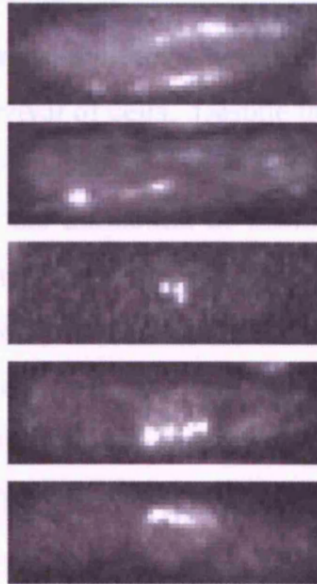


Fig. 2.2.5 Localisation of Alp14-GFP. Cells containing *alp14⁺-GFP* grown in rich media culture were visualised under live fluorescent microscopy, showing Alp14 localisation in interphase and mitosis. Scale bar represents 10 μm .

CHAPTER 3

Analysis of *alp14* partial deletions

The function of the TOG family of proteins has been widely studied and shown to be of utmost importance to the survival of cells. Despite this, the role of the highly conserved TOG domains has yet to be elucidated. Because fission yeast contains two functional homologues in this family, the dissection of fission yeast TOG may reveal specific functions of TOG proteins masked in other organisms. Domain analysis of fission yeast TOG protein is carried out by *alp14* partial deletions. Construction and analysis of *alp14* partial deletion mutants are described in this chapter. Results reveal that the first TOG domain is responsible for its role in the spindle assembly checkpoint. The second TOG domain, together with the diverse C-terminal region stabilises microtubules, possibly by promoting their elongation. Finally, the C-terminal tail of Alp14 is also required for localisation, which is supported by interaction with its binding partner Alp7, a protein of the TACC family.

The interaction between spindles and kinetochores is central to chromosome segregation. By capturing the kinetochores, mitotic spindles are able to pull replicated sister chromatids toward opposite poles, thereby separating them prior to septation and cytokinesis. When the interaction between spindles and kinetochores is compromised, for example when kinetochores are unattached or tensionless, a checkpoint mechanism is activated to delay anaphase onset until the error has been corrected. The spindle assembly checkpoint consists of a set of highly conserved proteins known as Mph1 (also known as Mps1), Mad1, Mad2, Mad3 (also known as BubR1 in higher eukaryotes), Bub1 and Bub3. It is thought that by interacting with an activator of anaphase promoting complex (APC), Mad2, Mad3 and Bub3 prevent APC-dependent degradation of securin, thereby inhibiting anaphase onset. The mitotic activator of APC is Slp1, which is known as Cdc20 in budding yeast and p55^{Fizzy} in higher eukaryotes. It has been shown that a complex of Mad2-Slp1/Cdc20 that lacks Mad3 and Bub3 also exist, which is also able to inhibit APC.

Studies of fission yeast TOG homologue, Alp14, has revealed two distinct roles. One is promotion of polymerisation at the plus-ends of cytoplasmic microtubules and mitotic spindles. The other is the maintenance of spindle assembly checkpoint (Garcia *et al.* 2001). When Alp14 function is compromised, the spindle checkpoint is activated in response to spindle damage but also fails to be maintained. Because these two processes are highly linked, it is difficult to elucidate detailed involvement of Alp14 in the assembly checkpoint by studying mutants that cause complete dysfunction of Alp14. By deleting specific domains of Alp14, we aim to isolate regions of Alp14 that are specifically responsible for each role of the protein, namely microtubule-stabilisation and spindle assembly checkpoint maintenance.

By domain analysis, the function of conserved TOG domains would also be clarified. Given its high sequence conservation at the N-terminal region, it is speculated that the highly conserved TOG domains possess a microtubule-stabilising activity. However, various studies have shown contradictory results. There have been several reports of the diverged C-terminal region being unexpectedly responsible for the conserved microtubule function (Nabeshima *et al.* 1995; Wang and Huffaker 1997; Spittle *et al.* 2000; Nakaseko *et al.* 2001). Another study indicates that the N-terminal TOG domains destabilise microtubules rather than stabilising them (Van Breugel 2003). This further

contradicts the consistent findings of the protein's overall functions. Further more, TOG domains contain HEAT repeats, which are hallmarks of protein-protein interaction activity (Neuwald and Hirano 2000). Despite this, a candidate protein that may interact at this domain is yet to be found. Given that Alp14 functions to establish stable bipolar spindle-kinetochore attachment and maintain the spindle assembly checkpoint, candidate proteins that may interact with TOG domains may be components of the kinetochore and the spindle checkpoint.

3.1 Systematic deletion of *alp14*⁺ from the C-terminus

Earlier report shows the C-terminus of Alp14 contains a microtubule-binding activity (Nakaseko *et al.* 2001). Given this result, deletion of the C-terminal region is expected to result in the loss of Alp14's localisation, at least to cytoplasmic microtubules and mitotic spindles. A predicted coiled-coil motif is also found within the microtubule-binding domain in Alp14, which suggests that microtubule localisation may be dependent on interaction with a partner protein. The ability to bind to microtubules is also likely to confer Alp14 to promote microtubule polymerisation.

3.1.1 Construction of *alp14* C-terminus-deletion mutants.

To systematically truncate Alp14 from its C-terminal, GFP fusions were used as this would also allow the localisation of the mutants to be visualised. The insertion of GFP at the C-terminal of wild type Alp14 does not affect the function of the protein and therefore is unlikely to disturb the folding of the protein. In addition to the predicted coiled-coil domain, the C-terminal region also contains an *in vitro* microtubule-binding domain at residues 639-696, shown in fig 3.1.1. (Nakaseko *et al.* 2001). To understand the *in vivo* function of this region, two constructs have been produced. One is the deletion of the C-terminal tail ($\Delta Tail-GFP$) at residues 696-809, leaving the microtubule-binding domain and coiled-coil region intact. The second construct ($\Delta MT-GFP$) deletes residues 639-809, disposing the predicted microtubule-binding domain from the C-terminal. Another construct ($\Delta Cter-GFP$) that deletes the entire diverse C-terminal region from 420-809, only leaving conserved TOG domains intact was produced to

analyse the function of the diverged region of Alp14. A schematic diagram of the constructs is shown in fig.3.1.1. Analysis of constructed *alp14* partial mutants is described below.

3.1.2 Deletion of the C-terminal region of Alp14 results in the loss of microtubule function and localisation.

When the microtubule function of Alp14 is lost, cells become temperature-sensitive. At the restrictive temperature (36°C), these cells exhibit retarded growth and bent / branched cells. These phenotypes are used to determine the loss of microtubule function in *alp14* C-terminal deletions. Fig. 3.1.2 shows that all constructs of *alp14* C-terminal deletion ($\Delta Tail-GFP$, $\Delta MT-GFP$ and $\Delta C-GFP$) display cell morphology defects at 36°C, indicating that microtubule function is lost when the C-terminal region is deleted. Because the microtubule-binding and coiled-coil domains remain intact in $\Delta Tail-GFP$, the loss of microtubule function in this construct suggests that the C-terminal regions, including the most C-terminal residues that do not contain known or predicted domains, are crucial for microtubule function. Consistently, immuno-staining of anti- α -tubulin confirms that deletion of Alp14 C-terminal regions results in short cytoplasmic microtubules and mitotic spindles, similar to deletion of full-length *alp14*⁺ (fig. 3.1.3).

The loss of microtubule function may reflect the loss of specific domains required for the protein's function to stabilise microtubules. Alternatively, it could also be caused by the loss localisation to microtubules. To investigate the localisation of these mutant proteins, cells were fixed with methanol and processed for immuno-staining with anti α -tubulin. Fig. 3.1.3 shows that Alp14 localisation is lost in all constructs that delete the C-terminal region. Live cell analysis at both permissive and restrictive temperatures confirms that Alp14 is no longer able to localise to microtubules, SPBs or kinetochore dots in these constructs (data not shown).

Because the localisation of Alp14 is lost, it would be inaccurate to study the affects of *alp14* partial deletion in these constructs. It is also possible that the loss of localisation is due to the insertion of GFP fusion, causing the folding of the protein to be hindered. Alternatively, partially deleted Alp14 mutant proteins may be unstable and are readily

degraded.

3.2 Systematic deletion of *alp14*⁺ from the N-terminus

The N-terminal regions of TOG proteins in yeast consist of two conserved TOG domains, containing HEAT repeats. HEAT repeats are hallmarks for protein-protein interaction domains (Neuwald and Hirano 2000), indicating a possible site for protein interaction in this region. Though studies have shown that it may have microtubule-depolymerising activity in vitro (van Breugel 2003), the in vivo role of TOG domains is yet to be elucidated. If TOG domains also depolymerise microtubules in vivo, their deletions are expected to cause hyper-stabilised microtubules, similar to that of microtubule-destabilising mutants such as $\Delta klp5/klp6$ (see chapter ⁵ ~~8~~).

3.2.1 Construction of *alp14* N-terminus-deletion mutants.

To analyse the function of the TOG domains, systematic deletions from the N-terminus was carried out (fig. 3.2.1 A). Truncations were facilitated by homologous recombination, which allows the sequence targeted for deletion to be replaced by a selective marker. Because of this, it is difficult to express truncated Alp14 by its natural promoter as the marker would have to reside upstream of the promoter region. To overcome this, *P81nmt* thiamine-inducible promoters, containing an upstream kanamycin-resistance marker (*kan*^r) were used to replace the deleted *alp14* N-terminal sequence.

To visualise the localisation of the partially deleted proteins, *P81nmt* was transformed into an *alp14*⁺ sequence with GFP fusion at the C-terminus. Because the *alp14*⁺-GFP construct also contains a *kan*^r gene, a marker swap was carried out by homologous recombination to replace the *kan*^r gene with a uracil marker (*ura4*⁺). A live observation showed that the marker swap did not affect Alp14-GFP localisation (fig. 3.2.1 B). The *alp14*⁺-GFP-*kan*::*ura4*⁺ strain was used for the truncation of the *alp14*⁺ gene from the N-terminal. A control construct (*FL*) was produced to express full length Alp14-GFP from *P81nmt* promoters. Fig. 3.2.1 C and D show that *FL* behaves like wild type in the

absence of thiamine, when the *nmt* promoter is expressed. At 36°C, *FL* does not show bent or branched cells, suggesting that the microtubule function is intact. When treated with TBZ, *FL* showed similar sensitivity as the wild type strain, confirming that the production of Alp14-GFP from the *P81nmt* promoter does not compromise Alp14 function. Note that when using TBZ on plates, cells were first grown in minimal media lacking thiamine, then spotted onto rich plates containing TBZ. This is to avoid technical inaccuracies that often arises from the different growth rates of cells on solid minimal media that contains TBZ (lab observation – unpublished data). Alp14-GFP was also expressed from the *FL* strain and visualised in a live microscopic analysis (fig. 3.2.1 E). In absence of thiamine, the *P81nmt* promoter is induced and Alp14-GFP localises to microtubules as observed in wild type.

Once the control strains were confirmed to be fully functional, partial deletions of Alp14 from the N-terminus were carried out. To understand the function of the TOG domains, two constructs were produced. One deletes the first TOG domain at residues 1-240 ($\Delta TOG1$). The second construct deletes both TOG domains and the entire conserved N-terminal region at residues 1-430 ($\Delta TOG2$). Other constructs delete the entire N-terminal region and the microtubule-binding domain at residues 1-696 ($\Delta N-M$) and most of the C-terminal region at residues 1-710, leaving only 100 residues intact ($\Delta N-C$). Analysis of *alp14* N-terminus-deletion mutants is described below.

3.2.2 The C-terminal tail of Alp14 is required for localisation.

Section 3.1 has shown that the C-terminal region of Alp14 may be required for its localisation. Localisation analysis of *alp14* deletions from the N-terminus confirms the findings. Fig. 3.2.2 shows that $\Delta TOG1$ and $\Delta TOG2$ are able to localise similarly to wild type Alp14-GFP. Surprisingly, although the microtubule localisation is substantially reduced in $\Delta N-M$, deletion of all known and predicted domains including the microtubule-binding and coiled-coil domains ($\Delta N-M$) is insufficient to completely delocalise the protein. Localisation is lost only with further deletion of the sequence C-terminal of the microtubule-binding domain ($\Delta N-C$ -fig. 3.2.2 F), suggesting that last 100 residues at the C-terminal region are responsible for the localisation of Alp14.

This result has been confirmed by another study in our lab, showing that Alp14 binds to Alp7, a member of the TACC family, at the C-terminal (Sato *et al.* 2004). By binding to Alp7, Alp14 is recruited to mitotic SPBs, and subsequently localise to mitotic spindles and kinetochores. A two-hybrid assay shows that $\Delta N-M$ (also known as $\Delta 696$ in Sato *et al.* 2004) binds strongly with Alp7, indicating that Alp14 C-terminal contains an Alp7-binding domain, essential for its mitotic localisation. Although the coiled-coil motif does not appear to act as an Alp7-binding domain, its deletion results in reduced Alp14 localisation ($\Delta N-M$ –fig. 3.2.2 E and Sato *et al.* 2004). Hence the coiled-coil motif may facilitate or stabilise Alp14-Alp7 binding. Alp14 localisation in interphase is also abolished in $\Delta N-C$, suggesting that the C-terminus may also contain a signal that allows Alp14 to be recruited to cytoplasmic microtubules. However, it is possible that $\Delta N-C$ is simply not expressed or readily degraded.

3.2.3 The second TOG domain, together with the C-terminus is required for microtubule stabilisation.

Complete deletion of *alp14*⁺ results in short microtubules and chromosome missegregation at 36°C (see chapter 2). Immuno-staining of α -tubulin in Alp14 N-terminal truncation constructs grown at 26°C shows that cytoplasmic microtubules and mitotic spindles are largely intact in *FL-GFP* and *$\Delta TOG1-GFP$* cells in comparison to wild type (fig. 3.2.2 A-C). In contrast, the *$\Delta TOG2-GFP$* , *$\Delta N-M-GFP$* and *$\Delta N-C-GFP$* constructs exhibit short cytoplasmic microtubules and abnormal spindles (fig. 3.2.2 D-F), suggesting that the 3'-prime region of *alp14*⁺ from the start of the second TOG domain is required for microtubule stabilisation or elongation. In addition, missegregating chromosomes are often observed in these cells. Given that Alp14 functions to stabilise the plus-ends of microtubules, the chromosome missegregation phenotype suggests that *$\Delta TOG2-GFP$* , *$\Delta N-M-GFP$* and *$\Delta N-C-GFP$* are defective in the mitotic spindle and fail to stabilise the spindle-kinetochore interaction.

Temperature-sensitivity and microtubule defects of *alp14* N-terminal deletion mutants.

Growth defects can be easily detected by phloxine B, a red dye that accumulates in dead or sick cells (Moreno *et al.* 1991). On plates containing phloxine B, wild type cells

appear to be light pink as they are able to repel and export the dye, whereas cells under duress such as growth retardation appear red. Fig. 3.2.3 A and B shows that wild type and $\Delta TOG1-GFP$ cells are able to maintain cell polarity and microtubule function at both 26°C and 36°C. In contrast, $\Delta TOG2-GFP$, $\Delta N-M-GFP$ and $\Delta N-C-GFP$ are temperature-sensitive and display severe bent / branched cell morphology at 36°C. The results indicate that the first TOG domain is not required for microtubule function, at least in the maintenance of cell polarity and shape. The second TOG domain, however, is required for microtubule function. Moreover, the bent and branched cell morphology in $\Delta TOG2-GFP$ appears to be identical to that of $\Delta N-M-GFP$ and $\Delta N-C-GFP$ at 36°C. This suggests that the loss of the second TOG domain disrupts microtubule function.

TBZ-sensitivity of *alp14* N-terminal deletion mutants.

The TBZ-sensitivity of $\Delta alp14$ may be caused by defects in the spindle assembly checkpoint as well as compromised microtubule stabilisation. Because $\Delta TOG2-GFP$, $\Delta N-M-GFP$ and $\Delta N-C-GFP$ displays compromised microtubule function, they are also expected to show hypersensitivity to TBZ. As fig. 3.2.4 shows the results are indeed as expected. Intriguingly, $\Delta TOG2-GFP$, $\Delta N-M-GFP$ and $\Delta N-C-GFP$ also appear to be more sensitive to the microtubule drug than $\Delta alp14$ at 26°C. An explanation for this may be that Dis1 is able to compensate for Alp14 function in $\Delta alp14$, whereas it is unable to do so in $\Delta TOG2-GFP$, $\Delta N-M-GFP$ and $\Delta N-C-GFP$ due to competition. Our results so far (the intact cell polarity and cell shape) show that $\Delta TOG1-GFP$ does not exhibit any observable microtubule defects, which implies that the first TOG domain may not be required for microtubule function. Despite this, $\Delta TOG1-GFP$ is sensitive to TBZ (fig. 3.2.4). This suggests that hypersensitivity of $\Delta TOG1-GFP$ to TBZ may be caused by a loss in spindle assembly checkpoint function.

To confirm that the temperature- and TBZ-sensitivity of the *alp14* partial deletions are caused by the loss of Alp14 function, a plasmid containing ectopic *alp14*⁺ was introduced. Fig. 3.2.5 shows that *palp14*⁺ restores growth and cell polarity at 36°C in $\Delta N-M-GFP$ cells. The plasmid also rescues the TBZ-sensitivity of the $\Delta TOG1-GFP$ and $\Delta N-M-GFP$.

3.3. The Requirement of Alp14 TOG1 in the spindle assembly checkpoint

Previously described results in this chapter show that the specific deletion of the first TOG domain in Alp14 results in hypersensitivity to the microtubule drug, TBZ. Despite this, the mutant does not exhibit any observable microtubule defects. The hypersensitivity to TBZ despite the lack of microtubule defects suggests that the first TOG domain may be a component of the spindle assembly checkpoint. In addition, studies of the *alp14-1270* mutant showed that it is incapable of maintaining high H1 kinase activity when microtubule-destabilising drugs are added (Garcia *et al.* 2001). So far, this function has not been found in other homologous TOG members. Given that two TOG proteins are functional in fission yeast and that the function of the homologues in this family show high functional conservation, it may be that the spindle checkpoint function is masked in other systems. This section describes studies undertaken to elucidate the involvement of Alp14 in the spindle checkpoint through analyses of the $\Delta TOG1$ mutant.

3.3.1 TOG1 is required to maintain the spindle assembly checkpoint

To confirm that spindle function is intact in $\Delta TOG1$, a strain harbouring simultaneous deletions of *klp5*⁺ and *TOG1* was constructed. Klp5 and Klp6 are microtubule-destabilisers that play a collaborative role with Alp14 and Dis1. Klp5/6 and Alp14/Dis1 stabilise spindle-kinetochore attachment by exerting their microtubule-regulating activity at the plus-ends of metaphase spindles (Garcia *et al.* 2002). Simultaneous deletions of Klp5 / Klp6 and Alp14 / Dis1 result in synthetic lethality (see chapter 5 and Garcia *et al.* 2002). If the first TOG domain were required to stabilise mitotic spindles, $\Delta klp5\Delta TOG1$ mutant would be lethal. Fig. 3.3.1 show that $\Delta klp5\Delta TOG1$ is viable. In addition, the double mutant exhibits elongated cells similar to that of $\Delta klp5$ (also see chapter5), indicative of a non-additive phenotype. Therefore, $\Delta TOG1$ does not show detectable microtubule or spindle defects, further suggesting that the first TOG domain may be specifically required for the spindle assembly checkpoint.

Cells lose viability and become cut in $\Delta TOG1$ in presence of TBZ.

As previously described, fig. 3.2.4 show that the $\Delta TOG1-GFP$ mutant is sensitive to TBZ when grown on solid medium. To confirm that $\Delta TOG1-GFP$ hypersensitivity to TBZ, a growth viability test was carried out. Cells were firstly inoculated in liquid cultures containing rich media to allow growth. TBZ was then added to the cultures at 50 μ g/ml. ← Samples were taken at hourly at from 0 to 6 hours and plated onto rich media containing at 200 cells per plate. Viability was calculated by the number of colonies formed on each plate at each time point against those at 0 hours. Fig. 3.3.2 A shows that in presence of TBZ, the viability of wild type and control *FL-GFP* cells declines slightly over the length of exposure to the drug. However, like $\Delta alp14$, $\Delta N-M-GFP$ and $\Delta mad2$ cells, $\Delta TOG1-GFP$ quickly loses the ability to survive in TBZ. After 3 and 4 hours in TBZ, the number of surviving $\Delta TOG1-GFP$ cells has dropped below 50% and 10%, respectively. Observation of DAPI-stained cells after 6 hours in the drug shows few cut cells in *FL-GFP* control strain, whereas in $\Delta mad2$ and $\Delta TOG1-GFP$ mutants, almost all cells observed were cut or showed severe chromosome segregation defects (fig 3.3.2 B). This suggests that like $\Delta mad2$, $\Delta TOG1-GFP$ is unable to delay anaphase in response to spindle damage, implicating that TOG1 functions in the spindle assembly checkpoint.

Cyclin B is degraded prematurely in $\Delta TOG1$ in presence of TBZ.

Mitotic entry is driven by activation of Cdk1-cyclin B complex in all eukaryotes. Fission yeast cyclin B, Cdc13, accumulates during G₂ in preparation of mitosis and is destroyed by APC upon initiation of mitotic exit (Hagan *et al.* 1988; Alfa *et al.* 1989; Booher *et al.* 1989). Localisation of Cdc13 is crucial in determining its functions throughout the cell cycle. A study has shown that Cdc13 is recruited to the nucleus during G₂ and S phase. In mitosis, Cdc13 localisation is dynamic and is indicative of anaphase onset. During prophase and metaphase, Cdc13 is found on both SPBs and mitotic spindles. Upon anaphase onset, APC ubiquitylates Cdc13, leading to its proteolysis and degradation (Decottignies *et al.* 2001).

In wild type the presence of microtubule damage causes the degradation of Cdc13 to be delayed, which indicates a mitotic arrest. A quantification of formaldehyde-fixed cells with visible Cdc13-GFP in the presence of a microtubule drug after synchronisation was carried out. In this condition, both wild type and $\Delta TOG1$ strains accumulate cells with visible Cdc13-GFP, showing spindle checkpoint activation (fig. 3.3.3 A). Unlike wild

type, however, $\Delta TOG1$ displays a sharp drop in the number of cells with Cdc13-GFP (fig. 3.3.3 A at 4 hours in microtubule drug), showing that the TOG domain is required to maintain the spindle assembly checkpoint. Fig. 3.3.3 B shows cells after 4 hours in the microtubule drug. Unlike wild type, $\Delta mad2$ and $\Delta TOG1$ cells failed to retain Cdc13-GFP after 4 hours in the drug. Interestingly, Cdc13-GFP localisation appears earlier in $\Delta TOG1$ than in wild type. This may be a reflection of some microtubule defects in $\Delta TOG1$ that were not detected in earlier experiments. Alternatively, this could reflect the role of TOG1 in the spindle assembly checkpoint. Note that the microtubule drug used here is carbendazole (CBZ), which destabilises microtubules in a similar manner as TBZ (Millband and Hardwick 2002). TBZ was not used here as the morphology of cells is often disturbed in presence of the drug when grown in minimal media, which is required to selectively express the *nmt* promoter.

Spindle assembly checkpoint maintenance in *cut7-446* mutant requires the first TOG domain of Alp14.

Spindle damage induced by the addition of microtubule drug is a condition that is somewhat artificial. To test the requirement of the TOG domain in condition where the spindle damage may occur in mutants, a *cut7-466* strain was used. Cut7 is a kinesin-like protein that belongs to the kinesin-5 family (previously known as the Bim C family – Hagan and Yanagida 1990 and 1992). Studies of *cut7* temperature-sensitive mutant, *cut7-466*, suggests that the protein is required for spindle formation (Hagan and Yanagida 1992; Drummond and Hagan 1998). Cut7 is recruited to SPBs throughout mitosis, specifically to the spindle midzone in anaphase B. In *cut7-466* cells, the spindle localisation is abolished and the bipolar spindles fail to form at 36°C, leading to activation of the spindle assembly checkpoint and anaphase delay (Hagan and Yanagida 1992; Drummond and Hagan 1998). Although the spindle checkpoint is activated in *cut7-466*, the spindle error cannot be corrected in the absence of functional Cut7. Because the spindle checkpoint cannot arrest cells in mitosis incessantly even in wild type, mitosis eventually progresses and *cut7-466* cells become cut (hence its name).

In $\Delta TOG1$ *cut7-466* double mutant, growth viability after temperature shift up from 26°C to 36°C was tested. Fig. 3.3.4 A shows that the viability of *cut7-466* and $\Delta TOG1$ *cut7-466* cells is similarly low in this condition even though we had expected a further drop in viability in $\Delta TOG1$ *cut7-466*. From our results, we speculate that in *cut7-466*, the spindle

checkpoint is activated to arrest cells in mitosis, thereby inhibiting growth in these cells. In $\Delta TOG1$ *cut7-466*, we predict that the spindle checkpoint cannot be maintained and cells become cut, which contributes to the drop in viability.

Like wild type cells, *cut7-466* exhibit condensed chromatin in metaphase when the spindle checkpoint is activated. To determine the role of TOG1 in the spindle checkpoint, the number of condensed DNA were counted in *cut7-466* and $\Delta TOG1$ *cut7-466* cells after temperature shift up. *cut7-466* cells show a sharp increase in the number of cells displaying condensed DNA, with the number of condensed DNA is stabilised over time (fig. 3.3.4 B). In contrast, the condensed DNA phenotype in $\Delta TOG1$ *cut7-466* shows a sudden steep drop after its peak. This indicates that the spindle checkpoint can be activated but not maintained in $\Delta TOG1$ *cut7-466*. Consistent with this, $\Delta TOG1$ *cut7-466* cells become cut after 6 hours at 36°C, whereas the majority of *cut7-466* cells still remain arrested in mitosis (fig. 3.3.4 C).

TOG1 and the spindle assembly checkpoint cascade.

The TOG1 domain is required for the maintenance of the spindle assembly checkpoint. The next question is where in the spindle checkpoint cascade does TOG function, and how it may do so. Various studies have shown that the spindle assembly checkpoint cascade may not be straightforward or linear. So far, Mad2 has been shown to function downstream of Mph1 (He *et al.* 1998). Other studies have shown that Mad2 inhibition of APC depends on Mad3 (Millband and Harwick 2002), while its localisation requires Mad1 (Hwang *et al.* 1998; Chen *et al.* 1999; Fraschini *et al.* 2001; Iouk *et al.* 2002). A model of the spindle checkpoint that is supported by genetic, biochemical and structural studies (see chapter1, fig.1.4) suggest that the checkpoint cascade is far from linear and that the functions of the components are interdependent. Moreover, despite Mad2 being considered as a major player in the checkpoint, Mad2-independent inhibition of APC have been reported. As a result, various branches of the ‘classical’ spindle checkpoint cascade have been proposed, including a Bub1-dependent tension checkpoint (Skoufias *et al.* 2001; Tournier *et al.* 2004). Not only would it be interesting to understand how the TOG domain might function in the checkpoint cascade, the elucidation of TOG1 may also shed light on the spindle assembly checkpoint itself.

Simultaneous deletions of spindle checkpoint proteins and TOG1.

Double deletions of a spindle checkpoint protein and TOG1 were carried out. Fig. 3.3.5 shows growth phenotypes of the double deletion constructs in comparison to wild type, deletion of TOG1 and deletions of checkpoint proteins. Non-additive phenotypes were observed in all double deletions (none of the double mutants show a more severe growth retardation than $\Delta TOG1$), except in $\Delta TOG1 \Delta mad1$ cells. Because Mad1 is reportedly required for Mad2 localisation, this may be a discrepancy in the experiment. Another explanation may be that although Mad1 localises Mad2 to the kinetochore, it might not be required to activate Mad2 inhibition of APC. From the overall result, non-additive phenotypes confirm that TOG1 functions in the spindle assembly checkpoint, and may function upstream of the spindle checkpoint cascade.

Overproduction of Mph1 and Mad2 is toxic in $\Delta TOG1$.

To further investigate the role of TOG1, multicopy plasmids containing checkpoint genes *mad2*⁺ and *mph1*⁺ expressed by *nmt* promoters were introduced to $\Delta TOG1$ cells. *mad2*⁺ and *mph1*⁺ were expressed by *P41-nmt* and *P3-nmt* promoters, respectively. These expression conditions have been shown to result in overproduction of the Mad2 and Mph1 proteins, resulting in mitotic arrest in the absence of spindle damage (He *et al.* 1998). The defect can be detected as toxicity and severe growth retardation. If the spindle assembly checkpoint were linear and TOG1 functioned downstream of Mph1 and Mad2, overexpression of these checkpoint proteins would not affect cell growth. On the other hand, if TOG1 were required upstream of the spindle checkpoint then overproduction of Mph1 and Mad2 may hyper-activate the checkpoint, leading to toxicity. Fig. 3.3.6 shows that overproduction of Mad2 and Mph1 is toxic when TOG1 is deleted. This suggests that TOG1 may function upstream of Mad2 and Mph1. Note that a control experiment introducing empty *pREP1* and *pREP41* plasmids (containing *P3nmt* and *P41nmt* promoter respectively) into wild type and $\Delta TOG1$ cells was also carried out and showed no evidence of toxicity or retarded growth (data not shown).

Mad2 and Mad3 hyper-accumulate transiently at the kinetochore when spindle is damaged in the absence of TOG1.

Spindle assembly checkpoint has been reported to be highly dynamic (Millband *et al.* 2002; Musacchio and Hardwick 2002) with rapid turnovers of components such as Mad2, Mad3 and Bub3, which are required to be rearranged or modified in order to bind to Slp1 in the MCC complex. It is thought that the kinetochore acts as a catalytic site for the turnover of these components (Sironi *et al.* 2002; Millband *et al.* 2002; Musacchio and Hardwick 2002). Overall, spindle checkpoint activation and maintenance are thought to occur in a two-step process. The first is recruitment of all checkpoint proteins to the kinetochores. The second is the rearrangement or modification of Mad2, Mad3 and Bub3 to bind to Slp1 (Millband *et al.* 2002; Musacchio and Hardwick 2002). To determine the requirement of TOG1 in the spindle assembly checkpoint, localisation of checkpoint proteins were tested. If checkpoint components are normally recruited, the involvement of TOG1 in the first step can be eliminated.

Because checkpoint components are interdependently recruited to kinetochores, Mad2, Mad3 and Bub1 localisation would imply that all other checkpoint components are also recruited. To test if TOG1 is required for the localisation of Mad2 to kinetochores, wild type and $\Delta TOG1$ cells grown in absence of thiamine were synchronised with hydroxyurea. They were then washed out and released in media containing microtubule drug CBZ. The number of cut cells was counted to confirm that the spindle checkpoint is not maintained in $\Delta TOG1$ in this condition. As Fig. 3.3.7 A shows, the number of cut cells in $\Delta TOG1$ cells raises sharply over time compared to wild type. Strong Mad2-GFP dots were also counted. The result shows that Mad2 is able to localise to the kinetochores in both wild type and $\Delta TOG1$ (fig. 3.3.7 A and B). Intriguingly, the percentage of cells showing strong Mad2 dots is much higher in $\Delta TOG1$ than in wild type cells. Moreover, localisation of Mad2-GFP was observed earlier in $\Delta TOG1$ than in wild type cells. This may suggest that the spindle checkpoint is activated earlier in $\Delta TOG1$. Another explanation may be that Mad2 is hyper-accumulated at the kinetochores in the absence of TOG1. These possibilities may be able to be distinguished by visualisation of other checkpoint proteins.

Mad3-GFP and Bub1-GFP recruitments to the kinetochores were tested in the same condition as above. Fig. 3.3.8 shows that, like Mad2, Mad3 also hyper-accumulates at

kinetochores of $\Delta TOG1$ cells in presence of spindle damage. In contrast, Bub1 did not hyper-accumulate at the kinetochore, though its recruitment is upregulated in the presence of spindle damage (fig. 3.3.9). Because Bub1 localises normally to the kinetochore in a similar timing to that in wild type cells, the possibility that the spindle checkpoint is activated earlier in $\Delta TOG1$ could be eliminated. Unlike Mad2 and Mad3, Bub1 is not required to be rearranged into the APC-inhibiting MCC complex with Slp1. Specific hyper-accumulation of Mad2 and Mad3, but not Bub1, at the kinetochore suggests that Mad2 and Mad3 may be unable to turnover and rearrange into the MCC complex in $\Delta TOG1$. Note that the recruitment of Mad2, Mad3 and Bub1 had been tested repeatedly in independent experiments and showed consistent results.

If Mad2 and Mad3 were unable to rearrange to form the MCC complex in $\Delta TOG1$, a fundamental question would be how the spindle assembly checkpoint could be activated in this condition. One possibility is that mechanisms of spindle checkpoint activation and maintenance are different. Some studies have shown that Mad2 can inhibit APC without localisation to the kinetochore (DeLuca *et al.* 2003; Rajagopalan *et al.* 2004). This suggests that there is a population of Mad2 that is not required to be modified or rearranged at the kinetochore. The cell's initial response to spindle damage may be by directly activating Mad2-Slp1 interaction rather than localising Mad2 to the kinetochore to be modified, as the latter would result in a more delayed response. However, as the population of 'modified' Mad2 becomes depleted, 'unmodified' Mad2 needs to localise to the kinetochore to allow for binding to Slp1 for maintenance of the spindle checkpoint.

If TOG1 directly maintained the spindle checkpoint by retaining Mad2 and Mad3 at the kinetochore, candidate targets of TOG1 could be proteins that facilitate Mad2 and Mad3 turnover. To date, it is little is known about how Mad2 and Mad3 are rearranged into the MCC complex. Mad1-Mad2 complex localises at the kinetochore. It has been postulated that this complex allows free Mad2 to be modified at the kinetochore. From what is known, candidate targets of TOG1 could be molecules upstream of the Mad1-Mad2 complex, including Mph1, Mad1 and Mad2.

Another possibility is that TOG1 indirectly maintains the spindle assembly checkpoint via a kinetochore protein. It is thought that the kinetochore acts as a catalytic site for rearrangements of checkpoint proteins, as well as a site for spindle attachment and

localisation of proteins such as microtubule polymerising and depolymerising proteins. The stability of the kinetochore structure is of utmost importance to chromosome integrity. An outer kinetochore complex known as the Nuf2-Ndc80 complex has been shown to be required for the localisation of spindle checkpoint proteins and may act as a component of the checkpoint.

3.4 Requirement of Alp14 TOG1 in kinetochore stability.

In this section, we address the stability of the kinetochore structure in $\Delta TOG1$. This is because the kinetochore acts as a catalytic site for the turnover of spindle checkpoint proteins, which may be defective in the absence of TOG1 causing Mad2 and Mad3 to hyper-accumulate. The kinetochore structure is built on by a series of protein complexes (Kniola *et al.* 2001; McAinsh *et al.* 2003; De Wulf *et al.* 2003; Amor *et al.* 2004). Inner kinetochore complexes are recruited to the centromeric region, and central and outer kinetochore protein complexes in turn load onto them. Stable kinetochore structure is essential for kinetochore-spindle attachment and, during spindle checkpoint activation, dynamic turnover of spindle assembly checkpoint proteins. A mutation in a single component of the inner or central kinetochore, such as *mis6* and *mis12* mutants, can lead to the disruption of stable kinetochore structure (Takahashi *et al.* 2000; Appलगren *et al.* 2003; Obuse *et al.* 2004; Amor *et al.* 2004). Mutations in the outer kinetochore Ndc80 complex, however, cause structural disruption of outer kinetochore but leave inner and central kinetochore intact (DeLuca *et al.* 2003; DeLuca *et al.* 2005). Various studies of the Ndc80 complex have shown evidence that it also acts as a component of the spindle assembly checkpoint (Nebetani *et al.* 2001; DeLuca *et al.* 2003; McClelland *et al.* 2003), with some groups suggesting that the Ndc80 complex prevents microtubule-dependent stripping of checkpoint proteins until stable kinetochore is formed (DeLuca *et al.* 2003; McClelland *et al.* 2003).

Nuf2 and Ndc80 are delocalised in $\Delta TOG1$ in presence of CBZ.

To test the stability of kinetochore structure, localisation of Ndc80 was tested in wild type and $\Delta TOG1$ cells. In fission yeast, the Ndc80 complex has been reported to localise to interphase kinetochores or SPBs then loaded onto kinetochores upon mitotic entry. As fig. 3.4.1 shows, asynchronous wild type cells display strong Ndc80-GFP staining at the

cytoplasmic regions as well as SPB / kinetochore dots. Interestingly, mitotic wild type cells no longer show strong cytoplasmic staining in metaphase cells, and instead show comparatively intense kinetochore dots (compare asynchronised and synchronised cell released into mitosis). Like wild type, $\Delta TOG1$ cells display weak cytoplasmic staining and intense kinetochore dots in metaphase cells in the absence of spindle damage. However, when microtubule drug CBZ is added, the intensity of Ndc80-GFP at the kinetochores becomes greatly reduced in $\Delta TOG1$ compared to wild type (fig. 3.4.1 A and B). This suggests that Ndc80 is delocalised in the absence of TOG1. Note that even though images were taken using the same setting and normalised to the background, Ndc80-GFP signal is very weak throughout the whole cells in $\Delta TOG1$, which suggests that Ndc80 may, alternatively, be degraded in this condition.

To confirm this finding, another component of the Ndc80 complex, Nuf2, was also visualised in both fixed and live cells. Fig. 3.4.2 A shows results in formaldehyde-fixed mitotic cells in the absence and presence of CBZ. Like Ndc80-GFP, Nuf2-CFP was also reduced in $\Delta TOG1$ cells when the spindle is damaged. Similar results were obtained from live cells (fig. 3.4.2 B), where Bub1-GFP was also used as a marker of spindle checkpoint activation. Quantification of Nuf2-CFP intensity at the kinetochores (circled region on cell pictures) confirms that unlike wild type cells, Nuf2 fails to display a peak at the kinetochore in $\Delta TOG1$ cells when the spindle is damaged. These results suggest that the first TOG domain of Alp14 is required for the localisation of the Ndc80 outer kinetochore complex, thereby contributing to the stabilisation of the kinetochore structure.

Alp14 binds to Nuf2

The next question we addressed is how Alp14 might localise the Ndc80 complex. One possibility is that Alp14 may bind to components of the complex or other kinetochore proteins. From sequence analysis of Alp14, three potential protein-protein interaction sites are found. One of these sites is the coiled-coil domain at the diverse C-terminal tail. We have determined that Alp7 binds to Alp14 at the C-terminal to allow Alp14 mitotic localisation. Although the coiled-coil domain itself is not required for Alp14-Alp7 binding, it is absolutely essential for complete Alp14 localisation.

The other two potential protein-protein interaction sites are the TOG domains at the conserved N-terminal TOG, containing HEAT repeats. HEAT repeats are hallmarks of protein-protein interaction domains and are thought to be able to bind a variety of proteins as protein-interaction adaptors (Neuwald and Hirano 2000). Consistently, HEAT repeats are found in a number of proteins with varying functions such as phosphatase, condensin, cohesin and coatomers. To date, no candidate proteins have been found to bind to members of the TOG family via the HEAT repeats.

To test if Alp14 binds to components of the Ndc80 complex, a co-immunoprecipitation assay was set up. Wild type cells carrying both *alp14⁺-13myc* and *nuf2⁺-CFP* and control strains grown asynchronously in rich media were extracted for protein and subjected to co-immunoprecipitation assay using anti-myc antibody conjugated with protein G beads. Western blotting analysis shows that Nuf2-CFP co-immunoprecipitates with Alp14-myc (fig. 3.4.3). This suggests that Alp14 binds to Nuf2 in vivo, which further supports earlier findings that the first TOG domain of Alp14 is required for Nuf2 localisation in the presence of spindle damage. From this, we postulate that Alp14 may bind to Nuf2 via its TOG domains. Because the C-terminal region of Alp14 carries out various functions, including microtubule stabilisation, microtubule binding in interphase and Alp7 binding for its mitotic localisation, this proposal is not unlikely.

Alp14 binding to Nuf2 suggests that Alp14 may maintain the spindle assembly checkpoint indirectly via Nuf2. To investigate if Alp14 also directly binds to major checkpoint components, Mad2 and Slp1, a two-hybrid assay was carried out. Fig. 3.4.4 shows that no binding was detected between various domains of Alp14 and Mad2 or Slp1. Control Ras and Raf binding shows that the assay was functional. Several attempts at co-immunoprecipitation also failed to show Alp14 binding to Mad2, Mad3 or Slp1 (data not shown).

3.5 Summary and concluding remarks

We have determined that the C-terminal tail of Alp14 is required for its localisation in interphase and mitosis, thereby allowing for the protein's overall microtubule function. In addition to localisation, the C-terminal region, together with the second TOG domain

(TOG2), are required to stabilise microtubules. Deletion of the TOG2 motif and C-terminal regions from the N-terminus resulted in short interphase microtubules and chromosome missegregation, suggesting that these domains stabilise microtubules by promotion of their polymerisation. Finally, in this chapter we have determined that the first TOG domain (TOG1) is required for the maintenance of the spindle assembly checkpoint. Fig. 3.5.1 summarises the role of Alp14 domains.

Investigation into the involvement of TOG1 in the spindle assembly checkpoint found that spindle damage induced by either addition of microtubule drugs or *cut7* mutation resulted in premature anaphase onset in the absence of TOG1. In $\Delta TOG1$, Mad2 and Mad3 hyper-accumulate at unattached kinetochores, suggesting that TOG1 may be required for the turnover of specific checkpoint proteins for their rearrangement into the anaphase-inhibiting complex. Upon investigation of kinetochore stability, which is required for the integrity of the spindle checkpoint, we found that the TOG1 domain is required for Nuf2 and Ndc80 localisation in spindle damaged conditions. Co-immunoprecipitation assay shows that Alp14 binds to Nuf2. From these results, we postulate that the TOG1 domain is required for Nuf2-Alp14 interaction or that Nuf2 directly interacts with the TOG1 domain. Overall, our findings suggest that TOG1 indirectly maintains the spindle assembly checkpoint via the Nuf2-Ndc80 kinetochore complex.

The microtubule function of Alp14

Partial deletion of Alp14 from the C-terminus resulted in the complete loss of Alp14 localisation. Further analysis using deletions of Alp14 from the N-terminus showed that the last 100 residues at C-terminal tail are required for the localisation of the protein. The localisation dependency of Alp14 on its C-terminal tail is supported by the finding that Alp14 binds to Alp7, a TACC homologue, at this region (Sato *et al.* 2003 and 2004). The interaction between fission yeast TOG and TACC proteins allows Alp14 to enter the nucleus, leading to its mitotic localisation (Sato and Toda – personal communication). This function is conserved as findings of interaction between TACC and TOG have been reported in frog and fly studies (Cullen and Ohkura 2001; Lee *et al.* 2001; Bellanger and Gonczy 2003; Srayko *et al.* 2003). Like Alp14, the interaction is absolutely required for the TOG proteins to be recruited to centrosomes and microtubules in order to exert their microtubule-regulating activity. In our study, the microtubule binding and coiled-coil

regions were intriguingly not required for either interaction with Alp7 or localisation. However, absence of these motifs resulted in reduced Alp14 localisation, suggesting that they may be required for stabilisation of Alp14-Alp7 binding to microtubules. Note that Alp7 requires Alp14 to localise to mitotic spindles, indicating that the Alp14-Alp7 complex binds to microtubules via Alp14 C-terminus, at least in mitosis (Sato *et al.* 2003).

Analysis of partial deletion mutants showed that both the C-terminal and the TOG2 domain function to stabilise microtubules. Deletion of the TOG2 domain (Δ TOG2) from the N-terminus resulted in lost of cell polarity, short cytoplasmic microtubules and chromosome missegregation. Further deletion into the C-terminal region displayed similar phenotypes, though cells exhibiting lagging chromosomes and cut phenotypes were more frequently found. It is possible that the microtubule function of TOG2 is a result of its close proximity to the C-terminal region, which leads it to contribute to formation of the tertiary structure required for microtubule-stabilisation. Another possibility is that this function of the TOG2 domain is highly conserved and its activity confers the C-terminal region to obtain a microtubule role, thereby enhancing the protein's function. An *in vitro* study in frog agrees with our findings. In this report, a region of XMAP215 located at the N-terminus containing TOG domains, was shown to possess microtubule polymerisation activity (Popov *et al.* 2001). The consistency between the studies in two very different organisms and systems leads us to postulate that TOG domains in close proximity to the C-terminal region may contain conserved microtubule function.

Microtubule growth may occur by direct addition of $\alpha\beta$ -tubulin subunits, prevention of shrinkage, inhibition of catastrophe and promotion of rescue. The initial breakthrough in this field involving *in vitro* studies in frog showed that as well as an increased growth, the rate of rescue was also augmented when purified XMAP215 was added to pure microtubules (Gard and Kirschner 1987; Vasquez *et al.* 1994). This suggests that the TOG family of proteins may prevent catastrophe as well as directly promoting growth at the plus-ends of microtubules, possibly by microtubule bundling at plus-ends. In our study, deletion of the TOG2 region resulted in short but bundled microtubules, further deletions into the C-terminus resulted in similar microtubule phenotypes, though higher rates of chromosome missegregation were detected. Further investigation into microtubule phenotypes needs to be carried out to clarify the specific role of Alp14

domains in promoting microtubule-stabilisation. We have addressed this point in the next chapter by overexpression of specific domains of Alp14.

The spindle assembly checkpoint function of Alp14

In this study we have found that the first TOG domain of Alp14 is required for spindle assembly checkpoint maintenance, which is novel function of TOG domain. Upon spindle damage, the spindle assembly checkpoint is activated but fails to be maintained in $\Delta TOG1$. In this condition, two intriguing phenotypes are observed. First is the hyper-accumulation of Mad2 and Mad3, but not Bub1. Structural studies have shown that the structure of Mad2 takes two forms, one that can readily bind to Slp1 and the other that cannot. It is thought that ‘free’ Mad2 cannot readily bind to Slp1, and needs to be modified at the kinetochore to allow its rearrangement into anaphase-inhibiting MCC complex (containing Slp1-Mad2-Mad3-Bub3 – Sudakin *et al.* 2001; Hardwick *et al.* 2000; Millband and Hardwick 2002; Sudakin and Yen 2004). Although the structure of Mad3 has yet to be studied, Mad3 is also thought to be required to rearrange into the MCC complex, using the kinetochore as a catalytic site for its modification (Sironi *et al.* 2002; Musacchio and Hardwick 2002). Put together, we postulate that specific hyper-accumulation of Mad2 and Mad3 in $\Delta TOG1$ may be caused by their inability to turnover from the kinetochore in the absence of TOG1.

As TOG1 is only required for maintenance of the spindle checkpoint, our speculation implies that Mad2 and Mad3 turnover is required for checkpoint maintenance but not activation. It has been reported that Mad2 can inhibit APC without localisation to the kinetochore (DeLuca *et al.* 2003; Tournier *et al.* 2004), which suggests that there is a population of Mad2 that can directly bind to Slp1. In support of this, a Mad2-Slp1/Cdc20 complex has been found to exist and able to inhibit APC (Sironi *et al.* 2001; Zhang and Lees 2001; Luo *et al.* 2002).

The second intriguing phenotype observed was the delocalisation of Nuf2 and Ndc80 from the kinetochore only when the spindle is damaged. We have also found that Alp14 binds to Nuf2 through a co-immunoprecipitation assay. From our results, we propose that the TOG domain is required for Nuf2-Alp14 interaction or that Nuf2 directly interacts with the TOG domain. Several studies have shown that unlike other kinetochore complexes, the Nuf2-Ndc80 complex, which includes Nuf2, Ndc80 (also known as Hec1

in higher eukaryotes), Spc24 and Spc25, also functions as a component of the spindle assembly checkpoint (Janke *et al.* 2001; McClelland *et al.* 2004). The requirement of the complex in the spindle assembly checkpoint is highly allele-specific, where different mutations within the same gene can lead to either hyper-activation or inactivation of the checkpoint (Nabetani *et al.* 2001; Meraldi *et al.* 2004). One common effect of these mutants, however, is the delocalisation of specific spindle checkpoint proteins from the kinetochore, suggesting that the Nuf2-Ndc80 complex regulates the localisation of checkpoint proteins. Frog xNdc80 and xNuf2 are required to recruit Mad1, Mad2, Bub1 and Bub3 to the kinetochore (DeLuca *et al.* 2003; McClelland *et al.* 2003 and 2004; Meraldi *et al.* 2004). Similarly, in chicken DT40 cell, Hec1 or Nuf2 depletion causes mitotic arrest with only BubR1 but not Mad2 localisation (Hori *et al.* 2003). In HeLa cells, there are reports that recruitment of hMps1, hMad1 and hMad2 requires hHec1 and hNuf2 (Martin-Lluesma *et al.* 2002). Lastly, depletion of hSpc25 showed a loss of Hec1 and hMad1, while hBub1 and hBubR1 recruitment were retained (Bharadwaj *et al.* 2004). In these studies, localisation of spindle checkpoint proteins can be restored by adding microtubule drugs, suggesting that the Ndc80 complex may function to prevent microtubule-dependent stripping of checkpoint proteins until stable kinetochore is formed (DeLuca *et al.* 2003).

From our results, we postulate a model, which is as follows. Given that the kinetochore acts as catalytic site for the turnover of specific checkpoint proteins, the stability of outer kinetochore proteins is important for the maintenance of the checkpoint. Upon spindle damage, an intact kinetochore is able to activate the spindle assembly checkpoint. However, as the damage persists and the checkpoint is maintained, the kinetochore structure needs to be stabilised to cope with a constant activity of Mad2 and Mad3 turnover. In $\Delta TOG1$, when the spindle is damaged Nuf2 and Ndc80 are delocalised and Mad2 and Mad3 hyper-accumulate at the kinetochore. Taking our results together, we propose that TOG1 is required to stabilise Nuf2 at the kinetochore when spindle is damaged to maintain the spindle assembly checkpoint (fig. 3.5.2). In this model, Alp14 is required for the recruitment or stabilisation of Nuf2 at the kinetochore, which in turn ensures spindle assembly checkpoint proteins to be stably retained at this site. In the absence of TOG1, the outer kinetochore is destabilised, causing unstable localisation of spindle checkpoint proteins and inhibition of APC via Mad2 and Mad3 cannot be maintained.

It is interesting that the delocalisation of Nuf2 in $\Delta TOG1$ only occurs in spindle-damaged condition. An explanation for this could be that Nuf2 becomes delocalised in $\Delta TOG1$ only when the spindle assembly checkpoint is activated due to a high level of protein binding and turnover at the kinetochore during checkpoint activation/maintenance. This implies that Alp14 stabilises Nuf2 during spindle checkpoint maintenance, suggesting that Alp14 may be able to localise to the kinetochore in a microtubule-independent fashion. Another possibility is that Alp14 interacts with Nuf2 in early mitosis, during which both proteins are localised to the SPB-centromere cluster. By binding to Nuf2, Alp14 could localise Nuf2 to the kinetochore, thereby stabilises the kinetochore structure. Nuf2 has been shown to localise to SPBs prior to being transferred onto the kinetochore (Nabetani *et al.* 2001; Appelgren *et al.* 2003). When the inner or central kinetochore is disrupted, for example in *mis12* mutant, the SPB-centromere cluster is abolished, with Nuf2 observed with the SPBs (Asakawa *et al.* 2005).

Separate functions of the two TOG domains

In this study we have determined two different functions of two separate TOG domains, namely the maintenance of the spindle assembly checkpoint which requires the first TOG domain (TOG1), and the stabilisation of microtubules which requires the second TOG domain (TOG2). Although the sequence and structure of the two TOG domains are highly conserved, they perform distinct functions. As TOG domains consist of HEAT repeats, which are protein-protein interaction sites (Neuwald and Hirano 2000), the role of the TOG domains may be determined by the protein that binds to them. In our study, we have found that Alp14 binds to Nuf2 in an asynchronous culture. We suggest that Alp14 may bind to Nuf2 at the N-terminal, possibly at the first TOG domain, as the C-terminal of Alp14 has already been shown to bind to Alp7 and microtubules (Sato *et al.* 2004). This suggestion is also in line with our finding that Nuf2 and Ndc80 are delocalised in the absence of the first TOG domain. However, to clarify the protein-binding properties of TOG1, a binding assay between TOG1 and Nuf2 would need to be carried out. An effort to finding TOG binding partners, for example by TAP-tagging TOG1 and TOG2 or two-hybrid screens, could lead to interesting results which would further elucidate the role of TOG domains.

The role of the TOG2 domain in microtubule-stabilisation is supported by a previous in vitro study in frog, which reports that an N-terminal region of XMAP215 promotes microtubule polymerisation while the C-terminus promotes catastrophe (Popov *et al.* 2001). This suggests that the microtubule role of the TOG domains is conserved, at least between fission yeast and frog. So far we have not determined if the TOG2 domain possess an in vivo protein-binding property. As mentioned earlier, it is possible that the TOG2 domain functions to stabilise microtubules due to its proximity to the C-terminus, which contains a microtubule-binding domain. By its location, it may be that presence of TOG2 enhances the folding of the protein, which allows it to regulate microtubule dynamics.

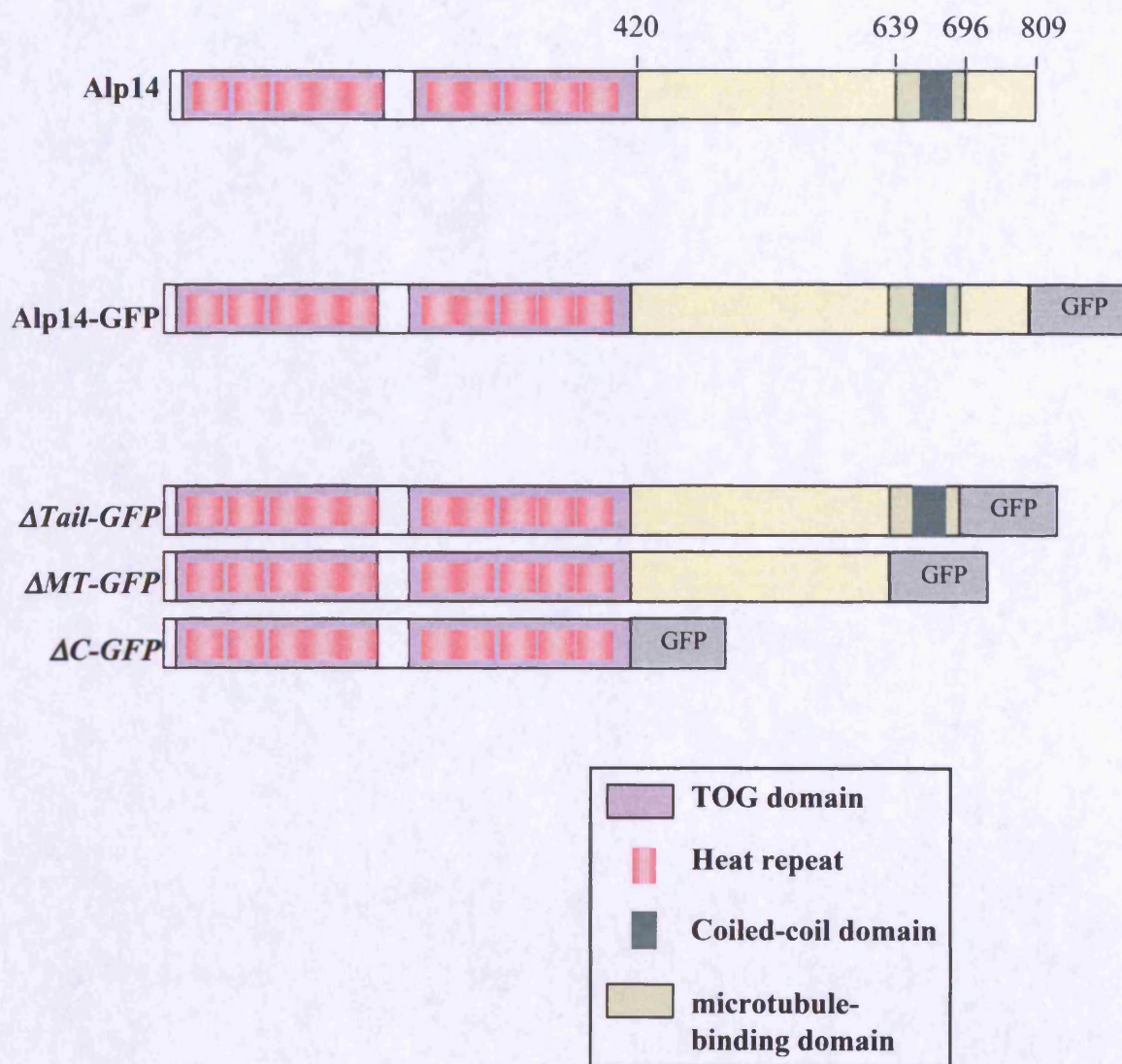


Fig. 3.1.1 Systematic deletion of *alp14*⁺ from the C-terminal. Structural diagram of wild type Alp14 and its deletions from the diverse C-terminal region using GFP. *$\Delta Tail$ -GFP* is the deletion of C-terminal tail at residues 696-809, leaving all known predicted domains intact. *ΔMT -GFP* represents the deletion of residues 639-809 which disposes the predicted microtubule-binding domain. *$\Delta Cter$ -GFP* is the deletion of the entire diverse C-terminal region from 420-809, leaving conserved TOG domains. Not drawn to scale.

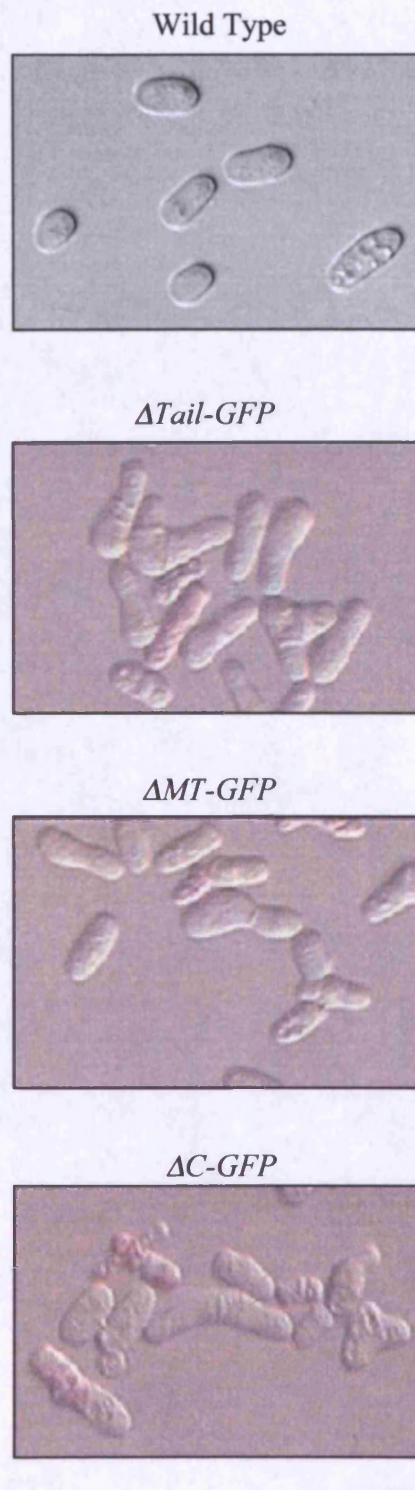
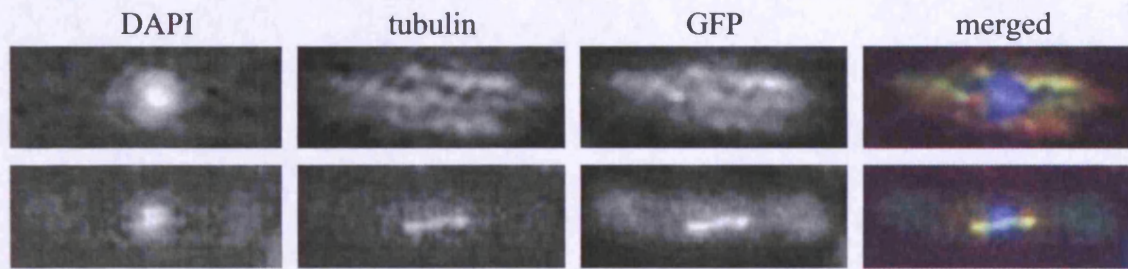
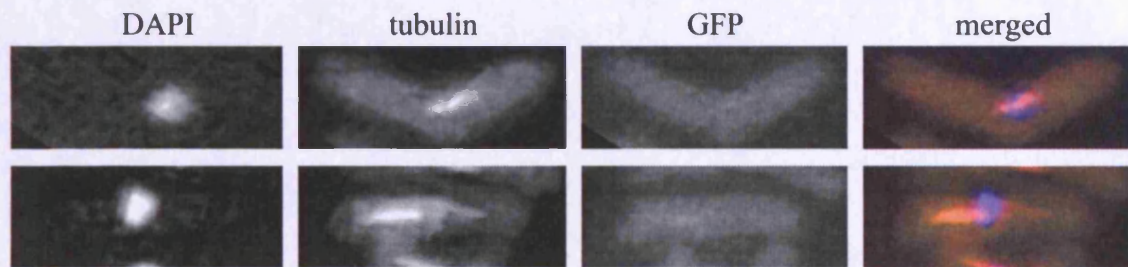


Fig. 3.1.2 Deletion of the C-terminal region of Alp14 results in cell polarity defects. Wild type, $\Delta Tail-GFP$, $\Delta MT-GFP$ and $\Delta C-GFP$ strains were streaked on rich media containing phloxine B and incubated for two days at 36°C. Branched cells indicate polarity defects in this condition. The scale bar represents 10 μ m.

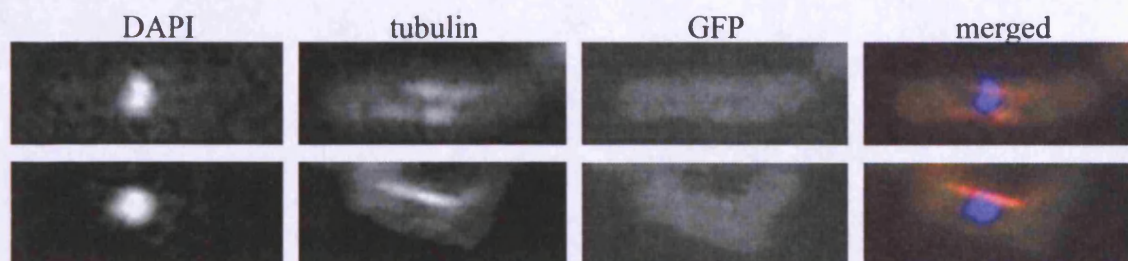
wild type



$\Delta Tail-GFP$



$\Delta MT-GFP$



$\Delta C-GFP$

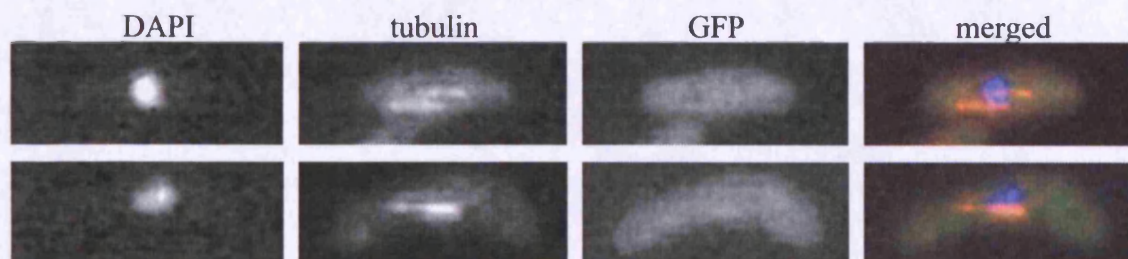


Fig. 3.1.3 The C-terminal region of Alp14 is required for localisation and microtubule function. Wild type *alp14⁺-GFP*, *ΔTail-GFP*, *ΔMT-GFP* and *ΔC-GFP* grown in rich media at 26°C were shifted up to 36°C for six hours and fixed with methanol and processed for immunostaining with anti-α-tubulin antibody. The scale bar represents 10μm.

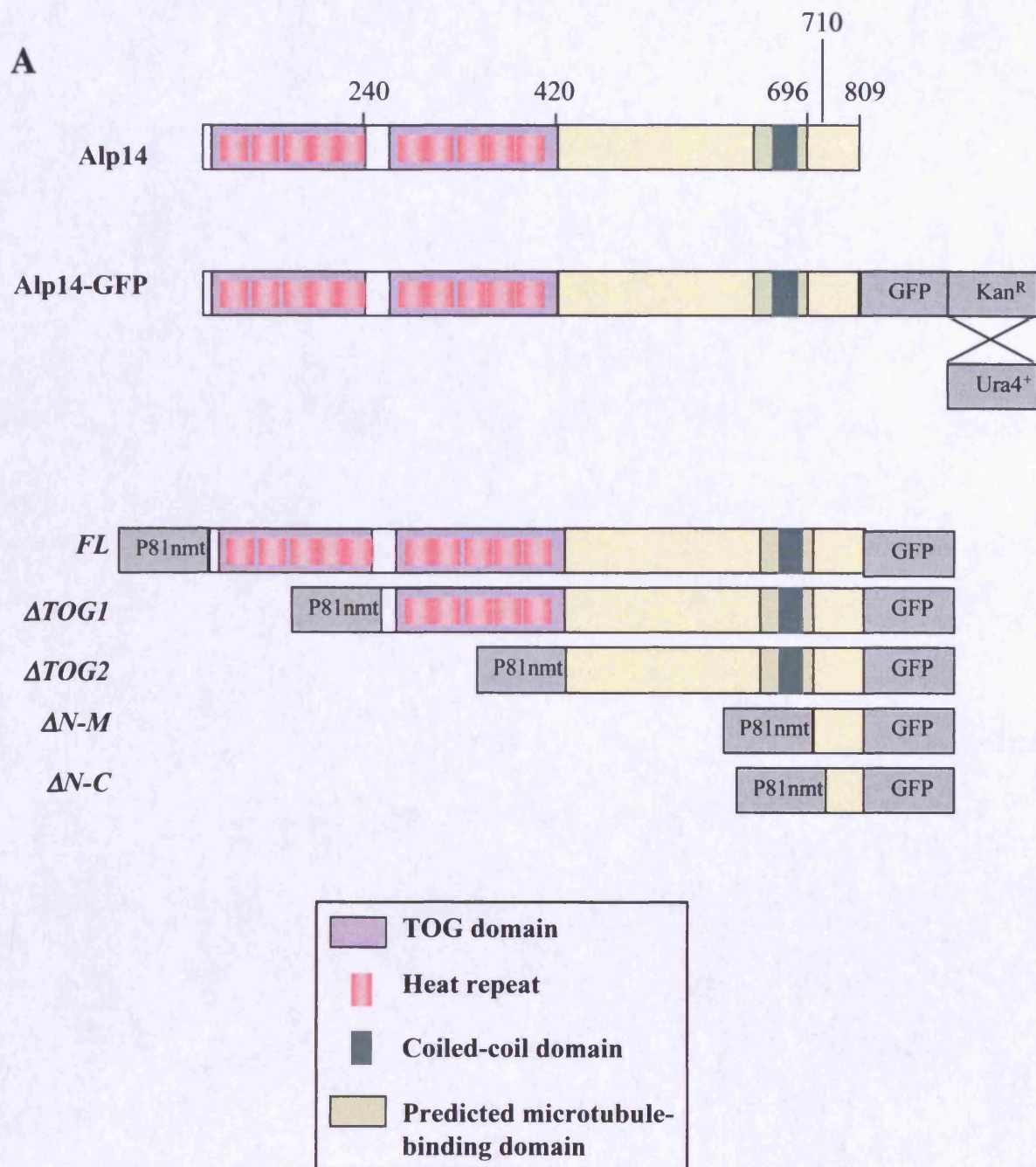
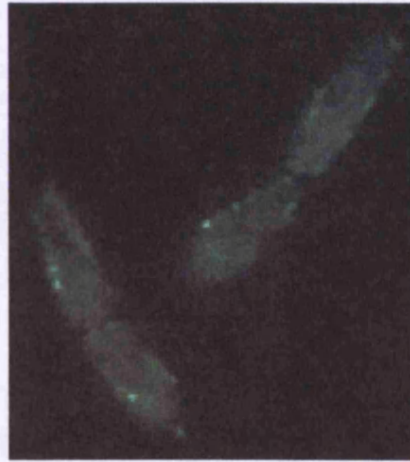


Fig. 3.2.1 A) Systematic deletion of *alp14*⁺ from the N-terminal. Structural diagram of wild type Alp14 and Alp14-GFP, and their deletions from the conserved N-terminal region using an inducible *P81nmt* promoter. *FL* represents full length Alp14 or Alp14-GFP controls expressed from *P81nmt* promoters. *ΔTOG1* is the deletion of the first TOG domain at residues 1-240. *ΔTOG2* is the deletion of residues 1-430, which disposes both TOG domains and the entire conserved N-terminal region. *ΔN-M* represents deletion of residues 1-696, where the entire N-terminal region and the microtubule-binding domain are deleted. *ΔN-C* is the deletion of the N-terminal and most of the C-terminal region, leaving just 100 residues intact. Not drawn to scale.

B

alp14⁺-GFP-Kan^R



alp14⁺-GFP-Kan^R::ura4⁺

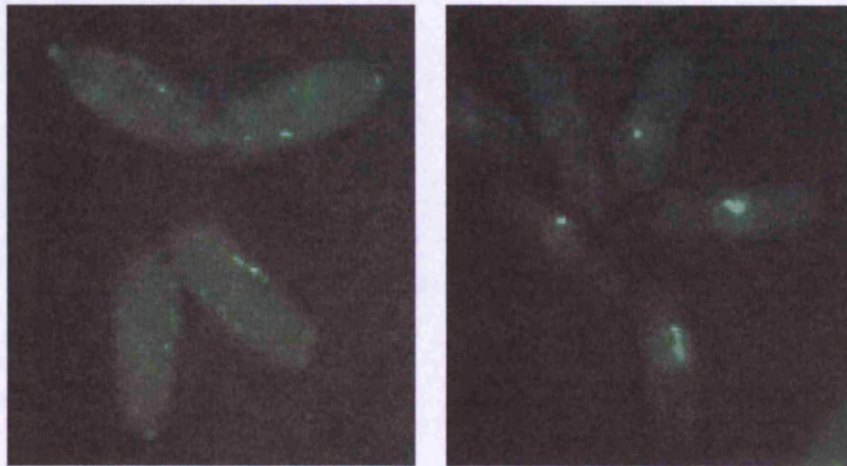


Fig. 3.2.1 B) Exchange of markers on Alp14-GFP does not disrupt Alp14 localisation. Cells containing *alp14⁺-GFP-Kan^R* and *alp14⁺-GFP-Kan^R::ura4⁺* grown on rich media were visualised under live fluorescent microscopy, showing Alp14 localisation in interphase and mitosis. The scale bar represents 10 μ m.

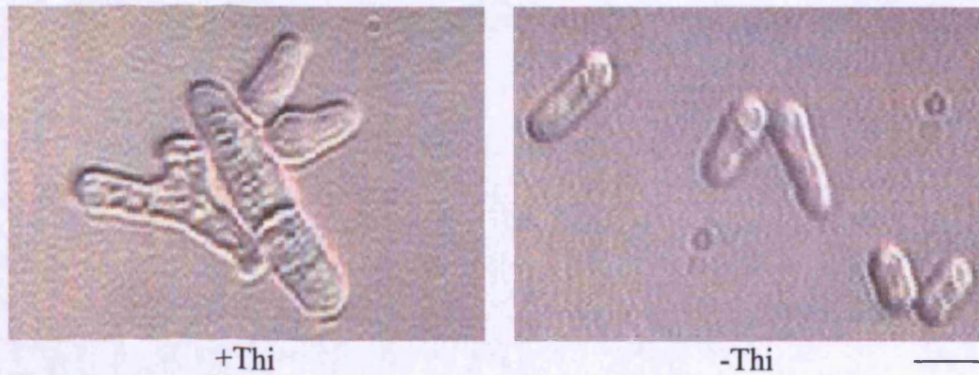
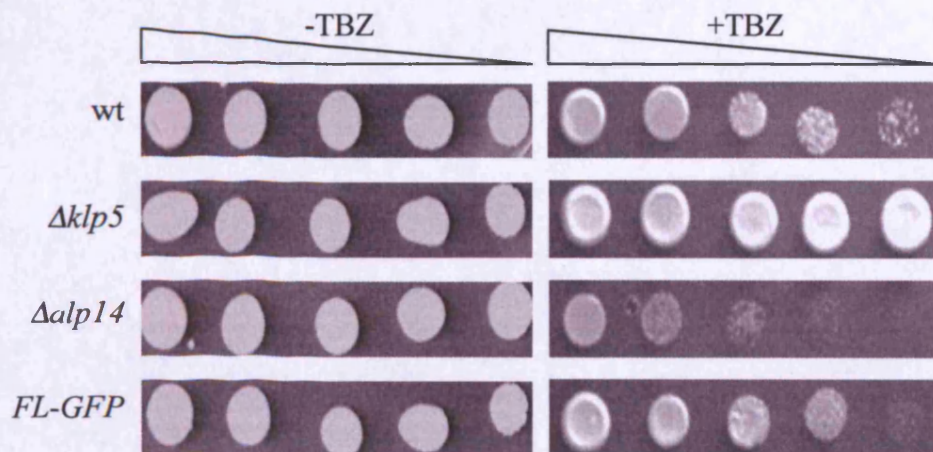
C*FL-GFP***D**

Fig. 3.2.1 C) and D) Full length Alp14 expressed from P81nmt promoter behaves like wild type Alp14. C) *FL-GFP* cells (with Alp14 expressed from a P81nmt promoter) were grown on minimal plates in absence or presence of thiamine for 4 days at the restrictive temperature of 36°C. In presence of thiamine the promoter is shut off, mimicking $\Delta alp14$ condition. In absence of thiamine, Alp14 is produced, mimicking wild type condition. D) Wild type, $\Delta klp5$, $\Delta alp14$ and *FL-GFP* strains were first grown on selective media lacking thiamine then spotted after serial dilution (10^6 to 10^2 cells) on rich plates in absence or presence of TBZ and incubated for 4 days at the permissive temperature of 26°C. The scale bar represents 10 μ m.

E

FL-GFP

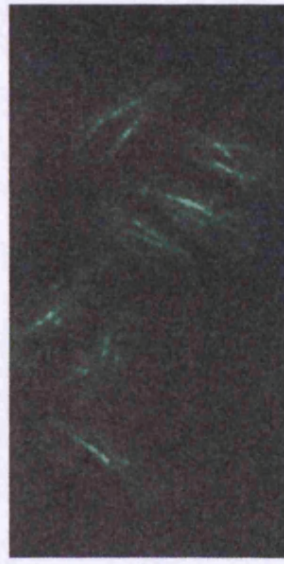


Fig. 3.2.1 E) Full length Alp14-GFP expressed from P81nmt promoter behaves like wild type Alp14. Cells containing *P81nmt-alp14⁺-GFP-Kan^R::ura4⁺* grown on minimal media lacking thiamine were visualised under live fluorescent microscopy. In absence of thiamine, Alp14 is produced, mimicking wild type condition. The scale bar represents 10 μ m.

A

WT Alp14-GFP

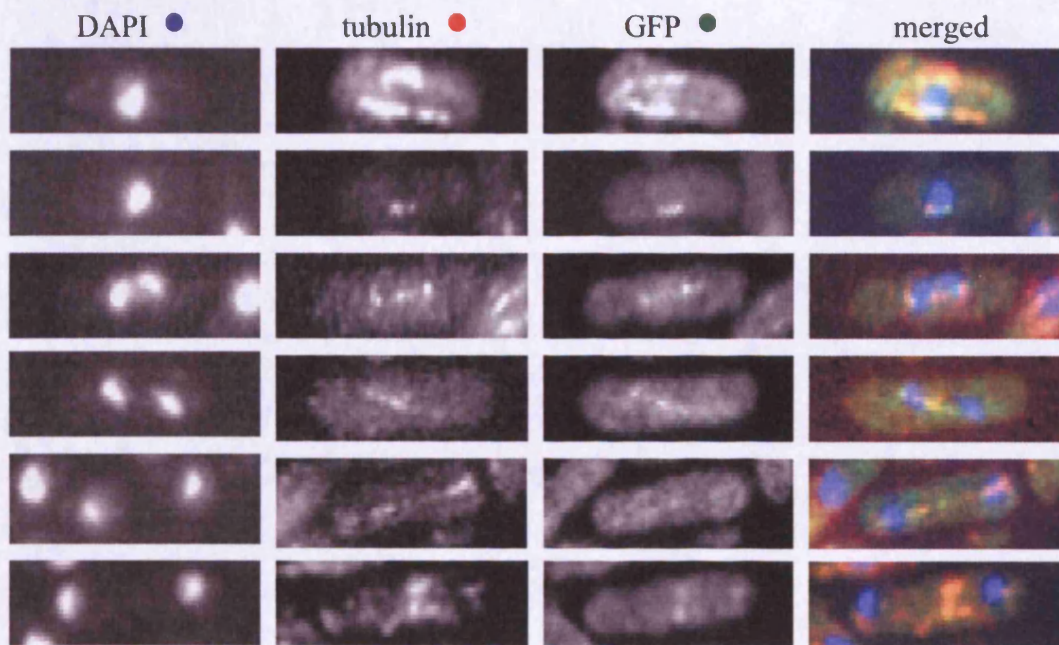
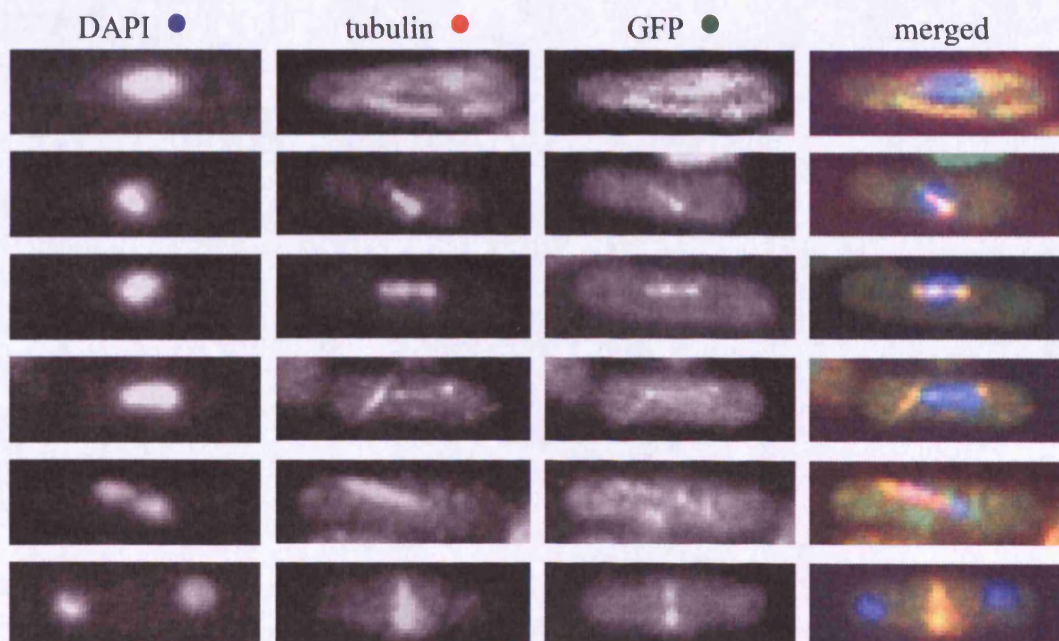
**B***FL-GFP*

Fig. 3.2.2 Localisation and microtubule morphology of *alp14* N-terminal deletions. Cells grown in minimal media in absence of thiamine at 26°C were fixed with methanol and processed for immunostaining with anti- α -tubulin antibody. **A) and B)** Visualisation of wild type Alp14-GFP and *FL-GFP* strains shows wild type microtubule morphology and Alp14 localisation. The scale bar represents 10 μ m. Continues on next pages.

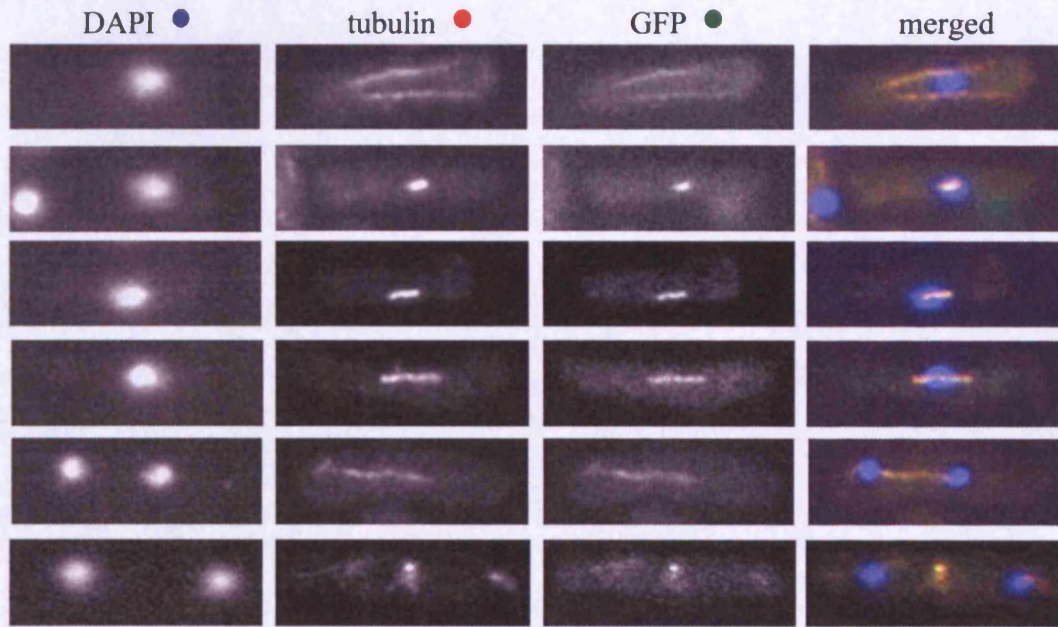
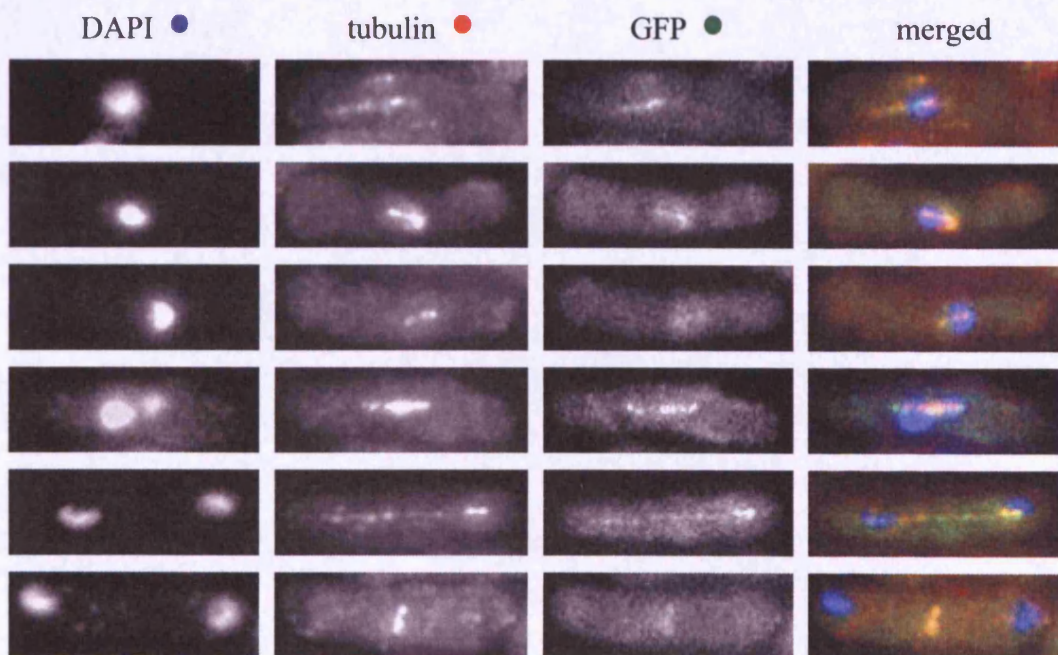
C*ΔTOG1-GFP***D***ΔTOG2-GFP*

Fig. 3.2.2 C) and D) Visualisation of *ΔTOG1-GFP* and *ΔTOG2-GFP* strains. Microtubule morphology is similar to wild type in *ΔTOG1-GFP* but is defective in *ΔTOG2-GFP*. Alp14 localisation remains similar to wild type in both strains. The scale bar represents 10μm. Continues on next page.

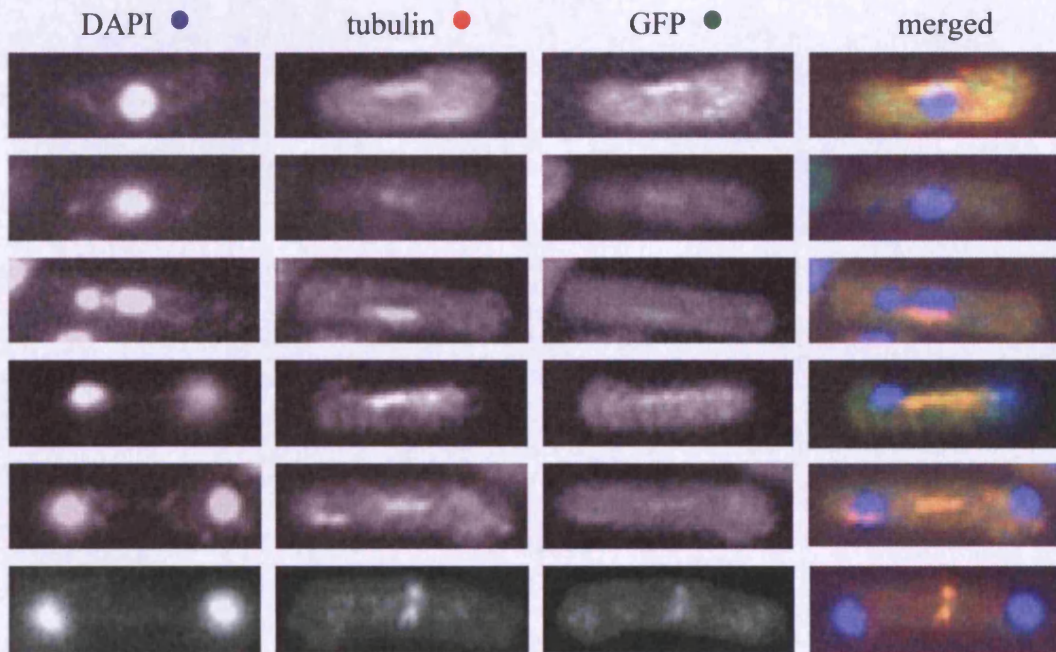
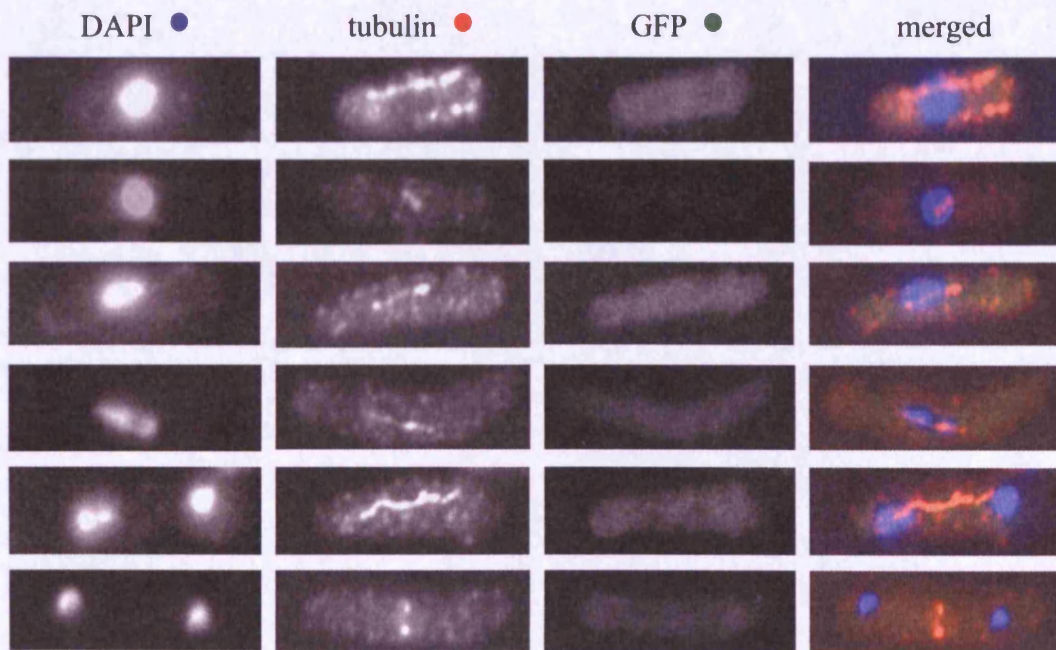
E*ΔN-M-GFP***F***ΔN-C-GFP*

Fig. 3.2.2 E) and F) Visualisation of *ΔN-M-GFP* and *ΔN-C-GFP* strains. *ΔN-M-GFP* and *ΔN-C-GFP* show microtubule defects. Alp14 localisation is weak in *ΔN-M-GFP* and is abolished in *ΔN-C-GFP*. The scale bar represents 10μm.

A

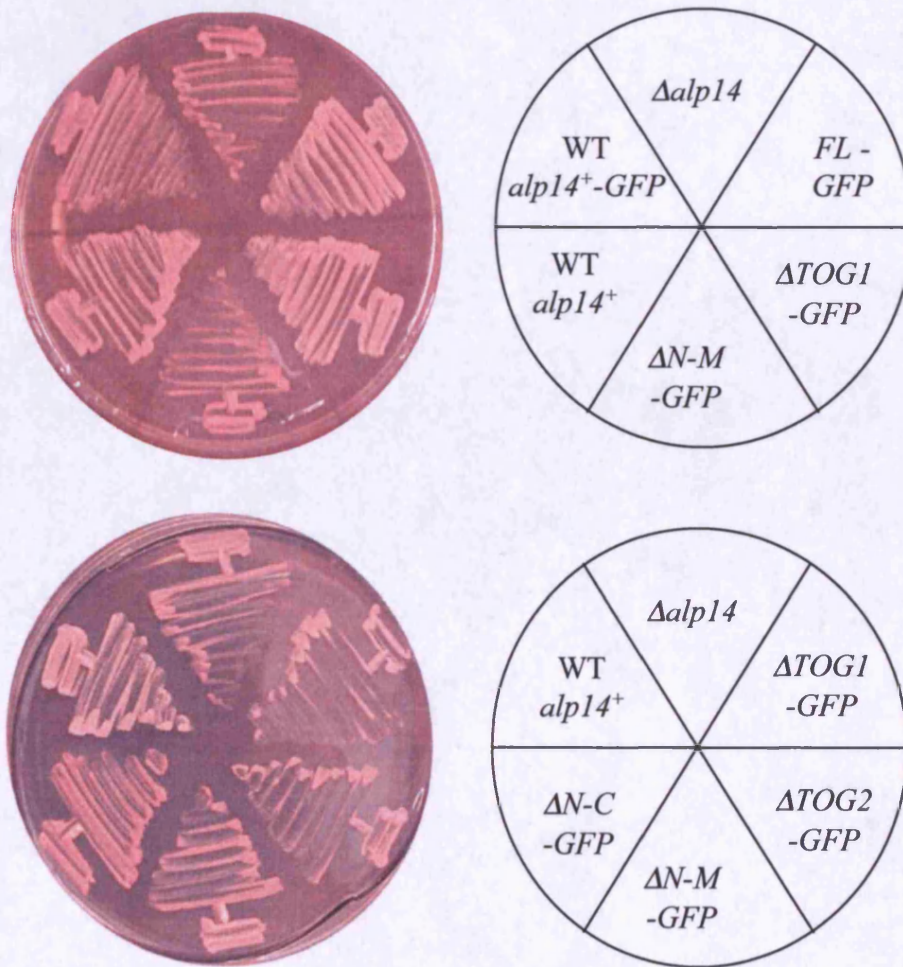
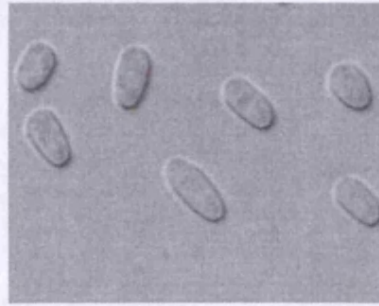


Fig. 3.2.3 Temperature-sensitivity and microtubule function of *alp14* N-terminal deletions. A) Wild type, $alp14^+-GFP$, $\Delta alp14$, FL-GFP, $\Delta TOG1-GFP$, $\Delta TOG2-GFP$, $\Delta N-M-GFP$ and $\Delta N-C-GFP$ strains were streaked on minimal media containing phloxine B and incubated for two days at 36°C. Red colonies are indicative of temperature-sensitivity in this condition. Continues next page.

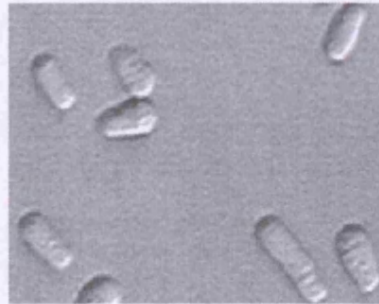
B

36°C

FL-GFP



ΔTOG1-GFP



ΔTOG2-GFP



ΔN-M-GFP



ΔN-C-GFP



Fig. 3.2.3 B) *FL-GFP*, *ΔTOG1-GFP*, *ΔTOG2-GFP*, *ΔN-M-GFP* and *ΔN-C-GFP* strains were streaked on minimal media at 36°C for 1 day and visualised. The scale bar represents 10μm.

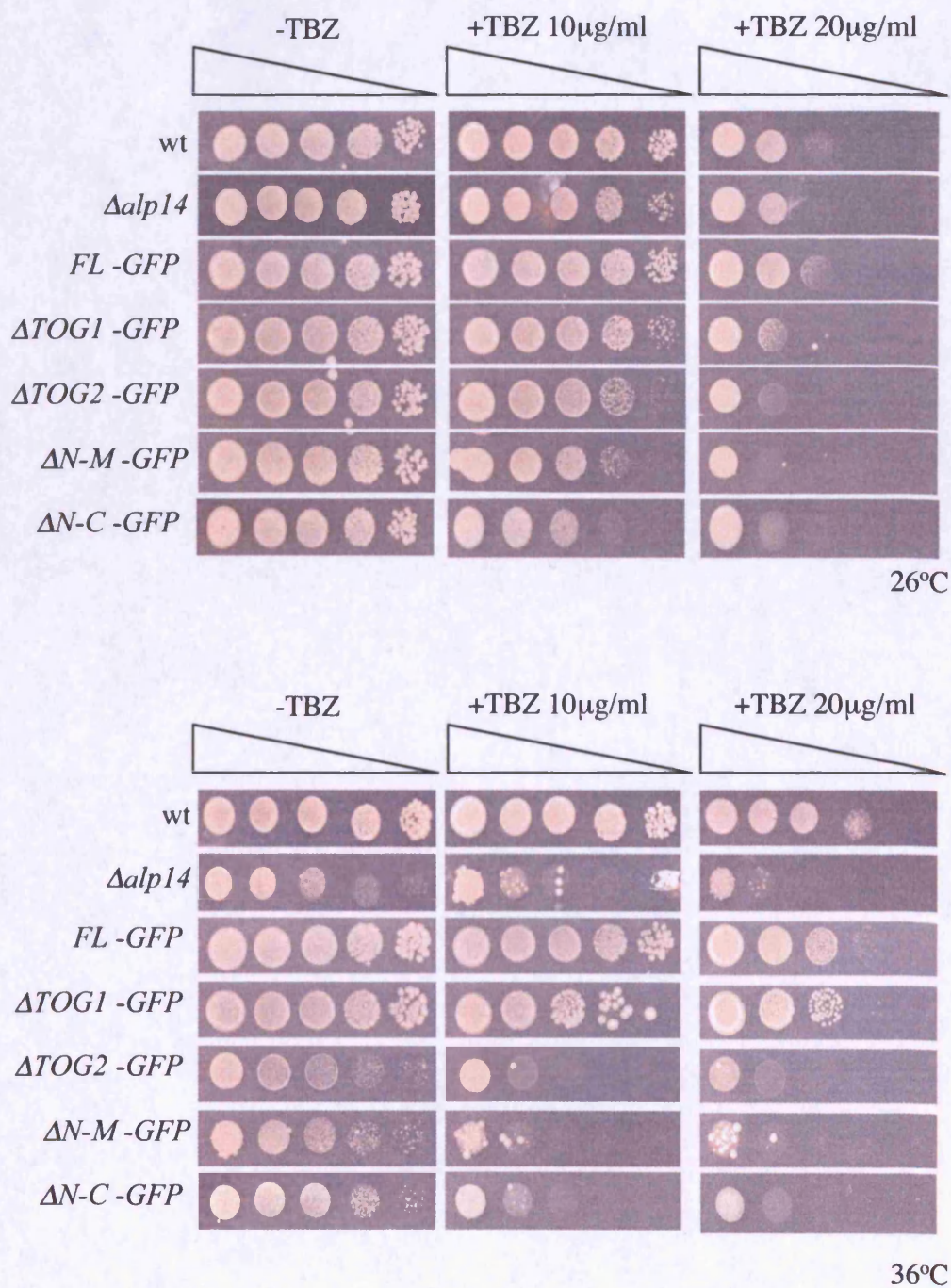


Fig. 3.2.4 TBZ-sensitivity of *alp14* N-terminal deletions. Wild type, $\Delta alp14$, FL-GFP, $\Delta TOG1$ -GFP, $\Delta TOG2$ -GFP, $\Delta N-M$ -GFP and $\Delta N-C$ -GFP strains were grown on minimal media lacking thiamine then spotted after serial dilution (10^6 to 10^2 cells) on rich plates in the absence or presence of 10 or 20μg/ml TBZ for 2-4 days at 26°C (top panels) and 36°C (bottom panels).

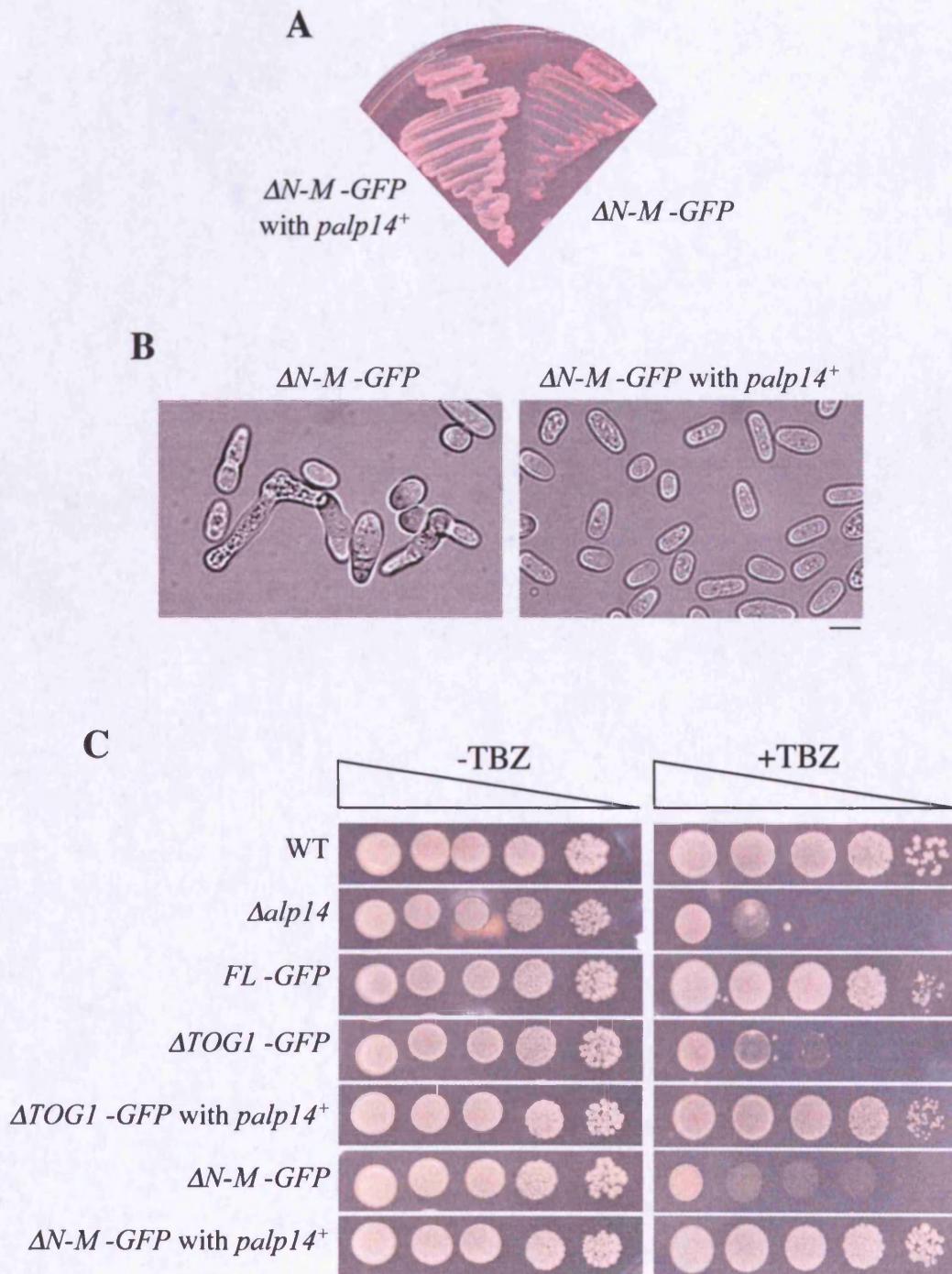


Fig. 3.2.5 Introduction of *palp14*⁺ abolishes the temperature- and TBZ-sensitivity of *alp14* N-terminal deletions. A) and B) $\Delta N-M-GFP$ with *palp14*⁺ and $\Delta N-M-GFP$ cells were streaked on minimal media containing phloxine B and incubated for two days at 36°C (A) and visualised by light microscopy (B). C) Wild type, $\Delta alp14$, FL-GFP, $\Delta TOG1-GFP$, $\Delta TOG1-GFP$ with *palp14*⁺, $\Delta N-M-GFP$ and $\Delta N-M-GFP$ with *palp14*⁺ strains were grown on minimal media lacking thiamine then spotted after serial dilution (10^6 to 10^2 cells) on rich plates in the absence or presence of 10 μ g/ml TBZ for 2-4 days at 26°C. The scale bar represents 10 μ m.

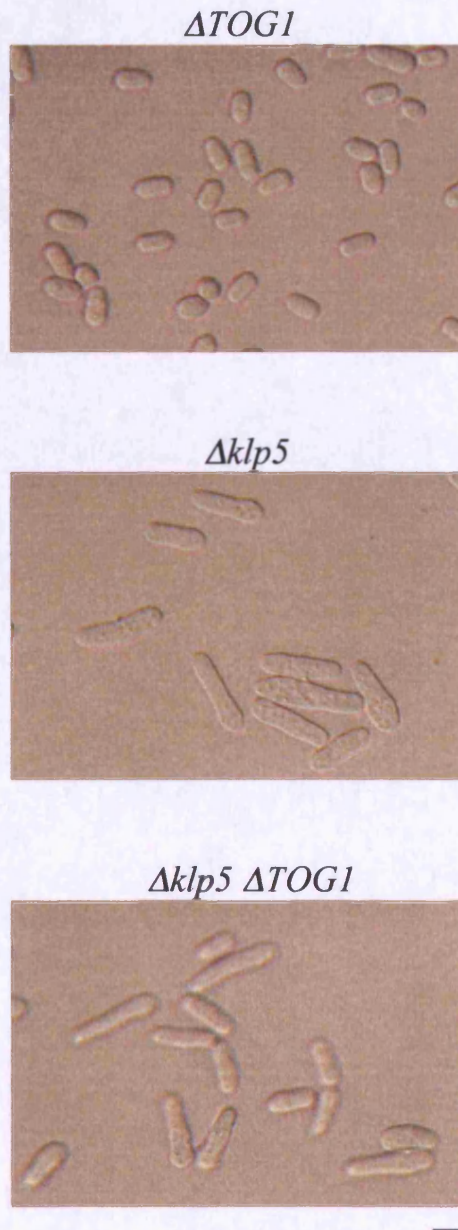


Fig. 3.3.1 $\Delta TOG1$ does not exhibit microtubule defects. *$\Delta TOG1$* , *$\Delta klp5$* and *$\Delta klp5 \Delta TOG1$* cells were streaked on minimal media in absence of thiamine 2 days at 27°C and visualised by light microscopy. *$\Delta klp5 \Delta TOG1$* does not show additive phenotype of *$\Delta klp5$* and *ΔTOG* , confirming that *ΔTOG* does not exhibit microtubule defects. The scale bar represents 10 μ m.

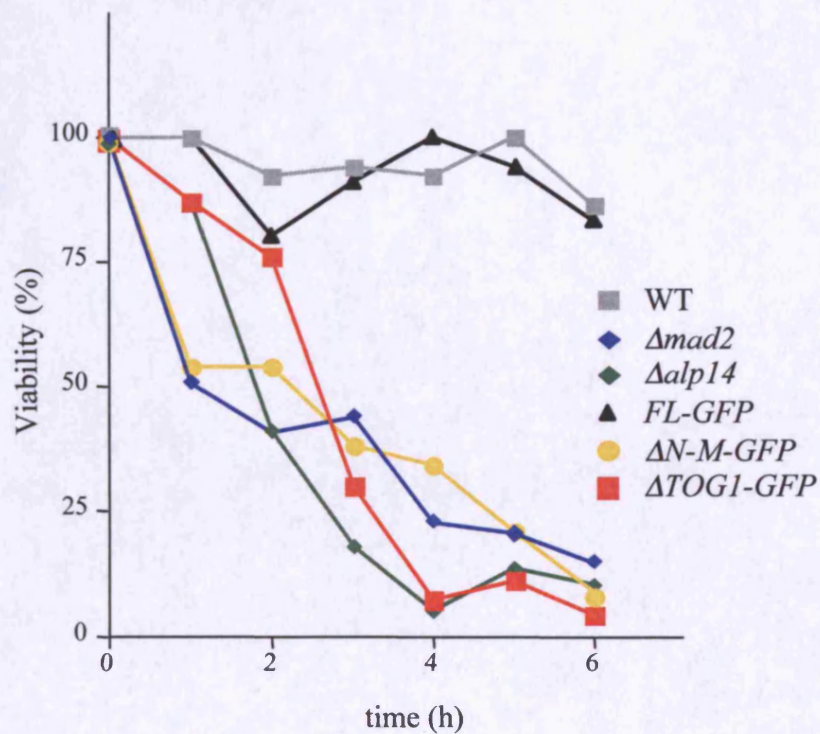
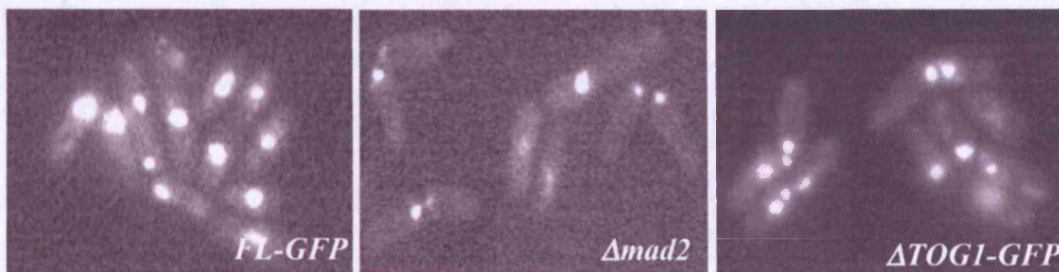
A**B**

Fig. 3.3.2 The first TOG domain of Alp14 is required for the spindle assembly checkpoint pathway. **A)** 50 μg/ml TBZ was added to wild type, $\Delta mad2$, $\Delta alp14$, *FL-GFP*, $\Delta N-M-GFP$ and $\Delta TOG1-GFP$ cells grown in minimal media lacking thiamine and incubated for up to 6 hours. Samples were taken hourly and plated onto fresh media at 200 cells per plate and incubated at 26°C for three days. Percentage of viability was determined by the number of colonies grown. **B)** Cells exposed to TBZ for 3 hours were fixed with formaldehyde and stained with DAPI. Like $\Delta mad2$, $\Delta TOG1-GFP$ displays cut cells, indicating that the spindle assembly checkpoint is defective in this mutant. The scale bar represents 10 μm.

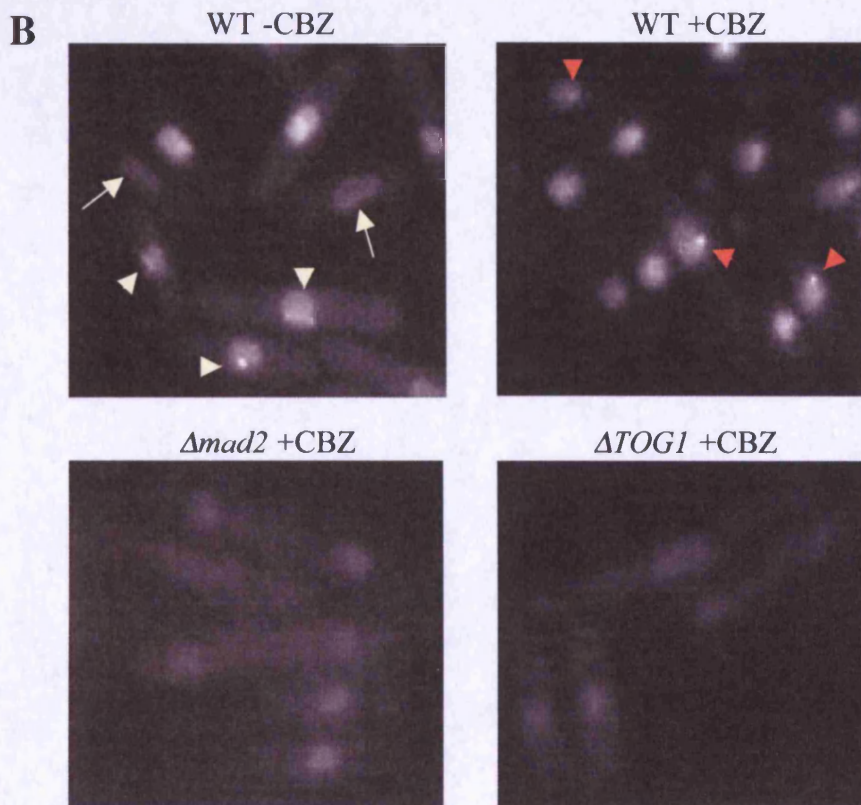
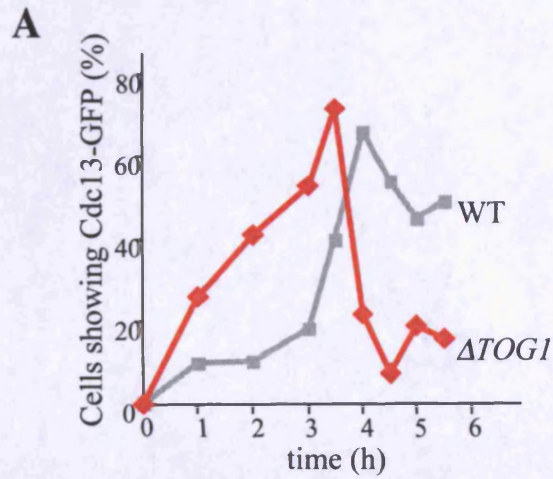


Fig. 3.3.3 Cyclin B is degraded prematurely in $\Delta TOG1$ in presence of TBZ. Wild type, $\Delta mad2$, and $\Delta TOG1$ cells containing Cdc13-GFP were grown in minimal media lacking thiamine, synchronised in HU for 4 hours at 27°C, washed out and resuspended in fresh HU-free minimal media in presence or absence of 50 μ g/ml CBZ for up to 6 hours. **A)** Samples of wild type and $\Delta TOG1$ cells in CBZ were counted for cells containing Cdc13-GFP signal. **B)** Cells at 4 hours after HU release in presence or absence of CBZ. White arrow heads and arrows show Cdc13-GFP localisation in normal mitosis and its degradation upon anaphase onset, respectively. Red arrow head shows Cdc13-GFP staining at SPBs in spindle damaged condition. The scale bar represents 10 μ m.

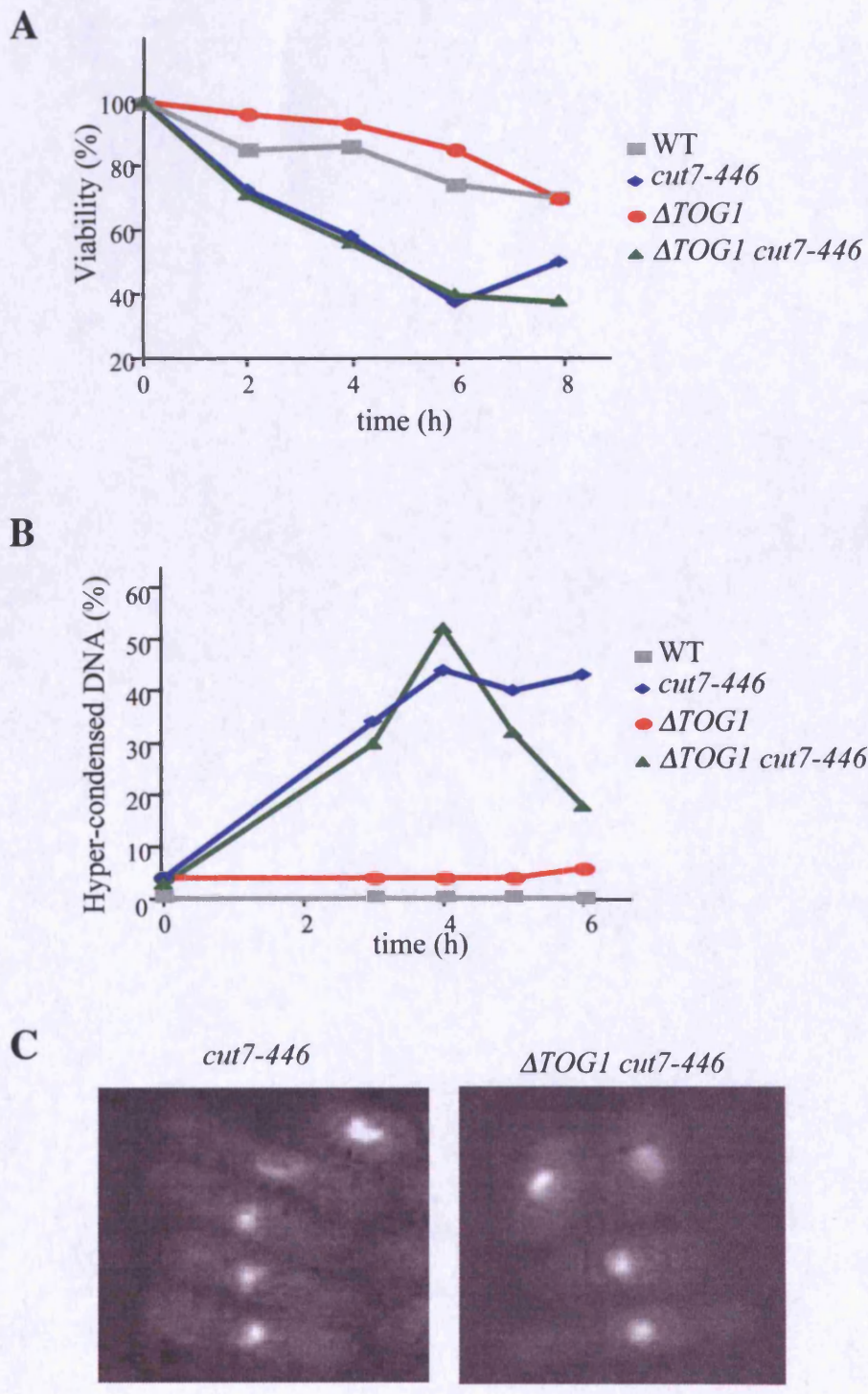


Fig. 3.3.4 The first TOG domain of Alp14 is required for the spindle assembly checkpoint pathway. Wild type, *cut7-446*, $\Delta TOG1$ and $\Delta TOG1 cut7-446$ cells grown in minimal media lacking thiamine at 26°C were shifted up to 36°C for up to 8 hours. **A)** Samples taken every two hours after temperature shift were plated onto fresh media at 200 cells per plate and incubated at 26°C for three days. Percentage of viability was determined by the number of colonies grown. **B)** Samples taken hourly from 3-6 hours were fixed with formaldehyde and stained with DAPI. Cells displaying hyper-condensed DNA were counted. **C)** DAPI-stained cells at 6 hours after shift up. The scale bar represents 10 μ m.

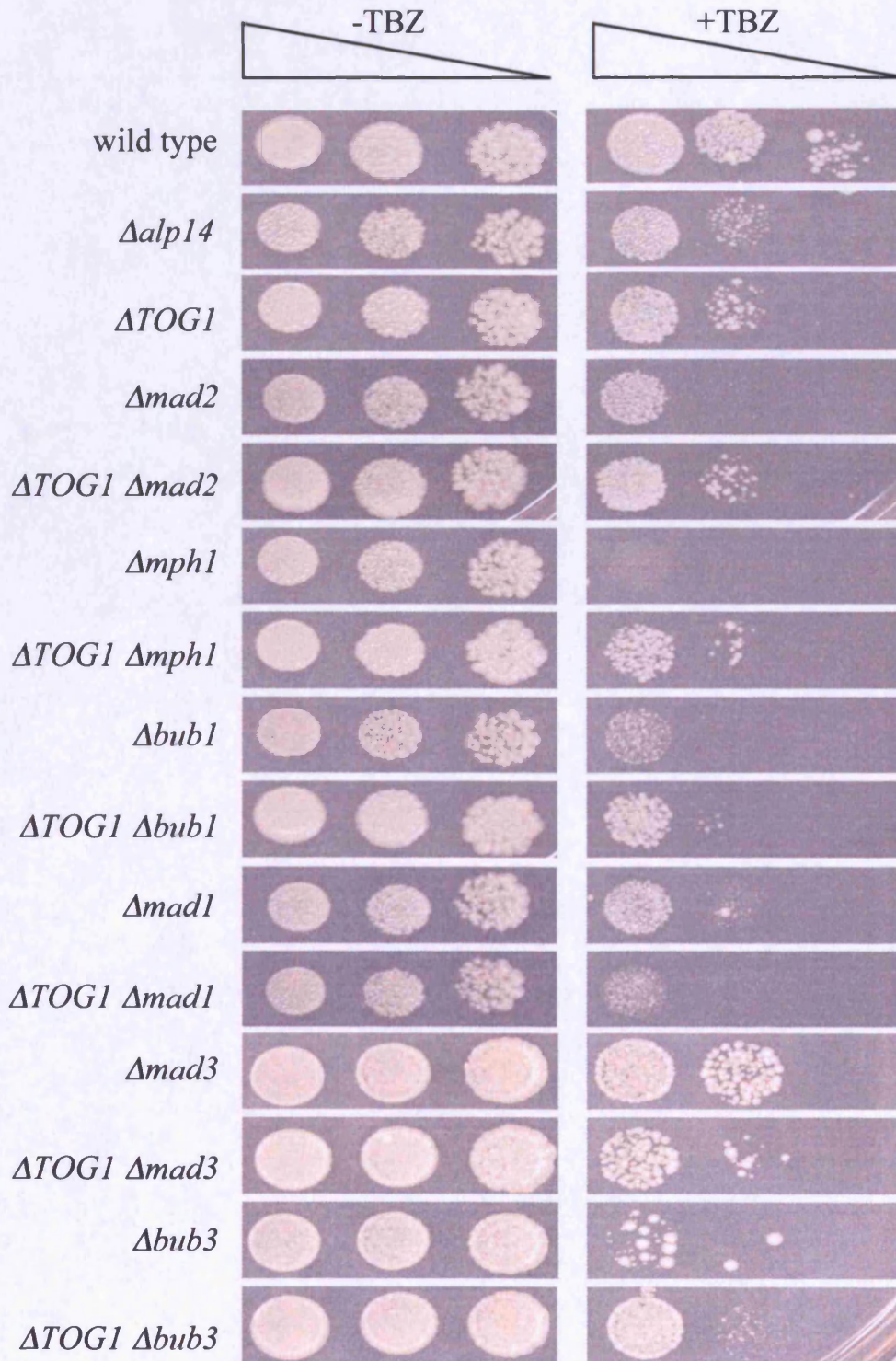
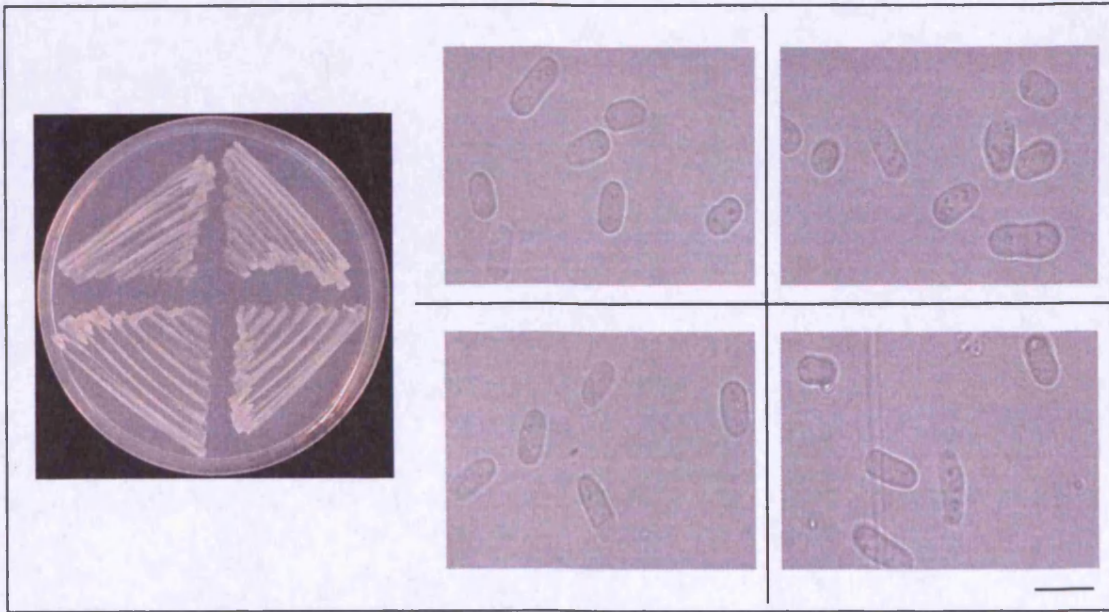


Fig. 3.3.5 Simultaneous deletions of spindle checkpoint proteins and TOG1 display non-additive phenotype in TBZ. Wild type, $\Delta alp14$, $\Delta TOG1$, $\Delta mad2$, $\Delta TOG1 \Delta mad2$, $\Delta mph1$, $\Delta TOG1 \Delta mph1$, $\Delta bub1$, $\Delta TOG1 \Delta bub1$, $\Delta mad1$, $\Delta TOG1 \Delta mad1$, $\Delta mad3$, $\Delta TOG1 \Delta mad3$, $\Delta bub3$ and $\Delta TOG1 \Delta bub3$ strains were grown in minimal media lacking thiamine then spotted after serial dilution (10^5 to 10^2 cells) on rich plates in the absence or presence of 20 μ g/ml TBZ for 4 days at 26°C.

WT + <i>pREP41x</i> <i>-mad2⁺</i>	Δ <i>TOG1</i> + <i>pREP41x</i> <i>-mad2⁺</i>
WT + <i>pREP3x</i> <i>-mph1⁺</i>	Δ <i>TOG1</i> + <i>pREP3x</i> <i>-mph1⁺</i>

+Thi



-Thi

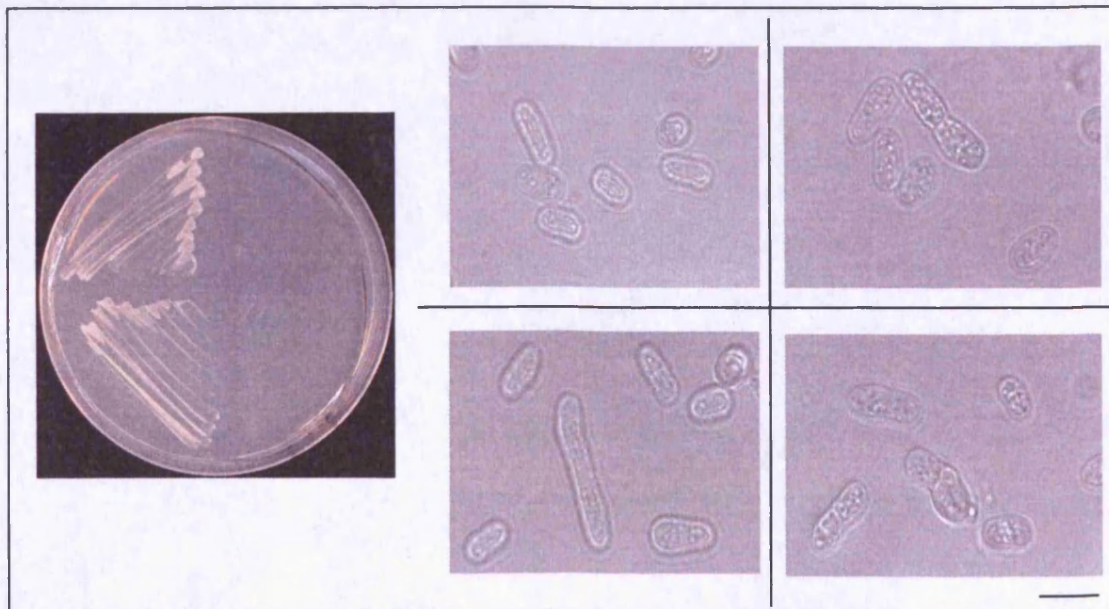


Fig. 3.3.6 Overproduction is toxic in Δ *TOG1*. Wild type and Δ *TOG1* cells transformed with vectors containing *mad2⁺* and *mph1⁺* overexpressed by *P3nmt* or *P41nmt* promoters were streaked onto minimal media in presence or absence of thiamine at 26°C for 2 days. The scale bar represents 10 μ m.

A

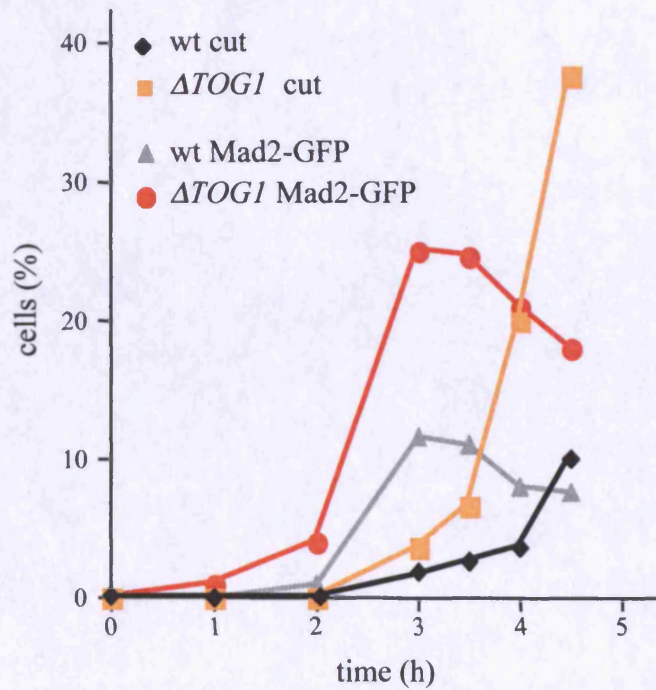
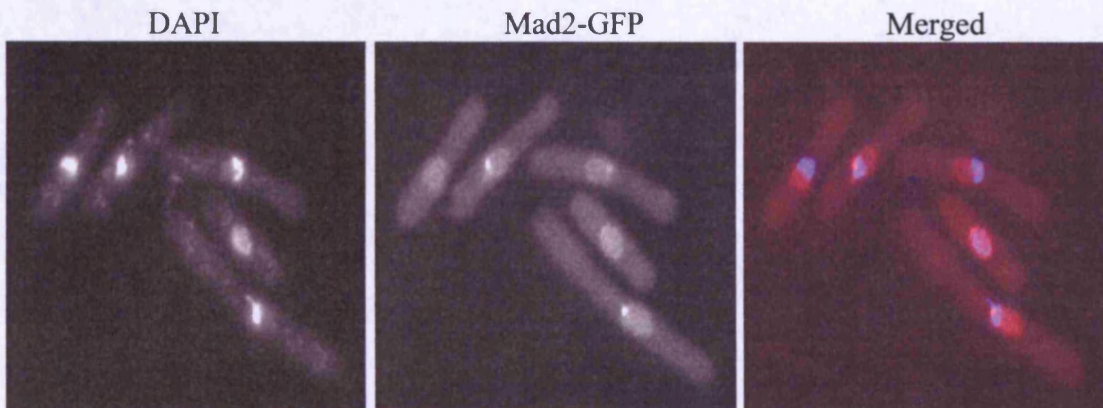


Fig. 3.3.7 Mad2 accumulates at $\Delta TOG1$ kinetochores when spindle is damaged. Wild type and $\Delta TOG1$ cells carrying *mad2*⁺-GFP were grown in minimal media lacking thiamine, synchronised in HU for 4 hours at 27°C, washed out and resuspended in fresh minimal media in presence of 50 μ g/ml CBZ for up to 5 hours. Samples were fixed with formaldehyde and stained with DAPI. A) The number of cells showing cut phenotype and those showing strong Mad2-GFP dots in metaphase were counted at each time point. Continues next page.

B

Wild type



ΔTOG1

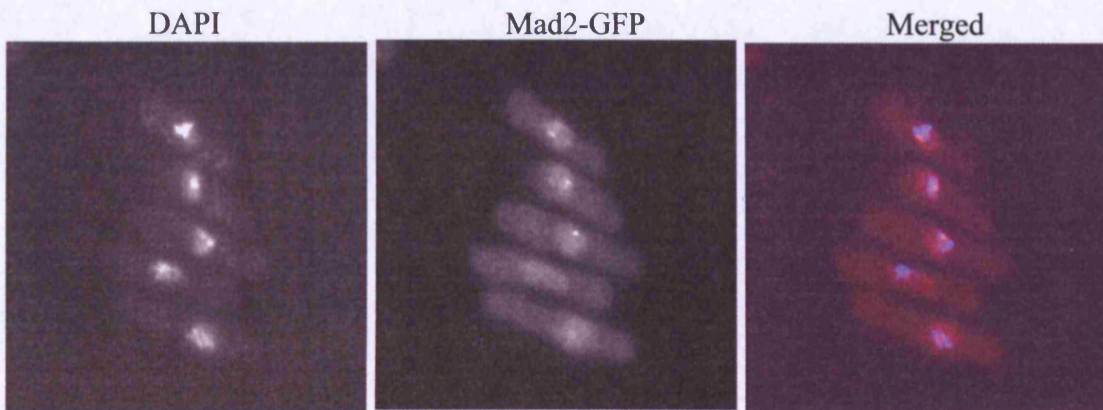


Fig. 3.3.7 B) Wild type and *ΔTOG1* cells showing strong Mad2-GFP dots in metaphase after 3.5 hours in microtubule drug CBZ. The scale bar represents 10 μ m.

A

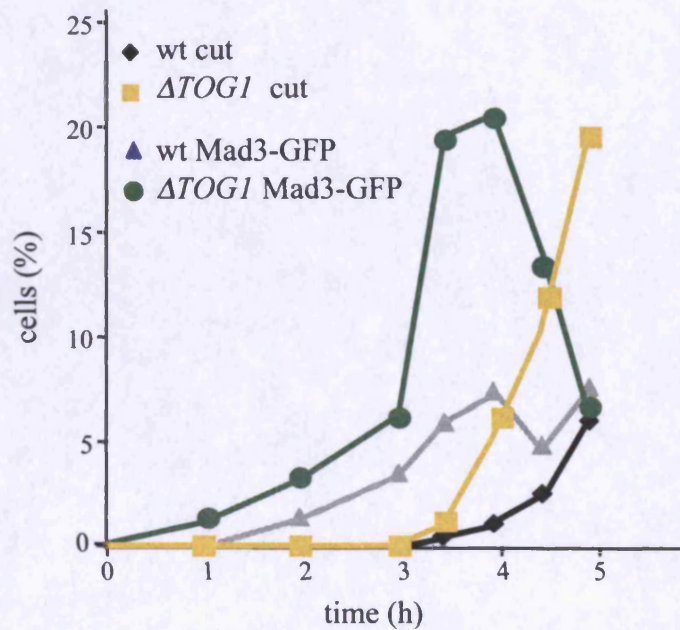
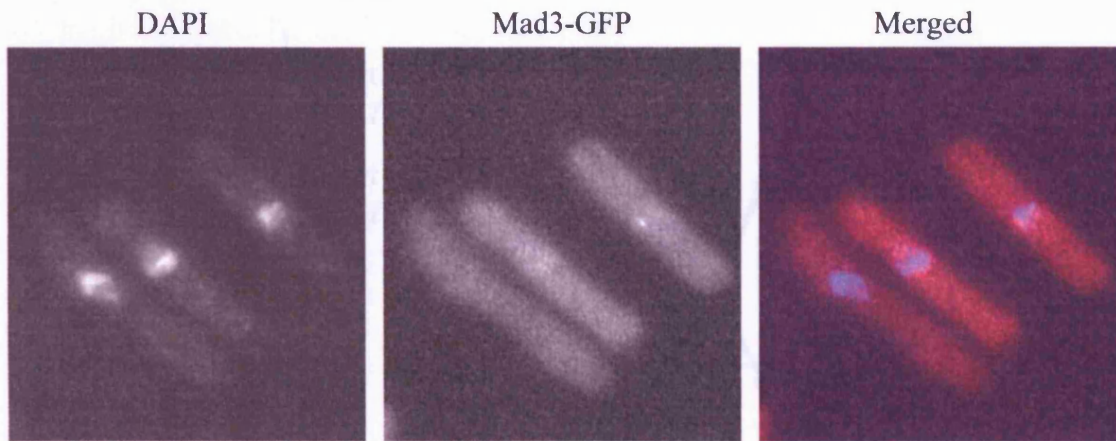


Fig. 3.3.8 Mad3 accumulates at $\Delta TOG1$ kinetochores when spindle is damaged. Wild type and $\Delta TOG1$ cells carrying *mad3*⁺-GFP were grown in minimal media lacking thiamine, synchronised in HU for 4 hours at 27°C, washed out and resuspended in fresh minimal media in presence of 50 μ g/ml CBZ for up to 5 hours. Samples were fixed with formaldehyde and stained with DAPI. A) The number of cells showing cut phenotype and those showing strong Mad3-GFP dots in metaphase were counted at each time point. Continues next page.

B

Wild type



ΔTOG1

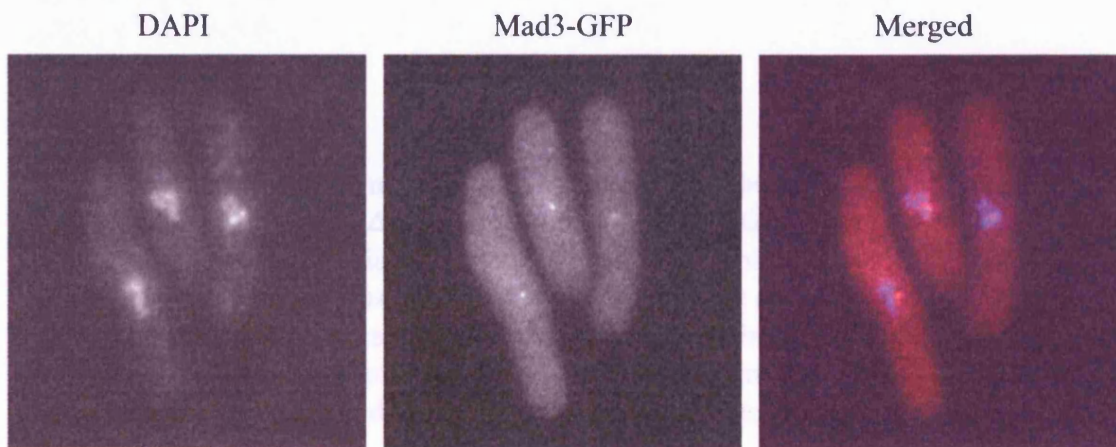


Fig. 3.3.8 B) Wild type and *ΔTOG1* cells showing strong Mad3-GFP dots in metaphase after 4 hours in microtubule drug CBZ. The scale bar represents 10 μ m.

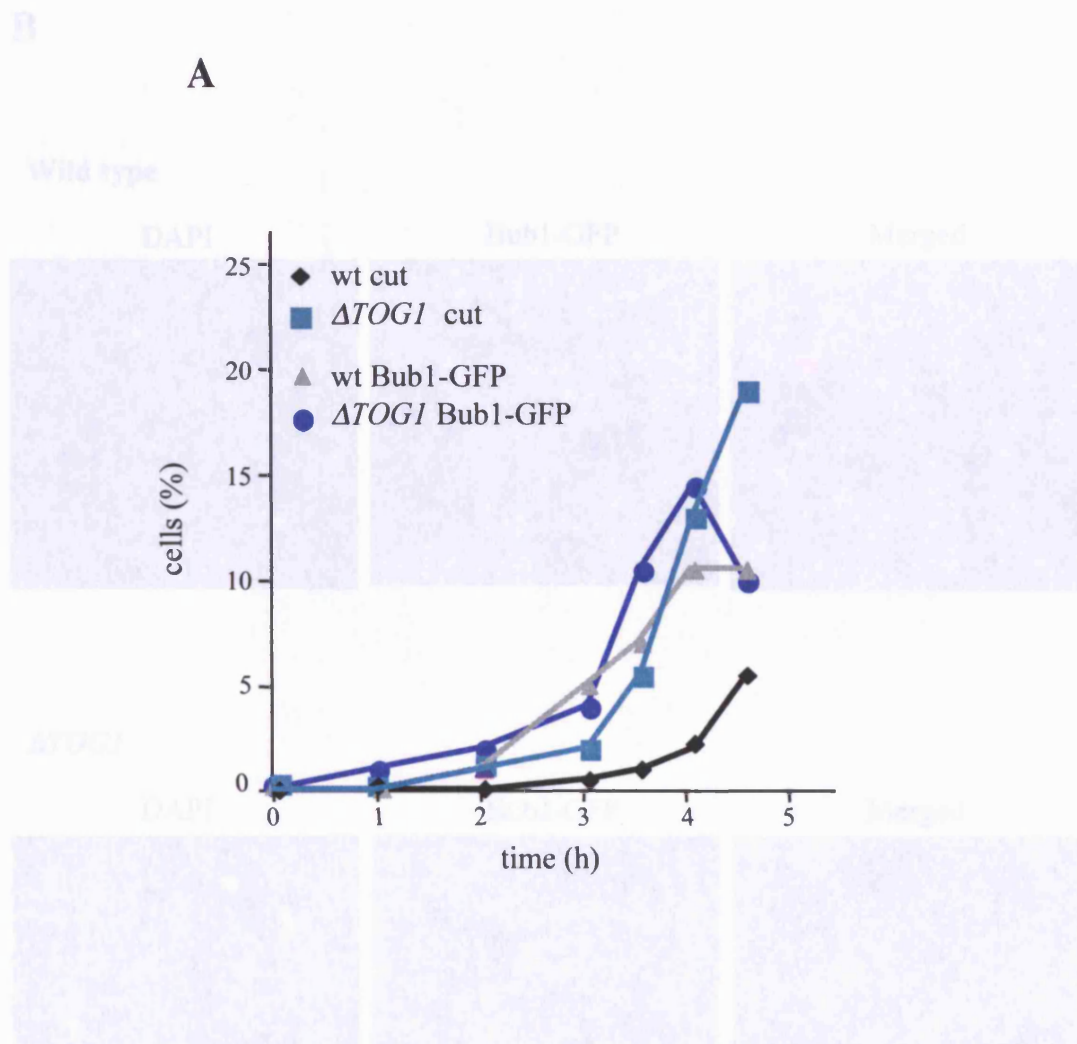
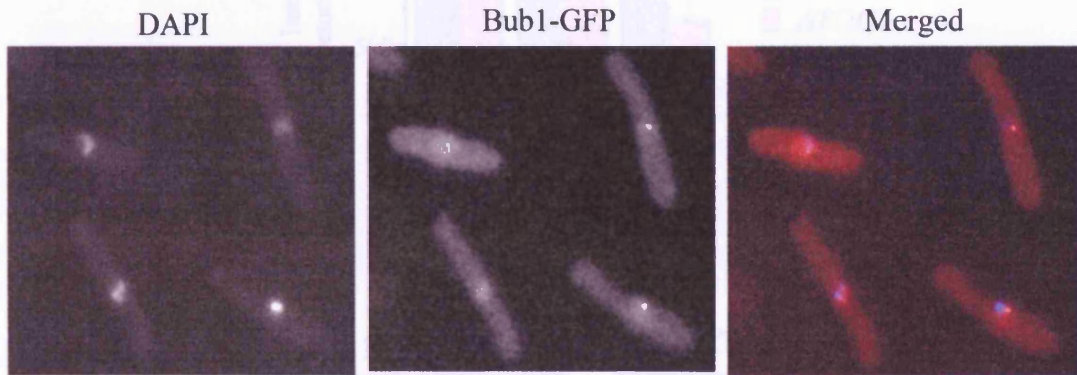


Fig. 3.3.9 Bub1 localises normally at $\Delta TOG1$ kinetochores when spindle is damaged. Wild type and $\Delta TOG1$ cells carrying $Bub1^+$ -GFP were grown in minimal media lacking thiamine, synchronised in HU for 4 hours at 27°C, washed out and resuspended in fresh minimal media in presence of 50 μ g/ml CBZ for up to 5 hours. Samples were fixed with formaldehyde and stained with DAPI. **A)** The number of cells showing cut phenotype and those showing strong Bub1-GFP dots in metaphase were counted at each time point. Continues next page.

B

Wild type



ΔTOG1

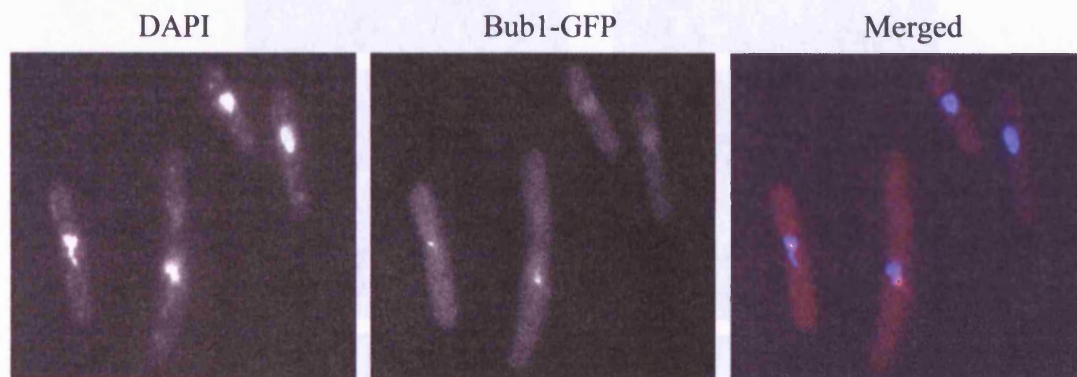


Fig. 3.3.9 B) Wild type and *ΔTOG1* cells showing strong Bub1-GFP dots in metaphase after 4 hours in microtubule drug CBZ. The scale bar represents 10 μ m.

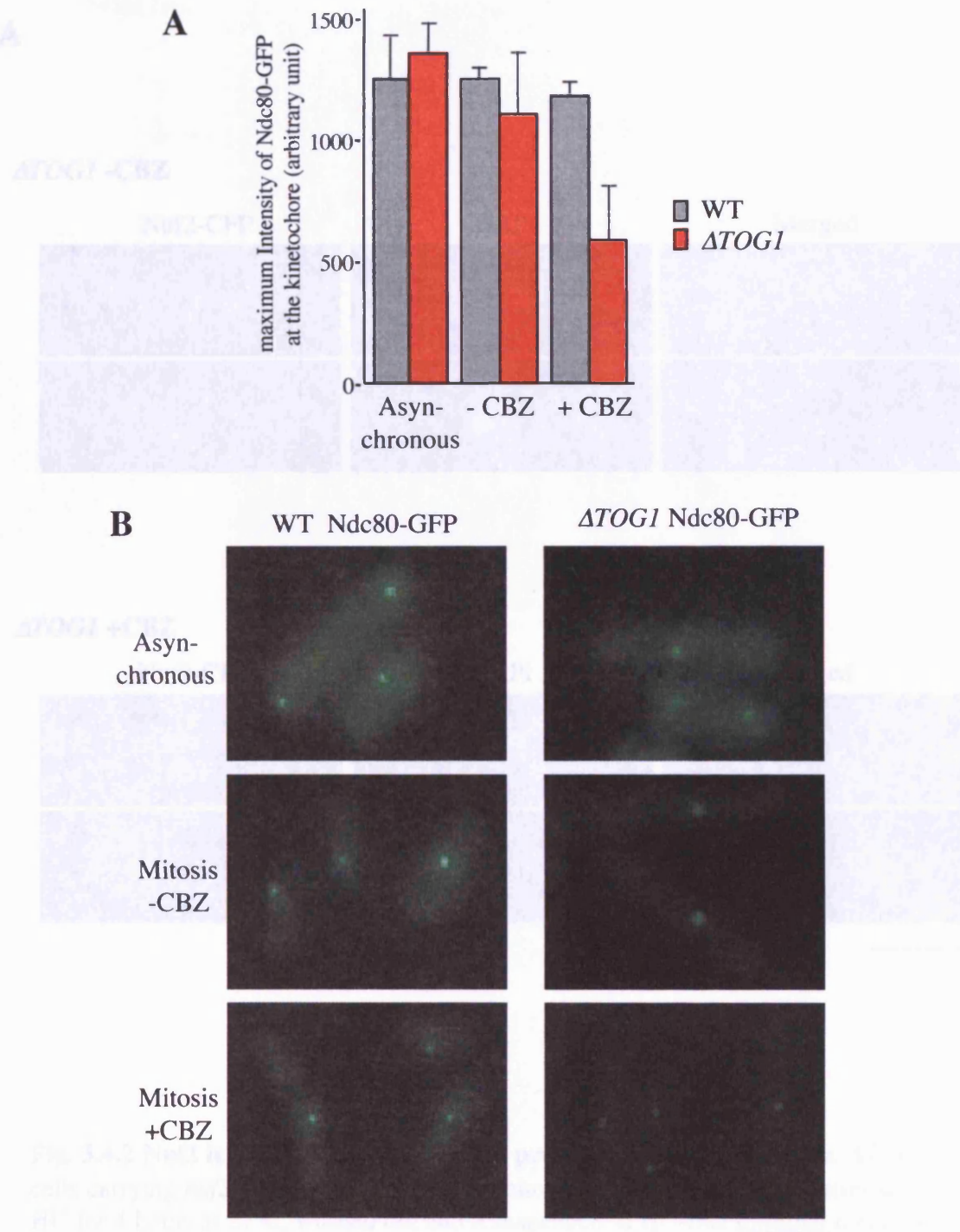


Fig. 3.4.1 Ndc80 is delocalised in $\Delta TOG1$ in presence of spindle damage. Wild type and $\Delta TOG1$ cells carrying *ndc80⁺-GFP* were grown in minimal media lacking thiamine. A sample of asynchronous cells was taken, while other samples were synchronised in HU for 4 hours at 27°C, washed out and resuspended in selective media in presence or absence of 50 μ g/ml CBZ for 3 hours. All samples were fixed with formaldehyde and stained with DAPI. Maximum intensities of Ndc80-GFP dot at the kinetochore in each sample were visualised and measured using the Improvion Velocity program. Note that all images were captured under the same settings and normalised to the background for all samples. The scale bar represents 10 μ m.

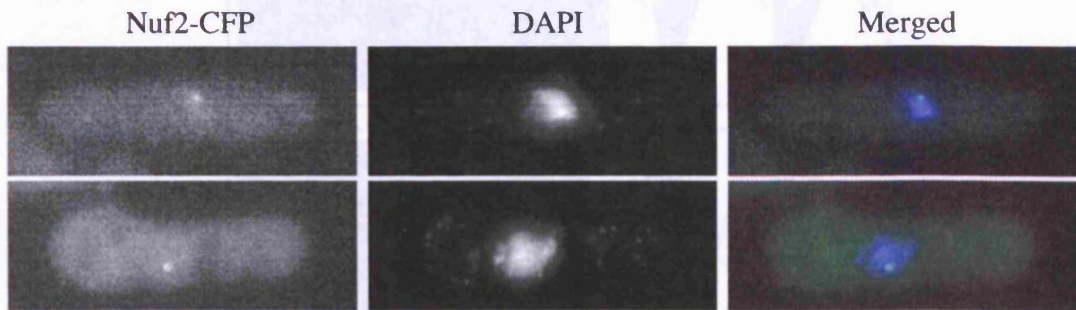
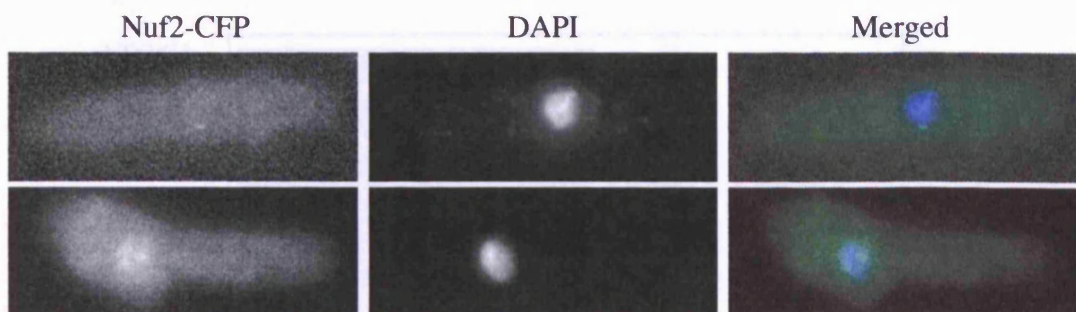
A***ΔTOG1* -CBZ*****ΔTOG1* +CBZ**

Fig. 3.4.2 Nuf2 is delocalised in *ΔTOG1* in presence of spindle damage. *ΔTOG1* cells carrying *nuf2*⁺-CFP were grown in minimal lacking thiamine, synchronised in HU for 4 hours at 27°C, washed out and resuspended in HU-free minimal media in presence or absence of 50µg/ml CBZ for 3 hours. A) *ΔTOG1* cells shows reduced Nuf2-CFP intensity at the kinetochore in formaldehyde-fixed cells in spindle damaged condition. Continues next page. The scale bar represents 10µm.

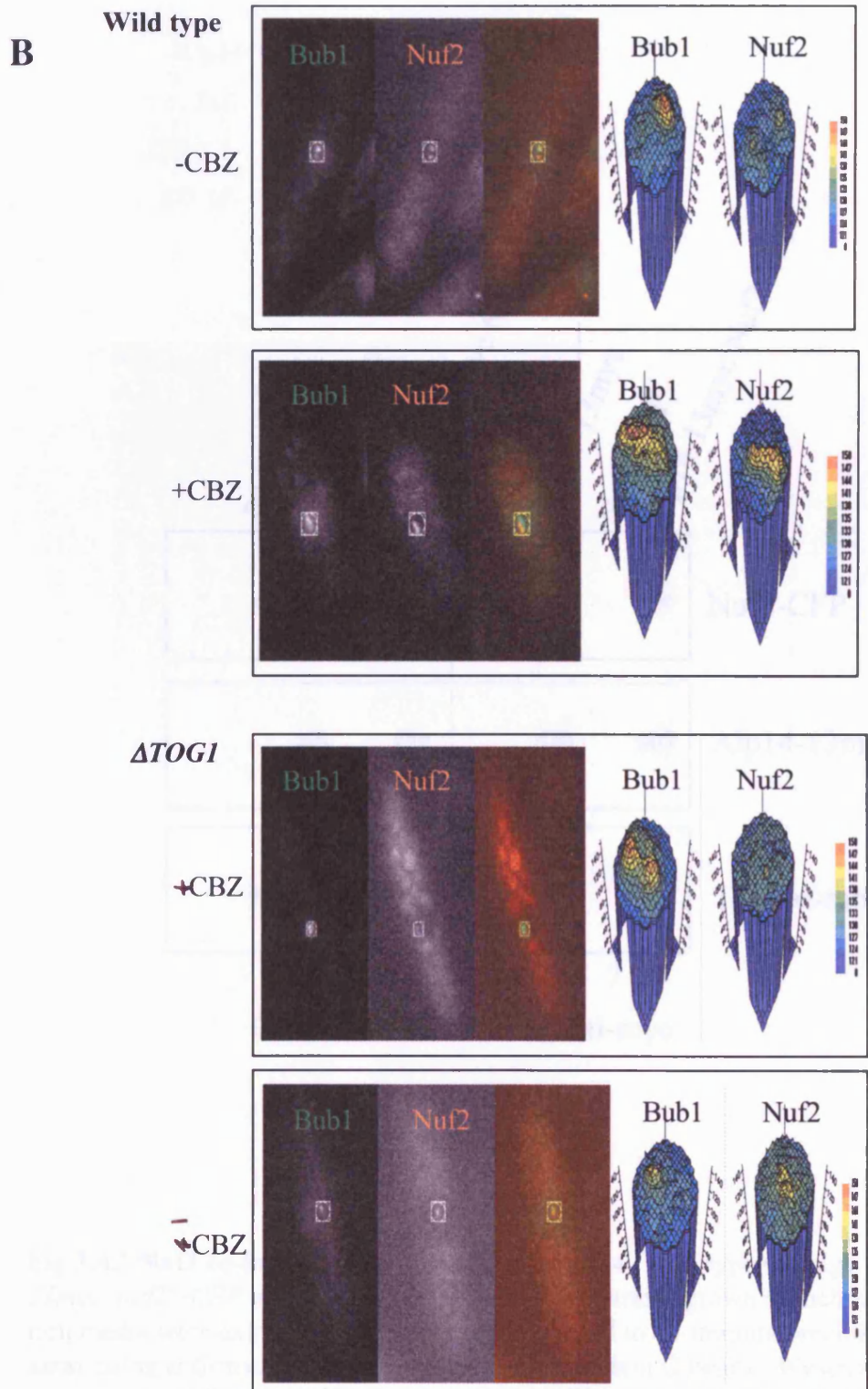


Fig. 3.4.2 B) Live wild type and $\Delta TOG1$ cells showing reduced Nuf2-CFP intensity at the kinetochore in in spindle damaged condition. Intensities of Nuf2-CFP dot at the kinetochore were visualised and measured using the Delta Vision program. Note that about 20 cells were visualised for each sample; representative cells are shown The scale bar represents 10 μm .

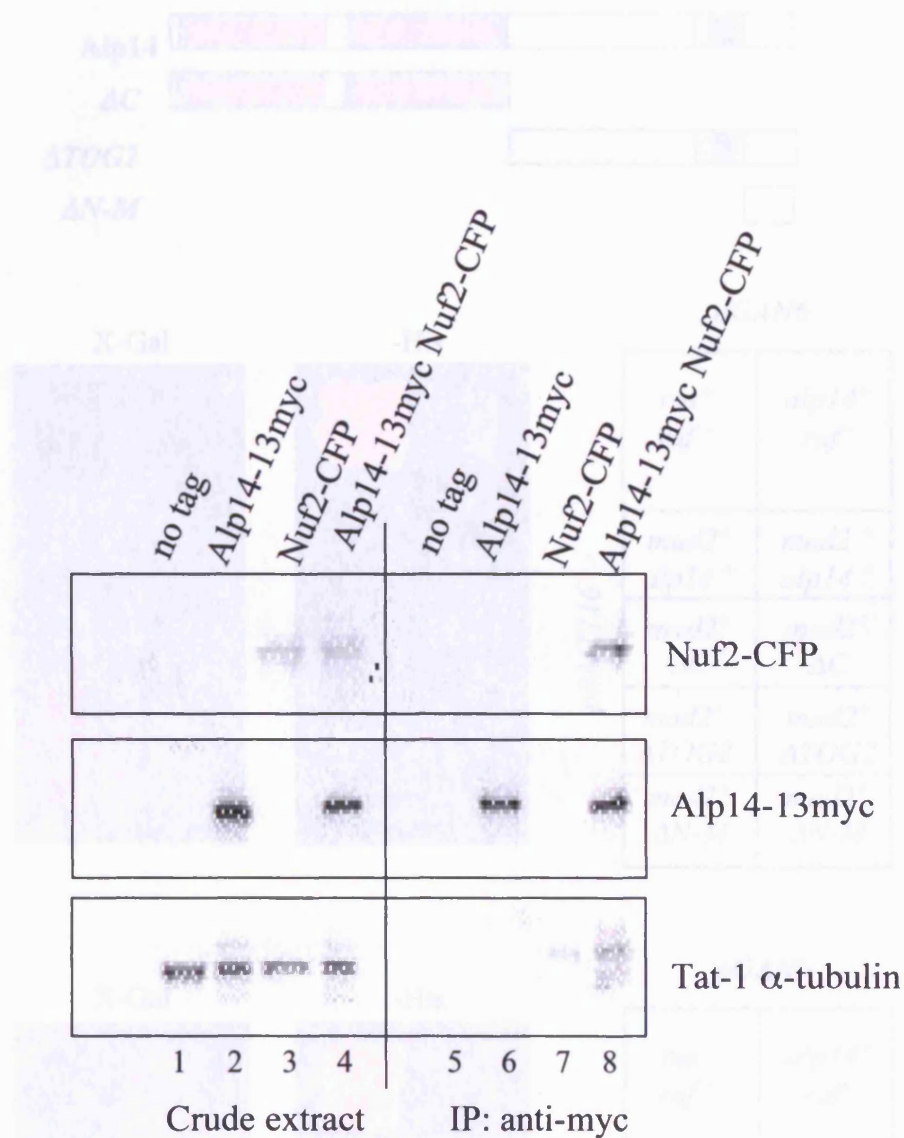


Fig 3.4.3 Nuf2 co-immunoprecipitates with Alp14. Wild type (no tag), *alp14⁺-13myc*, *nuf2⁺-CFP* and *alp14⁺-13myc nuf2⁺-CFP* strains grown asynchronously in rich media were extracted for protein and subjected to co-immunoprecipitation assay using anti-myc antibody conjugated with protein G beads. Western blotting using an anti-GFP antibody shows that Nuf2-CFP is pulled down with Alp14-myc. Probing against TAT1 was carried out as loading control. 30ng of proteins were loaded in lanes 1-4 and 3mg of proteins were used for the co-immunoprecipitation assay and loaded in lanes 5-8.

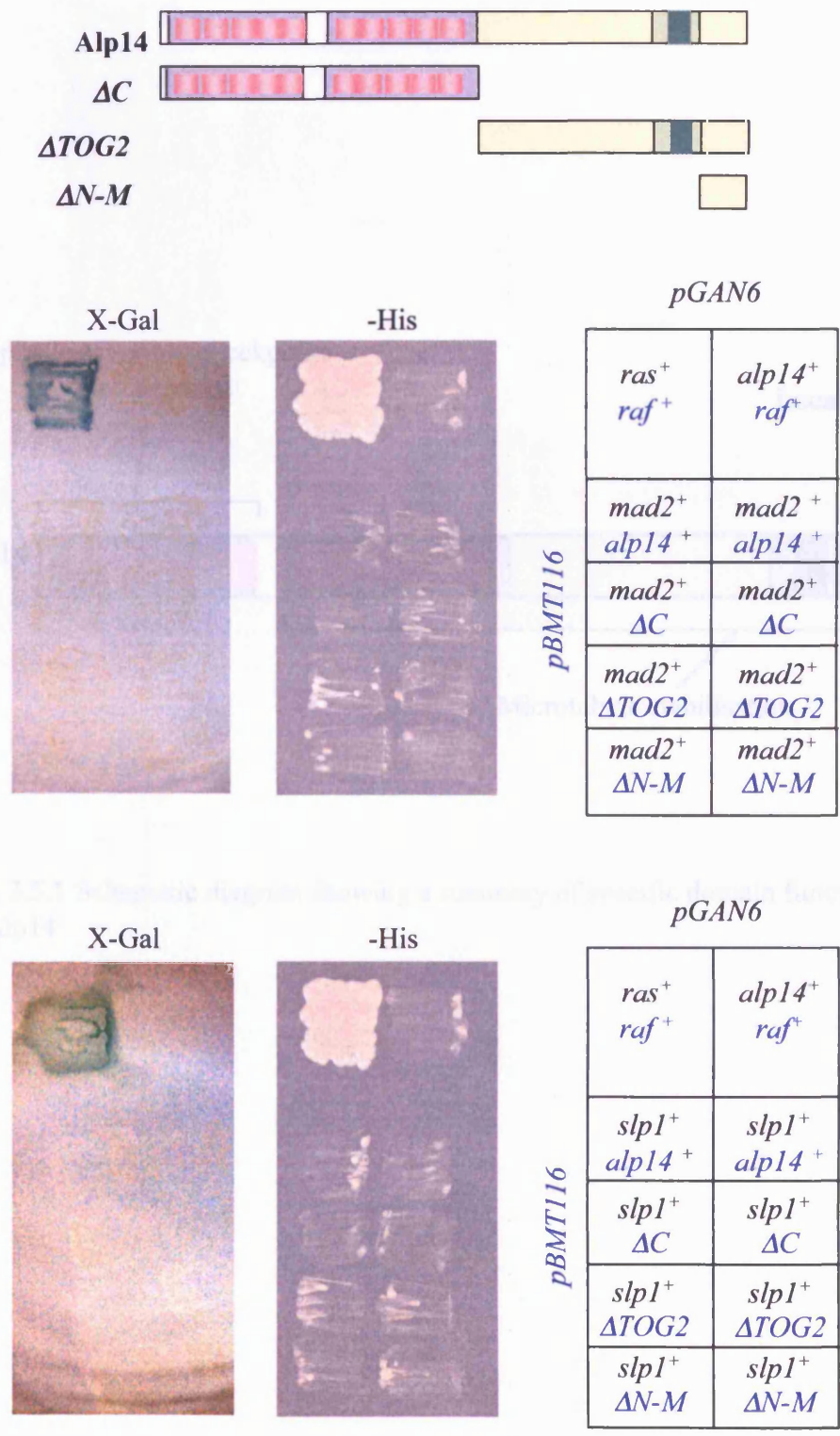


Fig. 3.4.4 Two-hybrid binding assays failed to show binding between **Alp14** and **Mad2** or **Slp1**. Budding yeast transformants expressing the indicated gene products were streaked on minimal medium lacking histidine (-His) or plates containing X-Gal (-gal). As positive and negative controls, *Ras - Raf* and *Alp14 - Raf* were expressed, respectively.

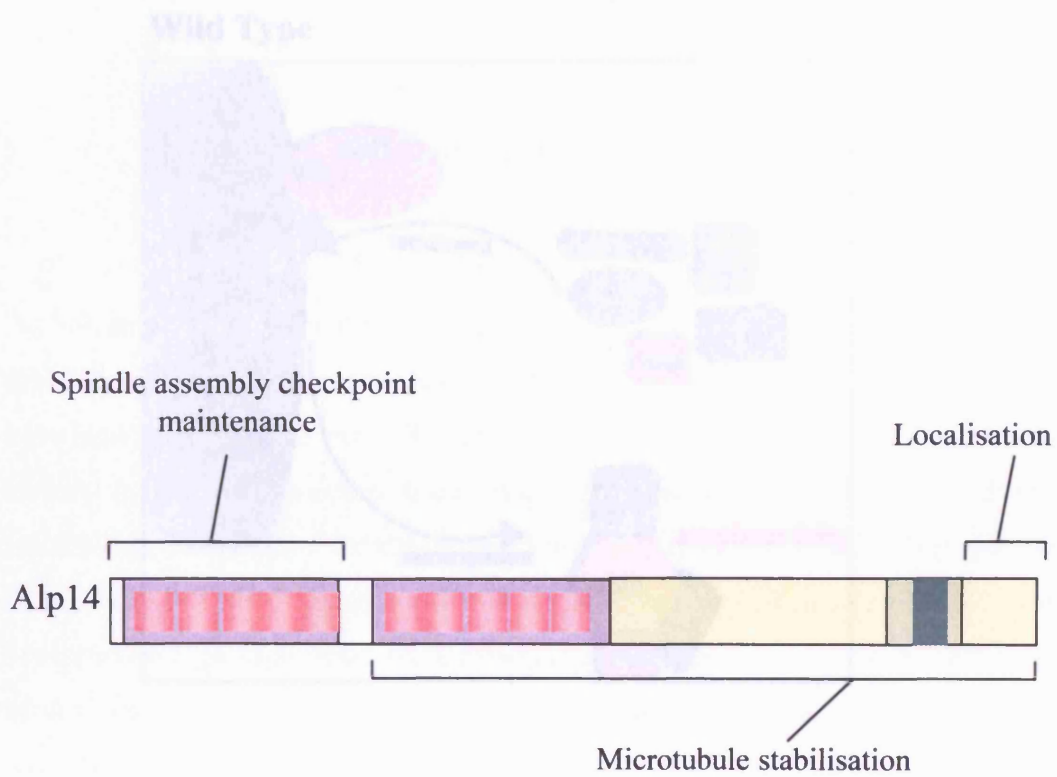
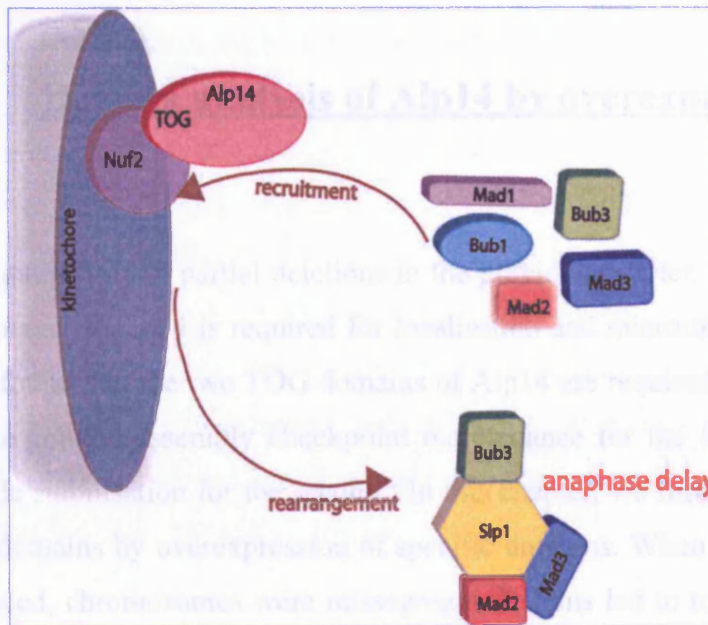


Fig. 3.5.1 Schematic diagram showing a summary of specific domain functions in Alp14.

Fig. 3.5.2 Our model: ATDGI mutation as the genetic assembly pathway for stabilisation of stage kinetochore protein. In the wild type, the recruitment and stabilisation of Ndc 80 to the kinetochore is a key step in the assembly checkpoint. In the ATDGI mutant, the recruitment of Ndc 80 to the kinetochore is blocked, leading to a failure to stabilise the kinetochore. This results in a failure to maintain the spindle checkpoint and a consequent failure to arrest the cell cycle. The ATDGI mutation is known to be a mutation in the ATPase domain of Alp14, which is a key component of the spindle checkpoint.

CHAPTER 3

Wild Type



$\Delta TOG1$

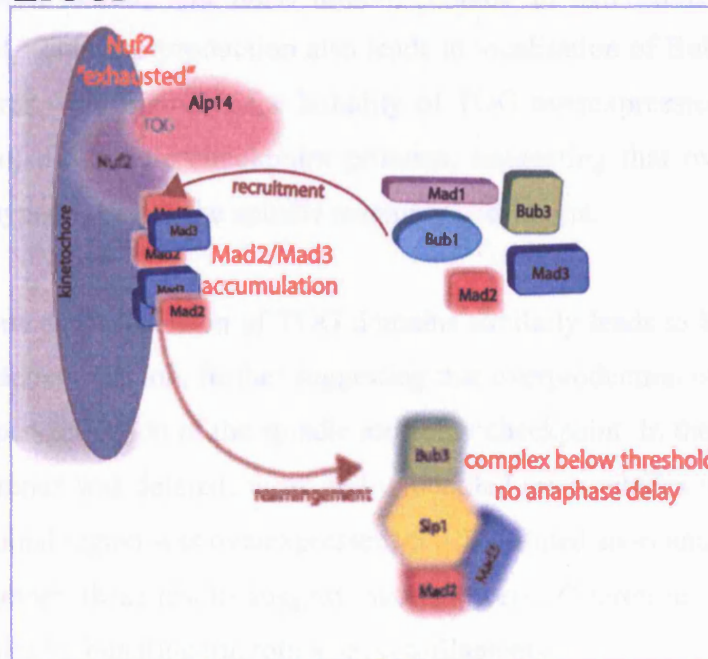


Fig. 3.5.2 Our model: TOG1 maintains the spindle assembly checkpoint by stabilisation of outer kinetochore protein, Nuf2. Alp14 is required for the recruitment or stabilisation of Nuf2 at the kinetochore, which in turn ensures spindle assembly checkpoint proteins to be stably retained at this site. In wild type, the kinetochore structure is stable and spindle checkpoint can be maintained when the spindle is damaged (upper panel). However, in the absence of TOG1, the outer kinetochore is destabilised, causing unstable localisation of spindle checkpoint proteins and inhibition of APC via Mad2 and Mad3 cannot be maintained.

CHAPTER 4

Domain analysis of Alp14 by overexpression

By investigating Alp14 partial deletions in the previous chapter, it was determined that the C-terminus of Alp14 is required for localisation and microtubule stabilisation. We have also found that the two TOG domains of Alp14 are required for distinct functions, namely the spindle assembly checkpoint maintenance for the first TOG domain and microtubule stabilisation for the second. In this chapter, we further investigate the role of Alp14 domains by overexpression of specific domains. When full length Alp14 was overproduced, chromosomes were missegregated. This led to toxicity and inability to enter further rounds of mitosis, causing cells to accumulate in interphase. In contrast, specific overproduction of TOG domains in a wild type background by plasmid expression is lethal, and most notably results in activation of spindle assembly checkpoint. This overproduction also leads to localisation of Bub1 but not Mad2 to the kinetochores. Surprisingly, the lethality of TOG overexpression is dependent on the presence of all spindle checkpoint proteins, suggesting that overproduction of TOG domains hyper-activates the spindle assembly checkpoint.

Endogenous overexpression of TOG domains similarly leads to lethality in a Mad2 and Bub1-dependent fashion, further suggesting that overproduction of the N-terminal region causes hyper-activation of the spindle assembly checkpoint. In these constructs, in which the C-terminus was deleted, weak and unbundled microtubules were also found. When the C-terminal region was overexpressed, cells exhibited short and bundled microtubules. Taken together, these results suggest that the diverse C-terminus of Alp14 may stabilise microtubules by bundling microtubule protofilaments.

The stability of microtubules is regulated by factors that affect their polymerisation, depolymerisation, catastrophe and rescue. Visualisation of microtubules by electron microscopy showed that microtubules are closely bundled at the growing end, appearing as “sheet-like” structures containing straight parallel lines of microtubules packed together when they are polymerised. In contrast, depolymerising microtubules show curved and bent microtubule filaments specifically at the plus-end (Alberts *et al.* 1994; Nogales *et al.* 2003). Bundling of protofilaments at microtubule-ends is crucial for microtubule stability as it facilitates the prevention of depolymerisation and catastrophe, and promotes polymerisation and rescue. In addition, microtubule bundling also allows proteins to cross-link protofilaments, which permits interaction of microtubule ends of the same polarity, for example at the spindle midzone to recruit proteins for septation and cytokinesis (Liao *et al.* 1994; Kashina *et al.* 1996).

In higher eukaryotes, defects in microtubule stability in interphase cells leads to catastrophic malfunctions in cell migration, transport and cell-to-cell communication, as well as abnormal cell shape. In mitosis, loss of microtubule stability hugely compromises the integrity of the genome as accurate chromosome segregation can no longer be ensured. Like yeast, higher eukaryotes employ the spindle assembly checkpoint to prevent chromosome missegregation by delaying anaphase onset when unattached or tensionless kinetochores are detected. Studies in human HeLa cells reveal that approximately 20% of wild type human cells experience a significant mitotic delay prior to anaphase in a single round of mitosis, making the role of the spindle assembly checkpoint indispensable (Reider *et al.* 1994). On the other hand, fission yeast wild type cells are thought to activate the spindle checkpoint far less frequently during normal mitotic cycles. Consistently, cells remain viable when components of the spindle checkpoint are deleted in this organism (He *et al.* 1997 and 1998; Bernard *et al.* 1998; Millband and Hardwick 2002; Ikui *et al.* 2002; Tournier *et al.* 2004; this study). However, it is not to say that the spindle checkpoint is insignificant in fission yeast. When spindle checkpoint proteins are overexpressed in this organism, the checkpoint is hyper-activated, leading to cell cycle arrest in mitosis without spindle damage, which in turns results in lethality (He *et al.* 1998).

In our study described in the previous chapter, we have determined that the first TOG domain of Alp14 (TOG1) is required to maintain the spindle assembly checkpoint

through analysis of *alp14* partial deletions. To complete our study, we investigate effects of overexpressing specific domains of Alp14 in this chapter. By overexpressing TOG domains, we seek to further elucidate and confirm the role of TOG1 in the spindle assembly checkpoint. In addition, we further analyse the role of the second TOG domain (TOG2) and C-terminus of Alp14 in microtubule-stabilisation.

4.1 Overproduction of full length Alp14

To analyse the effects of overproducing specific domains, overexpression of full length Alp14 is first carried out as a control. In vivo studies of Alp14 has shown that it stabilises microtubules, both during interphase and in mitosis, and is essential to maintain the spindle assembly checkpoint (Garcia *et al.* 2001; chapter 2 and 3). We expect Alp14 overexpression to cause hyper-stabilised microtubules, which in interphase could be exhibited as elongated or bent cell shapes. In mitosis, defects in spindle dynamics caused by the overexpression are likely to result in spindle assembly checkpoint activation and/or chromosome missegregation. Because Alp14 is also required for the maintenance of the spindle checkpoint, overexpression of the protein also results in mitotic arrest or cut cells.

It is important to note that Alp14 localisation in mitosis is dependent on its binding to Alp7. For this reason, the overproduced Alp14 may not be able to localise and exert its functions if wild type Alp7 is not expressed at a similarly high level. In this scenario, overproduction of Alp14 would be expected to produce hyper-stabilised microtubules only in interphase without causing mitotic defects. Another possibility is that the overproduced Alp14 protein may still be able to exert some mitotic function.

Overexpression of *alp14*⁺ results in microtubule defects, chromosome missegregation and cell cycle arrest.

To induce overproduction of full length Alp14, a *P3nmt* promoter has been endogenously integrated to replace natural promoters of *alp14*⁺. In the absence of thiamine, the *nmt* promoter is induced and Alp14 is overexpressed. Results show that *ov-alp14* displays severe growth defects on plates in the absence of thiamine, indicative of lethality in this condition (data not shown). Viability of wild type and *ov-alp14* cells tested at 0 and 12

to 22 hours in absence of thiamine shows that wild type cells are able to grow in the absence of thiamine (fig. 4.1.1 A). However, a gradual loss of viability was observed for *ov-alp14* cells in overexpressed condition. The gradual loss may be a reflection of cells accumulating defects as they go through rounds of cell division. Microscopic analysis *ov-alp14* cells grown on plates show abnormal cell shape, with some cells displaying elongated shape, while others exhibiting expanded cell ends (fig. 4.1.1 B). These cell morphologies are suggestive of compromised microtubule dynamics. Elongated cells could be caused by long microtubules, which may occur when the rate of catastrophe is abnormally low as a result of defects in microtubule regulators. Alternatively, elongated cells could be a result of hyper-stabilised microtubules. In this case, hyper-stabilised or hyper-elongated microtubules may push or curve at the cell ends instead of undergoing rapid catastrophe once they have reached cell ends. This would also lead to elongated or expanded cell ends as we have observed in *ov-alp14*.

To visualise the effect of overproducing Alp14 on microtubules, wild type and *ov-alp14* cells were processed for immuno-staining with anti- α tubulin (anti-TAT1) and anti-SPB (anti-Sad1) after inducing the *P3nmt* promoter for 20 hours. Compared to wild type, *ov-alp14* cells show few microtubules in this condition (fig. 4.1.2). Of those few microtubules, some appear to curve at the cell ends, which is consistent with the expanded cell ends morphology observed in fig 4.1.1. The presence of curved microtubules indicates that the rate of catastrophe may be substantially decreased when Alp14 is overproduced. One explanation for this is that Alp14 may possess a microtubule-bundling activity, thereby inhibiting catastrophe and consequently stabilising microtubules. When Alp14 is overexpressed, microtubule protofilaments may be hyper-stable, leading to overgrowth at cell ends.

Interestingly, very few mitotic spindles were observed after 20 hours in overexpressed condition. Despite this, inaccurate chromosome segregation and defective SPB separation were observed in this condition (fig. 4.1.2). To quantify the number of cells with missegregated chromosomes, wild type and *ov-alp14* cells were fixed with formaldehyde and stained with DAPI at 13-23 hours in overexpressed condition. As fig. 4.1.3 shows, the number of missegregated chromosome increased gradually over time in Alp14 overexpression, whereas it remained non-existent in wild type. Assuming that overexpressed Alp14 is functional in mitosis, this result is expected as wild type Alp14

regulates spindle growth and stabilises spindle-kinetochore interaction. We reason that overproduction of Alp14 may cause hyper-stabilised spindles, leading to abnormal chromosome segregation.

As mentioned earlier, no mitotic spindles were observed after Alp14 has been expressed for 20 hours despite chromosome and SPB missegregation defects (fig. 4.1.2). A count of the number of mitotic cells in this condition reveal that unlike wild type cells where nearly 10% of mitotic cells were found, *ov-alp14* cells displayed virtually no mitotic cells. Instead, most cells accumulated at an interphase or G₁-like stage (fig. 4.1.4). It is crucial to note that after 20 hours in overexpressed condition the viability of cells has dropped substantially, suggesting that this accumulation in interphase is representative of the terminal phenotype of Alp14 overexpression. We propose that overexpression of Alp14 causes gross chromosome segregation defects, which leads cells to be unable to enter further rounds of mitosis and subsequently accumulate interphase, results in lethality.

4.2. Overexpression of *pTOG*⁺

From our analysis in chapter 3, the TOG1 domain is required for maintenance of the spindle assembly checkpoint. In this section, we aim to further elucidate and confirm the role of Alp14 in the spindle assembly checkpoint by overexpression of the TOG domain ectopically. Although our study so far has not implicated the TOG2 domain to also function in checkpoint, we decided to overexpress both TOG1 and TOG2 as we reasoned that flanking regions of TOG1 may be required for its full spindle checkpoint function. By expressing both TOG domains, we would be able to fully analyse TOG1 function in the spindle assembly checkpoint. In this experiment, we overproduced TOG1 and TOG2 by expression of multicopy plasmids containing the TOG motifs. To construct the plasmid, Alp14 residues 1-430, which contain the two TOG domains, were amplified by primers containing additional *NdeI* and *SmaI* digestion sites. The PCR-amplified sequence was then subcloned into *pREP1* plasmids. Because the *pREP1* plasmid contains a *P3nmt* promoter, the overexpression of the TOG domains can be regulated by addition of thiamine.

As well as microtubule stabilisation, the C-terminal of Alp14 is also required for localisation. Because of this, it is unclear whether the overproduced $pTOG^+$ would be able to localise and exert its functions. Previous studies have shown that overproduction of spindle checkpoint components leads to mitotic arrest and lethality that can be detected by growth retardation on plates lacking thiamine (He *et al.* 1998; Abrieu *et al.* 2001). If overexpressed TOG domains were functional, it may hyper-activate the spindle checkpoint, leading to cell cycle arrest in mitosis, observed as growth lethality on plates lacking thiamine. As fig. 4.2.1 shows, cells overproducing $pTOG^+$ indeed are lethal on plates lacking thiamine. Note that growth retardation is also detected in the presence of thiamine, which may be because the thiamine-inducible $P3nmt$ promoter is unable to completely suppress expression of $pTOG^+$ in this condition, as this is often the case in the fission yeast system (Hirata *et al.* 1998). We next investigate detailed effects of overexpression of $pTOG^+$ to further elucidate and confirm the role of TOG domains in the spindle assembly checkpoint.

4.2.1 Overexpression of $pTOG^+$ activates the spindle assembly checkpoint.

Because our study has indicated that the first TOG domain is required to maintain the spindle assembly checkpoint, the overproduced $pTOG^+$ could cause abnormalities in the checkpoint. We have already shown that $pTOG^+$ overproduction is toxic (above – fig. 4.2.1), which could be caused by defects in the spindle checkpoint. If this were the case, it is a possibility that upon spindle damage $pTOG^+$ cells may be able to maintain the spindle checkpoint for a longer period than wild type cells. Alternately, overproduced $pTOG^+$ could hyper-activate the spindle checkpoint without spindle damage in a similar manner as Mad2 or Mph1 overexpression (as briefly described above -He *et al.* 1998; Hardwick *et al.* 1996; Draviam *et al.* 2004; Kadura *et al.* 2005; Abrieu *et al.* 2001). In this scenario, $pTOG^+$ overexpression would lead to severe cell cycle arrest in mitosis and growth lethality. Another explanation for the toxicity in $pTOG^+$ cells could be severe microtubule defects. A series of experiments carried out to investigate these possibilities is described below.

The lethality of $pTOG^+$ overexpression is rescued by deletion of any components of the spindle assembly checkpoint.

So far, studies (Garcia *et al.* 2001 and this thesis) suggest that TOG1 may function upstream of the spindle assembly checkpoint. If, like overexpression of Mad2 or Mph1,

the toxicity of cells overexpressing $pTOG^+$ were caused by hyper-activation of the spindle checkpoint, then the lethality of $pTOG^+$ would be dependent on the function of spindle checkpoint proteins. To test this possibility, $pTOG^+$ was introduced to cells deleted for spindle checkpoint proteins. Results show that $pTOG^+$ lethality is rescued by the absence of Mph1, Mad1, Mad2, Bub1 and Bub3 (fig. 4.2.2 and table 4.2.3). Although we were not able to obtain colonies that simultaneously overexpress $pTOG^+$ and lack Mad3, we would expect the lethality of $pTOG^+$ to also be rescued in the absence of Mad3. However, it is possible that we could not obtain $pTOG^+$ in a $\Delta mad3$ strain because the combination is not viable. It is important to note that Mad2 overexpression did not cause cell cycle arrest in cells lacking Mad3, while it did so when other components of the checkpoint were deleted (summarised in fig. 4.2.3 – adapted from Millband and Hardwick 2002). The dependency of $pTOG^+$ lethality on spindle checkpoint proteins suggests that the TOG domains may function upstream of these proteins, and that $pTOG^+$ overexpression may hyper-activate the spindle assembly checkpoint even in the absence of spindle damage.

To ensure that the spindle assembly checkpoint is activated when the TOG domains are overexpressed, we sought to quantify the number of mitotic cells in $pTOG^+$. To address this, $pTOG^+$ cells were stained with anti-TAT-1 after 16 hours in overexpressed condition and counted for the number of mitotic cells against the total number of cells. Fig. 4.2.4 A shows that the percentage of mitotic cells reaches nearly 30% when $pTOG^+$ is overexpressed, which is about three times higher than in wild type strains in similar conditions (also see chapter 5 for mitotic index in wild type cells). However, when $mad2^+$ is deleted, the percentage of mitotic cells drops to about 10%, which suggests that overexpression of $pTOG^+$ leads to a cell cycle arrest in mitosis in a Mad2-dependent fashion, consistent to our previous finding. To investigate the cell cycle stage in which $pTOG^+$ cells are arrested, the number of cells in each phase of mitosis were counted against the total number of mitotic cells. Fig. 4.2.4 B shows that cells overexpressing $pTOG^+$ accumulated in prometaphase and metaphase, while they are not arrested in anaphase, indicating the spindle assembly checkpoint is activated in this condition.

The next question we addressed is how may $pTOG^+$ overexpression hyper-activate the spindle assembly checkpoint. Our data in chapter 3 suggests that TOG1 maintains the spindle checkpoint by localising the Nuf2/Ndc80 complex at the outer kinetochore in

spindle damage. Because, $\Delta TOG1$ results in weak Nuf2/Ndc80 staining, we would expect Nuf2/Ndc80 localisation to the kinetochore to be more intense in $pTOG^+$ overexpression. However, visualisation of Nuf2-CFP and Ndc80-GFP in $pTOG^+$ failed to show weaker or more intense fluorescence signal in comparison to wild type cells (data not shown). Although Nuf2/Ndc80 dots resembled that of wild type in $pTOG^+$, we cannot rule out the possibility that $pTOG^+$ overexpression may still hyper-activate the spindle checkpoint via the Nuf2/Ndc80 complex.

Overexpression of $pTOG^+$ results in Bub1 but not Mad2 localisation to the kinetochore.

Because the activation of the spindle checkpoint in $pTOG^+$ is dependent on checkpoint proteins, we would expect the kinetochore-recruitment of these proteins to be augmented when $pTOG^+$ is overexpressed. To test this possibility, we observed Mad2-GFP and Bub1-GFP in cells overexpressing that $pTOG^+$. As fig. 4.2.5 shows, strong kinetochore localisation of only Bub1-GFP but not Mad2-GFP was observed to be significantly higher than wild type after 16 hours in overexpressed condition.

Although this finding appears to be rather surprising, it is not completely unexpected as outer kinetochore protein Nuf2 has been shown to be required for kinetochore-recruitment of specific proteins (Martin-Lluesma *et al.* 2002; DeLuca *et al.* 2003; Gillett *et al.* 2004; Meraldi *et al.* 2004; Bharadwaj *et al.* 2004). A study of human HeLa cells showed that when hHec1 is depleted, Mad2 is unable to localise to kinetochores while Bub1 recruitment is reduced by approximately 50% during spindle checkpoint activation (Martin-Lluesma *et al.* 2002). Another group reported a similar finding that the kinetochore-localisation of Mps1, Mad2, and Mad3 but not BubR1 or Bub1 is lost when either hHec1 or hNuf2 is depleted (Meraldi *et al.* 2004). Similarly, when hSpc25 is lost, Mad1 and Hec1 can no longer be found at the kinetochore, whereas the localisation of Bub1 and BubR1 remain largely unaffected (Bharadwaj *et al.* 2004). In budding yeast, Mad2 and Bub1 are found at the kinetochores in *ndc80-1* but not *spc25-7* mutants (Gillett *et al.* 2004).

In addition, these studies have also suggested that the spindle checkpoint can be activated without observable Mad2 localisation to the kinetochore in some allele of *nuf2* mutants or hHec1/hNuf2 depletion (Martin-Lluesma *et al.* 2002; Meraldi *et al.* 2004; Gillett *et al.*

2004). Like overexpression of *pTOG*⁺, whose mitotic arrest and lethality is dependent on Mad2 and yet did not display Mad2 localisation to the kinetochore, simultaneous depletion of hHec1 and hMad2 resulted in catastrophic mitotic exit even though the spindle checkpoint was activated without Mad2 localisation (Martin-Lluesma *et al.* 2002). Because TOG1 maintains the spindle checkpoint via Nuf2, it is therefore unsurprising that overexpression of *pTOG*⁺ would lead to spindle checkpoint activation in a similar manner as *nuf2* mutants with regards to the recruitment of specific checkpoint proteins.

4.2.2 Overexpression of *pTOG*⁺ results in long astral microtubules.

Because we have shown the TOG2 domain to contribute to microtubule-stabilising activity of Alp14 (chapter 3), we next investigated the possibility that microtubules are defective in *pTOG*⁺ cells, as the plasmid overexpresses both TOG domains. *pTOG*⁺ cells stained with an anti- α -tubulin antibody (anti-TAT-1) after 16 hours in overexpressed condition showed long cytoplasmic microtubules in interphase (fig. 4.2.6). In mitosis, astral spindles also appeared to be elongated in specifically anaphase, while pole-to-kinetochore and pole-to-pole spindles appear normal in all phases of mitosis (fig. 4.2.6). In metaphase, astral spindles have been shown to grow within the confines of the nuclear envelope, suggesting that they are emanated from intra-nuclear SPBs (Zimmerman *et al.* 2004). On the other hand, astral spindles that appear in anaphase are emanated from extra-nuclear MTOCs, which reside in the cytoplasm (Zimmerman *et al.* 2004). Specific elongation of cytoplasmic microtubules in interphase and astral spindles in anaphase suggests that microtubules emanated from cytoplasmic MTOCs are specifically defective in the overexpression mutant. It is important to note that no chromosome segregation defects were observed. In addition, deletion of *mad2*⁺ in the *pTOG*⁺ overexpression strain did not further aggravate the elongated microtubule phenotype (fig. 4.2.6). This suggests that despite Mad2-dependent mitotic arrest in *pTOG*⁺ cells, the microtubule defects are independent of spindle assembly checkpoint roles. Overall, this data, together with the absence of missegregated chromosomes and lack of mitotic arrest in anaphase, suggest that overexpression of *pTOG*⁺ hyper-activates the spindle assembly checkpoint without damage to metaphase spindles.

In summary, *pTOG*⁺ overexpression resulted in two distinct phenotypes. One is the hyper-activation of the spindle checkpoint leading to lethality, which is dependent on the

function of spindle checkpoint proteins. The second is the elongation of microtubules that emanate from cytoplasmic MTOCs. These phenotypes have shown to be distinct because *pTOG*⁺ cells were not arrested in anaphase despite the presence of long anaphase astrals, and deletion of *mad2*⁺ did not further affect the elongated microtubule phenotype. Because deletion of TOG1 did not exhibit any defects in cell polarity, microtubules or chromosome segregation at the restrictive temperature (chapter 3), the microtubule defect in *pTOG*⁺ is suggested to be caused by overexpression of the TOG2 domain. Taken together, we postulate that the TOG1 domain is required to maintain the spindle checkpoint in spindle damage conditions. When overexpressed, the spindle assembly checkpoint is hyper-activated similarly to Mad2 or Mph1 overexpression, resulting in mitotic arrest and lethality. On the other hand, the TOG2 domain may function to elongate cytoplasmic microtubules. When TOG2 is overproduced, microtubules emanated from cytoplasmic MTOCs such as cytoplasmic microtubules and anaphase astral spindles become hyper-elongated. Note that this postulation is consistent with the overall microtubule function of Alp14 and could be clarified by specific expression of the TOG2 region by plasmid expression.

In addition to overexpression of TOG domains by multicopy plasmid in a wild type background, we also expressed them endogenously using a *P3nmt* promoter in strains where the C-terminal regions are absent. By investigating these strains, we were able to study the role of the C-terminus in further detail as well as confirm our findings of the TOG1 domain. Analyses of these strains are described below.

4.3 Overproduction of Alp14 domains from the N-terminus.

To overexpress Alp14 N-terminal domains endogenously, two constructs were produced. The first construct, *ov-TOG2*, specifically overexpresses both TOG domains from the N-terminal at residues 1-420 (fig. 4.3). Like *pTOG*⁺ overexpression described in the previous section, this construct expresses both TOG domains. However, in this experiment (*ov-TOG2*), the C-terminus is also deleted. In the second construct, *ov-TOG2-C*, the diverse C-terminal region that lacks the microtubule-binding and coiled-coiled domains is also overexpressed in addition to TOG at residues 1-639 domains (fig. 4.3).

In these constructs, the C-terminal tail of the protein is missing. Therefore, phenotypes would be contributed to both the loss of the C-terminal and the overproduction of the N-terminal. Note that the TOG2 domain and the diverged C-terminal region are required for complete microtubule function of the protein. By studying the *ov-TOG2* construct, which leaves the TOG2 domains intact, the microtubule functions of the second TOG domain and the C-terminal region may be able to be distinguished.

Cells overexpressing of *alp14* N-terminal regions display microtubule defects.

Because the C-terminal regions are absent in the *ov-TOG2* and *ov-TOG2-C* constructs, we first sought to test for microtubule defects in these strains. *ov-TOG2* and *ov-TOG2-C* cells grown for 3 days on plates containing or lacking thiamine displayed elongated and branched phenotypes in overexpressed condition (fig. 4.3.1). The cell morphology observed is similar to that of strains where the C-terminus is missing and the microtubule-stabilising role is compromised (chapter 3 – figs. 3.1.2 and 3.2.3), which suggests that the cell polarity defect may be caused by the absence of the C-terminus. Consistently, the overexpression of TOG domains in wild type background containing intact *alp14*⁺ did not display cell polarity defects (*pTOG*⁺ - described in the previous section).

To visualise microtubules, an immuno-staining of α -tubulin after 12 hours in overexpressed condition was carried out. Fig. 4.3.2 A shows that *ov-TOG2* is defective in cytoplasmic microtubules and mitotic spindles. Although microtubules in *ov-TOG2* appear to resemble that of wild type in length, they look weak and unbundled. After 24 hours in overexpressed condition, terminal phenotypes are observed (fig. 4.3.2 B). In this condition, *ov-TOG2* shows weak microtubule, with some cells lacking any observable microtubules altogether. From our results, we propose that the C-terminus of Alp14 may function to bundle microtubule protofilaments, thereby stabilising microtubules.

To address the effects of *ov-TOG2* in mitosis, a DAPI staining of *ov-TOG2* cells was carried out after 18 hours in overexpressed condition. We reason that if the absence of the C-terminus in *ov-TOG2* lead to weak mitotic spindles, defects in chromosome

segregation would be detected. As fig 4.3.3 shows, missegregated chromosomes were observed in this condition. Because Alp14 functions to stabilise spindle-kinetochore interaction during mitotic metaphase, we tested the possibility that *ov-TOG2* may cause defects in metaphase that leads to chromosome missegregation by visualisation of Nuf2 localisation. In wild type conditions, outer kinetochore protein Nuf2 can be observed as kinetochore dots that remain within close proximity during metaphase. On the other hand, metaphase Nuf2 dots are more dispersed from each other when microtubules are compromised, such as in *nda3* mutants (defective in β -tubulin –Hiraoka *et al.* 1984). Fig. 4.3.4 shows that Nuf2 dots are clearly dispersed in *ov-TOG2* cells after 18 hours in overexpressed condition. Our results suggest *ov-TOG2* cells to contain weak mitotic spindles. The microtubule and mitotic defects in *ov-TOG2* may be caused by either the lack of the C-terminal region or the overexpression of the TOG domains. To distinguish between these possibilities, multicopy plasmids containing *alp14*⁺ were introduced to *ov-TOG2* cells. As fig. 4.3.5 shows, *palp14*⁺ rescues growth defects of overexpressed *ov-TOG2*, suggesting that weak and unbundled microtubule phenotypes and mitotic defects are caused by the absence of the C-terminal region of Alp14.

Overexpression of *alp14* N-terminal activates the spindle assembly checkpoint.

We have shown that overexpression of Alp14 TOG domains in wild type background causes lethality that is dependent on functions of all spindle checkpoint proteins (*pTOG*⁺-section 4.2). This result led to the proposal that overexpression of TOG domains causes the spindle checkpoint to be hyper-activated. To test the possibility that *ov-TOG2* overproduction also hyper-activates the checkpoint, components of checkpoint were deleted. Fig. 4.5.6 shows that like *pTOG*⁺ overexpression, deletions of *mad2*⁺ and *bub1*⁺ rescue the toxicity and growth defects of *ov-TOG2* (fig. 4.3.6). Surprisingly, deletions of other checkpoint proteins (Mph1, Mad1, and Bub3) did not rescue the growth defects of *ov-TOG2* as effectively as $\Delta mad2$ and $\Delta bub1$. It is also of note that deletion of *mad3*⁺ did not appear to rescue the defect, which may explain why we were unable to obtain strains carrying *pTOG*⁺ in $\Delta mad3$ background due to lethality. Examination of the *ov-TOG2-C* strain shows that deletion of *mad2*⁺ and *bub1*⁺, but not other checkpoint genes could rescue the toxicity in this condition. Note that *ov-TOG2-C* also overexpresses a part of the C-terminal region, which is expected to cause further spindle damage and may explain the apparent differences in checkpoint dependencies.

To confirm that the spindle assembly checkpoint is activated in *ov-TOG2*, localisations of Mad2-GFP and Bub1-GFP to the kinetochores were observed (fig. 4.3.7 A). Quantifications of intense Mad2-GFP and Bub1-GFP dots at the kinetochore show that the recruitments of both Mad2 and Bub1 are highly increased in *ov-TOG2* in comparison to wild type (fig. 4.3.7 B). Note that this result is different from that of *pTOG⁺* overexpression, where the localisation of Bub1 but not Mad2 was observed.

An explanation for the differences in the requirement of the spindle checkpoint between *pTOG⁺* and *ov-TOG2* overexpressions is the presence of Alp14 C-terminus. While overexpression of *pTOG⁺* was carried out in wild type background that contains intact *alp14⁺*, the *ov-TOG2* strain lacks the C-terminus of Alp14 required for microtubule stabilisation. Consistently, unlike *pTOG⁺* cells, weak and unbundled microtubules are found in *ov-TOG2*. In response to microtubule defects in *ov-TOG2*, the spindle assembly checkpoint is activated. In summary, *pTOG⁺* hyper-activates the spindle assembly checkpoint without spindle damage. *ov-TOG2*, on the other hand, displays two phenotypes. One, caused by the absence of the C-terminus, is weak cytoplasmic microtubules and mitotic spindles, which leads spindle checkpoint activation. The second, caused by overexpression of TOG domains, is the hyper-activation of the spindle assembly checkpoint.

4.4 Overexpression of Alp14 from the C-terminus.

To complete our overexpression study, we also constructed strains that overproduced the the C-terminal regions of Alp14. The C-terminal tails of Alp14 were overexpressed at residues 710-809 (*ov-tail1*) and 697-809 (*ov-tail2*), respectively (fig. 4.4). The *ov-tail1* construct specifically overexpresses the C-terminal tail lacking the microtubule binding and coiled-coil domains, whereas these two domains are overexpressed in the *ov-tail2* strain. The TOG domains are overexpressed in constructs named *ov-C-TOG1* and *ov-C-TOG2*, where residues 241-809 and 151-809 are overproduced respectively (fig. 4.4). Only the second TOG domain is expressed from the C-terminal region in *ov-C+TOG1*. *ov-C+TOG2*, however, also expresses half of the first TOG domain because flanking regions of the second TOG domain may be required for its function. It is important to note that the constructs overexpress Alp14 endogenously, which implies that the N-

terminal regions are deleted. Therefore, phenotypes observed will be reflective of two defects. The first is the overexpression of the C-terminus; the second is the absence of the N-terminal regions.

Overexpression of Alp14 C-terminus is toxic and results in microtubule defects and spindle assembly checkpoint activation.

Our study has shown that the C-terminus of Alp14, together with the second TOG domain, stabilises microtubules. When this region is overexpressed, we would expect hyper-stabilised microtubules to be observed. To address possible microtubule defects in *alp14* partial overexpressions, *ov-tail1*, *ov-tail2*, *ov-C-TOG1* and *ov-C-TOG2* strains were streaked onto rich media containing phloxine B at 26°C and 36°C. Results show *ov-tail1* and *ov-tail2* to grow as red cells on phloxine B at 36°C, indicating that they are temperature-sensitive (fig.4.4.1 A). Visualisation of cells grown on plates indicates that *ov-tail1* and *ov-tail2* cells are bent and branched (fig. 4.4.1 B). Because these constructs do not carry the microtubule-binding domain or the coiled-coiled motif (fig. 4.4), these results are expected. On the other hand, the *ov-C-TOG1* and *ov-C-TOG2* constructs, which contain the entire region required for microtubule stabilisation, are not temperature sensitive and are shaped similarly to cells overexpressing full length Alp14, with expanded cell ends (fig. 4.4.1). Abnormal cell morphology is also observed in presence of thiamine (data not shown). This is because the *P3nmt* promoter is unable to fully suppress gene expression in fission yeast (Hirata *et al.* 1998).

For further analyse the role of Alp14 in microtubule stabilisation, we have chosen to focus on the *ov-C-TOG1* construct as it expresses the entire region required for microtubule stabilisation (the region stretching from second TOG domain to the C-terminal tail, residues 241-809). To test for growth defects caused by *ov-C-TOG1* overproduction, wild type and *ov-C-TOG1* cells were subjected to a viability test. Results show that although growth defects are undetected on plates in *ov-C-TOG1*, viability of cells is lost in overexpressed condition (fig. 4.4.2). We next addressed the effects of *ov-C-TOG1* overexpression on microtubules by immuno-staining of anti- α tubulin to allow visualisation of microtubules. After 12 hours in overexpressed condition, *ov-C-TOG1* cells display short and thick cytoplasmic microtubules in comparison to wild type (fig. 4.4.3). This suggests that interestingly, microtubules are stabilised by a bundling activity in *ov-C-TOG1* cells. Consistently, in mitosis short and broken spindles are observed,

leading to chromosome segregation defects (fig. 4.4.4).

To test for spindle assembly checkpoint activation in *ov-C-TOG1*, kinetochore-localisation spindle checkpoint protein, Mad2, is visualised. Quantification of strong Mad2 dots at the kinetochores shows that Mad2 localisation is more than three times higher in *ov-C-TOG1* than wild type cells (fig. 4.4.5), which indicates that the spindle assembly checkpoint is activated. In fact, the spindle assembly checkpoint is absolutely required for the viability of *ov-C-TOG1* cells as deletion of *mad2*⁺ in the *ov-C-TOG1* strain renders it lethal, even in the presence of thiamine (data not shown).

4.5 Summary and concluding Remarks

In this chapter, we have determined that when full length Alp14 was overproduced, chromosomes were missegregated, which led to the inability of cells to enter further rounds of mitosis, causing them to accumulate in interphase. Overproduction of both TOG domains in a wild type background (*pTOG*⁺) is lethal, which is dependent on the presence of all spindle checkpoint proteins. This suggests that overproduction of TOG domains hyper-activates the spindle assembly checkpoint. Hyper-activation of the spindle assembly checkpoint in *pTOG*⁺ intriguingly led to kinetochore-localisation of Bub1 but not Mad2. Endogenous overexpression of TOG domains which also deletes the C-terminus similarly lead to lethality in a Mad2 and Bub1-dependent fashion. Weak and unbundled microtubules were also found, and determined to be caused by the absence of the C-terminal domains. When the second TOG domain and the C-terminal region was overexpressed, cells exhibited short and bundled microtubules, suggesting that Alp14 may stabilise microtubules by bundling microtubule protofilaments.

The role of Alp14 in microtubule stabilisation

In the previous chapter, we have determined that the C-terminal tail of Alp14 is required for its localisation in interphase and mitosis, thereby allowing for the protein's overall microtubule function. In addition to localisation, the C-terminal region, together with the second TOG domain (TOG2), also stabilises microtubules. Deletion of the TOG2 motif and C-terminal regions from the N-terminus resulted in short interphase microtubules

and chromosome missegregation, suggesting that these domains stabilise microtubules by promotion of their polymerisation.

In this chapter, we examined the role of the TOG2 domain and the C-terminus in Alp14 in microtubule-stabilisation. We have found that this region promotes formation of thick microtubule bundles (*ov-C-TOG1* – section 4.4), suggesting that Alp14 may promote microtubule stabilisation and growth by bundling microtubule protofilaments together. Electron microscopic analysis of microtubule dynamics showed that polymerising microtubules are closely bundled at the growing end, while depolymerising microtubules show curved and bent microtubule filaments specifically at the growing end. Given that Alp14 is localised as punctuated dots along the microtubule, particularly at the plus-ends, we postulate that Alp14 may bundle microtubule protofilaments at the plus-ends, thereby reducing the rate of catastrophe and subsequently promoting overall microtubule growth (fig. 4.5.1 A).

Additional analysis of TOG domain overexpression (*pTOG⁺* - section 4.2), suggest that the TOG domains may also function to elongate cytoplasmic microtubules. Even though both TOG domains are overexpressed in this construct, we reason that because the first TOG domain does not appear to possess microtubule activity (results from $\Delta TOG1$), microtubule defects were a result of TOG2 overexpression. Cells expressing *pTOG⁺* showed elongated cytoplasmic microtubules and anaphase astral microtubules. These microtubules are emanated from MTOCs that specifically reside outside of the nucleus. From this finding, we suggest that the second TOG domain of Alp14 may promote cytoplasmic microtubule polymerisation in vivo. However, we acknowledge that this speculation had not been proven in our study and addition experiments (for example specific deletion or overexpression of the TOG2 motif) need to be performed to clarify this point.

Overall, our speculation is consistent with reports of in vitro studies in frog, which showed that addition of only XMAP215 to purified tubulin causes microtubule polymerisation (Gard and Kirschner 1987; Vasques *et al.* 1994). Taken together, we postulate that the second TOG domain may promote microtubule polymerisation and the C-terminal region facilitates this activity by bundling microtubule protofilaments at the

growing ends. Fig. 4.5.1 B summarises the functions of specific domains of Alp14 found in this study.

The role of Alp14 in the spindle assembly checkpoint

The previous chapter has investigated the role of the first TOG domain in Alp14 (TOG1) by analysing effects of TOG1's absence. Deletion of TOG1 results in failure to maintain the spindle assembly checkpoint in spindle damaged conditions, which is accompanied by Nuf2 and Ndc80 delocalisation from the kinetochore and specific hyper-accumulation of Mad2 and Mad3 at the kinetochore. Given that our results also indicate that Alp14 binds to Nuf2, we postulate that TOG1 is required to maintain the spindle assembly checkpoint by localising Nuf2 at the kinetochore, thereby stabilising the kinetochore structure for Mad2 and Mad3 turnover. In this chapter, we investigate the effects of overproducing TOG domains. Overexpression of both TOG domains was found to result in elongated cytoplasmic microtubules. We propose that this is an effect of the second TOG domain (TOG2) as our previous studies suggest that TOG1 does not possess microtubule-regulating function. We have also found that overexpression of *pTOG*⁺ is lethal in a Mad2- and Bub1- dependent manner suggesting that TOG1 hyper-activates the spindle assembly checkpoint in this condition. Intriguingly, accumulation of Bub1 but not Mad2 was detected in *pTOG*⁺ overexpression.

The lethality of *pTOG*⁺ is dependent on the presence of all spindle checkpoint proteins. Despite TOG1 dependency on all checkpoint components, Bub1 is recruited to the kinetochore without Mad2, suggesting that Mad2 localisation to the kinetochore is not essential for spindle checkpoint activation. Previous studies of the requirement of Mad2 have been somewhat controversial. In vivo studies have often used Mad2 localisation to the kinetochore as a hallmark of spindle checkpoint activation (Li and Benezra 1996; Chen *et al.* 1996; Waters *et al.* 1998; Howell *et al.* 2000). However, some reports, including in vivo studies, have suggested the existence of the non-kinetochore Mad2-Slp1 complex, which is able to inhibit APC (Meraldi *et al.* 2004; Gillett *et al.* 2004). In addition, in *nuf2* mutants or Nuf2/Ndc80/Hec1 depletion, the spindle assembly checkpoint is activated even though Mad2 is not recruited to the kinetochore (Martin-Lluesma *et al.* 2002; Meraldi *et al.* 2004; Gillett *et al.* 2004). However, lack of Mad2 recruitment was not representative of Mad2 requirement as simultaneous depletion of hHec1 and hMad2 resulted in catastrophic mitotic exit (Martin-Lluesma *et al.* 2002).

This report displays a close resemblance to our finding in *pTOG*⁺ overexpression that Mad2 is not recruited to the kinetochores even though the overexpression led to mitotic arrest and lethality in a Mad2-dependent fashion.

In our study, the localisation of Bub1 without Mad2 in *pTOG*⁺ could be a result of direct Mad2-Slp1 binding, without Mad2 turnover at the kinetochore. If this were true, it would suggest that TOG1 could directly regulate the spindle assembly checkpoint via Mad2. Alternately, our localisation data (Bub1 without Mad2) could be a reflection of TOG1 function via the Nuf2/Ndc80 complex. The outer-kinetochor complex has repeatedly been shown to be crucial for recruitment of specific checkpoint proteins by independent groups (Martin-Lluesma *et al.* 2002; DeLuca *et al.* 2003; Gillett *et al.* 2004; Meraldi *et al.* 2004; Bharadwaj *et al.* 2004). For example, lost of hHec1 localisation at the kinetochore by RNAi or anti-body depletion in HeLa cells causes kinetochore-localisation of Mps1, Mad2, and Mad3 to be lost (Martin-Lluesma *et al.* 2002; Meraldi *et al.* 2004). In these studies, the recruitment of Bub1 or BubR1 were intriguing unaffected, suggesting that the Nuf2/Ndc80 complex may regulate the spindle assembly checkpoint specifically via Mph1, Mad1 and Mad2. This supports earlier findings that the spindle checkpoint cascade is probably not linear and may contain branches (Waters *et al.* 1998; Hoffman *et al.* 2001; Tang *et al.* 2001; Rajagopalan *et al.* 2004; Tournier *et al.* 2004). Although the Nuf2/Ndc80 proteins appear to localise as wild type in *pTOG*⁺ in our study, we cannot exclude the possibility that Nuf2/Ndc80 function is compromised in this condition.

Overall, our findings suggest that the first TOG domain of Alp14 specifically functions to maintain the spindle assembly checkpoint. Although artificial conditions were often used in the study, results of TOG1 deletion and overexpression have consistently implicate the function of TOG1 in the spindle checkpoint cascade. Despite sequence and functional conservation of the TOG family of proteins, the role of TOG domains in the spindle assembly checkpoint has never been reported previously. The role of TOG proteins in the spindle checkpoint may be masked by their functions in microtubule-stabilisation in other organisms. It is of note that like TOG homologues in budding yeast and higher eukaryotes, the spindle checkpoint is also activated in *alp14* mutants at the restrictive temperature, where the lack of functional Alp14 causes weak spindles and spindle-kinetochore interaction. It is only when spindle damage is induced at the

permissive temperature in *alp14* temperature-sensitive mutants that Alp14's role in spindle checkpoint becomes evident. By systematic truncations of Alp14, we have been able to separate the spindle checkpoint function from the microtubule-stabilising function, facilitating the study of the protein's involvement in the spindle assembly checkpoint.

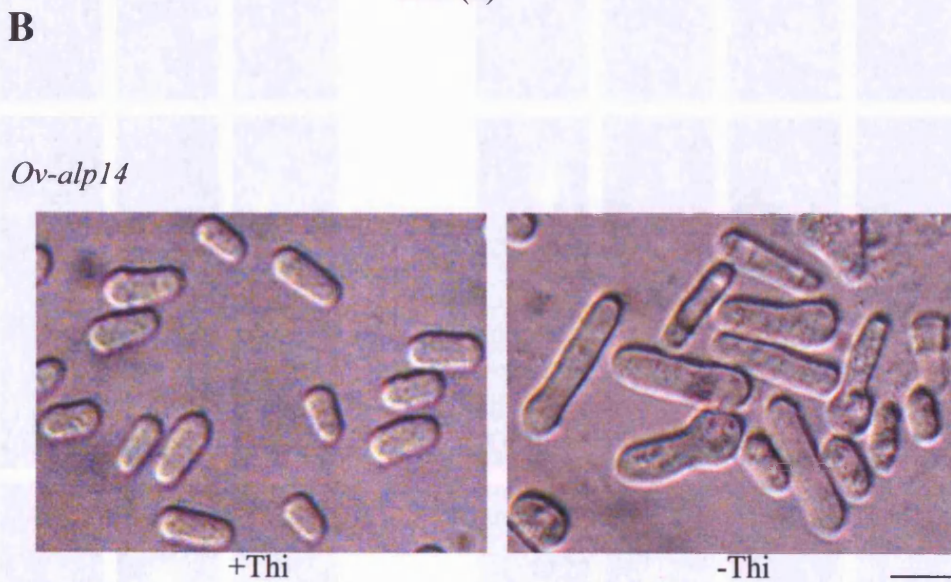
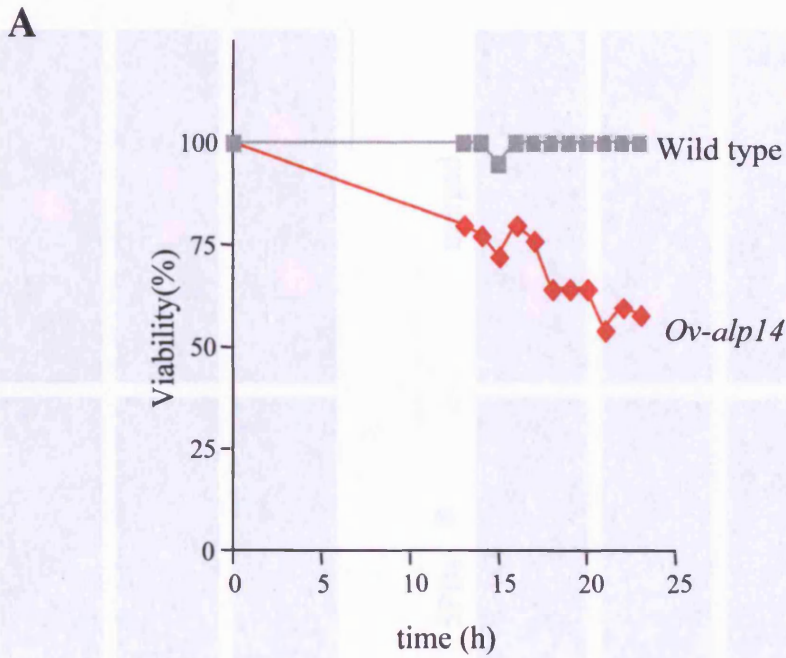
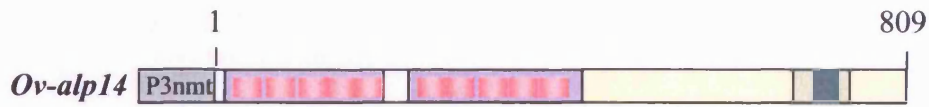
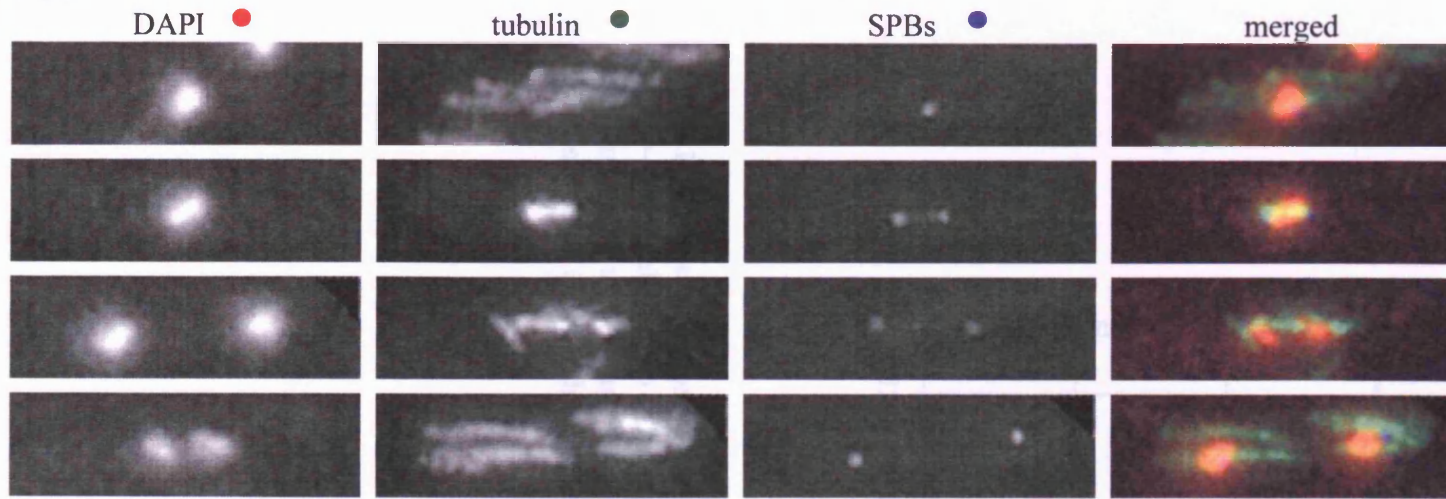


Fig. 4.1.1 Overexpression of *alp14*⁺ is toxic. **A)** Wild type and *ov-Alp14* cells grown in rich media were filtered and inoculated in media lacking thiamine for up to 23 hours. Samples were taken hourly and plated onto fresh media at 200 cells per plate and incubated at 30°C for three days. Percentage of viability was determined by the number of colonies grown. **B)** *Ov-Alp14* cells were streaked onto minimal media in presence or absence of thiamine and incubated at 30°C for two days. Inducible promoter expresses Alp14 in absence of thiamine. The scale bar represents 10µm.

Wild type



*Ov-*alp14**

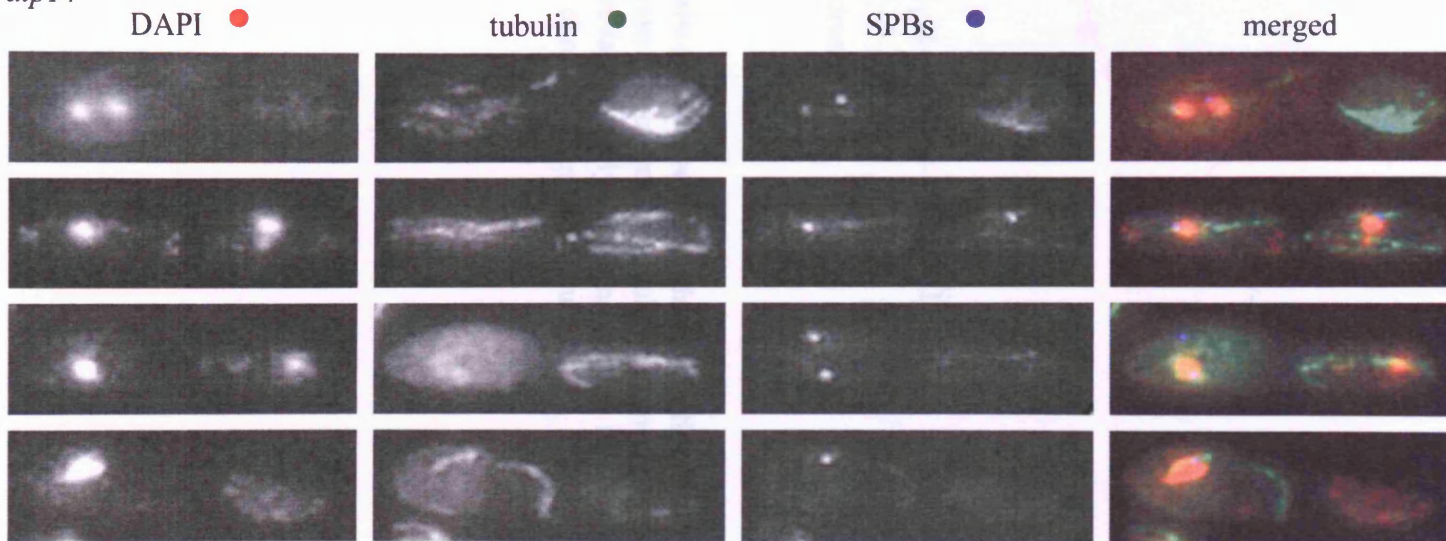


Fig. 4.1.2 Overexpression of *alp14*⁺ results in chromosome missegregation and microtubule defects. Wild type and *ov-Alp14* cells grown in rich media were filtered and reinoculated in media lacking thiamine for 20 hours. Cells were fixed with methanol and processed for immunofluorescence with anti-tubulin and anti-SAD1 staining. The scale bar represents 10 μ m.

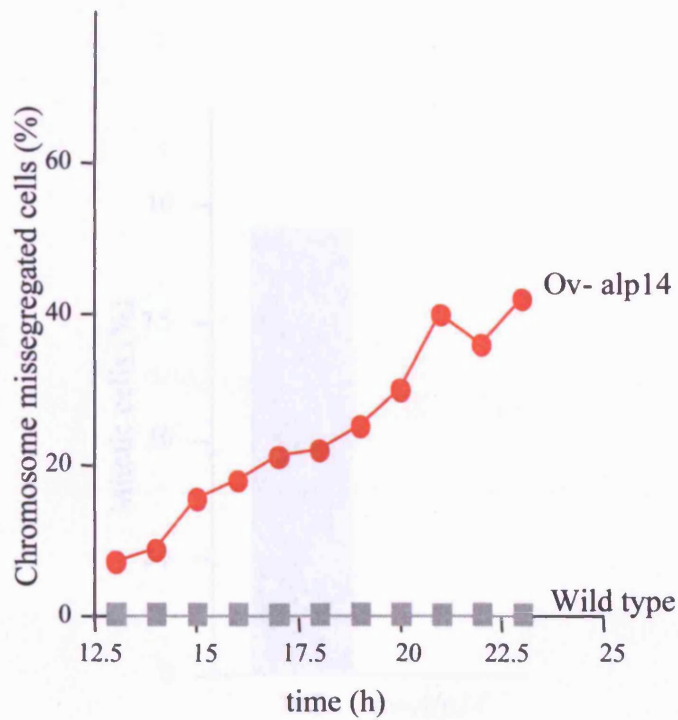


Fig. 4.1.3 Overexpression of *alp14*⁺ results in chromosome missegregation. Wild type and *ov-Alp14* cells grown in rich media were filtered and reinoculated in media lacking thiamine for up to 23 hours. Samples were taken hourly for formaldehyde fixation and DAPI staining. Cells with missegregated chromosomes were counted.

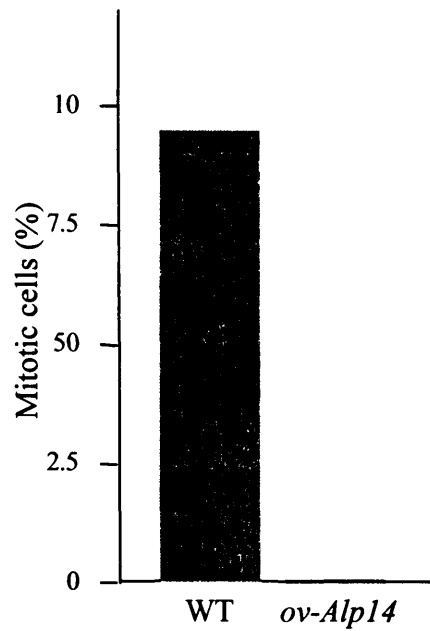


Fig. 4.1.4 Overexpression of *alp14*⁺ results in accumulation of cells in interphase. Wild type and *ov-Alp14* cells grown in rich media were filtered and reinoculated in media lacking thiamine for 20 hours. Cells processed for immunofluorescence with anti-tubulin and DAPI staining were counted.

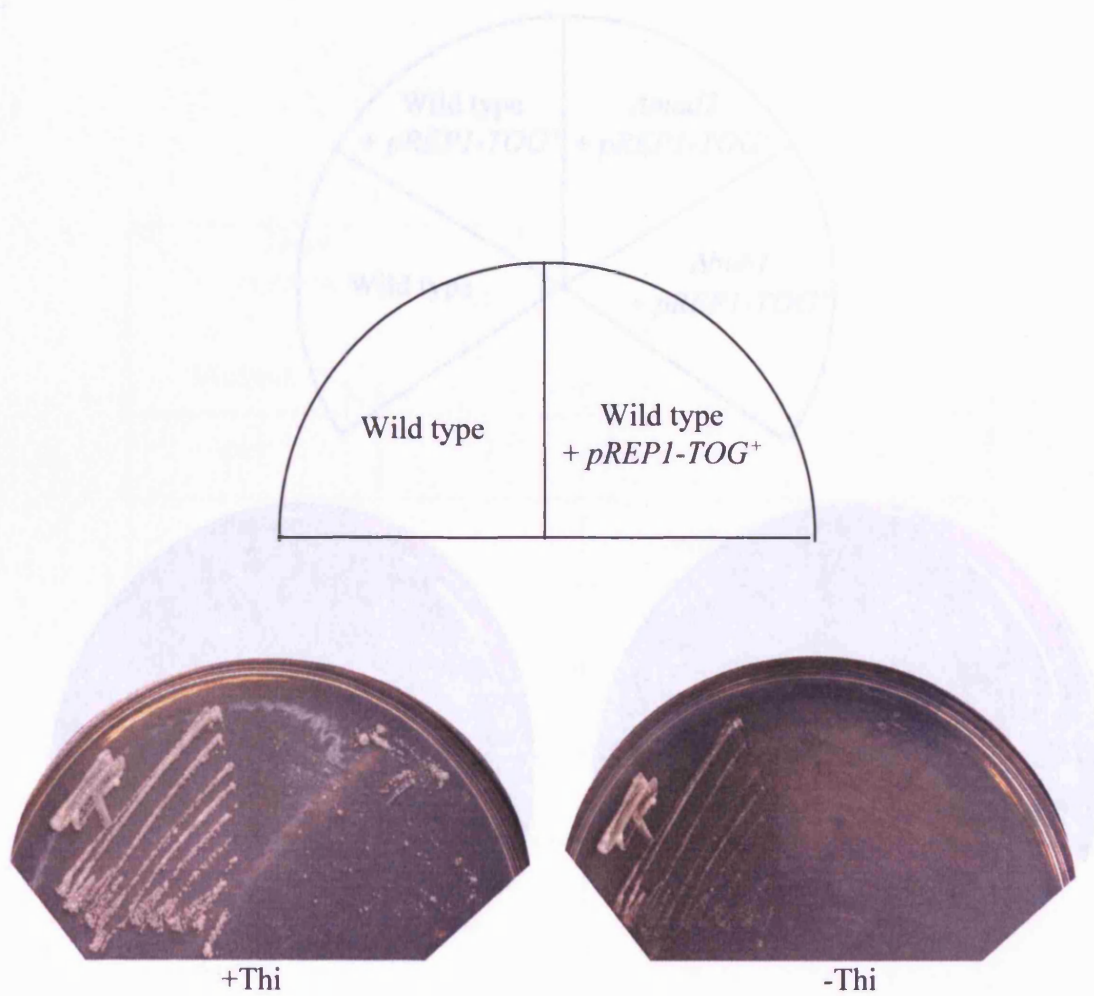


Fig. 4.2.1 Overexpression of $pTOG^+$ results is toxic. Wild type cells containing pREP1 or $pREP1-TOG^+$ were streaked onto selective media in presence or absence of thiamine at 27°C for 3 days. Note that wild type cells containing empty pREP1 showed normal growth on plates (data not shown).

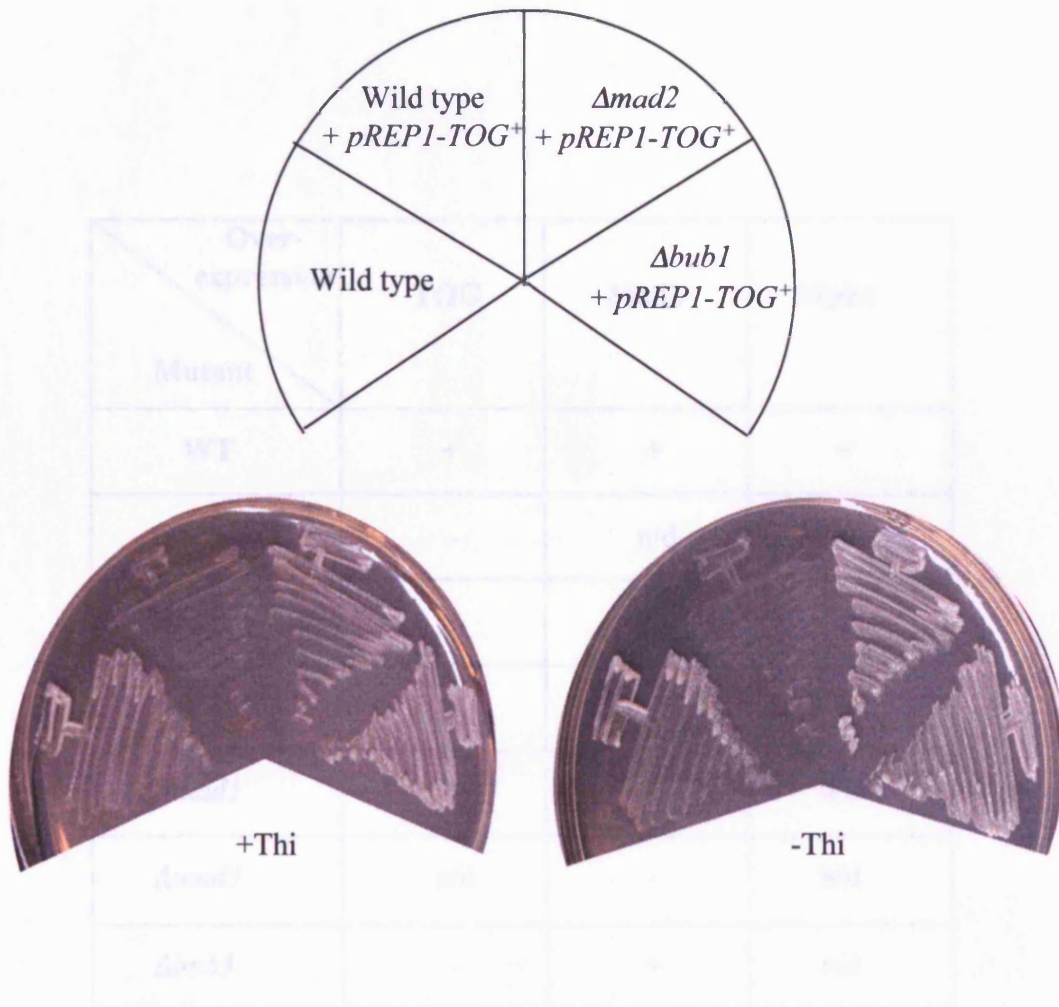


Fig. 4.2.2 Toxicity of $pTOG^+$ overexpression is dependent on the presence of Mad2 and Bub1. Wild type, $\Delta mad2$ and $\Delta bub1$ cells containing $pREP1-TOG^+$ were streaked onto selective media in presence or absence of thiamine at 27°C for 2 days.

Over-expression Mutant	TOG	Mad2	Mph1
WT	+	+	+
<i>Δmad2</i>	-	n/d	-
<i>Δbub1</i>	-	+	-
<i>Δmph1</i>	-	+	+
<i>Δmad1</i>	-	+	n/d
<i>Δmad3</i>	n/d	-	n/d
<i>Δbub3</i>	-	+	n/d

Table. 4.2.3 Toxic-dependency of overproduction of TOG or spindle checkpoint proteins. Wild type, *Δmad2*, *Δbub1*, *Δmph1*, *Δmad1*, *Δmad3* and *Δbub3* cells containing *pREP1-TOG⁺*, *pREP41x-mad2⁺* or *pREP41x-mph1⁺* were streaked onto selective media in presence or absence of thiamine at 27°C for 2 days. The + symbol represents growth arrest / toxicity. The - symbol represents non-toxicity. n/d represents non-determined phenotypes. Note that the Mad2 overexpression data presented above is adapted from Millband and Hardwick 2002.

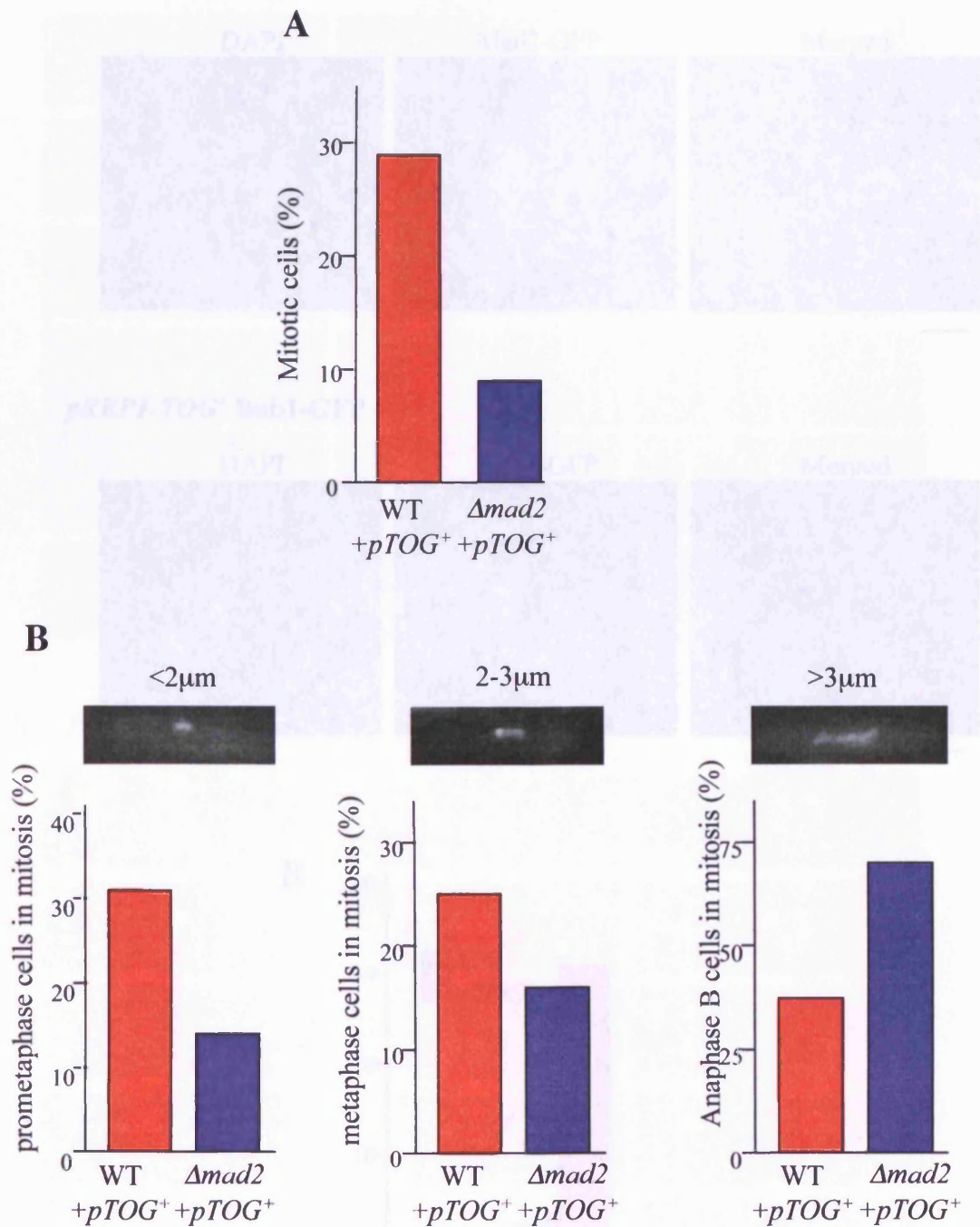
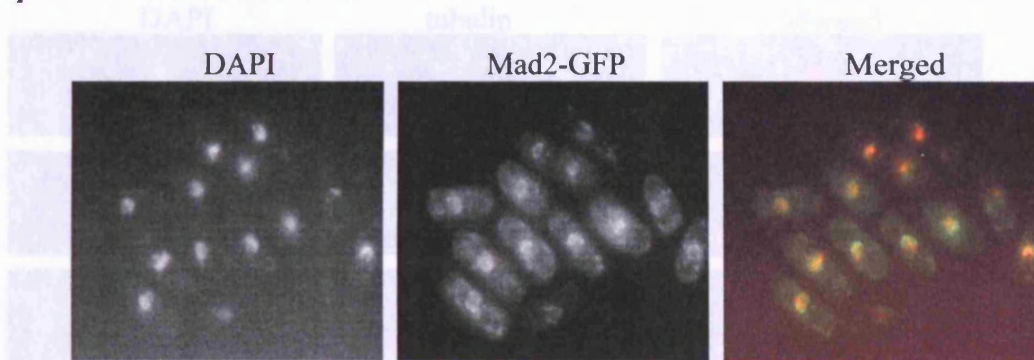


Fig. 4.2.4 Overexpression of $pTOG^+$ results Mad2-dependent metaphase arrest. Wild type and $\Delta mad2$ cells containing $pREP1-TOG^+$ were grown in rich media, filtered and reinoculated in selective media in absence of thiamine at 26°C for 16 hours. They were then fixed with methanol and processed for immunostaining with anti- α -tubulin antibody. **A)** The percentage of mitotic cells after 6 hours in overexpression condition. **B)** Of the mitotic cells, the percentage of prometaphase (spindles <2 μ m), metaphase (spindles 2-3 μ m), and anaphase (spindles >3 μ m) cells were counted.

A *pREP1-TOG⁺ Mad2-GFP*



pREP1-TOG⁺ Bub1-GFP

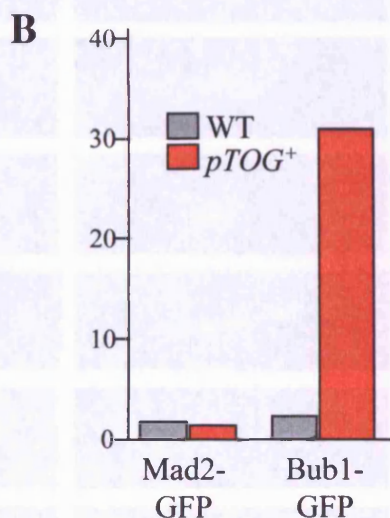
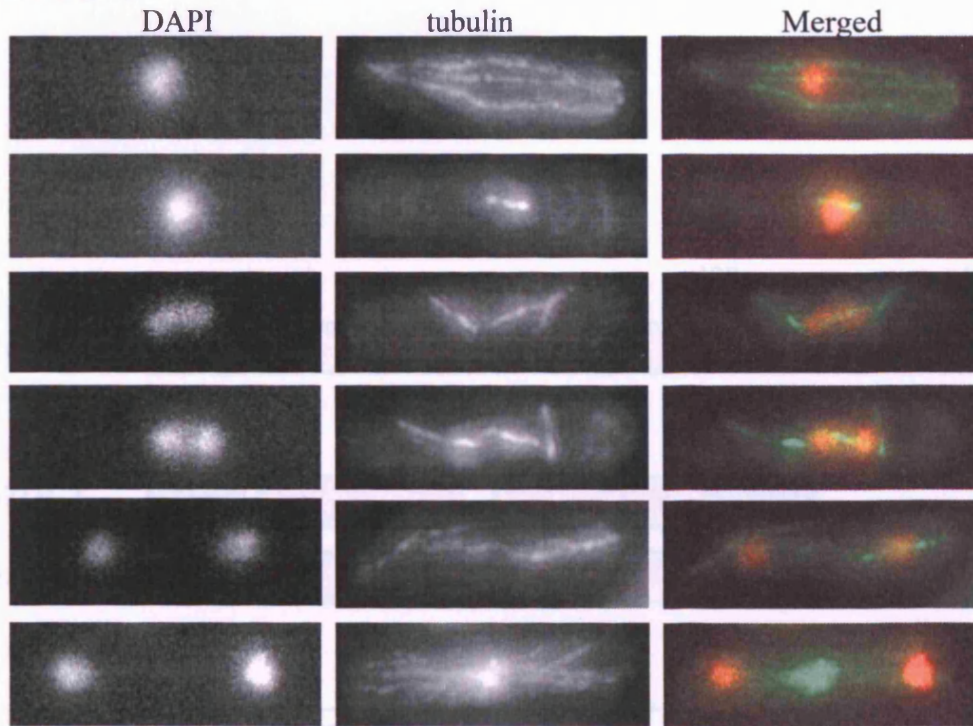


Fig. 4.2.5 Overexpression of *pTOG⁺* results localisation of Bub1 but not Mad2. Wild type cells containing *pREP1-TOG⁺* and *mad2⁺-GFP* or *bub1⁺-GFP* were grown in rich media, filtered and reinoculated in selective media in absence of thiamine at 26°C for 6 hours. **A)** Cells showing Mad2-GFP and Bub1-GFP localisation. **B)** The percentage of cells showing strong Bub1 or Mad2 dots at the kinetochore. The scale bar represents 10µm.

pREP1-TOG⁺ WT



pREP1-TOG⁺ $\Delta mad2$

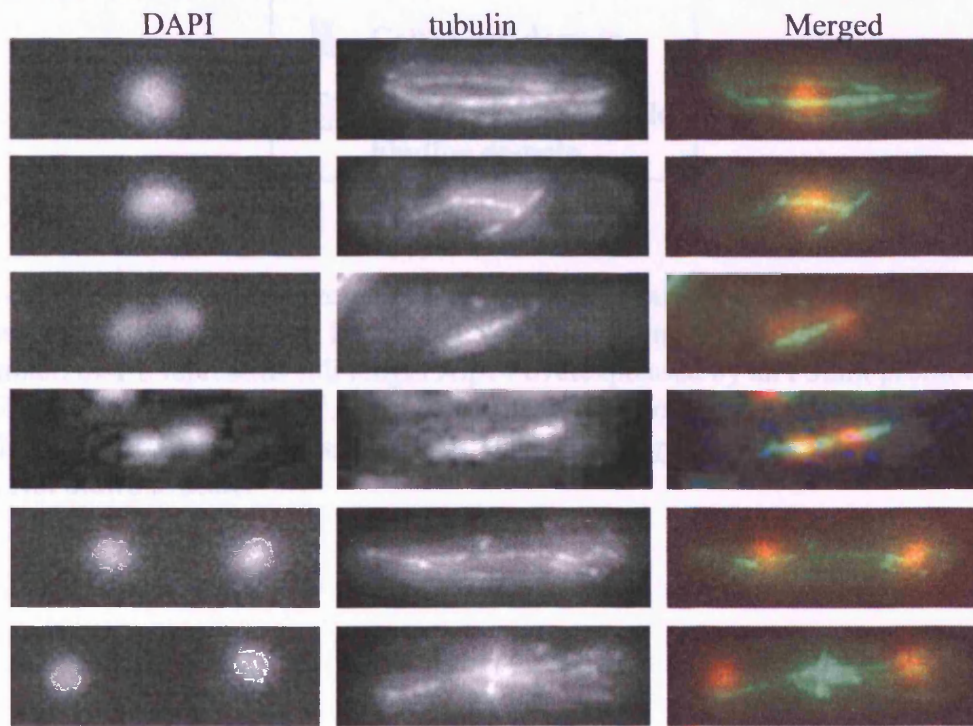


Fig. 4.2.6 Overexpression of *pTOG*⁺ results in long astral microtubules. Wild type and $\Delta mad2$ cells containing *pREP1-TOG*⁺ were grown in rich media, filtered and reinoculated in selective media in absence of thiamine at 26°C for 16 hours. They were then fixed with methanol and processed for immunostaining with anti- α -tubulin antibody. Visualisation of cells shows cytoplasmic microtubules in interphase and astral spindles in anaphase to be elongated. Note that wild type cells carrying empty pREP1 display normal microtubule phenotypes (data not shown). The scale bar represents 10 μ m.

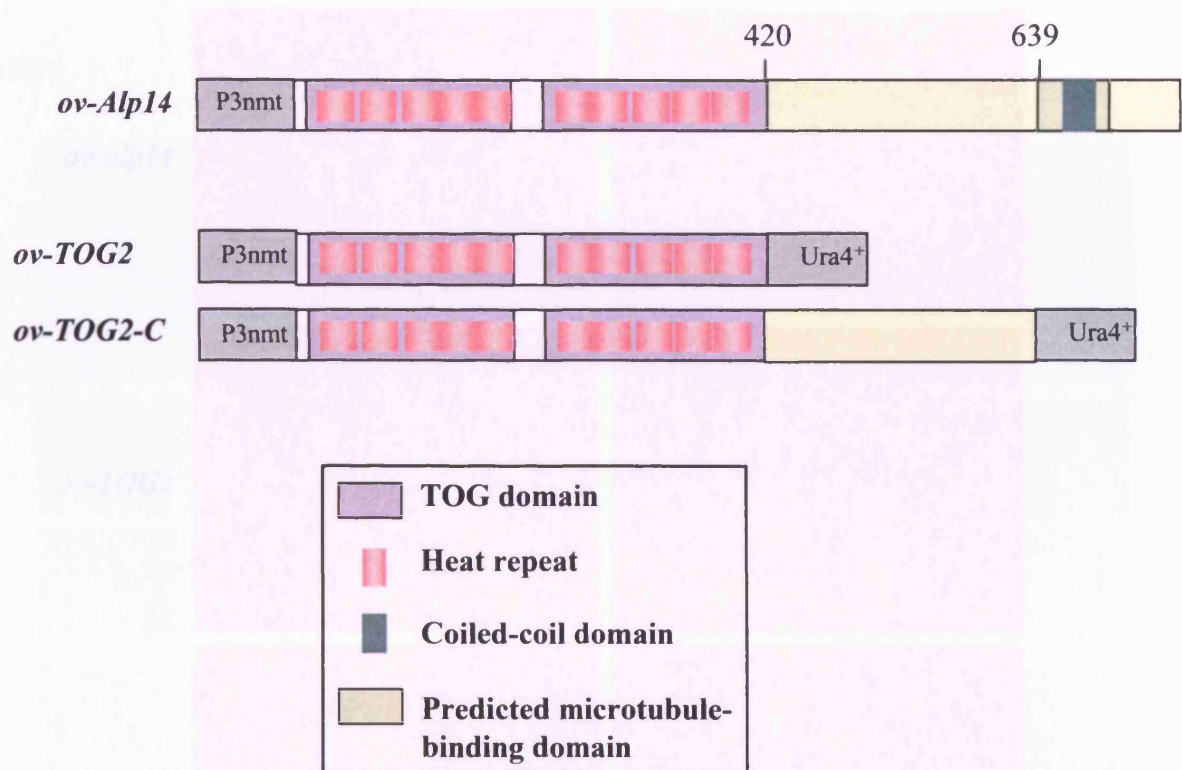


Fig. 4.3 Systematic overexpression of *alp14*⁺ N-terminal. Structural diagram of overexpressions of Alp14 full length and N-terminal using an inducible P3nmt promoter. *ov-FL* represents full length Alp14 overexpressed by an P3nmt promoter. *ov-TOG2* is an overexpression of Alp14 N-terminal TOG domains at residues 1-420. *ov-TOG2-C* represent overexpression of the TOG and C-terminal region at residues 1-639. Not drawn to scale.

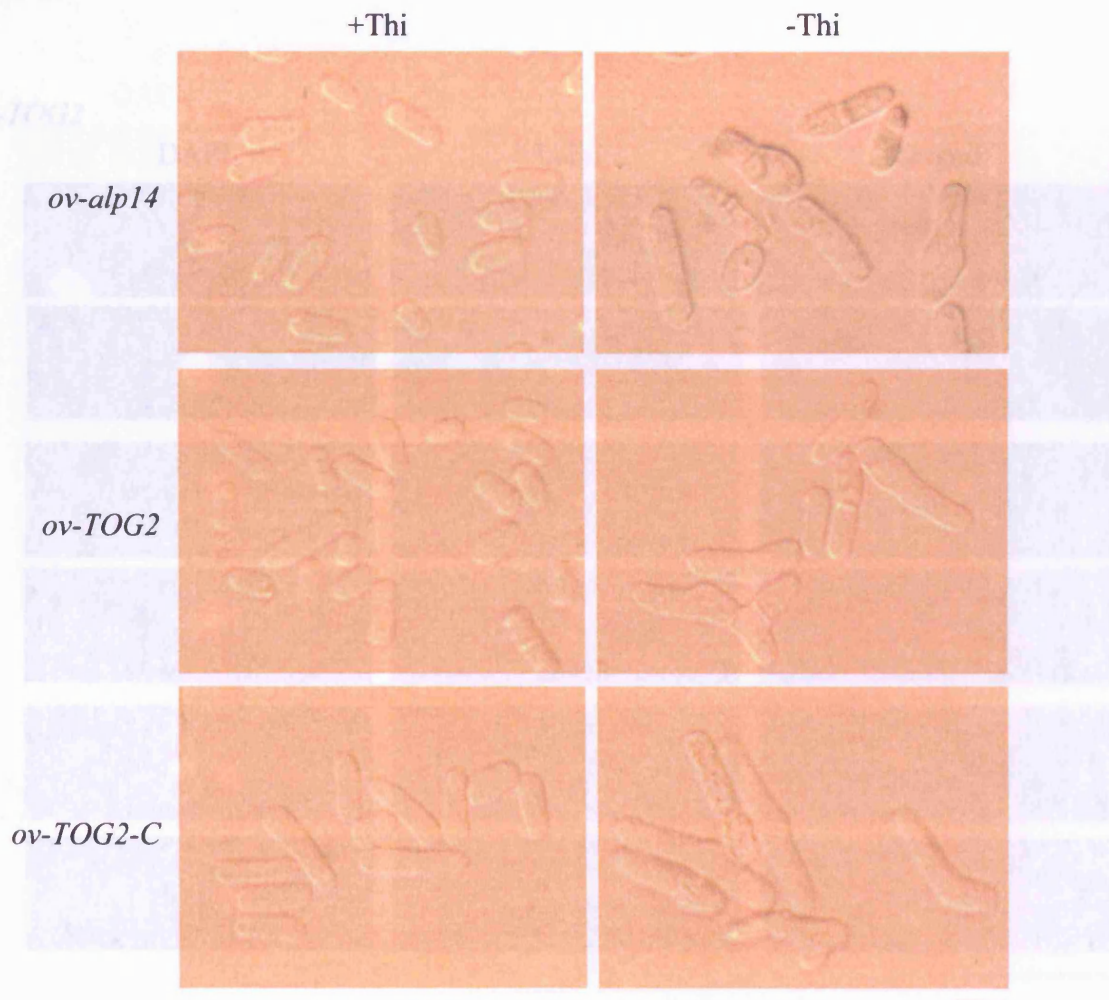


Fig. 4.3.1 Overexpression of *alp14* N-terminal results in cell polarity defects. *ov-*alp14**, *ov-*TOG2** and *ov-*TOG2-C** cells grown on plates containing minimal media in absence or presence of thiamine at 27°C for 3 days and visualised. The scale bar represents 10µm.

Fig. 4.3.1 Overexpression of *alp14* N-terminal results in cell polarity defects. *ov-*alp14**, *ov-*TOG2** and *ov-*TOG2-C** strains grown on plates containing minimal media in absence or presence of thiamine at 27°C for 3 days and visualised. The scale bar represents 10µm.

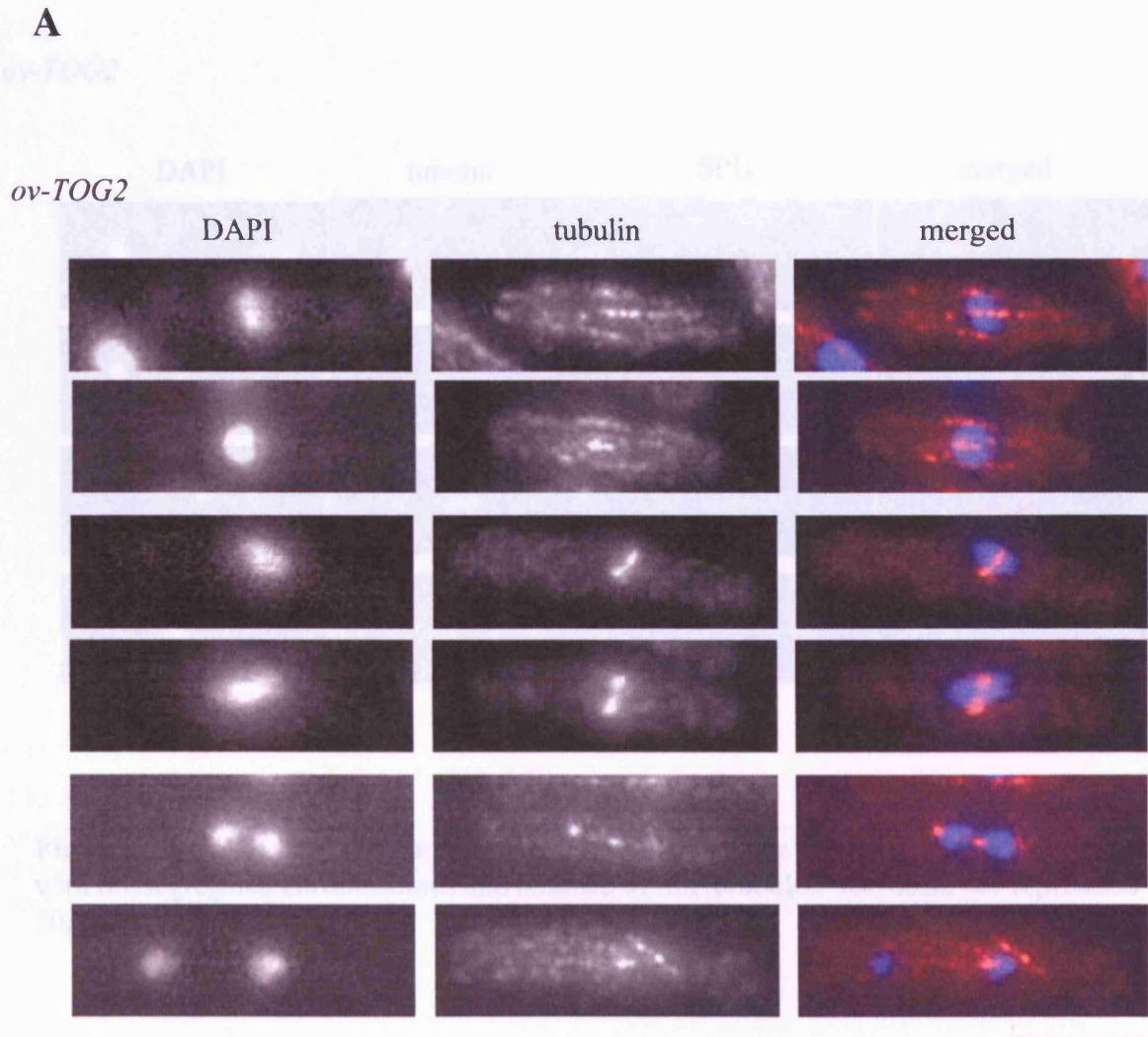


Fig. 4.3.2 Overexpression of *alp14* N-terminal results in microtubule defects. *ov-TOG2* and *ov-TOG2-C* cells grown in rich media were filtered and reinoculated in media lacking thiamine at 30°C for 12-24 hours. Cells were fixed with methanol and processed for immunofluorescence staining with anti α -tubulin. **A)** Cells after 12 hours in overexpressed condition show weak microtubules. Continues next page. The scale bar represents 10 μ m.

B

ov-TOG2

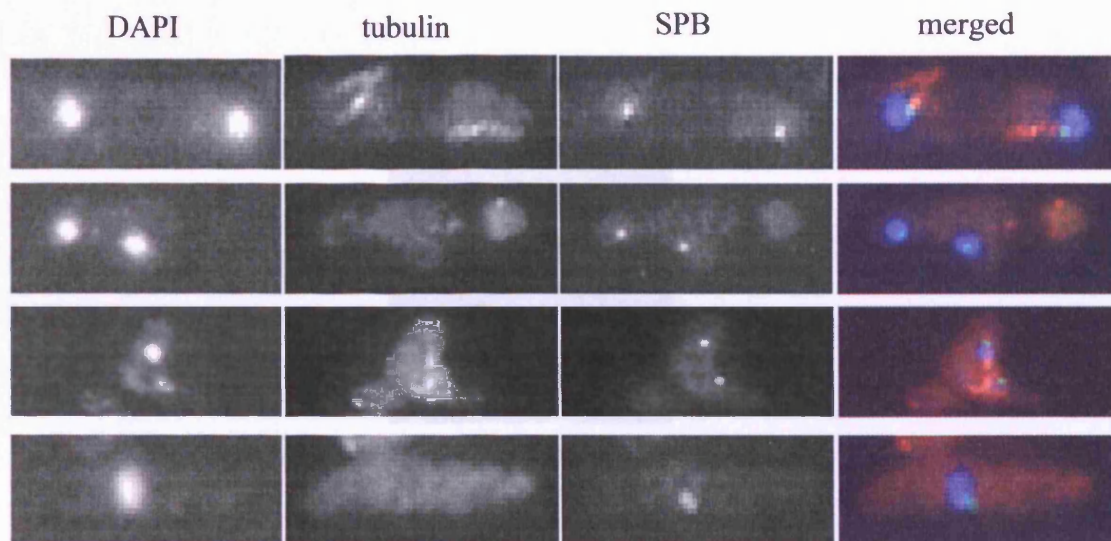


Fig. 4.3.2 B) Cells after 24 hours in overexpressed condition show terminal phenotype, with missegregated chromosomes and absence of microtubules. The scale bar represents 10µm.

Fig. 4.3.2 B) Cells after 24 hours in overexpressed condition show terminal phenotype, with missegregated chromosomes and absence of microtubules. The scale bar represents 10µm.

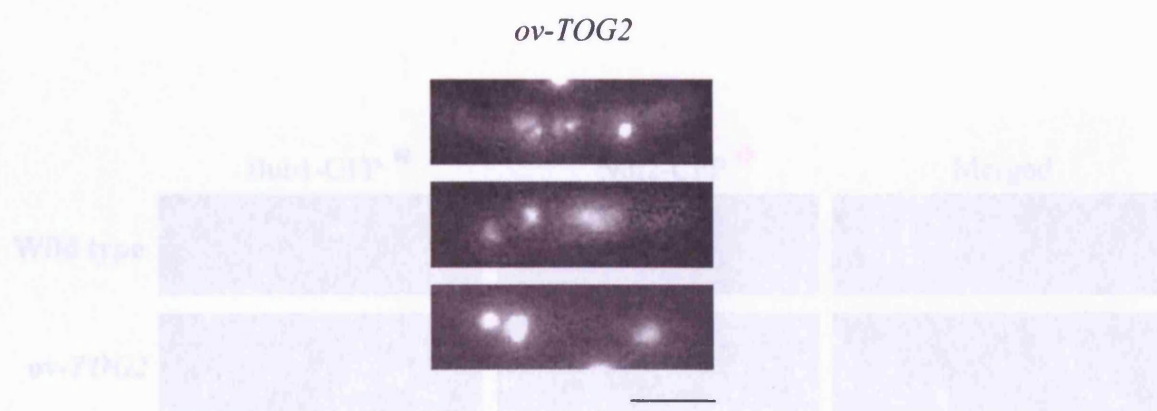


Fig. 4.3.3 Overexpression of *alp14* N-terminal results in chromosome missegregation. *ov-TOG2* cells grown in rich media were filtered and reinoculated in media lacking thiamine for 18 hours and processed for formaldehyde fixation and DAPI staining. Cells with missegregated chromosomes are shown. The scale bar represents 10 μ m.

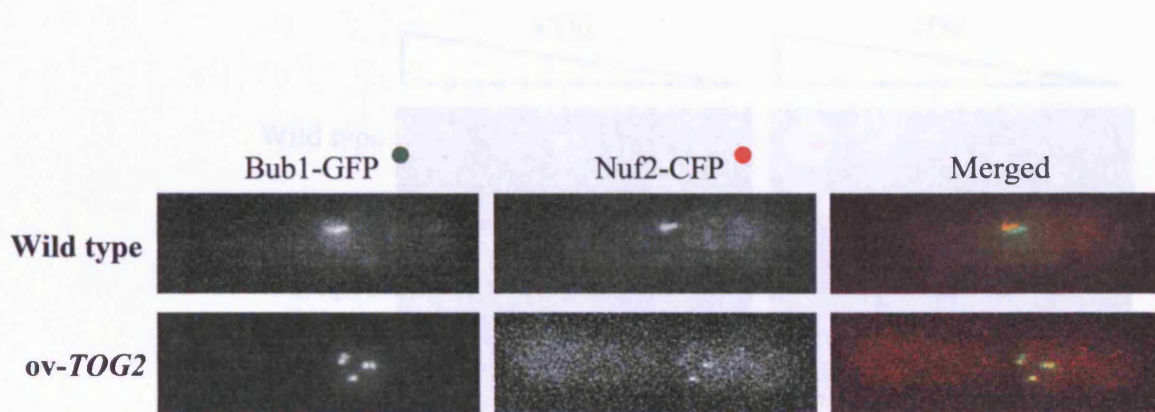


Fig. 4.3.4 Overexpression of *alp14* N-terminal results in dispersed kinetochores. *ov-TOG2* cells carrying *bub1*⁺-GFP and *nuf2*⁺-CFP were grown in rich media, filtered and reinoculated in media lacking thiamine for 18 hours. Bub1-GFP and Nuf2-CFP were observed in a live microscopic analysis. The scale bar represents 10µm.

Fig. 4.3.5 The toxicity of *alp14* N-terminal overexpression is alleviated by presence of *put14*⁺. Wild type, *del14*, *ov-TOG2*, *ov-TOG2* with *put14*⁺, *ov-TOG2* and *ov-TOG2* with *put14*⁺ strains were spotted in five serial dilutions (10⁷ to 10¹ cells) on minimal plates in the absence or presence of thiamine for 6 days at 27°C.

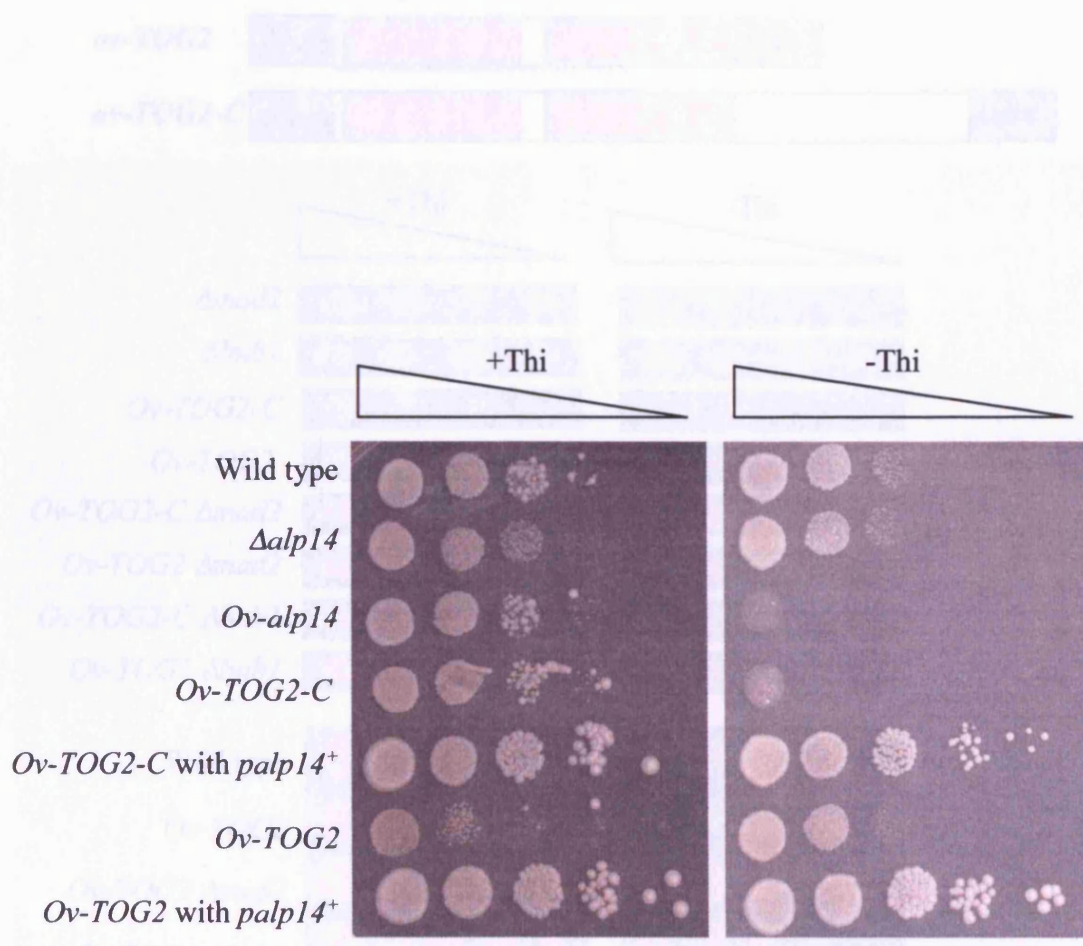


Fig. 4.3.5 The toxicity of *alp14* N-terminal overexpression is alleviated in presence of *palp14*⁺. Wild type, $\Delta alp14$, *ov-alp14*, *ov-TOG2-C*, *ov-TOG2-C* with *palp14*⁺, *ov-TOG2* and *ov-TOG2* with *palp14*⁺ strains were spotted after serial dilution (10^5 to 10^1 cells) on minimal plates in the absence or presence of thiamine for 6 days at 27°C.

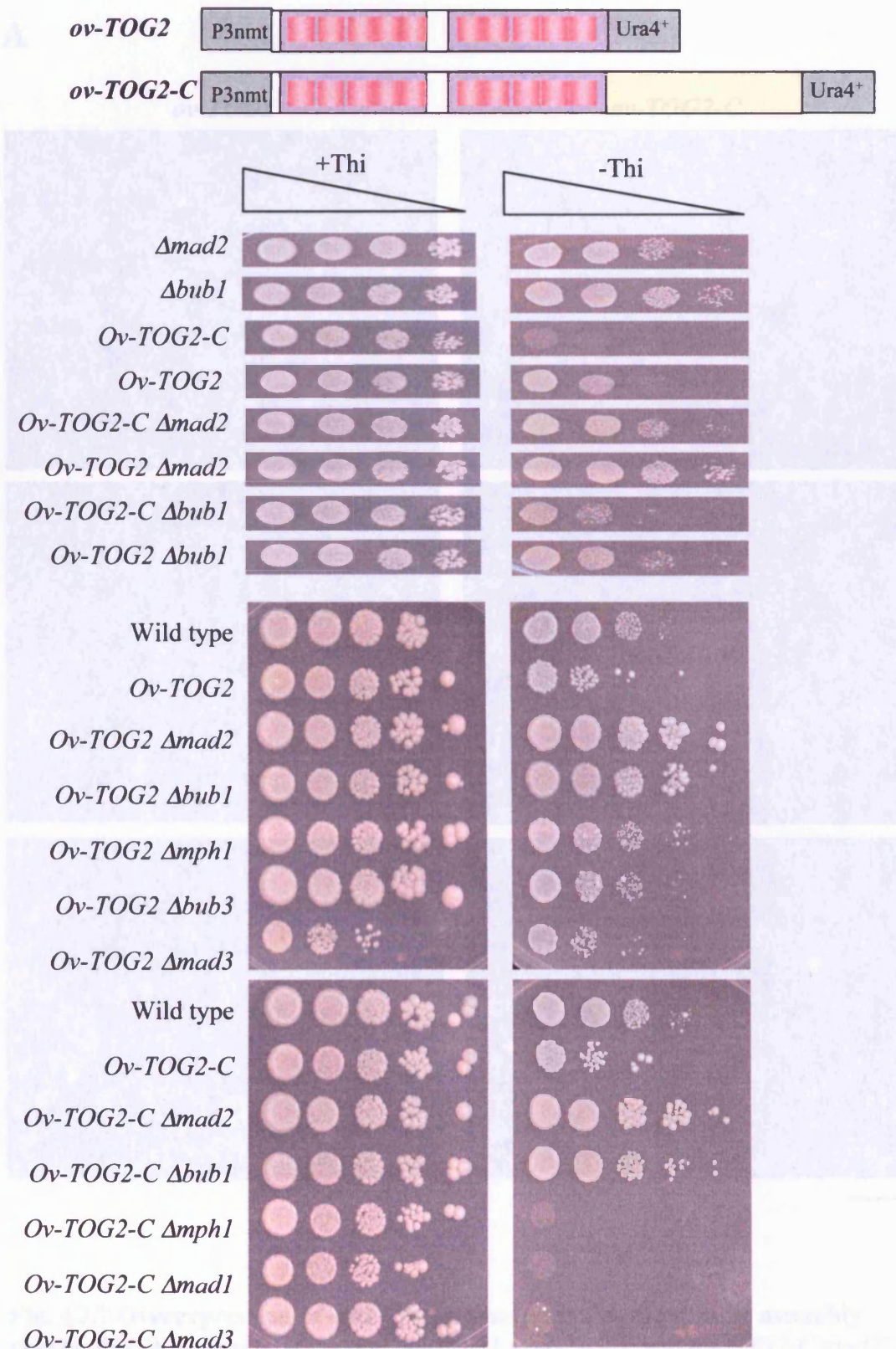


Fig. 4.3.6 The toxicity of *alp14* N-terminal overexpression is dependent on the presence of Mad2 and Bub1. Wild type, *ov-TOG2*, *ov-TOG2 Δmad2*, *ov-TOG2 Δbub1*, *ov-TOG2 Δmph1*, *ov-TOG2 Δbub3*, *ov-TOG2 Δmad3*, *ov-TOG2-C*, *ov-TOG2-C Δmad2*, *ov-TOG2-C Δbub1*, *ov-TOG2-C Δmph1*, *ov-TOG2-C Δmad1* and *ov-TOG2-C Δmad3* strains were spotted after serial dilution (10⁵ to 10¹ cells) on minimal plates in the absence or presence of thiamine for 6 days at 27°C. The toxicity of *alp14* N-terminal overexpression is alleviated when Mad2 or Bub1 are deleted.

A

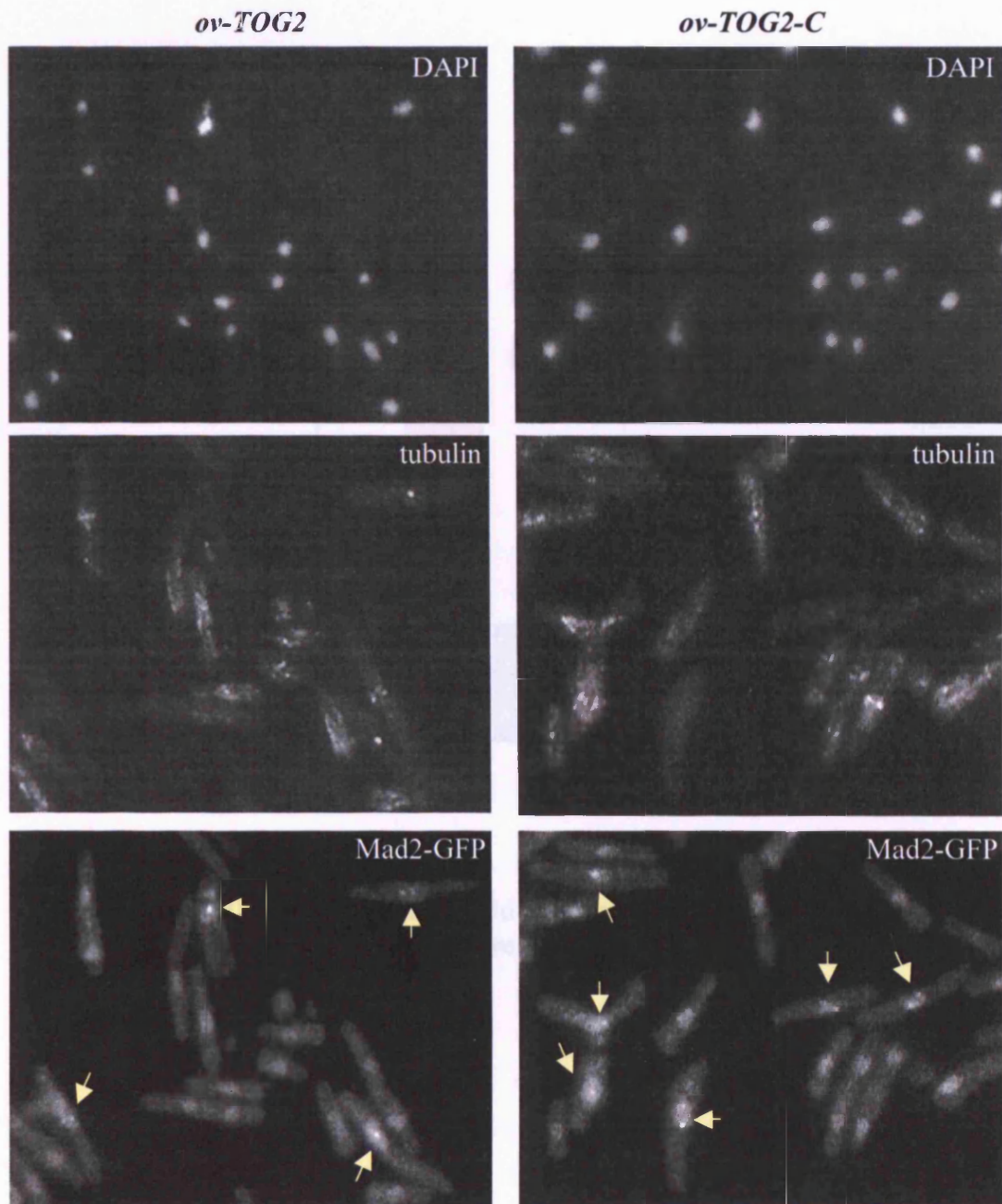


Fig. 4.3.7 Overexpression of *alp14* N-terminal activates the spindle assembly checkpoint. Wild type *mad2⁺-GFP*, *ov-TOG2 mad2⁺-GFP* and *ov-TOG2-C mad2⁺-GFP* cells grown in rich media were filtered and reinoculated in minimal media lacking thiamine for 14-30 hours. Cells were fixed with methanol and processed for immunofluorescence staining with anti-tubulin. **A)** Cells after 20 hours in overexpressed condition showing Mad2-GFP. The scale bar represents 10 μ m. Continues next page.

B

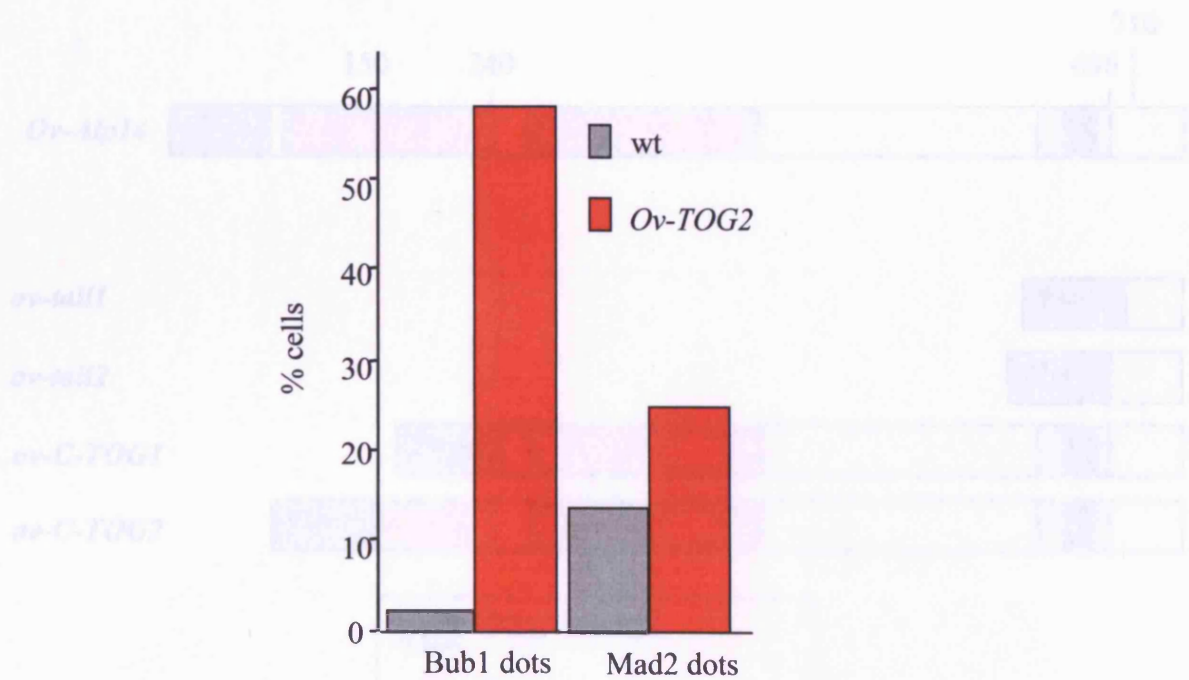


Fig. 4.3.7 B) Quantification of wild type and *ov-TOG2* cells containing Mad2 and Bub1 dots at kinetochores at 20 hours in overexpressed condition.

Fig. 4.3 Systematic overexpression of α 14 *Oocytes contain a single copy of*
overexpression of α 14 full length with increased stability in the presence of
*proteases. *ov- α 14/1* represents full length α 14 protein with a myc tag. *ov- α 14/2**
**ov-tell1* and *ov-tell2* are overexpression of α 14. *ov-tell1* and *ov-tell2* represent*
*and 697-809, respectively. *ov-C-TOG1* and *ov-C-TOG2* represent overexpression of*
*the C-terminal and TOG domain, at a wt wt 341-804 and 1-809, respectively. *ov-**
down to scale.

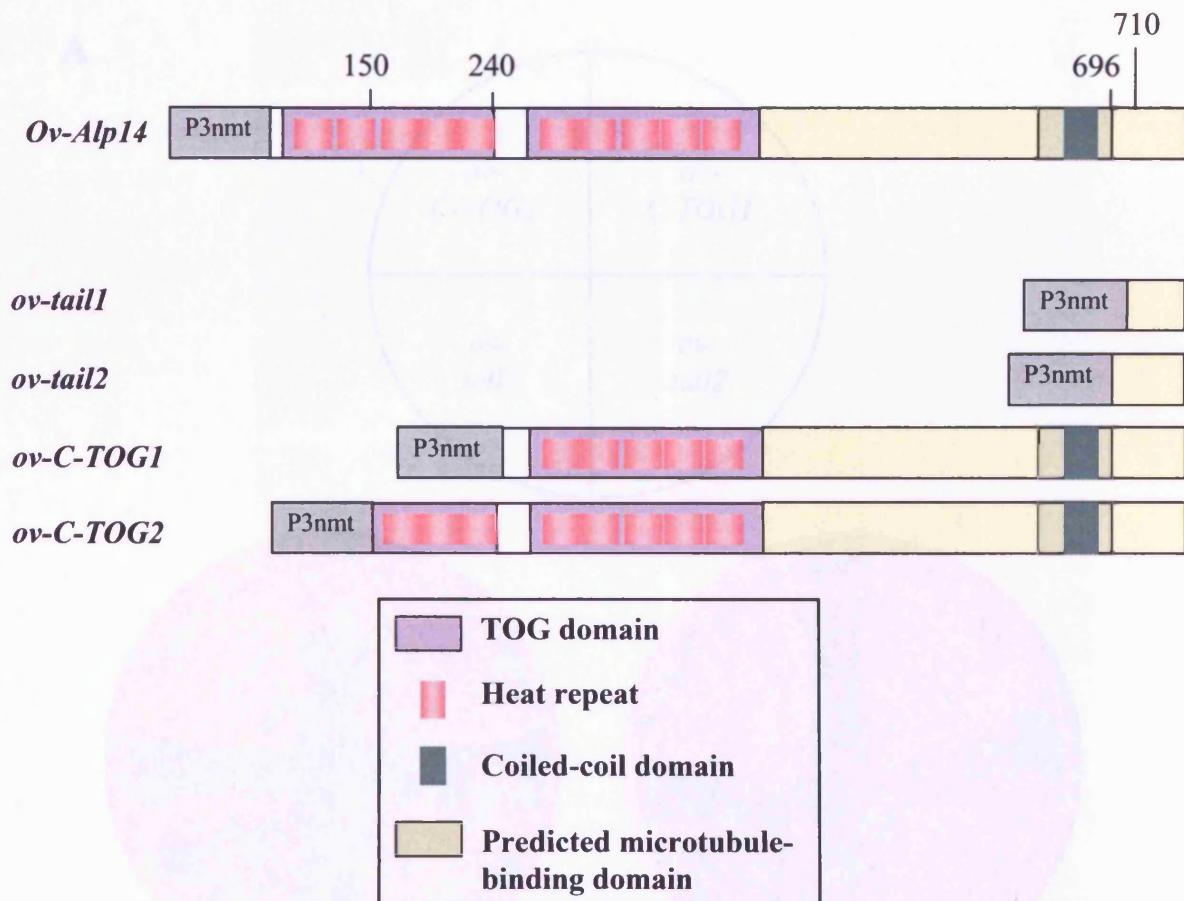


Fig. 4.4 Systematic overexpression of *alp14*⁺ C-terminal. Structural diagram of overexpressions of Alp14 full length and C-terminal using an inducible *P3nmt* promoter. *ov-Alp14* represents full length Alp14 overexpressed by an *P3nmt* promoter. *ov-tail1* and *ov-tail2* are overexpressions of Alp14 C-terminal tail at residues 710-809 and 697-809, respectively. *ov-C-TOG1* and *ov-C-TOG2* represent overexpressions of the C-terminal and TOG domains at residues 241-809 and 151-809, respectively. Not drawn to scale.

A

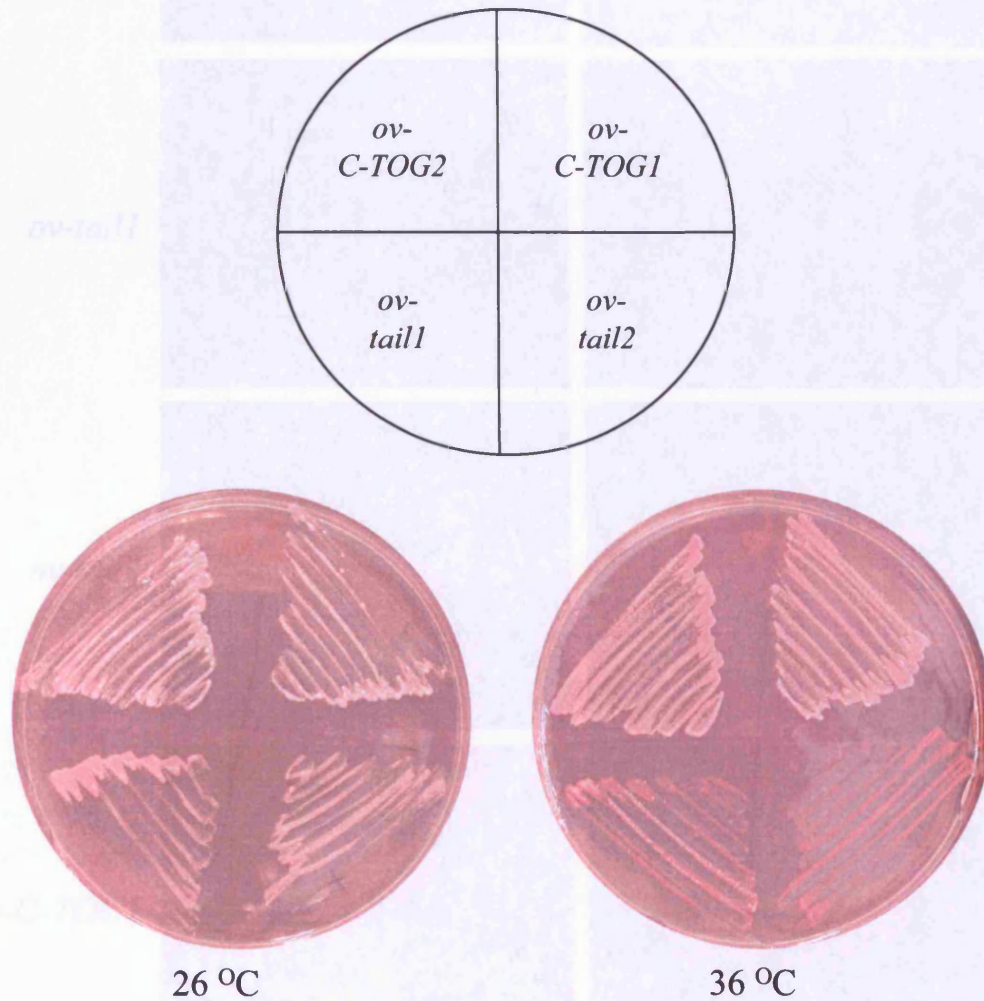


Fig. 4.4.1 The absence of the C-terminus results in temperature-sensitivity. A) *ov-tail1*, *ov-tail2*, *ov-C+TOG1* and *ov-C+TOG2* strains were streaked onto minimal media containing phloxine B at 26°C or 36°C for 2-3 days. Red colonies at 36°C are indicative of temperature-sensitivity. Continues next page.

Fig. 4.4.1 *Δalp14*, *ov-tail1*, *ov-tail2*, *ov-C+TOG1* and *ov-C+TOG2* strains grown on plates containing minimal media in the presence of phloxine B at 26°C or 36°C for 2-3 days and photographed. The scale bar represents 1 cm.

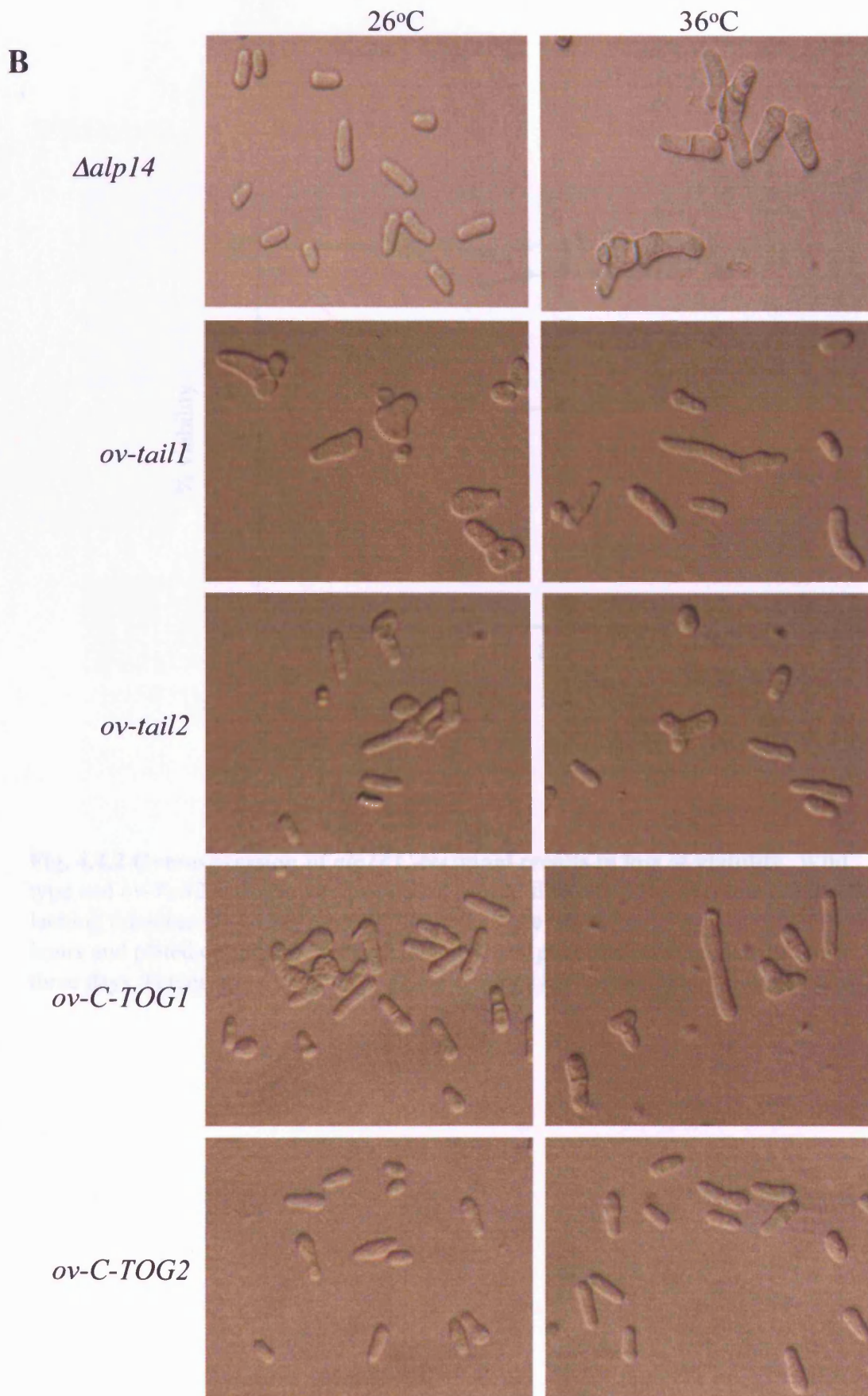


Fig. 4.4.1 *Δalp14*, *ov-tail1*, *ov-tail2*, *ov-C+TOG1* and *ov-C+TOG2* strains grown on plates containing selective media in absence of thiamine at 26°C or 36°C for 2-3 days and visualised. The scale bar represents 10µm. 165

Wild type

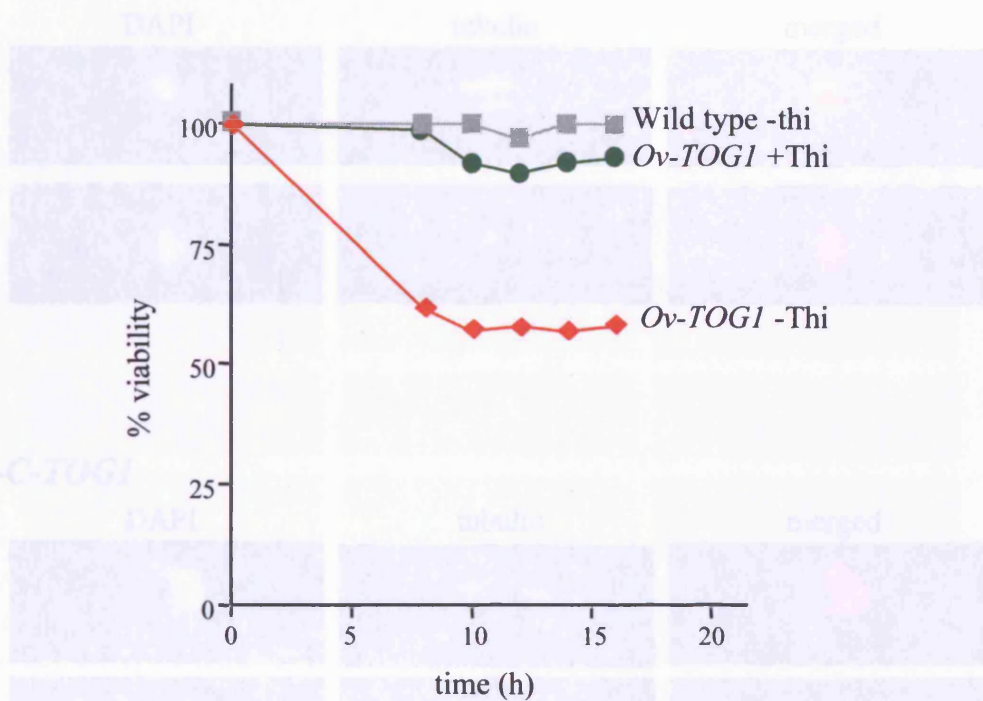
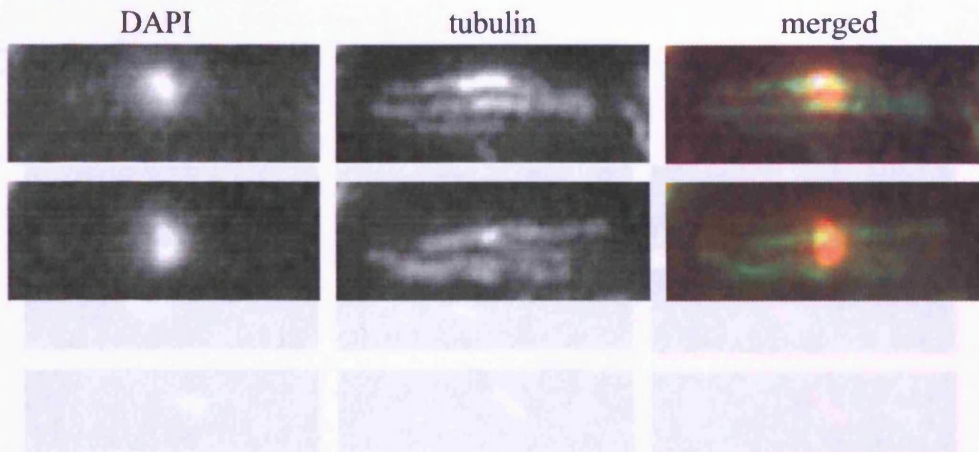


Fig. 4.4.2 Overexpression of *alp14* C-terminal results in loss of viability. Wild type and *ov-Tail2* cells grown in rich media were filtered and reinoculated in media lacking thiamine for up to 16 hours. Samples were taken every two hours from 8-16 hours and plated onto fresh media at 200 cells per plate and incubated at 30°C for three days. Percentage of viability was determined by the number of colonies grown.

Fig. 4.4.3 Overexpression of *alp14* C-terminal results in microtubule defects. Wild type and *ov-C-TOG1* cells grown in rich media were filtered and reinoculated in media lacking thiamine for 12 hours. Cells were fixed with methanol and processed for immunofluorescence staining with anti- α -tub. The scale bar represents 10 μ m.

Wild type



ov-C-TOG1

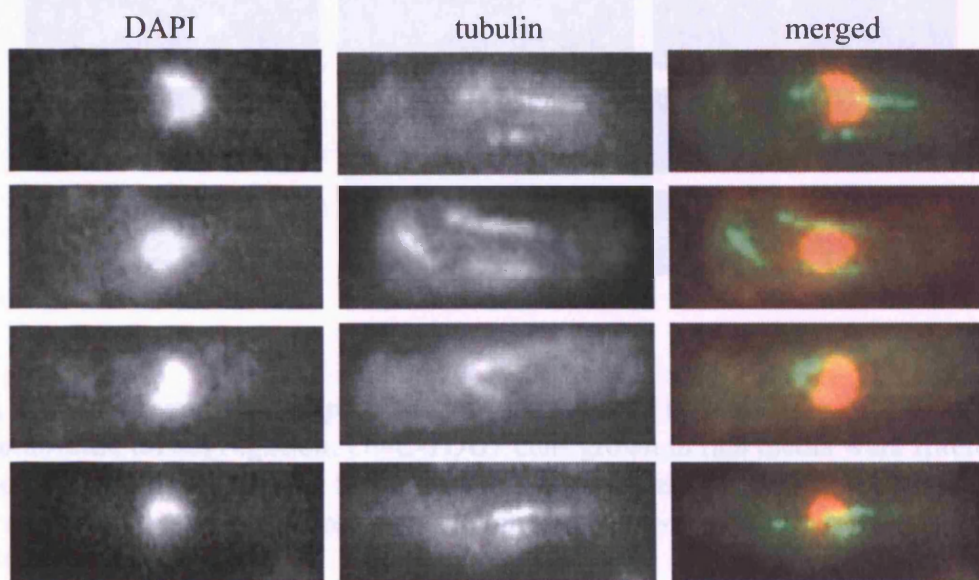


Fig. 4.4.3 Overexpression of *alp14* C-terminal results in microtubule defects.

Wild type and *ov-C-TOG1* cells grown in rich media were filtered and reinoculated in media lacking thiamine for 12 hours. Cells were fixed with methanol and processed for immunofluorescence staining with anti-tubulin. The scale bar represents 10 μ m.

Ov-C-TOG1

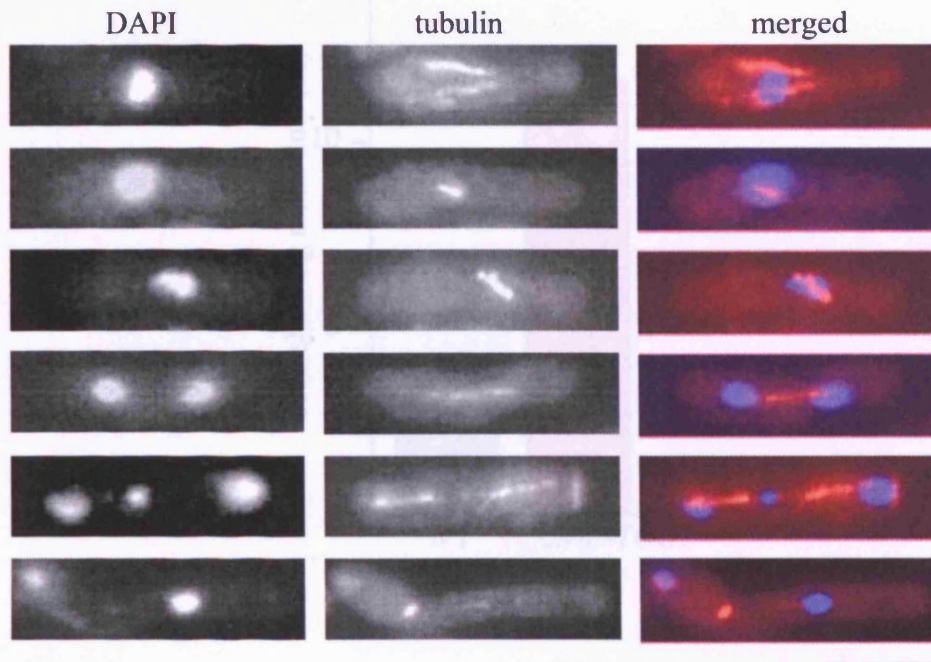


Fig. 4.4.4 Overexpression *alp14* C-terminal results in microtubule defects and chromosome missegregation. *Ov-C-TOG1* cells grown in rich media were filtered and reinoculated in media lacking thiamine for 12 hours. Cells were fixed with methanol and processed for immunofluorescence staining with anti-tubulin. The scale bar represents 10 μ m.

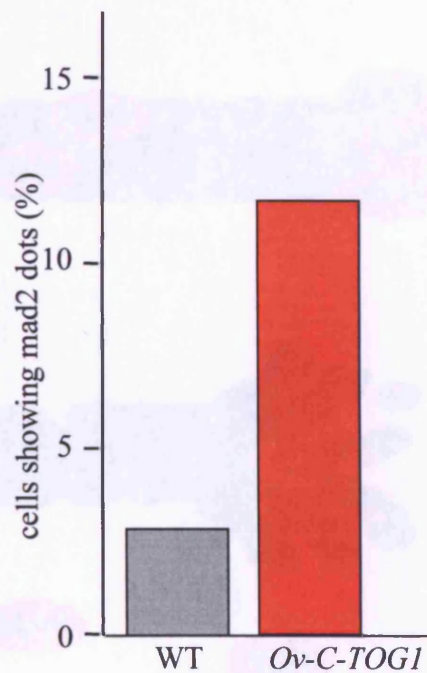
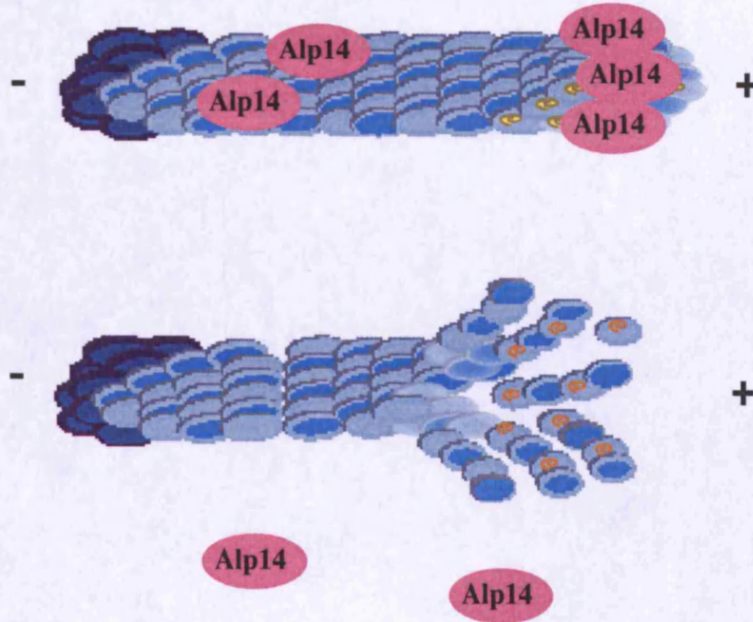


Fig. 4.4.5 Overexpression of *alp14* C-terminal activates the spindle assembly checkpoint. Wild type *mad2⁺-GFP* and *ov-C-TOG1 mad2⁺-GFP* cells grown in rich media were filtered and reinoculated in media lacking thiamine for 12 hours. Cells were fixed with methanol and processed for immunofluorescence staining with anti-tubulin. Cells containing Mad2 dots at kinetochores were counted.

A



B

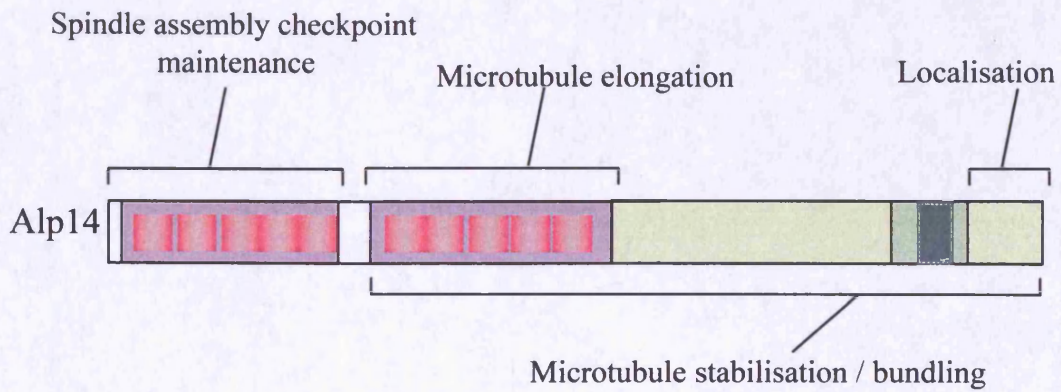


Fig. 4.5.1 A) Alp14 prevents catastrophe by bundling microtubule protofilaments at the growing ends. B) Schematic diagram showing a summary of specific domain functions in Alp14.

Timely and accurate chromosome segregation is crucial to the integrity and stability of cells in all organisms. Central to the accuracy of cell division in eukaryotes are mitotic spindles, which polymerised from opposite poles to capture replicated sister chromatids at the kinetochores. Once kinetochores are stably captured, spindles are depolymerised, resulting in a poleward pulling force that segregates the DNA. Bipolar attachment, stabilisation of spindle-kinetochore interaction and generation of poleward force are key factors in ensuring accurate chromosome segregation. When these processes are compromised, cells delay anaphase onset by activation of the spindle assembly checkpoint to allow the error to be corrected (Li and Nicklas, 1995; Chen *et al.* 1996; Zhou *et al.* 2002). It is thought in response to unattached DNA, it is essential that spindle checkpoint component Mad2 is recruited to the kinetochores established (Rieder *et al.* 1994; Chen *et al.* 1996; Li and Benezra 1996; Waters *et al.* 1998). However, Mad2-independent spindle checkpoint activation have also been observed (Waters *et al.* 1998; Hoffman *et al.* 2001; Tang *et al.* 2001; Rajagopalan *et al.* 2004; Gachet *et al.* 2001 and 2004; Tournier *et al.* 2004).

Proteins that regulate spindle dynamics play vital roles in bipolar kinetochore attachment, stability and tension generation. These proteins include members of microtubule-associated TOG family (also known as Dis1 / XMAP215 family) and Kinesin-13 family. Homologues of the TOG family have been consistently shown to promote microtubule polymerisation and stability (Gard and Kirschner 1987; Vasquez *et al.* 1994; Severin *et al.* 2001; Garcia *et al.* 2001; Nakaseko *et al.* 2001). Previous studies have shown fission yeast TOG members, Alp14 and Dis1, to act a link between plus ends of spindles and kinetochore, thereby facilitating kinetochore capture and stabilisation of spindle-kinetochore interaction (Garcia *et al.* 2001; Nakaseko *et al.* 2001).

The Kinesin-13 family of proteins have also been suggested to be main players in spindle-kinetochore stabilisation. MCAK and frog XKCM1 are both required for microtubule depolymerisation and accurate chromosome segregation in vivo (Kline-Smith *et al.* 2004; Walczak *et al.* 1996; Desai *et al.* 1999; Kline-Smith and Walczak 2002; Walczak *et al.* 2002). Although sequence analysis indicates that yeast does not contain homologues of Kinesin-13, studies of the closest orthologue of the Kinesin-13 family in budding yeast (classified as a member of the Kinesin-8 family) have shown functional homology. Like human MCAK and frog XKCM1, budding yeast Kip3 also

promotes microtubule destabilisation (Straight *et al.* 1998; Cottingham *et al.* 1999). However, efforts to determine the role of Kip3 in cell division indicate that it is involved in nuclear positioning during mitosis, a mechanism that is specific to the organism (DeZwaan *et al.* 1997; Miller *et al.* 1998; Cottingham *et al.* 1999). Detailed involvements of microtubule-destabilising kinesins in cell division remains to be elucidated. In this study, we aim to determine the role of Kinesin-8/-13 in chromosome segregation by analysis of fission yeast homologues, Klp5 and Klp6. In addition, we also address the effects of *klp5* and *klp6* mutants on the spindle assembly checkpoint and the relationship between TOG and Kinesin-8/13 members in fission yeast.

5.1. Identification of Klp5 and Klp6

A full genome-wide search at the Sanger database for Kinesin-8 homologues was carried out using budding yeast Kip3 as a quest. It has shown that the fission yeast harbours two members, Klp5 and Klp6 (for kinesin-like protein 5 and 6), with 50% identity and 69% homology between them. A summary of sequence identity/homology and an alignment of frog XKCM1, budding yeast Kip3, and fission yeast Klp5 and Klp6 are shown in fig.5.1.1. Klp5 and Klp6 share 56% homology to both human MCAK and frog XMKCM1.

An evolutionary phylogenetic tree deduced from sequence similarities using the Clustal X program shows that yeast kinesin-8 proteins are evolutionarily divergent from their orthologues, kinesin-13, in frog and human (fig. 5.1.2). Two members of the kinesin-13 family have been identified in human as KIF2 and MCAK (Aizawa *et al.* 1992; Noda *et al.* 1995; Wordeman and Mitchison 1995). Despite this, human MCAK appears to share a higher similarity with frog XKCM1, which is consistent with the reports that both proteins possess a microtubule depolymerising activity (Maney *et al.* 2001; Hunter *et al.* 2003). The kinesin-13 family members share a common kinesin domain near the middle of the protein, where the majority of the sequence homology is shared. In order to find other possible domains, searches in the pbase database and the matchbox domain prediction program were carried out. Fig. 5.1.3 shows predicted coil-coiled domains in frog XKCM1 and fission yeast Klp5 and Klp6. No coiled-coiled domains were predicted in human MCAK and budding yeast Kip3. The presence of the coil-coiled domains

indicates that these proteins may function via protein-protein interaction.

5.2. Analysis of *klp5*⁺ and *klp6*⁺ gene products

To address the protein level of Klp5 and Klp6, the kinesin genes were endogenously tagged with 3HA under the native promoters. Level of expression of Cut2 has been previously determined as 20,000 molecules/cell (Funabiki *et al.* 1996; Fujita *et al.* 2002). By using this information and comparison of band intensity of Cut2-3HA to Klp5-3HA and Klp6-3HA on an SDS gel, the protein levels of Klp5 and Klp6 could be estimated. Wild type (untagged strain), Klp5-3HA, Klp6-3HA and Cut2-3HA proteins from asynchronous cultures were run and subjected to a Western blot using an anti-HA antibody. Klp5 and Klp6 levels were estimated to be 31,600 and 20,000 molecules/cell, respectively (fig. 5.2.1 A). This shows that Klp5 and Klp6 are present in abundance. However, asynchronous cultures contain cells in a variety of cell cycle stages, making it impossible to predict the effect of Klp5 and Klp6 levels on their functions in this condition.

To synchronise cell cycle progression, a strain carrying a mutation in the *cdc25*⁺ gene was used. Cdc25 is a phosphatase whose activity is absolutely required for mitotic entry. Cdc25 initiates mitotic onset by dephosphorylating Cdc2 cyclin-dependent kinase (CDK) at tyrosine 15. When the function of Cdc25 is compromised, the cell cycle is arrested in G₂. Cells harbouring the *cdc25-22* mutation fail to progress from G₂ at restrictive temperatures, and can be used to arrest and release cells by temperature shifts. To analyse Klp5 and Klp6 levels at different stages of the cell cycle, cells containing both *klp5*⁺-13myc / *klp6*⁺-3HA and *cdc25-22* mutation were shifted up to 36°C to arrest cells in G₂. After four hours, the cultures were shifted down to 26°C for release into mitosis. Samples were taken every 15 minutes after G₂ release and processed for Western blotting and staining with calcofluor, a fluorescent reagent that stains the septa, to follow cell cycle progression. To test if levels of Klp5 is regulated throughout the cell cycle, we blotted against α -tubulin for comparison of band intensities. Results (data not shown) show similar fluctuations of band intensity between α -tubulin and Klp5-13myc throughout the cell cycle, indicating that Klp5 and Klp6 levels are not cell cycle regulated.

In these studies, Klp5-3HA, Klp5-13myc and Klp6-3HA always appeared as multiple bands, which raises the possibility that their functions may be regulated by protein modification, such as phosphorylation. Fig. 5.2.1 B shows Klp5-13myc to consistently appear as multiple bands throughout the cell cycle. This suggests that either Klp5 is modified throughout the cell cycle, or that its function is throughout the cell cycle is regulated by another means, such as protein-protein interaction. The appearance of multiple bands may also be a reflection of protein degradation.

5.3. Analysis of *klp5* and *klp6* deletion mutants.

Gene disruptions of *klp5*⁺ and *klp6*⁺ were carried out in order to address the in vivo roles of Kinesin-8 in fission yeast. Single and simultaneous deletions of *klp5*⁺ and *klp6*⁺ were viable. Analysis as to how these mutants may affect microtubule stability, chromosome segregation and chromosome stability are described below.

Klp5 and Klp6 destabilise microtubules in vivo.

Many mutants affecting microtubule stability show a sensitivity or resistance to the microtubule destabilising drugs. Thiabendazole (TBZ) is a microtubule drug that destabilises microtubules by inhibiting the addition of $\alpha\beta$ tubulin subunits to microtubule protofilaments. When TBZ is added to cells microtubules are broken down, resulting in mitotic arrest. Previous studies have shown that frog Kinesin-13 homologue, XKCM1, have an intrinsic microtubule depolymerising activity (Walczak *et al.* 1996; Desai *et al.* 1999; Kinoshita *et al.* 2001). If Klp5 and Klp6 were also able destabilise microtubules, $\Delta klp5$ and $\Delta klp6$ would be expected to show resistance to TBZ. To test this possibility, cells deleted for *klp5*⁺ and/or *klp6*⁺ were spotted after serial dilutions at 10⁶ to 10² cells onto rich media in absence or presence of 10 μ g/ml of TBZ. Wild type and $\Delta alp14$ strains were used as controls. Alp14 has been shown to act as a microtubule-stabilising factor, and mutants of *alp14*⁺ are known to be TBZ-sensitive (Garcia *et al.* 2001). Fig. 5.3.1 shows that $\Delta klp5$, $\Delta klp6$, and $\Delta klp5\Delta klp6$ are resistant to TBZ, suggesting that like frog XKCM1 and budding yeast Kip3, Klp5 and Klp6 function as a microtubule-destabilising factor.

To further investigate the involvement of Klp5 and Klp6 in microtubule dynamics, $\Delta klp5$, $\Delta klp6$ and $\Delta klp5\Delta klp6$ cells were processed for immunofluorescence staining with anti-tubulin (TAT-1) antibody. Visualisation by fluorescence microscopy shows microtubules in $\Delta klp5$, $\Delta klp6$ and $\Delta klp5\Delta klp6$ cells to be elongated and curved, a microtubule defect that has never been observed in wild type cells (fig. 5.3.2). Upon further analysis, the elongated and curved phenotype was only found in interphase and post-anaphase cells, where microtubules were emanated from cytoplasmic MTOCs. In contrast, no obvious defects in the morphology of the mitotic spindles were observed.

In above tests for the role of Klp5 and Klp6 in regulating microtubule stability, single $\Delta klp5$ and $\Delta klp6$ mutants showed no obvious difference in defective phenotypes between them. Moreover, simultaneous deletion of both genes did not increase the severity of the defects. This suggests that Klp5 and Klp6 may work together, for example as complex. Indeed, another member of the team has discovered that Klp5 and Klp6 co-localise and form a heterocomplex (Garcia *et al.* Curr. Biol. 2002). For this reason, some of the experiments described further have only been carried out using either $\Delta klp5$ or $\Delta klp6$.

Klp5 and Klp6 are involved in the fidelity of chromosome segregation.

Despite the lack of obvious defects in spindle morphology, it is intriguing how the loss of microtubule destabilising proteins may affect chromosome segregation. In mitosis, temporal regulation of spindle dynamics is absolutely crucial. To capture the kinetochores, spindles must grow from opposite poles towards sister chromatids. Once the kinetochores have been captured, spindles must then shrink at the site of capture, creating tension and stabilisation of the attachment. If Klp5 and Klp6 function to destabilise mitotic spindle as well as cytoplasmic microtubules, defects in chromosome segregation would be observed in $klp5/6$ deletion mutants. To test the fidelity of chromosome segregation in $klp5/6$ mutants in comparison to wild type, chromosome loss assays using a nonessential minichromosome 16 was carried out according to Niwa *et al.* 1989. The minichromosome is derived from the centromeric region of chromosome 3 and contains *ade6-m216* allele that is able to compensate for the *ade6-m210* mutation, which is carried endogenously in the genome. The minichromosome is stably maintained in normal mitosis but when DNA replication or segregation defects occur, the minichromosomes are lost and can be observed as red auxotrophs. Fig. 5.3.3. A shows high number of red and sectorial colonies in $\Delta klp5$. When the number of colonies

containing red sectors was counted against the total number of colonies, the percentage of chromosome loss in $\Delta klp5$ is shown to be more than 200 times that of wild type (fig. 5.3.3. B). The rate of chromosome loss was also calculated (half-sectored cells indicate chromosome loss in the first cell division) to be 9.2×10^{-2} per cell division. The chromosome loss phenotype suggests defects in chromosome segregation.

Consistently, microscopic analysis of $\Delta klp5$ and $\Delta klp6$ cells in mitosis shows stretched and lagging chromosome phenotypes, leading to unequal chromosome segregation. Wild type and $\Delta klp6$ cells were processed for immunofluorescence staining with anti α -tubulin (TAT-1) antibody. DAPI staining of these cells shows that $\Delta klp6$ causes missegregated chromosomes (fig. 5.3.4. A). However, the process of immuno-staining required fixation with methanol, which disturbs the DNA and causes fussing of DAPI when observed. In addition, the immuno-staining procedures may have disrupted spindle structures in this particular experiment as they appear weaker than expected of $\Delta klp6$ microtubules (compare fig. 5.3.4 A to figs. 5.3.2 and 5.3.5 C). To better visualise DNA, wild type and $\Delta klp5$ cells were fixed with formaldehyde and stained with DAPI. Formaldehyde-fixed $\Delta klp5$ cells clearly show chromosome segregation defects that are never found in wild type (fig. 5.3.4 B).

Defects in spindle function often cause mitosis to prolong in order for the error to be corrected. If the error occurs prior to anaphase causing the kinetochore to be unattached or the attachment is destabilised, anaphase onset is delayed by the spindle assembly checkpoint. To investigate if $\Delta klp5$ causes mitosis to delay, and if so at which stage, the percentage of cells in each mitotic phase has been counted in wild type, $\Delta klp5$, $\Delta klp6$ and $\Delta klp5\Delta klp6$. Cells were first processed for immunofluorescence to stain α -tubulin and DNA. Phases of mitotic cells were determined by the length of spindles in combination with the number of DNA mass. Fig. 5.3.5 shows that mitotic cells are accumulated in $\Delta klp5$, $\Delta klp6$ and $\Delta klp5\Delta klp6$, in particular those with mono-nucleate cells and short spindles, representative of cells in prometaphase to anaphase A. This suggests that $klp5/6$ deletion mutants may be defective in the spindle-kinetochore attachment.

5.4. Analysis of *klp5* and *klp6* overexpression mutants.

To induce single and simultaneous overproductions of Klp5 and Klp6 proteins, P3nmt promoters have been endogenously integrated to replace natural promoters of *klp5*⁺ and *klp6*⁺. In the absence of thiamine, the nmt promoter is induced and Klp5/6 are overexpressed, leading to retarded growth on plates after three days at 30°C (fig.5.4.1. A). To test the viability of *klp5/6* overexpression mutants, of *P3nmt-klp6* cells were grown in liquid culture in presence or absence of thiamine. Samples were taken at 0 hour and then hourly at from 12 to 18 hours and plated onto rich media containing thiamine at 200 cells per plate. Viability was calculated by the number of colonies formed on each plate at each time point against those at 0 hours. Fig. 5.4.1 B shows that overproduction of Klp6 causes the loss of viability.

Klp5 and Klp6 are required for microtubule function and accurate chromosome segregation.

Cytoplasmic microtubules are essential to maintain the cell shape and polarity. When the function of cytoplasmic microtubules is compromised, cells become abnormally shaped, often observed as branched or bent cells (Toda *et al.* 1983; Sawin and Nurse 1998). Because Klp5 and Klp6 regulate microtubule dynamics by promoting their depolymerisation, it is expected that *klp5/6* mutants would show abnormal cell shape. Indeed, overproduction of Klp5/6 results in accumulation of elongated and branched cells (fig. 5.4.2 and fig. 5.4.3 A).

The effects of Klp5/6 overproduction in mitosis also reflect their regulation of spindle dynamics. Immuno-staining of tubulin in cells expressing *P3nmt-klp6*⁺ show abnormally short or absence of microtubules in some cells, leading severe chromosome missegregation (fig. 5.4.3. A and B). Missegregated cells increase sharply over time in overexpression condition and eventually become cut as shown by DAPI staining of formaldehyde-fixed cells (fig. 5.4.3. C). Cut cells occur when mitotic progresses and cytokinesis occurs even though spindles are still unable to segregate sister chromatids.

In *P3nmt-klp6*⁺ cells observed, the abnormally elongated cell shape often occurred in binucleate cells. One reason for this could be that these cells are able to go through rounds of cell division without physically undergoing cytokinesis. To test this possibility,

P3nmt-klp6⁺ cells grown in presence or absence of thiamine were fixed and stained with calcoflour to mark the cells septa. The percentage of septated cells in overexpression condition was abnormally low (fig. 5.4.4. A). This implies that either cells are unable to septate or that they are arrested in a cell cycle stage prior to cytokinesis in response to the chromosome segregation defect. Of the septated cells, cytokinesis defects visualised as thick, wavy or multiple septa were observed (fig. 5.4.4. B). The percentage of cells showing abnormal septa increase sharply over time in both absence and presence of thiamine. This may be because the *P3nmt* promoter is unable to completely suppress the production of Klp6, as this is often the case in fission yeast.

5.5. *klp5* and *klp6* mutants activate the spindle assembly checkpoint

Given that Klp5 and Klp6 promote microtubule destabilisation and that spindle shrinkage is required to create tension and stabilisation of spindle-kinetochore attachment, it is possible that Klp5 and Klp6 are involved in tension-generation. If Klp5 and Klp6 were involved in the stabilisation of spindle-kinetochore attachment, the spindle assembly checkpoint would be activated when Klp5/6 function is compromised. To test this possibility, a central player of the spindle checkpoint, *mad2*⁺, was deleted in $\Delta klp5$ and *P3nmt-klp5/6* strains. When *mad2*⁺ is deleted, mitotic progression can no longer be delayed even when the spindle-kinetochore attachment has not been established (Rieder *et al.* 1994; Chen *et al.* 1996; Li and Benezra 1996; Waters *et al.* 1998).

Previously described minichromosome loss experiment (fig. 5.3.3.) has shown that Klp5 functions to ensure chromosome stability. Here, the rate of chromosome loss is compared between $\Delta klp5$, $\Delta mad2$ and $\Delta klp5\Delta mad2$. The rate of chromosome loss in $\Delta mad2$ was not increased dramatically compared wild type cells (<0.1% - no red or sectorised colonies were observed – data not shown) and as predicted, a significant rate of chromosome loss is detected in $\Delta klp5$. However, when both *klp5*⁺ and *mad2*⁺ were deleted, virtually no Ade⁺ colonies were retained, with the rate of chromosome loss calculated to be 6.3×10^{-1} (fig. 5.5.1). This suggests that Mad2 plays an important role in securing genome stability when Klp5 function is compromised. The finding has also been supported by results of another member of the team. By analysing timing of securin destruction, it was found that delay in anaphase onset in $\Delta klp5$ is eliminated in absence

of Mad2 (Garcia *et al.* Curr Biol. 2002). Therefore, Klp5 and Klp6 facilitate spindle-kinetochore attachment in prometaphase.

Similar to Klp5/6 overexpression, deletion of *mad2*⁺ in these strains is toxic and shows retarded growth on plates in absence of thiamine (fig. 5.5.2 A). Although cells quickly lose viability and become branched when *klp6* is overexpressed, when *mad2*⁺ is deleted, the severity of the defects is grossly amplified (fig. 5.5.3 B and C), suggesting that overproduction of Klp6 also activate the spindle assembly checkpoint. Consistent with this, $\Delta mad2$ -*P3nmt-klp5/6* display fewer missegregated cells and accumulate far more cut cells than *P3nmt-klp5/6* alone (fig. 5.5.3).

5.6. Genetic interaction between *klp5*⁺/*klp6*⁺ and *alp14*⁺/*dis1*⁺

In vitro studies of frog XKCM1 and XMAP215 have determined that they function antagonistically to depolymerise and polymerise microtubules, respectively to regulate microtubule dynamics (Tournebize *et al.* 2000; Kinoshita *et al.* 2001). In fact, it has been proposed that dynamic instability can be achieved solely with opposing activities of these two proteins in vitro (Kinoshita *et al.* 2001). In vivo studies in budding yeast also supports the possibility that Kip3 may interact with members of the TOG family. Defects in spindle elongation found in mutants of budding yeast TOG, Stu2, were rescued by deletion of Kip3 protein (Severin *et al.* 2001). Fission yeast homologues of the TOG family are Alp14 and Dis1. Alp14 and Dis1 share a role in microtubule stabilisation to ensure interaction between the spindle and the kinetochores (Nabeshima *et al.* 1995 and 1998; Nakaseko *et al.* 1996; Garcia *et al.* 2001). Because Klp5 and Klp6 are essential for proper spindle-kinetochore attachment in prometaphase, it is possible that despite possessing antagonistic roles in microtubule dynamics, Klp5/6 and Alp14/Dis1 might play a collaborative role in mitosis.

Fission yeast Kinesin-8 and TOG proteins play a collaborative role.

Genetic analysis was carried out by simultaneously deleting *klp5*⁺, *klp6*⁺, *alp14*⁺ and *dis1*⁺ in various combinations. Table 5.6.1 summarises viability of the resulting strains. Single deletions of *alp14*⁺ or *dis1*⁺ result in temperature- and cold-sensitivity, respectively. At restrictive temperatures, these deletion mutants show retarded growth,

microtubule defects and sensitivity to TBZ. Double deletion of *alp14*⁺ and *dis1*⁺ is lethal at any temperature, which can be rescued by an introduction of a multicopy plasmid containing *dis1*⁺. As discussed earlier, single or double deletions of *klp5*⁺ and *klp6*⁺, on the other hand, are viable and show no additive-phenotype. This suggests that other microtubule depolymerising factors exist in fission yeast to compensate for the loss of poleward force in absence of Klp5/6.

Any combination of simultaneous deletions of *klp5/6*⁺ and *alp14*⁺/*dis1*⁺ resulted in lethality at any temperature. In this case, the lethality could have been a result of Klp5/6 overproduction in absence of Alp14/Dis1, as overproductions of Klp5 and/or Klp6 are toxic. To test this, *alp14klp5klp6* and *dis1klp5klp6* deletion mutants were constructed and shown to be lethal, discarding the above-mentioned possibility. This indicates that fission yeast TOG and Kinesin-8 members play a collaborative role, and that *klp5/6* and *alp14* or *dis1* mutants were kept viable only by the other's functions.

Klp5/6 and Alp14/Dis1 play a common role in mitotic progression.

The next question is at which stage do Klp5/6 and Alp14/Dis1 share such an essential function. To address this, *alp14dis1*, *alp14klp5* and *dis1klp5* deletion mutants kept viable by plasmids containing *alp14*⁺ or *dis1*⁺ were subjected to a plasmid loss assay. Although the plasmid vectors were mitotically stable, their loss (at 20-30%) could be induced upon nitrogen starvation followed by re-feeding. This experiment allows defective phenotypes that lead to lethality in the mutants to be examined. *alp14dis1*, *alp14klp5* and *dis1klp5* mutants carrying *alp14*⁺ or *dis1*⁺ plasmids were starved of nitrogen for 12 hours, washed and resuspended in rich media at 30°C. Tubulin-staining of these cells at 7 hours after G₁ release indicate identical chromosome missegregation phenotypes for all mutants (fig.5.6.2 A and B). Spindles in cells lacking *alp14*⁺ and *dis1*⁺ have been previously shown to be unable to properly capture the kinetochore. The very same, but more severe, phenotype (fig.5.6.2 C) observed in *alp14klp5* and *dis1klp5* mutants suggest that Klp5/6 and Alp14/Dis1 play a common essential role to establish and stabilise spindle-kinetochore interaction.

***alp14klp5* and *dis1klp5* activate the spindle assembly checkpoint.**

In addition to chromosome missegregation, formaldehyde fixation and DAPI-staining in *alp14dis1*, *alp14klp5* and *dis1klp5* mutants in the plasmid loss assay also show the DNA

to be hyper-condensed (fig.5.6.3). Because this phenotype often observed when the spindle assembly checkpoint is activated, deletion of *mad2*⁺ was carried out in the *dis1klp5* + *pdis1*⁺ strain. Plasmid loss assay was carried out and cells were formaldehyde-fixed and stained with DAPI. Fig. 5.6.4 A shows that when *mad2*⁺ was deleted, *dis1klp5* no longer exhibited hyper-condensed chromosomes, suggesting that the spindle assembly checkpoint is activated. Activation of the checkpoint, however, was unable to overcome the defect as the cell cycle eventually progresses, resulting in gross segregation defects and lethality.

Deletion of *mad2*⁺ in cells harbouring prometaphase defects usually leads to the presence of cut cells. However, no cut cells were seen and instead cells exhibiting a “stretched” chromosome phenotype were observed. There were fewer cells showing chromosome missegregation (lagging chromosomes) in *mad2dis1klp5* than *dis1klp5* (fig. 5.6.4). It is thought that the stretched chromosome phenotype, which represents cells undergoing difficulties in segregating their DNA, may replace the chromosome missegregation phenotype in some *mad2dis1klp5* cells. Because *dis1klp5* is already synthetic lethal, it is difficult to determine if deletion of *mad2*⁺ increases the severity further. However, because *mad2dis1klp5* exhibits a different phenotype than that of *dis1klp5*, it is likely that the spindle assembly checkpoint is activated when Klp5/Klp6 and Alp14/Dis1 functions are compromised.

Proper mitotic localisation of Klp5 is dependent on Alp14.

We have determined that Klp5/6 and Alp14/Dis1 function together to ensure accurate cell division. The next question we asked is if they are required for each other's localisation in mitosis. Alp14 is recruited to SPBs upon mitotic onset, and are then transferred onto spindles observed as punctuated dots along the spindles (Garcia *et al.* 2001). Alp14 has also been found to bind to the kinetochore by microscopy and chromatin immunoprecipitation (Garcia *et al.* 2001). In $\Delta klp5$, Alp14-GFP is able to normally localise (studies from another member of the team - Garcia *et al.* EMBO 2002). Similarly, Klp5 and Klp6 are recruited to mitotic spindles and kinetochores in mitosis. In addition, in anaphase B Klp5 and Klp6 are also found at the spindle midzone. Cells harbouring integrated *klp5*⁺-GFP and $\Delta alp14$ were grown at 26°C then shifted up to 36°C, a restrictive temperature for $\Delta alp14$. As shown in fig. 5.6.5 A, the intensity Klp5-GFP after two hours at restrictive temperature appears to be lower than that of wild type.

Upon further analysis, the number of cells containing Klp5-GFP at the kinetochore was grossly reduced just after one hour at 36°C (fig. 5.6.5 B). Although Klp5 was still able to localise to the kinetochore in 10 percent of *Δalp14* cells, more than 50 percent of *Δalp14* show mitotic defects in this condition, showing that Klp5 is unable to localise to the kinetochore in 80 percent of mitotic *Δalp14* cells.

5.7 Summary and concluding remarks

The study described in this chapter has determined that Klp5 and Klp6 are microtubule destabilising factors whose functions are required to establish stable bipolar spindle-kinetochore attachment in mitosis. Please note that the results from this study and from other members of the team have been successfully accepted for publication (Garcia *et al.* Curr. Biol. 2002; Garcia *et al.* EMBO 2002).

Klp5 and Klp6 promote microtubule depolymerisation and ensures accurate chromosome segregation.

klp5/6 deletion mutants analysed in this study clearly show long and curved cytoplasmic microtubules and are resistant to microtubule drug TBZ. These findings indicate that Klp5 and Klp6 are microtubule destabilisers. In support of this, a cold-shock experiment carried out by another member of the team, showed that microtubules of *klp5/6* deletion mutants were more resistant to the cold than those of wild type. They were also able to rapidly recover microtubules after temperature shift up (Garcia *et al.* EMBO 2002). These findings suggest that although Klp5 and Klp6 belong to the Kinesin-8 family, like kinesin-13 homologues, Klp5 and Klp6 function to promote microtubule depolymerisation. This further supports previous speculation that yeast Kinesin-8 are functional orthologues of Kinesin-13 in higher eukaryotes (Severin *et al.* 2001).

In vitro studies have indicated that XKCM1 function at the plus-ends of microtubules to increase the rate of catastrophe and shrinkage (Walczak *et al.* 1996; Desai *et al.* 1999; Kinoshita *et al.* 2001). Although our in vivo system makes it impossible to determine if Klp5 and Klp6 also directly destabilises microtubules at the plus-ends, the localisation pattern of the proteins do suggest so. As well as interphase microtubules and mitotic

spindles, Klp5 and Klp6 are also recruited to spindle midzones and kinetochores, where the plus-ends of mitotic spindles are located (Garcia *et al.* Curr. Biol. 2002).

The mitotic localisation of Klp5 and Klp6 are also suggestive of their roles in ensuring accurate chromosome segregation. Indeed, analysis of *klp5/6* deletion and overexpression mutants in this study suggests that they are essential to prevent genome instability and chromosome missegregation. Upon detailed investigation, *klp5/6* mutants showed prolonged prometaphase (West *et al.* 2001 and 2002; Garcia *et al.* Cur. Biol. 2002). Deletion of spindle checkpoint component Mad2 in *klp5/6* mutants resulted in gross chromosome segregation and lethality, suggesting that the defects caused *klp5/6* mutants to engage the spindle assembly checkpoint. The activation of the spindle assembly checkpoint suggests that in *klp5/6* mutants the kinetochore is either unattached or tensionless. By analysing the localisation of spindle assembly checkpoint proteins, another member of the team showed that some *klp5/6* kinetochores display two patterns of spindle checkpoint protein localisation. One is the kinetochore-recruitment of both Mad2 and Bub1, the second is the kinetochore-localisation of Bub1 without Mad2. It is believed that the former is indicative of unattached kinetochores, whilst the latter may be representative of tension-less kinetochores. The recruitment of Bub1 without Mad2 is of particular interest as it is rarely observed in wild type fission yeast cells. This is because amphitelic attachment directly leads to tension generation in wild type cells. Errors in kinetochore capture resulting in merotelic and monotelic in wild type cells lead to unattached kinetochores and localisation of both Mad2 and Bub1. It is only when syntelic attachment occurs that kinetochores are attached but tensionless (see introduction fig. 1.5).

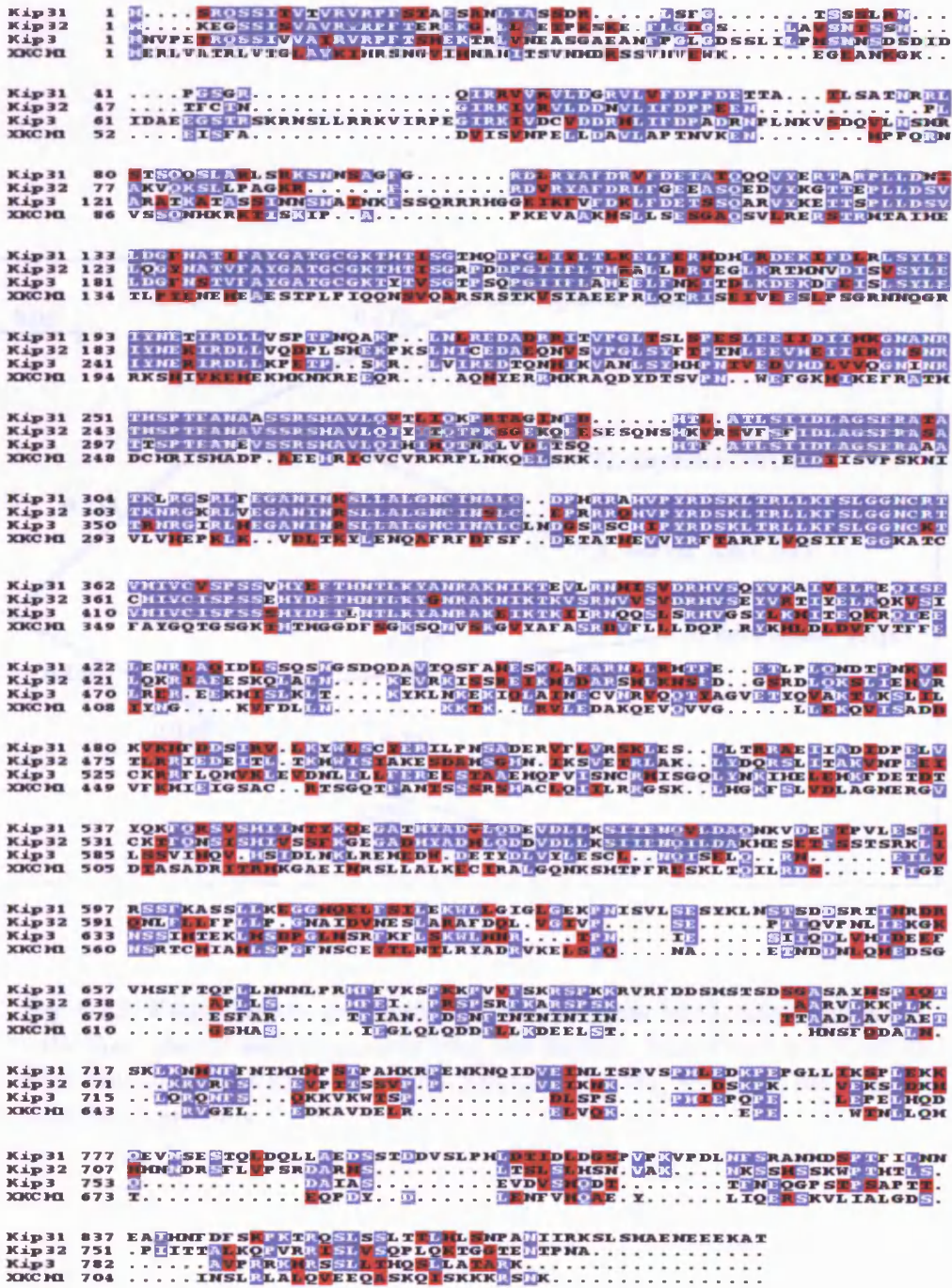
In summary, the presence of the both Mad1 and Bub1 localisation in *klp5/6* cells suggests that Klp5 and Klp6 are required for spindle-kinetochore capture or the stabilisation of the interaction. The recruitment of Bub1 with Mad2 in *klp5/6* cells also suggests that Klp5 and Klp6 function to generate tension at the kinetochore. We propose that by depolymerising the spindle plus-ends in metaphase, Klp5 and Klp6 provide a poleward pulling force at the kinetochore. This allows the stability of the spindle-kinetochore interaction to be tested. The poleward pulling force also generates tension, which provides a signal for anaphase onset.

The Klp5/Klp6 and Alp14/Dis1 collaborate to ensure stable bipolar attachment in mitosis.

We have also determined that although Klp5/Klp6 possess opposing roles in microtubule regulation to Alp14/Dis1, they play collaborative roles to establish stable bipolar spindle-kinetochore interaction. Alp14 has been proposed to function as a linker between the spindle and kinetochore, thereby ensuring spindle-kinetochore attachment. Because Klp5 localisation is reduced in *alp14* mutant, it is possible that Klp5/Klp6 localisation to the kinetochore is dependent on Alp14. This implicates that the function of Klp5/Klp6 at the kinetochore cannot be effective until Alp14 has reached the kinetochore, ie. until the spindle has captured the kinetochore. In this model, we propose that Alp14 facilitates the spindle-kinetochore attachment by promoting spindle growth at the plus-ends and Klp5 and Klp6 generates tension by promoting spindle shrinkage, leading to generation of poleward force (fig. 5.7.1).

Contrary to our findings, studies in frog and budding yeast suggest that kinesin-13 and TOG proteins function antagonistically, where simultaneous deletions lead to rescue of single deletion defects (Tournebize *et al.* 2000; Kinoshita *et al.* 2001; Severin *et al.* 2001). Although it appears that the collaborative roles of Alp14/Dis1 and Klp5/Klp6 in mitosis may not be evolutionarily conserved, it has been shown that vertebrate Kinesin-13 and TOG proteins function together to create dynamic instability (Kinoshita *et al.* 2001). In addition, all known homologues of Alp14/Dis1 and Klp5/Klp6 show similar or identical mitotic localisation. Overall, we envision that although TOG proteins and Kinesin-8/-13 members function in an opposed manner in terms of microtubule regulation (that is TOG polymerises microtubules, whilst Kinesin-8/13 depolymerises them), these two proteins play collaborative roles *in vivo* to establish microtubule dynamics.

A



B

PROTEINS	IDENTITY	HOMOLOGY
XKCM1 & Kip3p	31%	47%
XKCM1 & Klp5	37%	55%
XKCM1 & Klp6	39%	56%
Kip3p & Klp5	39%	53%
Kip3p& Klp6	56%	70%
Klp5 & Klp6	50%	69%

Fig. 5.1.1 Comparison between Klp5, Klp6 and their closest kinesin homologues. **A)** Sequence alignment between Klp5, Klp6 and their homologues in frog and budding yeast, XKCM1 and Kip3. Klp5 and Klp6 are labelled as Kip31 and Kip32, respectively. Blue signifies conserved residues, red signifies similar residues. **B)** Percentage of identity and homology between Kinesin-8 and Kinesin-13 family members.

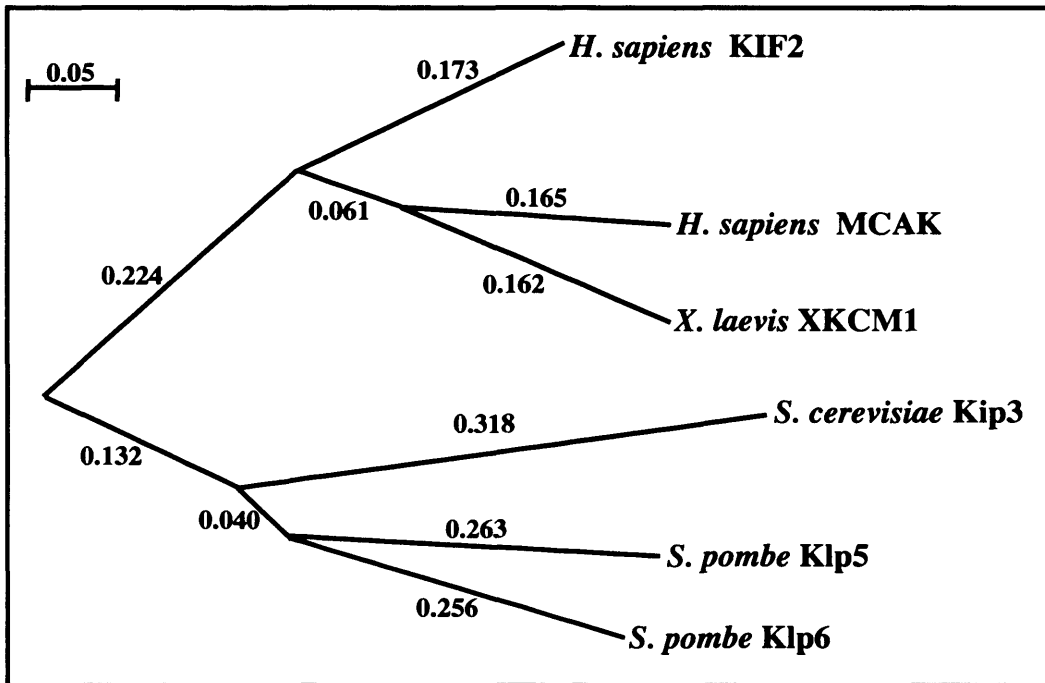
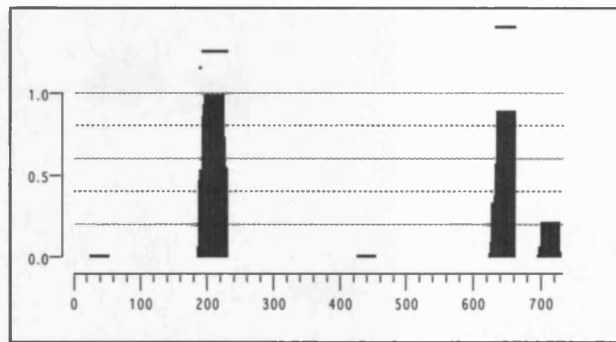


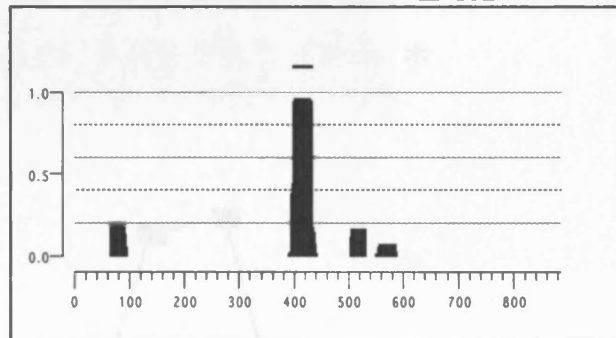
Fig. 5.1.2 Evolutionary relationship between yeast Klp5, Klp6 and Kip3 with their closest homologues in frog and human. Note that Klp5, Klp6 and Kip3 belong to the Kinesin-8 family, whereas XKCM1, KIF2 and MCAK, are Kinesin-13 proteins.

A

Xenopus XKCM1



S. pombe Klp5



S. pombe Klp6

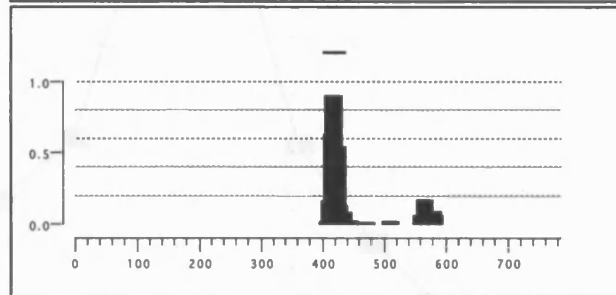
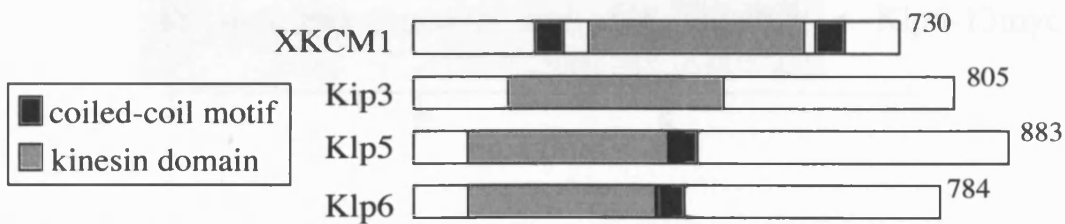
**B**

Fig.5.13 Structural comparison between Klp5 and Klp6 and their homologues in frog and budding yeast. A) Domain search reveals predicted coiled-coil regions in frog XKCM1 and fission yeast Klp5 and Klp6. Note that similar searches shows no predicted coiled-coiled regions in human MCAK and budding yeast Kip3. **B)** Structural comparison, showing positions of kinesin and coiled-coiled domains.

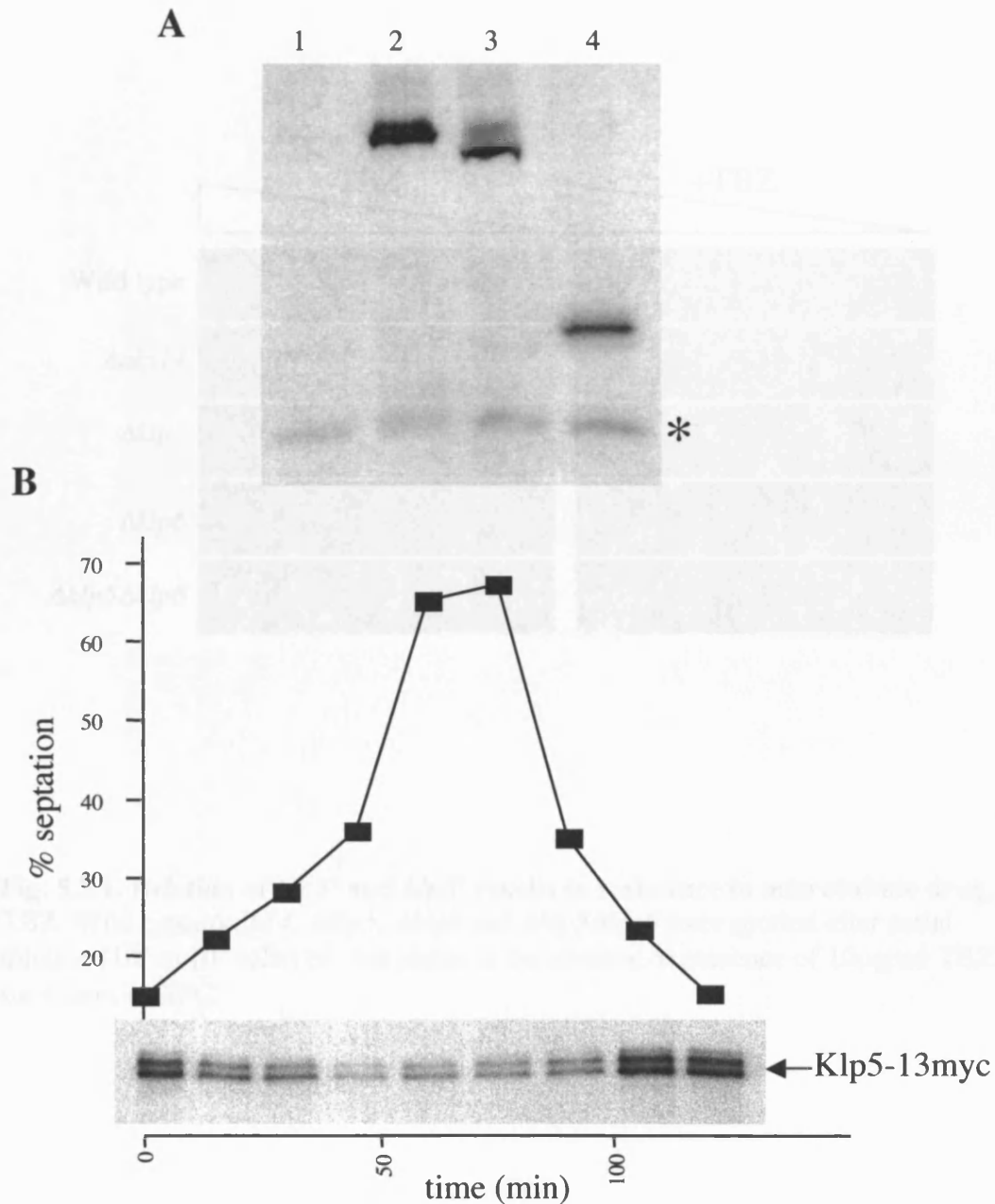


Fig.5.2.1 Estimation of Klp5 and Klp6 protein expression level. A) Wild type (untagged strain), Klp5-3HA, Klp6-3HA and Cut2-3HA cells grown in an asynchronous culture were extracted for protein, run on an 10% SDS gel and subjected to a Western blot using an anti-HA antibody. The level of expression was estimated by comparison of band intensity of Klp5-3HA and Klp6-3HA to that of Cut2-3HA, against the intensity of the non-specific bands (marked with asterisk). Level of expression of Cut2 has been previously determined as 20,000 molecules/cell. Klp5 and Klp6 are estimated to be produced at 31,600 and 20,000 molecules/cell, respectively. **B)** Cells containing both *klp5⁺-13myc* and *cdc25-22* mutation grown in rich media were shifted up to 36°C for four hours, then shifted down to 26°C. Sample were taken every 15 minutes and processed for Western blotting using an anti-myc antibody and calcofluor staining. Klp5-13myc shows multiple bands throughout the cell cycle. Blotting for tubulin control bands indicate that Klp5 level is not cell cycle regulated (data not shown).

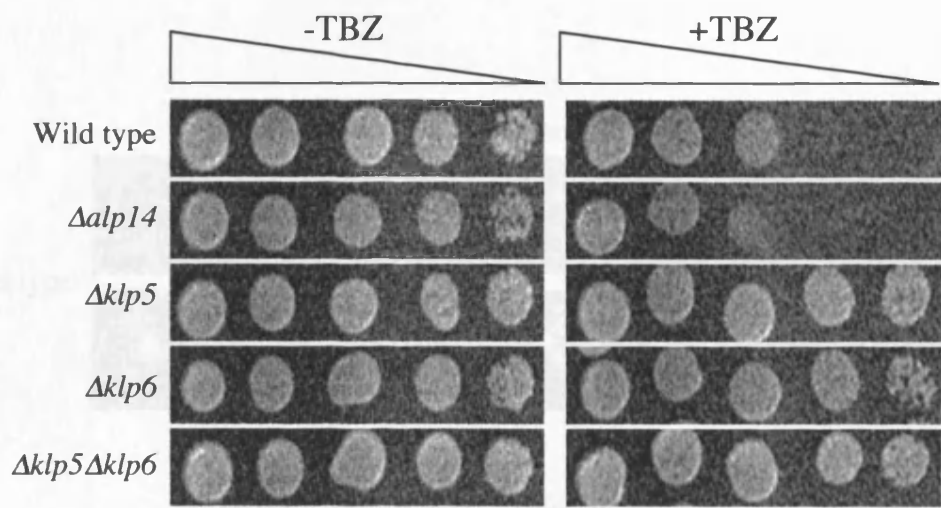


Fig. 5.3.1. Deletion of *klp5*⁺ and *klp6*⁺ results in resistance to microtubule drug, TBZ. Wild type, $\Delta alp14$, $\Delta klp5$, $\Delta klp6$ and $\Delta klp5\Delta klp6$ were spotted after serial dilution (10^6 to 10^2 cells) on rich plates in the absence or presence of $10\mu\text{g/ml}$ TBZ for 4 days at 26°C .

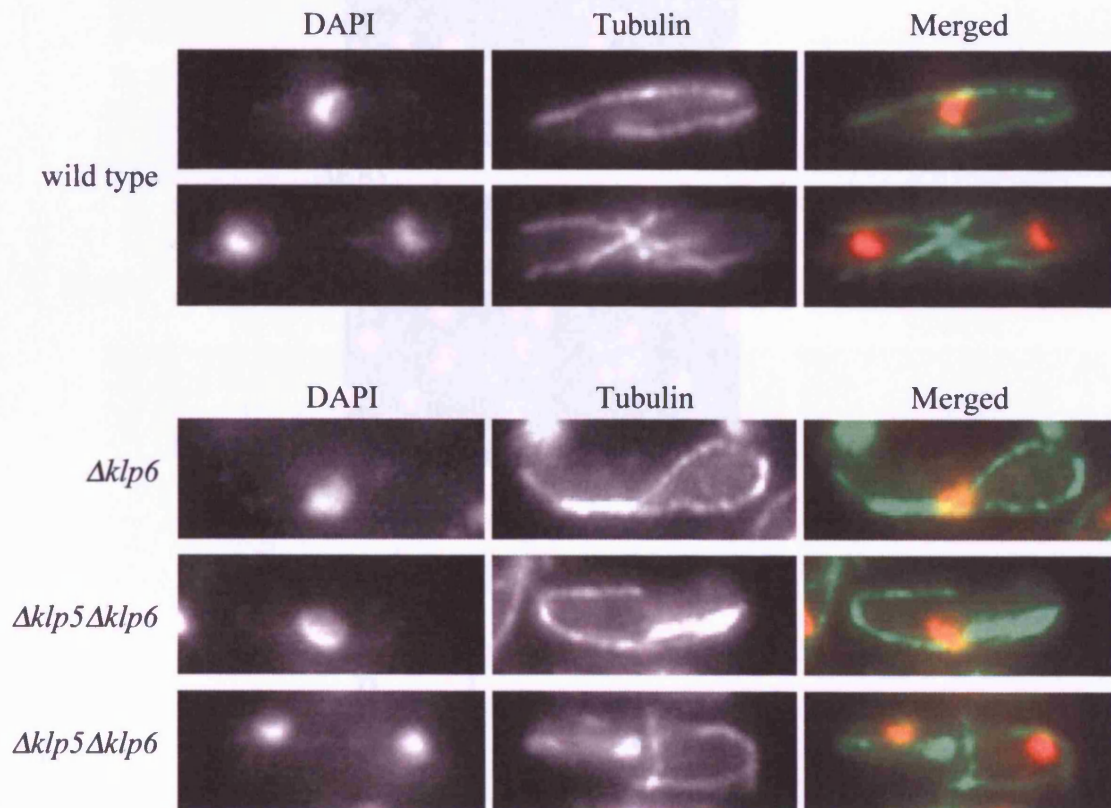


Fig.5.3.2 Deletion of $klp5^+$ and $klp6^+$ shows elongated and curved microtubules. Wild type, $\Delta klp5$, $\Delta klp6$ and $\Delta klp5\Delta klp6$ cells were fixed with methanol and processed for immunostaining with anti- α -tubulin antibody. Visualisation by fluorescence microscopy shows elongated and curved cytoplasmic microtubules in $\Delta klp6$ and $\Delta klp5\Delta klp6$ in comparison with wild type. The scale bar indicates 10 μ m.

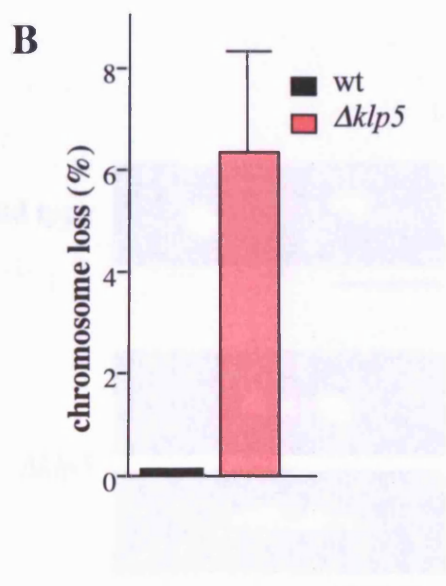
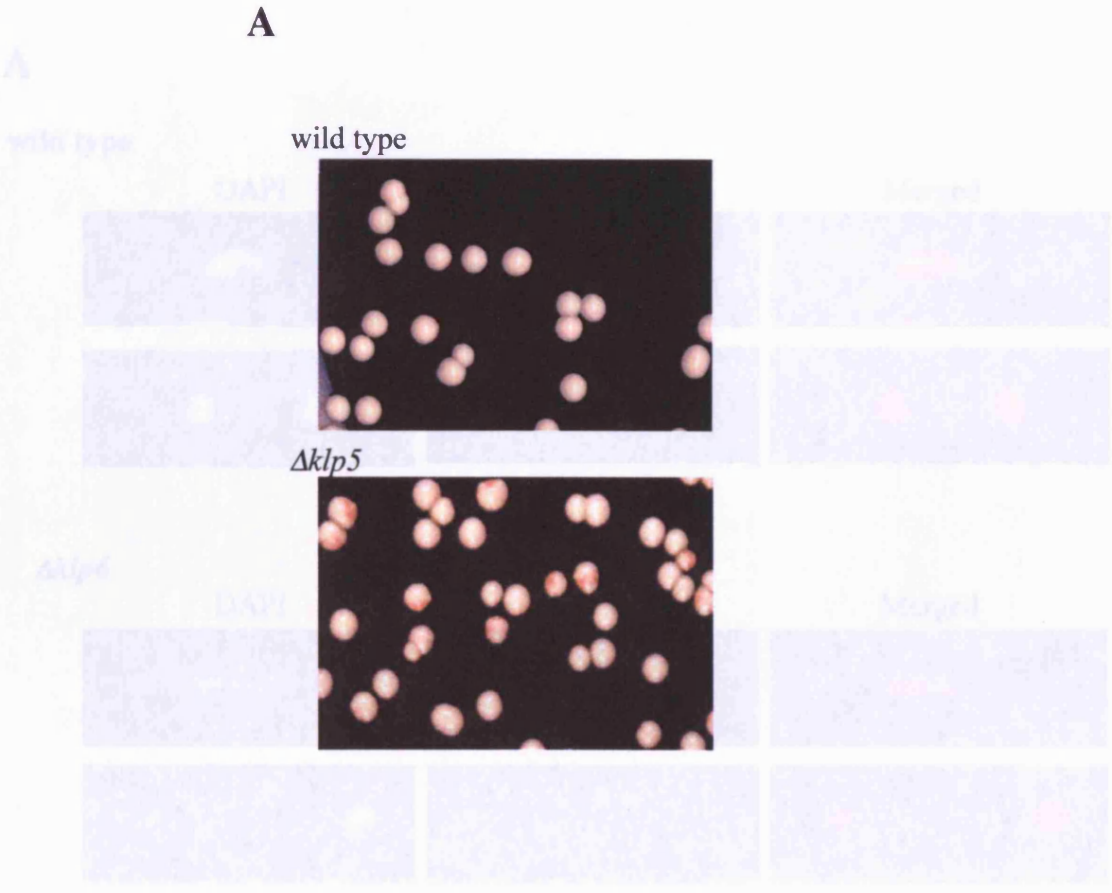


Fig.5.3.3 Deletion of $klp5^+$ and $klp6^+$ causes mini-chromosome loss. Wild type, $\Delta klp5$, $\Delta rad3$ and $\Delta klp5 \Delta rad3$ cells containing linear mini-chromosome grown on selective media (to retain mini-chromosome) were plated on rich media and incubated at 30°C for four days. **A)** $\Delta klp5$ colonies show sectoring adenine auxotroph, indicative of mini-chromosome loss. **B)** The percentage of mini-chromosome loss (red sectoring colonies). The rate of mini-chromosome loss is 0.092 per division.

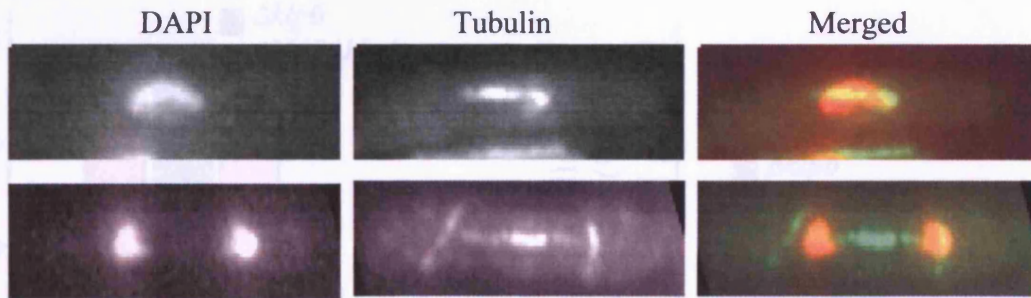
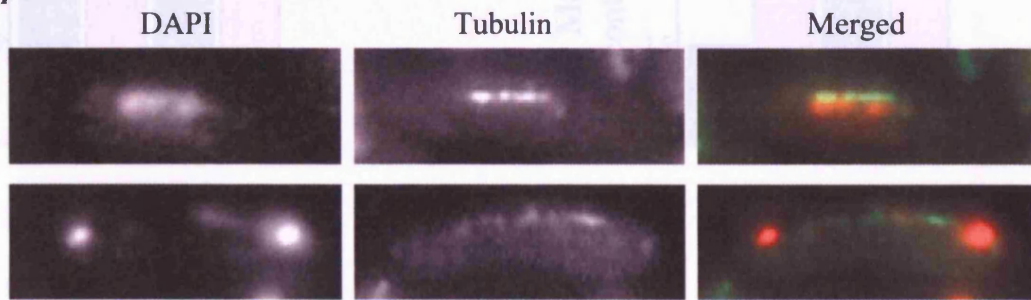
A**wild type** **$\Delta klp6$** **B****wild type** **$\Delta klp5$** 

Fig.5.3.4. Deletion of $klp5^+$ and $klp6^+$ causes chromosome missegregation. A) Wild type and $\Delta klp6$ cells were fixed with methanol and processed for immunostaining with anti- α -tubulin antibody. Visualisation by fluorescence microscopy shows chromosome segregation defects in anaphase. B) Wild type and $\Delta klp5$ cells were fixed with formaldehyde and stained with DAPI dye. Chromosome missegregation phenotype in $\Delta klp5$ is shown. The scale bar indicates 10 μ m.

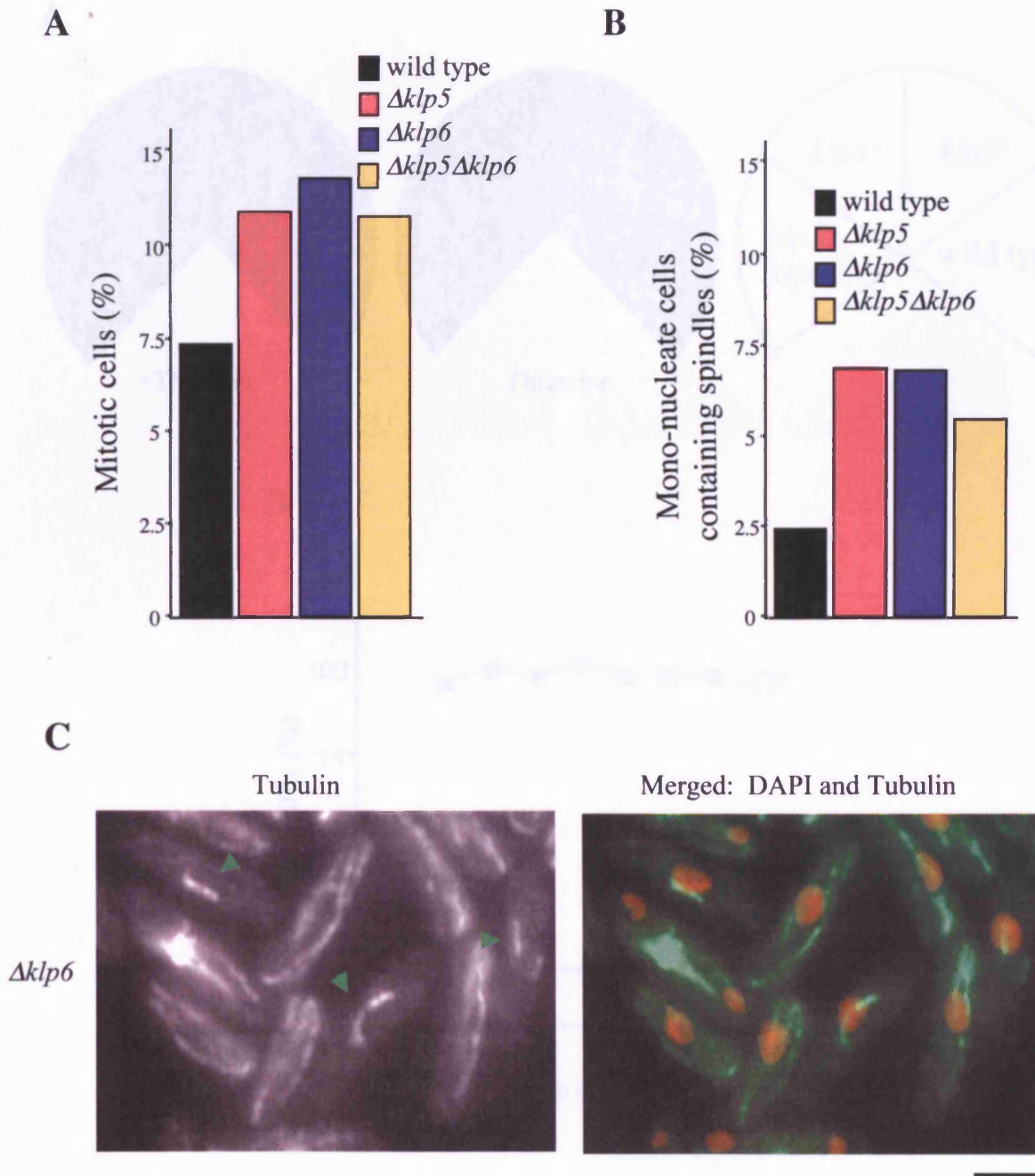


Fig.5.3.5. Deletion of $klp5^+$ and $klp6^+$ causes delay in mitotic progression. Wild type, $\Delta klp5$, $\Delta klp6$ and $\Delta klp5\Delta klp6$ cells were fixed with methanol and processed for immunostaining with anti- α -tubulin antibody. Cells in each phase of the cell cycle were visualised by fluorescence microscopy and counted. **A)** Accumulation of mitotic cells in $\Delta klp5$, $\Delta klp6$ and $\Delta klp5\Delta klp6$. **B)** Quantification of cells in each phase of mitosis shows accumulation of mono-nucleate cells containing spindles (corresponding prometaphase to anaphase A) in $\Delta klp5$, $\Delta klp6$ and $\Delta klp5\Delta klp6$. **C)** Mono-nucleate cells containing spindles (arrow heads). The scale bar indicates 10 μ m.

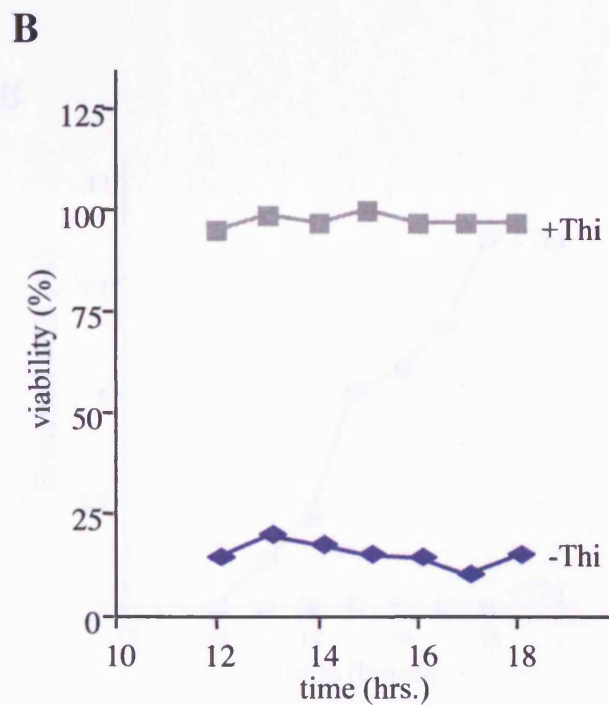
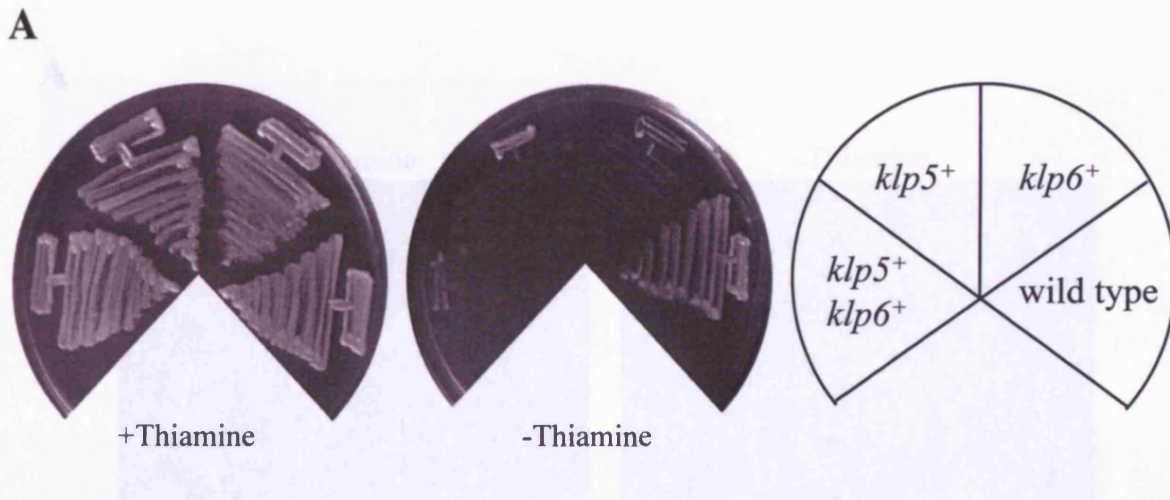


Fig. 5.4.1. Overexpression of *klp5*⁺ and *klp6*⁺ is toxic. **A)** Wild type, *P3nmt-klp5*⁺, *P3nmt-klp6*⁺ and *P3nmt-klp5*⁺-*P3nmt-klp6*⁺ strains were streaked onto minimal media in presence or absence of thiamine and incubated at 30°C for three days. Inducible promoter expresses gene product in absence of thiamine. **B)** *P3nmt-klp6*⁺ cells grown in minimal media in presence or absence of thiamine was plated onto fresh media at 200 cells per plate and incubated at 30°C for three days. Percentage of viability was determined by the number of colonies grown.

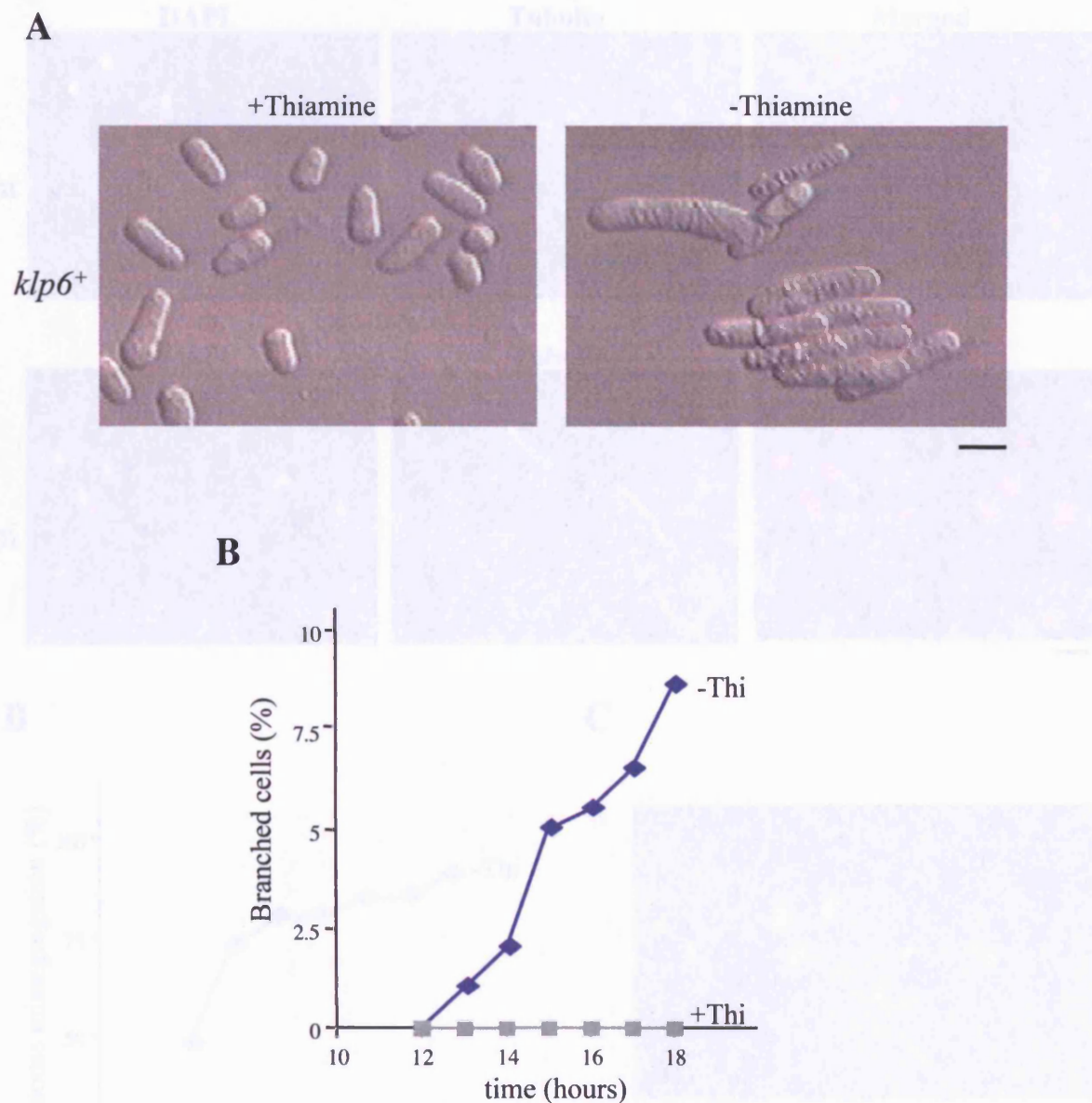


Fig.5.4.2. Overexpression of *klp5*⁺ and *klp6*⁺ results in defective cell shape. *P3nmt-klp6*⁺ cells grown in rich media was transferred into fresh minimal media in presence or absence of thiamine and incubated at 30°C. Samples were taken hourly from 12-18 hours. **A)** Morphology of the cells visualised by light microscopy at 16 hours shows elongated and branched cells in overexpressed condition. **B)** Percentage of branched cells increases sharply in overexpressed condition. The scale bar indicates 10 μ m.

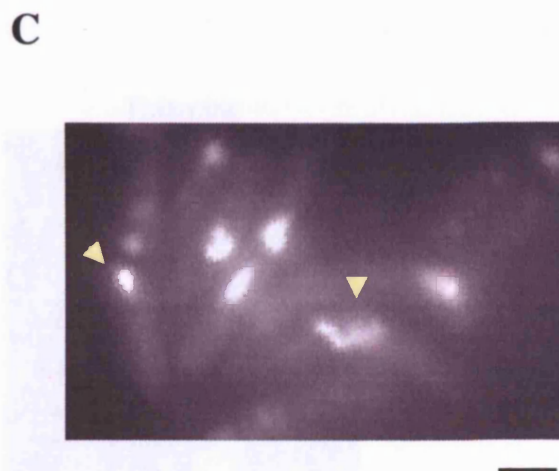
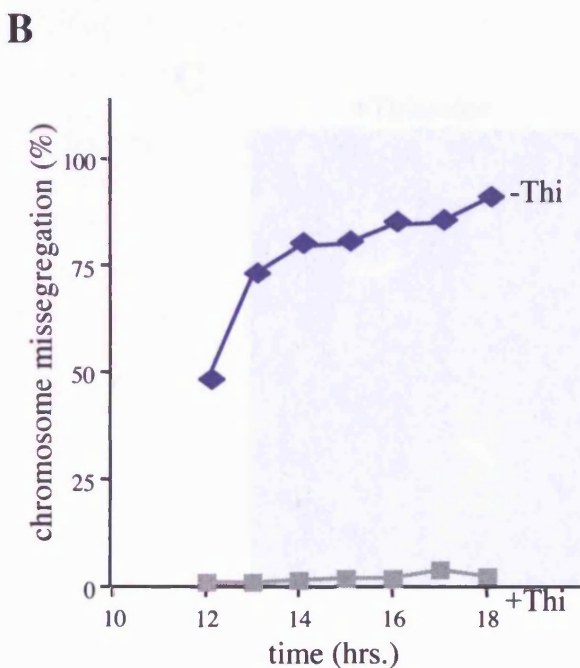
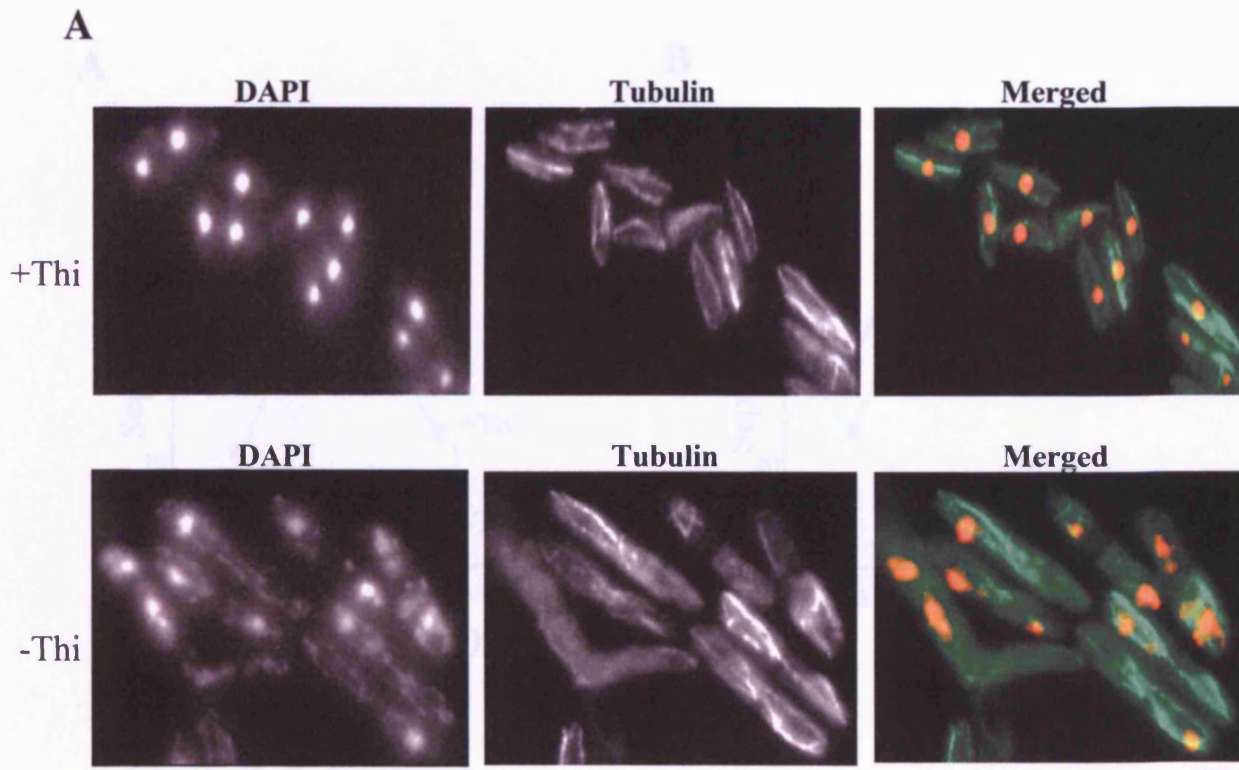


Fig.5.4.3. Overexpression of *klp5+* and *klp6+* results in mitotic spindle defects and chromosome missegregation. *P3nmt-klp6+* cells grown in rich media was transferred into fresh minimal media in presence or absence of thiamine and incubated at 30°C. Samples were taken hourly from 12-18 hours. **A)** Tubulin and DAPI stained cells, showing compromised spindles and chromosome segregation defects after 16 hours in overexpression condition. **B)** Quantification of the number of cells with missegregated chromosomes. **C)** DAPI-stained cells, showing cut phenotype after 22 hours in overexpression condition (arrow heads). The scale bar indicates 10 μ m.

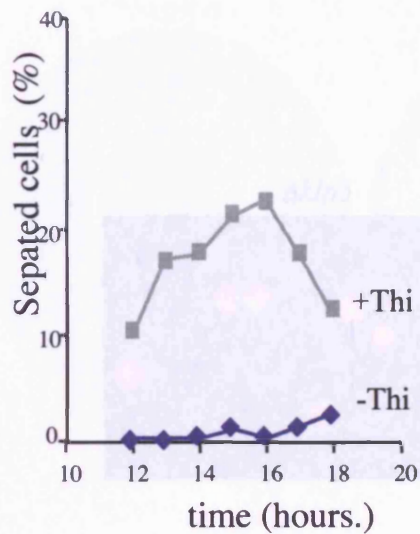
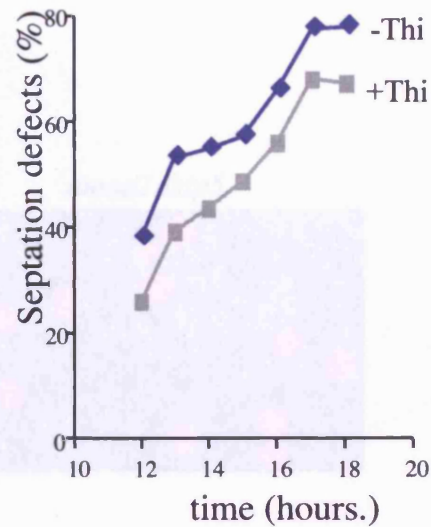
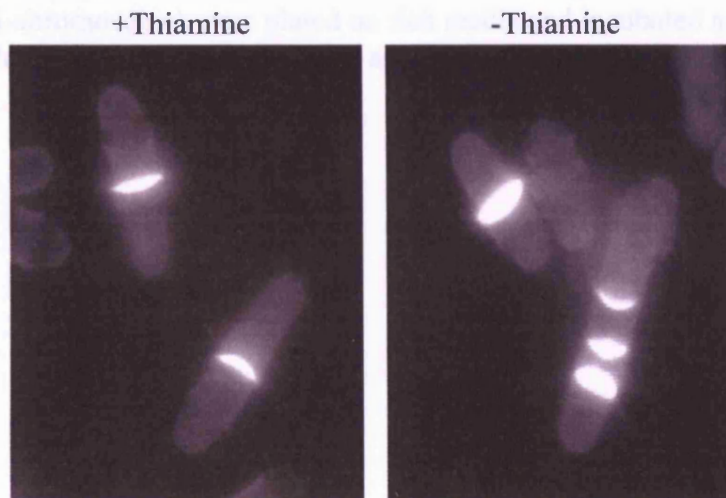
A**B****C**

Fig.5.4.4. Overexpression of *kfp5*⁺ and *kfp6*⁺ shows defects in septation. *P3nmt-kfp6*⁺ cells grown in rich media was transferred into fresh media in presence or absence of thiamine and incubated at 30°C. Samples were taken hourly from 12-18 hours, fixed with formaldehyde and stained with calcofluor. **A)** The percentage of septated cells is abnormally low in overexpression condition. **B)** Quantification of septated cells showing septation defects such as thick, wavy or multiple septa. **C)** A cell showing multiple septation defect after 16 hours in overexpression condition.

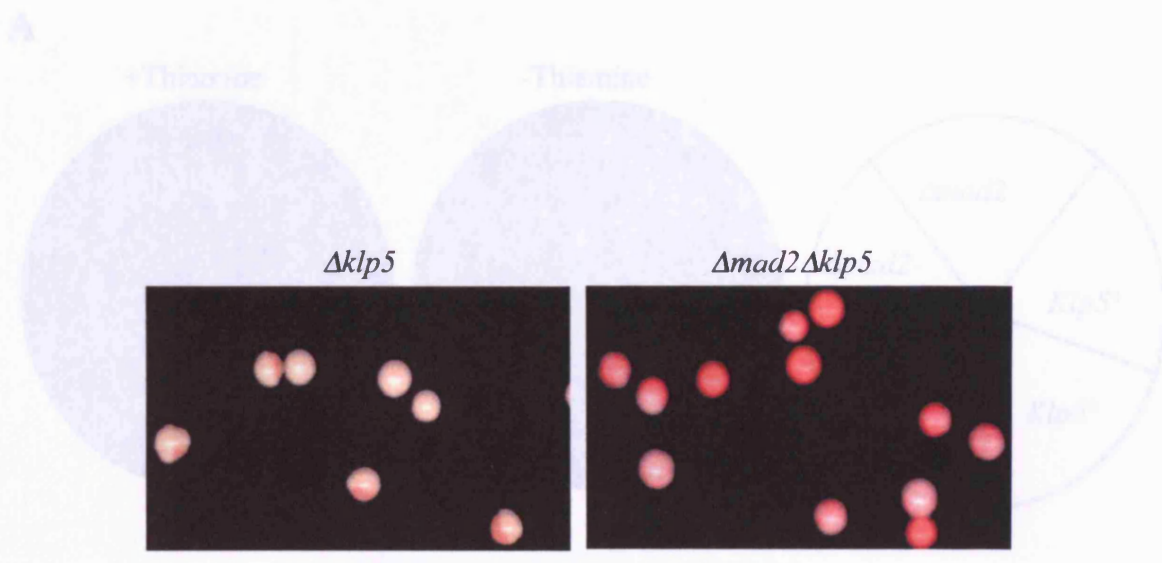


Fig.5.5.1. Deletion of *mad2*⁺ in *Δklp5* mutant exacerbates chromosome loss. *Δklp5* and *Δmad2Δklp5* cells containing linear mini-chromosome grown on selective media (to retain mini-chromosome) were plated on rich media and incubated at 30°C for four days. Colonies show sectorized adenine auxotroph, indicative of mini-chromosome loss.

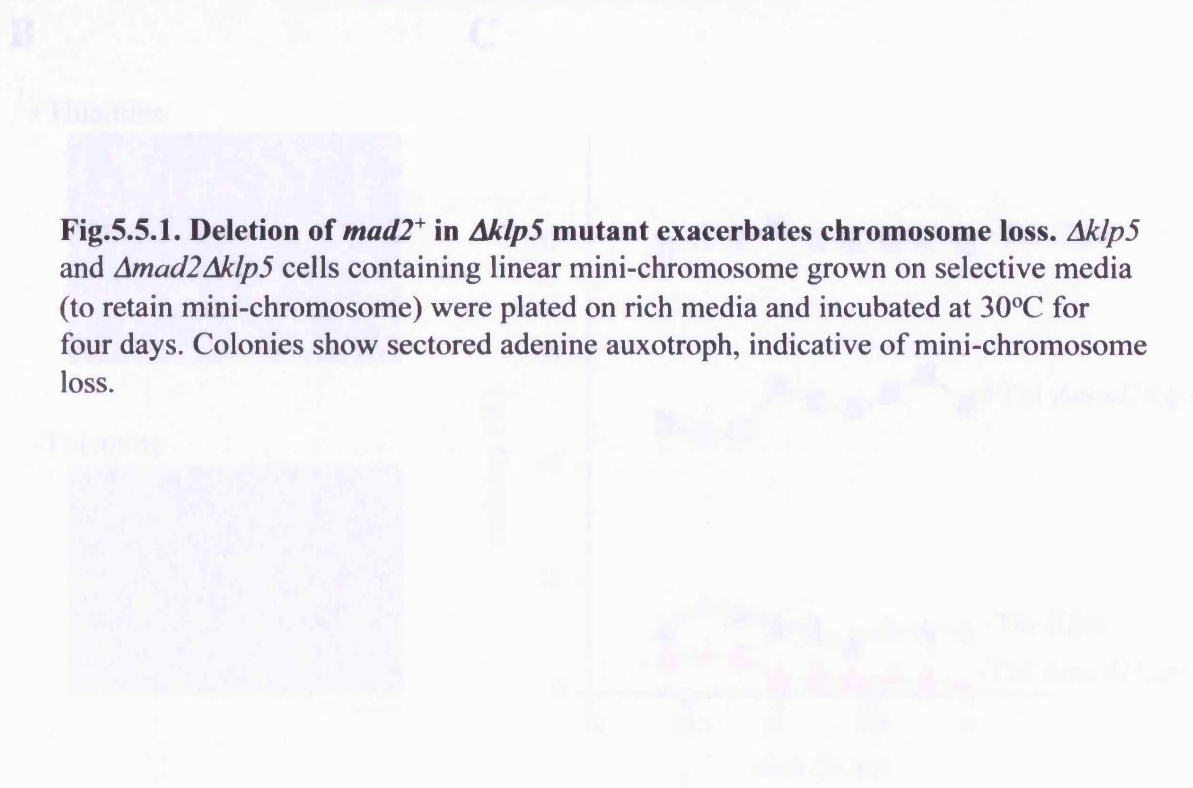


Fig.5.5.2. Deletion of *mad2*⁺ by itself with wild-type *klp5* does not exacerbate chromosome loss. *Δmad2* and *Δmad2Δklp5* cells containing linear mini-chromosome were grown on selective media (to retain mini-chromosome) and plated on rich media and incubated at 30°C for four days. *Δmad2* cells show no sectorization indicating no chromosome loss. *Δmad2Δklp5* cells grown on rich media do not show sectorization in the absence of thiamine, which is indicative of chromosome loss. *Δmad2* cells were plated at 10⁶ cells per plate and incubated at 30°C for four days. *Δmad2Δklp5* cells were plated at 10⁶ cells per plate and incubated at 30°C for four days. The sectorization of *Δmad2Δklp5* cells was observed in the absence of thiamine. The scale bar is 100 μm.

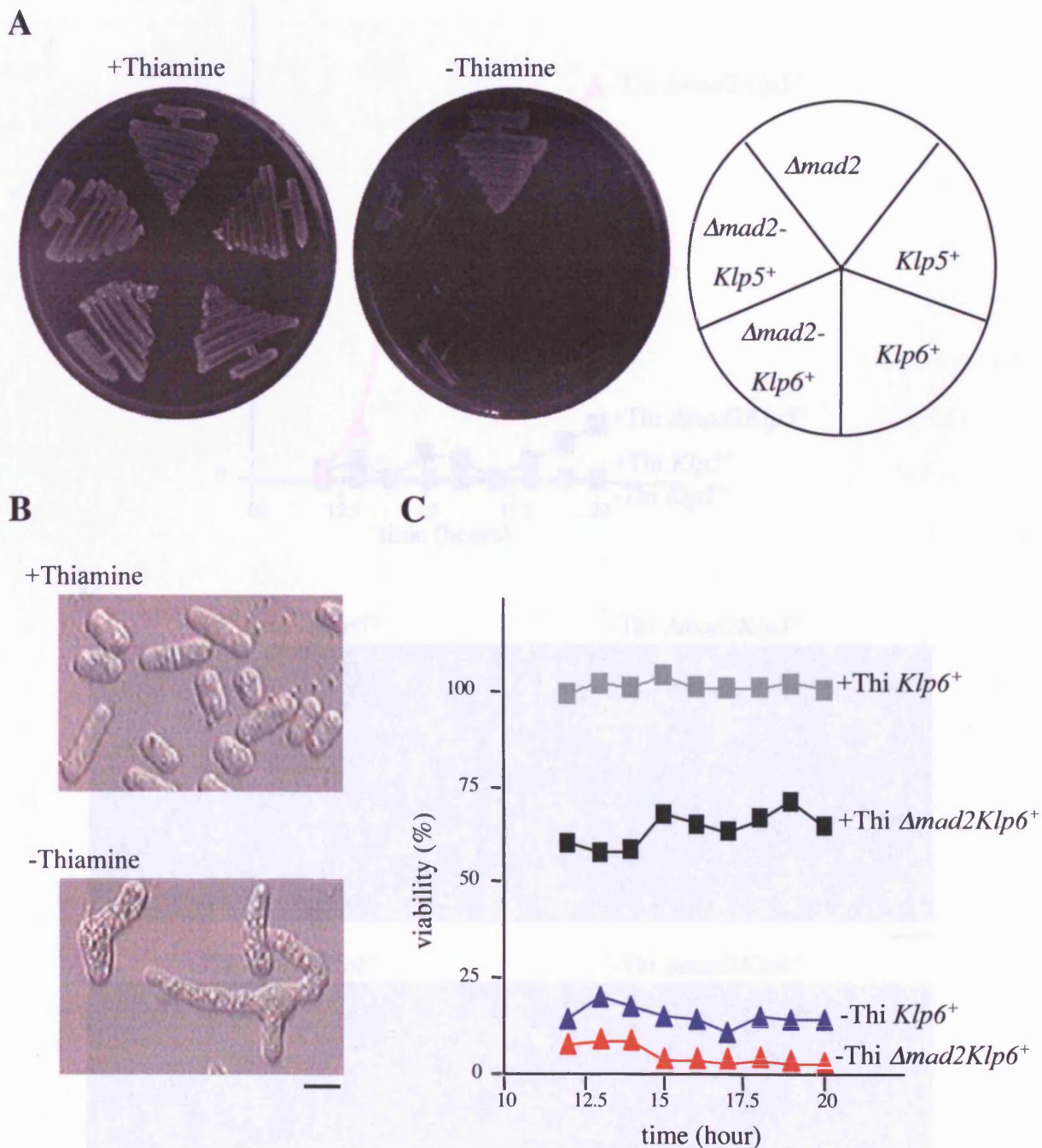


Fig.5.5.2. Deletion of *mad2*⁺ in *klp5* and *klp6* overexpression mutant exacerbates toxicity. A) Wild type, *P3nmt-klp5*⁺, *P3nmt-klp6*⁺ and Δ *mad2-P3nmt-klp5*⁺, Δ *mad2-P3nmt-klp6*⁺ strains were streaked onto rich media in presence or absence of thiamine and incubated at 30°C for 3 days. B) *P3nmt-klp6*⁺ cells show severe branching morphology. C) *P3nmt-klp6*⁺ and Δ *mad2-P3nmt-klp6*⁺ cells grown in rich media in presence or absence of thiamine was plated onto fresh media at 200 cells per plate and incubated at 30°C for three days. Percentage of viability was determined by the number of colonies grown. The scale bar indicates 10 μ m.

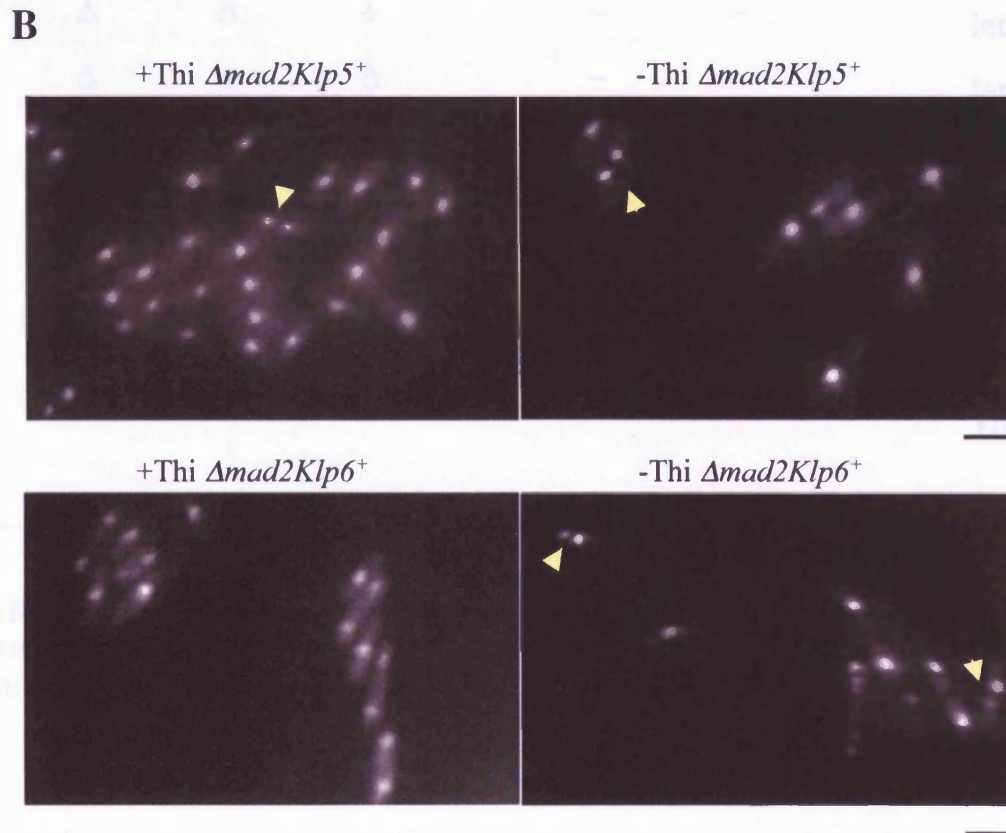
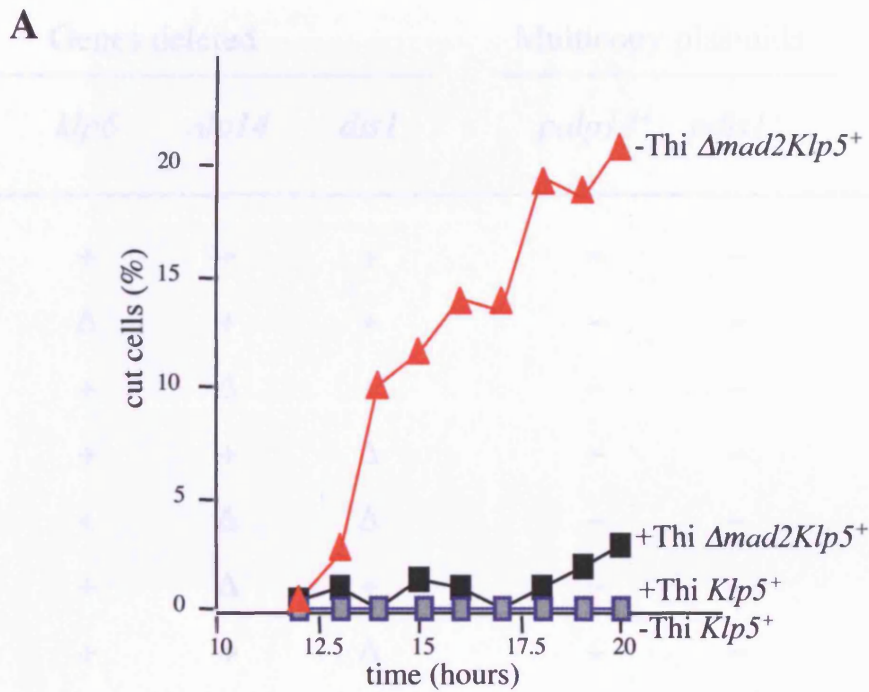


Fig.5.5.3. Deletion of $mad2^+$ in $klp5$ and $klp6$ overexpression mutant results in cut cells. $P3nmt-klp5^+$, $P3nmt-klp6^+$, $\Delta mad2-P3nmt-klp5^+$ and $\Delta mad2-P3nmt-klp6^+$ cells grown in rich media were transfer to fresh media in presence or absence of thiamine and incubated at 30°C. Samples for taken hourly and stained with DAPI. **A)** Quantification of cut cells in $P3nmt-klp5^+$ and $\Delta mad2-P3nmt-klp5^+$. **B)** $\Delta mad2-klp5^+$ and $\Delta mad2-klp6^+$ cells after 16 hours in presence or absence of thiamine, showing cut phenotype (arrow heads). The scale bar indicates 10 μm .

Genes deleted				Multicopy plasmids		Viability
<i>klp5</i>	<i>klp6</i>	<i>alp14</i>	<i>dis1</i>	<i>palp14⁺</i>	<i>pdis1⁺</i>	
Δ	+	+	+	-	-	viable
+	Δ	+	+	-	-	viable
+	+	Δ	+	-	-	viable, ts
+	+	+	Δ	-	-	viable, cs
+	+	Δ	Δ	-	-	lethal
Δ	+	Δ	+	-	-	lethal
Δ	+	+	Δ	-	-	lethal
+	Δ	Δ	+	-	-	lethal
+	Δ	+	Δ	-	-	lethal
Δ	Δ	Δ	Δ	-	-	lethal
+	+	Δ	Δ	-	+	viable
Δ	+	+	Δ	-	+	viable
Δ	+	Δ	+	+	-	viable
Δ	Δ	Δ	+	+	-	viable

Table 5.6.1 Genetic interaction between *klp5⁺*, *klp6⁺*, *alp14⁺* and *dis1⁺*. + indicates wild type alleles and Δ represents deletion mutants. cs and ts denote cold- and temperature-sensitive, respectively.

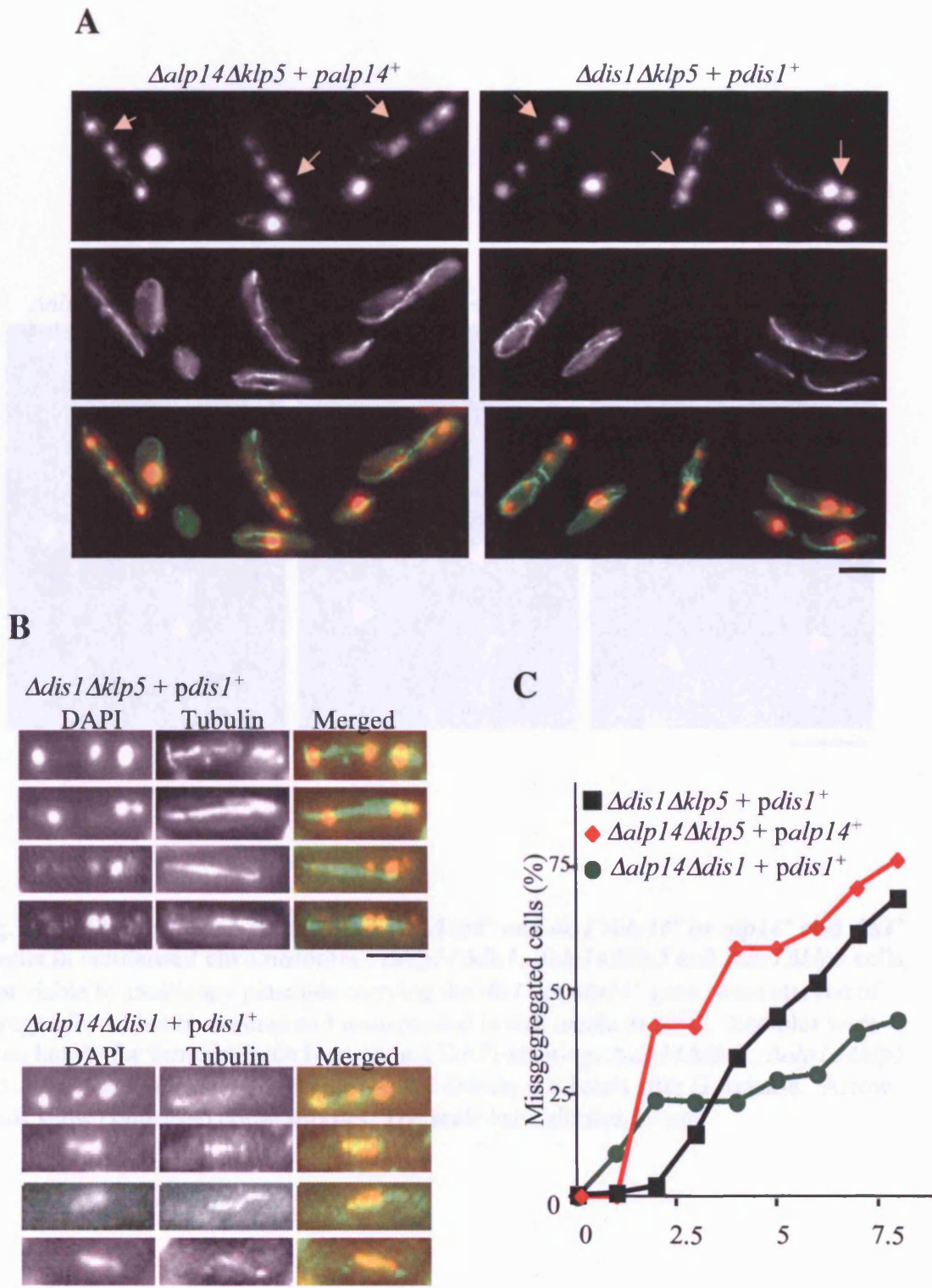


Fig. 5.6.2. Klp5/Klp6 and Dis1/Alp14 share an essential function in mitotic progression. *Δalp14Δklp5*, *Δdis1Δklp5* and *Δalp14Δdis1* cells, kept viable by multicopy plasmids carrying the *dis1⁺* or *alp14⁺* gene, were starved of nitrogen for 12 hours, washed and resuspended in rich media at 30°C. Samples were taken hourly for methanol fixation and anti-tubulin staining. **A)** Defective phenotypes of *Δalp14Δklp5* and *Δdis1Δklp5* at seven hours after G₁ release, leading to lethality. Missegregated chromosomes in post-anaphase cells are shown by arrows. **B)** Representative mitotic defects in *Δdis1Δklp5* and *Δalp14Δdis1* cells at seven hours after G₁ release. **C)** Quantification of cells showing chromosome segregation defects. The scale bar indicates 10 μm. 203

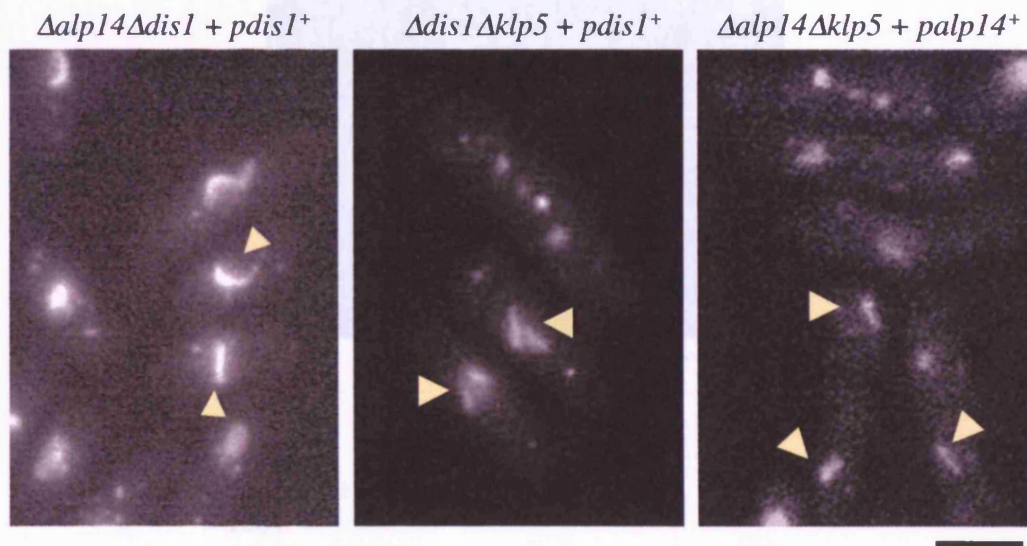
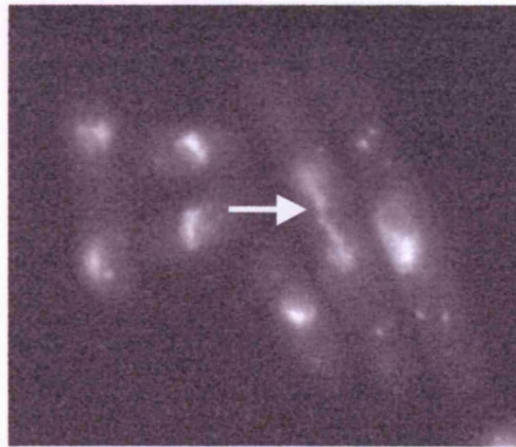


Fig. 5.6.3. Simultaneous deletion of *klp5*⁺/*klp6*⁺ and *dis1*⁺/*alp14*⁺ or *alp14*⁺ and *dis1*⁺ results in condensed chromosomes. *Δalp14Δdis1*, *Δalp14Δklp5* and *Δdis1Δklp5* cells, kept viable by multicopy plasmids carrying the *dis1*⁺ or *alp14*⁺ gene, were starved of nitrogen for 12 hours, washed and resuspended in rich media at 30°C. Samples were taken hourly for formaldehyde fixation and DAPI-staining. *Δalp14Δdis1*, *Δalp14Δklp5* and *Δdis1Δklp5* cells showing chromosome defects at 6 hours after G₁ release. Arrow heads show condensed chromosomes. The scale bar indicates 10 μm.

A

Δmad2Δklp5-dis1-203 +pdis1⁺



B

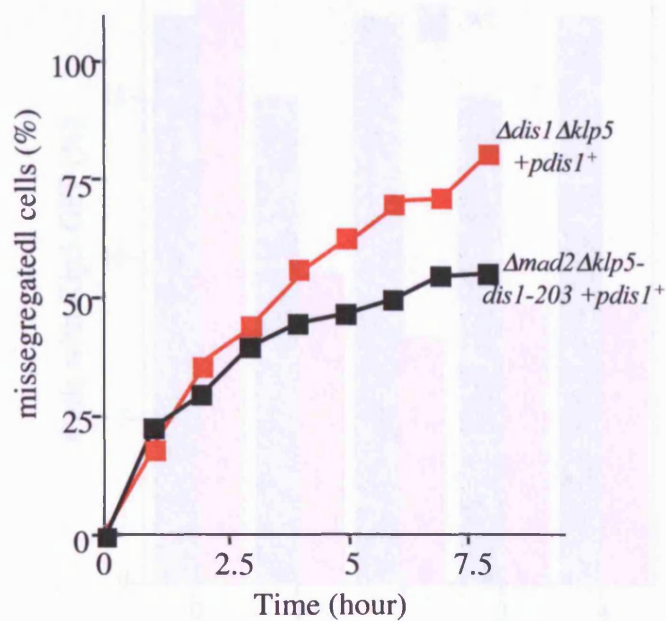


Fig. 5.6.4. Mutations in *mad2⁺*, *dis1⁺/alp14⁺* and *klp5⁺/klp6⁺* cause stretched chromosome phenotype. *Δmad2Δklp5-dis1-203* cells, kept viable by multicopy plasmids carrying the *dis1⁺* gene, were starved of nitrogen for 12 hours, washed and resuspended in rich media at 30°C. Samples were taken hourly for formaldehyde fixation and DAPI-staining. **A)** *Δmad2Δklp5-dis1-203* cells showing stretched chromosomes at six hours after G₁ release (arrow heads). **B)** Quantification of chromosome missegregation defects. The scale bar indicates 10 μm.

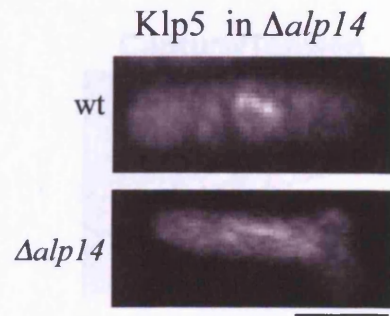
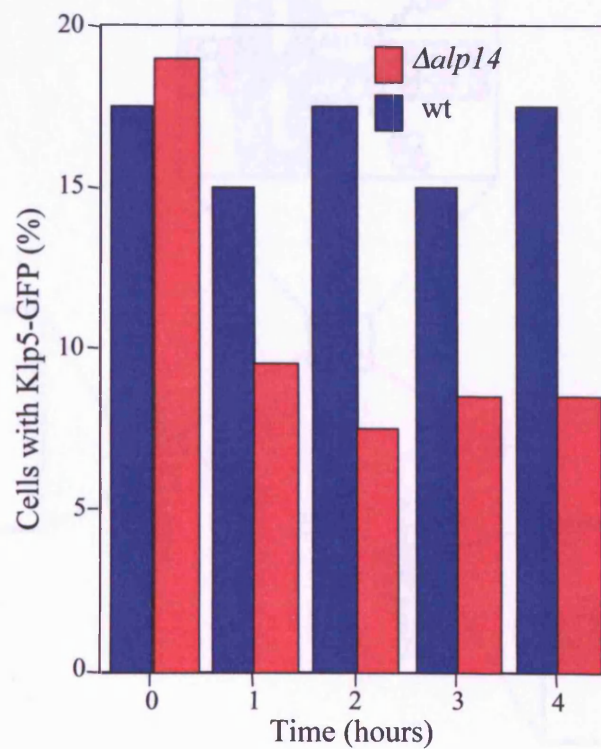
A**B**

Fig. 5.6.5. Deletion of $alp14^+$ causes the kinetochore localisation of Klp5 to be reduced. $\Delta alp14$ cells containing Klp5-GFP grown in rich media at 26°C were shift up to 36°C. Samples for taken hourly for four hours after temperature shift up. In $\Delta alp14$ cells, Klp5-GFP localisation to the kinetochore is reduced. The scale bar indicates 10 μ m.

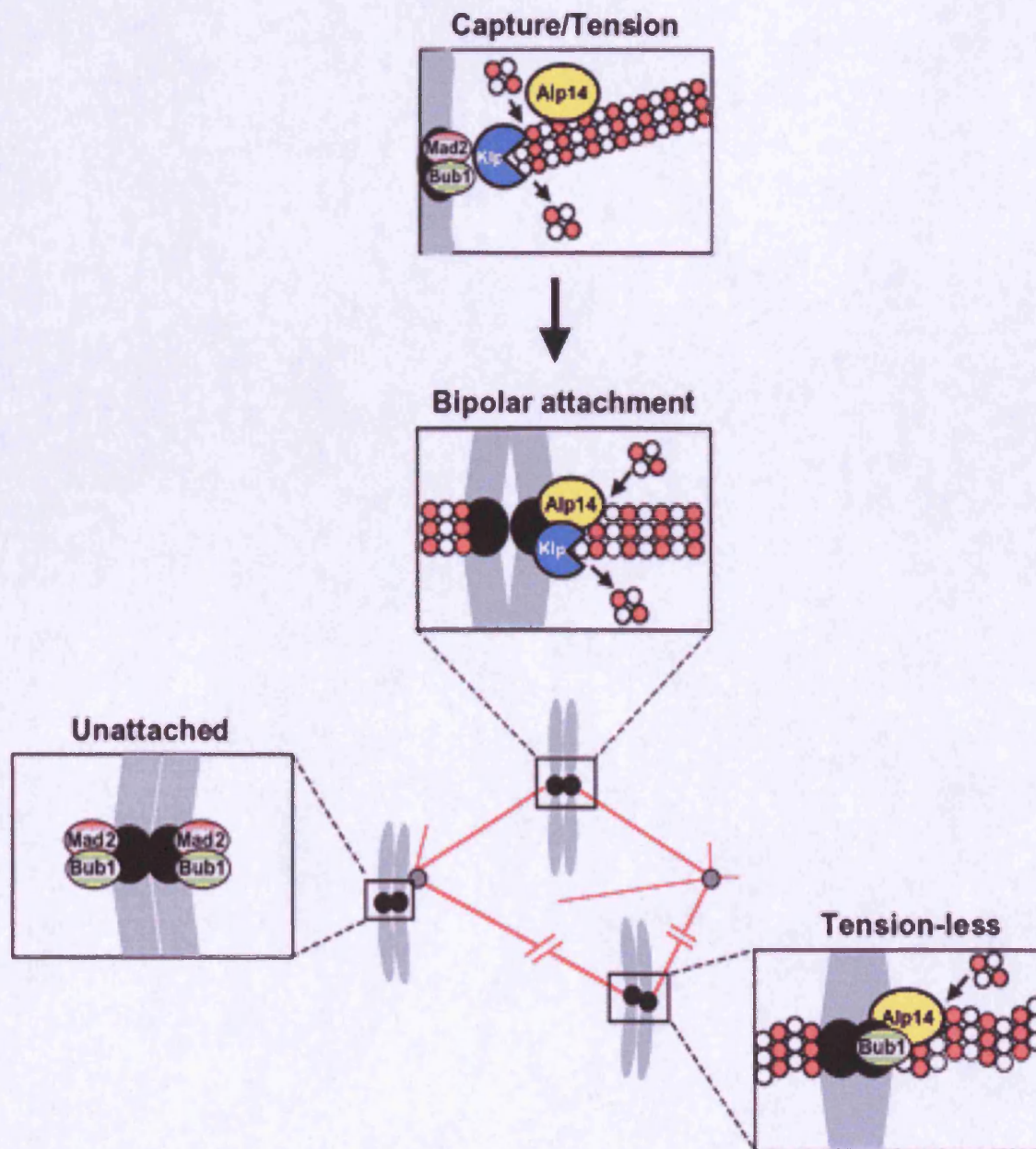


Fig. 5.7.1 A role for Klp5/Klp6 and Alp14/Dis1 in the formation of bipolar mitotic spindles. Klp5/Klp6 (shown as Klp) and Alp14/Dis1 (shown as Alp14) localise to both the mitotic spindles and the mitotic kinetochores. Alp14/Dis1 facilitates the spindle-kinetochore attachment by promoting spindle growth at the plus-ends and Klp5/Klp6 generates tension by promoting spindle shrinkage, leading to generation of poleward force. In the absence of Alp14, spindles fail to capture the kinetochores, resulting in Bub1 and Mad2 recruitment to the kinetochore (depicted as closed black circles). Klp5 and Klp6 have an additional role in generation of tension at the kinetochores upon attachment, and in their absence tension fails to be generated. These tension-less kinetochores recruit Bub1, but not Mad2.

CHAPTER 6

Discussion

Microtubule dynamics is tightly controlled during cell division to ensure accurate and timely chromosome segregation. In mitosis, the spindle is first polymerised from opposite poles to capture replicated sister chromatids at the kinetochores. Once kinetochores are stably attached, spindles are depolymerised, resulting in a poleward pulling force that segregates the DNA. When regulators of spindle dynamics are absent or defective, bipolar attachment and stabilised spindle-kinetochore interaction are compromised. In wild type cells, this leads to a delay in anaphase onset by activation of the spindle assembly checkpoint to allow the error to be corrected (Li and Nicklas, 1995; Chen *et al.* 1996; Zhou *et al.* 2002). However, in conditions where the spindle assembly checkpoint is also defective, gross chromosome missegregation occurs, leading to aneuploidy and lethality. In this thesis, we study the role of microtubule regulators, Alp14 and Klp5 / Klp6, in their separate and collaborative roles in mitosis.

A previous study of fission yeast Alp14 of the highly conserved TOG family revealed that it is required for microtubule stabilisation in interphase and mitosis. In the absence of functional Alp14, cytoplasmic microtubules become short and broken, resulting in cell polarity defects. In mitosis, cells with compromised Alp14 display gross chromosome missegregation, accompanied by weak mitotic spindles (Garcia *et al.* 2001). Subsequently, Alp14 was determined to be crucial to establish spindle bipolarity and was postulated to act as a linker between plus-ends of spindles and kinetochores (Garcia *et al.* 2001). In addition, Alp14 was found to be required for the spindle assembly checkpoint (Garcia *et al.* 2001). In the present study described in this thesis, specific domains of Alp14 are investigated to separate and further elucidate the protein's dual roles in microtubule dynamics and the spindle checkpoint.

From analyses of several constructs that delete or overexpress specific domains of Alp14, we reveal consistent results, showing the surprising finding that the two TOG domains in Alp14 are required for distinct mechanisms despite their high structural conservation. From our data, the first TOG domain (TOG1) is shown to be required for the spindle

assembly checkpoint. Its deletion results in failure to maintain the spindle checkpoint in spindle damaged conditions, while its overproduction causes hyper-activation of the checkpoint apparently without spindle damage. On the other hand, the second TOG domain (TOG2) functions to stabilise microtubules. Further analyses of TOG1's role in the spindle assembly checkpoint suggest that Alp14 may maintain the checkpoint via the outer kinetochore Nuf2/Ndc80 complex. Alp14 is found to bind to Nuf2, while deletion of TOG1 causes Nuf2 and Ndc80 to be delocalised from kinetochore in spindle damaged conditions. Lastly, our study of Klp5 and Klp6 shows that unlike Alp14, they depolymerise microtubules, but similarly to Alp14, they are also required for mitotic progression and accurate chromosome segregation. Investigation into the relationship between Alp14/Dis1 and Klp5/Klp6 shows that they genetically interact, and despite apparent opposing activities towards microtubule stability the families of microtubule associated proteins share an essential mitotic function to ensure spindle-kinetochore attachment and tension-generation.

Detailed results and their implications are discussed below. Note that this discussion spans results found in chapters 2-4, while the discussion for chapter 5 has been included within the chapter.

6.1 The C-terminal tail of Alp14 is required for localisation

From studies in chapter 3, we have determined that the C-terminal tail of Alp14 is required for localisation throughout the cell cycle. The first results that implicated the region in the localisation function were from constructs that delete Alp14 from the C-terminus (section 3.1). In all of these constructs, defects in cell polarity were displayed at the restrictive temperature. Upon further investigation, it became apparent in live microscopy and in fixed samples (co-stained with anti α -tubulin) that Alp14 localisation was lost in all constructs. Because it is also possible that the loss of localisation was due to the insertion of GFP fusion or that the mutant proteins were unstable and readily degraded, the Alp14 protein was also deleted from the N-terminus.

Consistent to above results, analyses of *alp14* N-terminal deletions showed Alp14 localisation to be reduced or lost in the absence of the C-terminal tail. Surprisingly,

when the microtubule-binding and coiled-coil regions were deleted ($\Delta N-M$), faint Alp14 localisation could still be observed. In fact, Alp14 localisation became completely lost only when further deletion into the C-terminal tail was carried out, which resulted in a 100-residue Alp14 mutant protein ($\Delta N-C$). Note that both $\Delta N-M$ and $\Delta N-C$ constructs displayed identical mutant phenotypes, including bent/branched cells, short/weak microtubules and chromosome missegregation. This suggests that even though the C-terminal tail allows for microtubule function by localisation, it may not in itself possess direct microtubule-stabilising activity or at least not be sufficient for this activity.

The localisation dependency of Alp14 on its C-terminal tail is supported by the finding that Alp14 binds to Alp7, a TACC homologue, at this region (Sato *et al.* 2004). In this report, the $\Delta N-M$ construct (reduced Alp14 localisation - also known as $\Delta 696$ in Sato *et al.* 2004) was necessary and sufficient for interaction with Alp7 in two-hybrid assays. The study also showed Alp14 localisation in mitosis to be entirely dependent upon Alp7. However, only Alp7 recruitment to spindles is dependent on Alp14. Taken together, the report suggests that Alp14 and Alp7 localise in mitosis as a complex. In this model, Alp7 recruits Alp14 to SPBs. Once on SPBs, Alp14 can then be recruited to spindles in an Alp7-independent manner. Alp7, on the other hand, requires Alp14 to localise to spindles. Note that although the $\Delta N-M$ construct could bind Alp7, our study shows its expression to result in reduced Alp14 localisation, suggesting that the microtubule and coil-coil motifs may be required for Alp14 binding to microtubules, which in turn is also required for the recruitment of Alp7 to mitotic spindles.

6.1.1 The Conservation of the C-terminus in the localisation function.

Like Alp7-Alp14, interaction between TACC and TOG family of proteins has also been reported in various organisms including human; frog, fly and worm (Gergely *et al.* 2000 and 2003; Cullen and Ohkura 2001; Lee *et al.* 2001; Bellanger and Gonczy 2003; Srayko *et al.* 2003). In all studies to date, TACC homologues have consistently been shown to recruit TOG proteins to centrosomes and microtubules. Like that of fission yeast, fly D-TACC also appears to interact with microtubules indirectly, and is speculated to interact with microtubules through its interaction with TOG homologue Msps (Lee *et al.* 2001). In worm, TAC-1 and TOG protein, ZYG-9, were also found to stabilise each other, which is thought of as a key feature that ensures microtubule assembly (Bellanger and Gonczy 2003).

Because TOG-TACC interaction and their localisation dependencies appear to be well conserved, it is attractive to postulate that all TOG proteins require a localisation partner. Unlike Alp14, Dis1 has not been found to require Alp7 for localisation in interphase or mitosis (Sato *et al.* 2004). Although Dis1 localisation partner has yet to be found, it's localisation dependencies on a binding partner cannot be ruled out. Like Alp14, all TOG homologues in yeast carry a coiled-coil motif at the C-terminus, suggesting that it may be possible to isolate TOG binding partners using the C-terminus as a bait, for example in a two-hybrid screen or TAP-tag biochemical assay. Although metazoan TOG proteins carry a C-terminal tail that is diverged from that of yeast and do not carry coiled-coil domains, it is possible that the localisation dependency on the C-terminus is conserved. In fly, the C-terminus of D-TACC was shown to be necessary and sufficient for microtubule-binding (Gergely *et al.* 2000). As mentioned earlier, further investigations showed that the C-terminus binds to microtubules indirectly and that D-TACC binds to TOG homologue Msps, leading to speculation that TACC interact with microtubules through its interaction with TOG in flies (Gergely *et al.* 2000; Lee *et al.* 2001). If the localisation dependency on the C-terminus were conserved, it would also be consistent with various findings that the C-terminus of TOG is required for microtubule function, as localisation to microtubules would allow the proteins to exert their function.

6.2 The second TOG domain (TOG2) and the C-terminus of Alp14 stabilise microtubules

In addition to localisation, our study has also shown the C-terminal region, together with the second TOG domain (TOG2), to stabilise microtubules. Evidence for this comes from analyses of both *alp14* partial deletions from the N-terminus (chapter 3, section 3.2) and specific overexpressions of Alp14 domains (chapter 4, sections 4.2.2, 4.3, 4.4). In cells carrying a construct where the first TOG domain is deleted ($\Delta TOG1$), defects in cell polarity, microtubule morphology and chromosome segregation were not observed at any temperature. Simultaneous deletions of the TOG1 motif and *kfp5*⁺ or *kfp6*⁺ genes were also viable and did not display additive phenotypes, even though $\Delta alp14 \Delta kfp5$ leads to

synthetic lethality. These data suggest that TOG1 is probably not required for microtubule function. However, upon further deletion of the N-terminus resulting in the absence of the second TOG domain ($\Delta TOG2$), cells become temperature-sensitive, showing bent/branched cells and chromosome missegregation at 36°C. This indicates that the TOG2 motif is required for microtubule function. Immuno-staining of $\Delta TOG2$ cells with anti- α -tubulin clearly shows short and weak cytoplasmic microtubules, which suggests that TOG2 may promote microtubule elongation, thereby stabilising them. Accordingly, when both TOG domains were overexpressed ($pTOG^+$) in a wild type background, cytoplasmic microtubules and anaphase astral spindles exhibited hyper-elongated phenotypes. Because the TOG1 domain has not been shown to be required for microtubule function, we speculate that microtubules become hyper-elongated upon overexpression of the TOG2 motif. Put together, we postulate that the second TOG domain of Alp14 stabilises microtubules by directly or indirectly elongating them. Although not carried out in this study, this point could be clarified by specifically overexpressing TOG2 by vector expression in a wild type background.

In our systematic truncation experiment, further deletion from the N-terminus into the C-terminal region results in similar phenotypes as $\Delta TOG2$, though lagging chromosomes and cut phenotypes were more frequently found. Increased chromosome missegregation events suggest that the C-terminus may carry an additional microtubule function to TOG2. However, our systematic deletion data remain inconclusive on this point, and an investigation of cells overexpressing TOG2 and C-terminus was carried out for clarification. When the TOG2 and C-terminal regions were endogenously overexpressed, cells exhibited hyper-bundled microtubules. This indicates that the C-terminus may indeed carry an additional microtubule function to TOG2, possibly a microtubule-bundling activity. Note that in these cells, the TOG1 motif is absent similarly to $\Delta TOG1$, where no microtubule defects were observed, which indicates that the bundled-microtubule phenotype is a result of TOG2 and C-terminus overexpression. Conversely, cells that simultaneously overexpress TOG domains and delete the C-terminus ($ov-TOG2$) display weak and unbundled microtubules. Note that this phenotype is distinctly different from that of $pTOG^+$, which suggests that hyper-bundling of microtubules is caused by the absence of the C-terminal domains in $ov-TOG2$.

Note that microtubule stabilisation could stem from direct addition of $\alpha\beta$ tubulin subunits, prevention of shrinkage, inhibition of catastrophe or promotion of rescue. In vitro studies in frog extracts found that as well as an increased growth, the rate of rescue was augmented when purified XMAP215 was added to pure microtubules (Gard and Kirschner 1987; Vasquez *et al.* 1994). The results from these reports suggest that XMAP215 prevents catastrophe as well as directly promoting growth at microtubule plus-ends. One way to achieve this is by microtubule bundling. Growing microtubules appear closely bundled and sheet-like under electron microscopy, while shrinking microtubules are specifically curved at the growing end (Alberts *et al.* 1994; Nogales *et al.* 2003). Given that Alp14 is localised as punctuated dots along the microtubule, particularly at the plus-ends, it is possible that Alp14 may also bundle microtubule protofilaments, thereby reducing the rate of catastrophe and subsequently promoting microtubule growth. Overall, from our observations we speculate that the second TOG domain of Alp14 promotes microtubule elongation and the C-terminal facilitates this activity by bundling microtubule protofilaments at the plus-ends.

6.2.1 How does Alp14 stabilise microtubules?

It has been reported that some microtubule associated proteins such as the Dam1 complex are bound to microtubules as rings (Westermann *et al.* 2005; Miranda *et al.* 2005). The ring structure is an attractive means to envisage how a protein might form complexes around microtubules that allow for bundling. In this structure, a protein complex would also be able to travel along microtubules and visualised as punctuated patterns as Alp14. However, Alp14 proteins have not been found to interact with each other, making the ring concept unlikely.

To date, the structure of TOG family of proteins have not been intensely studied and the molecular structure of TOG proteins are unknown. However, a study using unidirectional shadowing and electron microscopy has shown frog XMAP215 to be an elongated molecule of approximately 60nm (Cassimeris *et al.* 2001). The results from this study interpret that XMAP215 is a thin, rod shaped molecule that could span up to eight tubulin dimers along a microtubule protofilament. Electron microscopy shows although most XMAP215 molecules were straight, a subset appears bent, which suggests that XMAP215 is flexible (Cassimeris *et al.* 2001). The study also shows that XMAP215 did not stiffen microtubules upon assembly, which suggests that although

XMAP215 binds to microtubule lattice, it is surprisingly unlikely to stimulate microtubule stability through the interaction. Instead, XMAP215 may enhance α/β tubulin dimer to be added onto microtubule plus-ends (Cassimeris *et al.* 2001). This proposal has also been suggested by other groups investigating TOG homologues in frog and human, based on the rate of microtubule assembly (Gard and Kirschner 1987) and binding affinity of XMAP215 to tubulin dimers (Spittle *et al.* 2000).

6.2.2 The Conservation of the TOG2 and the C-terminus in microtubule stabilisation.

Given its high sequence conservation at the N-terminal region, it is speculated that the highly conserved TOG domains possess a microtubule-stabilising activity. However, various studies have shown contradictory results, including several reports that the diverged C-terminal regions are unexpectedly responsible for the conserved microtubule function (Nabeshima *et al.* 1995; Wang and Huffaker 1997; Nakaseko *et al.* 2001). In our study, the C-terminal tail of Alp14 has been shown to be required for Alp7-binding and localisation. This function may be conserved given that TACC-TOG homologues have been found to bind in various organisms and that this is absolutely required for localisation of TOG homologues to SPBs (Cullen and Ohkura 2001; Lee *et al.* 2001; Bellanger and Gonczy 2003; Srayko *et al.* 2003). It is possible that the requirements of the C-terminus for microtubule-stabilisation in above-mentioned reports are solely because the region localises the protein, allowing for microtubule function. However, results from our study also agree with the reports that as well as localisation, the C-terminus also stabilises microtubules, possibly by bundling protofilaments.

Surprisingly, the second TOG domain of Alp14 is also required for microtubule stabilisation, even though the first TOG domain possesses a distinct function. The requirement of the TOG2 domain is in agreement with an *in vitro* finding that the N-terminal region of XMAP215 carries a microtubule polymerisation activity (Popov *et al.* 2001). In addition, microtubule-binding assays of human ch-TOG and its specific domains demonstrated that two microtubule-binding domains are found in this organism. Consistent to our finding, one of the microtubule-binding domains is located within a region of approximately 600 amino acids near the N terminus, and the second in the C-terminus of the protein (Spittle *et al.* 2000). The consistency between these studies in fission yeast, frog and human suggests that the conserved N-terminus and diverged C-

terminal regions of TOG homologues may be functionally conserved to stabilise microtubules.

Compatible to the flexibility of XMAP215 visualised by electron microscopy (Cassimeris *et al.* 2001), HEAT repeat proteins are thought to be flexible (Kobe *et al.* 1999). This suggests that conserved HEAT repeats within TOG domains may interact with microtubules protofilaments to exert their function (Cassimeris *et al.* 2001). Also, as HEAT repeats are known protein-protein interaction sites (Neuwald and Hirano 2000), the role of the TOG domains may be determined by the protein that binds to them. In our study no binding partner of the TOG2 domain has been found. An effort to isolate binding partners of TOG domains could yield some very interesting answers to the functional conservation of TOG proteins. Apart from TOG2 binding to microtubules or microtubule proteins, the TOG2 domain may also stabilise microtubules by its proximity to the C-terminus, which contains a microtubule-binding domain. By its location, it may be that the presence of TOG2 enhances the folding of the protein, thereby allowing it to regulate microtubule dynamics.

Lastly, it is important to mention a surprising report that budding yeast Stu2 depolymerises microtubules *in vitro* (Van Breugel *et al.* 2003). The contrast in microtubule function between budding yeast and other organisms may be reflective of functional divergence. Budding yeast cell division requires an organism-specific process to migrate the nucleus to the bud-neck, which involves kinesin Kip3 (DeZwaan *et al.* 1997; Straight *et al.* 1997). Given that Stu2 and Kip3 and their homologues functionally oppose each other on a molecular level (Tournebize *et al.* 2001; Kinoshita *et al.* 2001; Severin *et al.* 2001; Garcia *et al.* EMBO 2002), it is probable that Stu2 has diversified to adapt to budding yeast processes and Kip3 function. It should be noted that Stu2 is reported to stabilise microtubule (Severin *et al.* 2001) or promote microtubule dynamics (Kosco *et al.* 2001)

6.3 The first TOG domain of Alp14 (TOG1) is required to maintain the spindle checkpoint in spindle damage

In this thesis, we have also determined a novel function of the TOG motif. From analyses of deletion and overexpression mutants, the first TOG domain of Alp14 is shown to be specifically required for the spindle assembly checkpoint. While deletion of TOG1 did not result in microtubule or chromosome defects at any temperature, when spindle damage is induced by either addition of microtubule drugs or *cut7* mutation, premature anaphase onset occurs (chapter 3, section 3.2 and 3.3). Like wild type, $\Delta TOG1$ cells are capable of activating the spindle checkpoint. However, the checkpoint fails to be maintained in this condition, resulting in cell cycle progression and appearance of cut cells. Synchronised $\Delta TOG1$ cells released into mitosis show accumulation of Cdc13-GFP upon addition of CBZ, but thereafter drops sharply and prematurely compared to wild type, showing spindle checkpoint activation followed by premature anaphase onset. Similarly, upon temperature shift up the $\Delta TOG1 cut7$ mutant accumulated condensed chromosome, reminiscent of spindle checkpoint activation. However, the checkpoint was not maintained and the number of condensed chromosomes rapidly declined while cut cells appeared. Moreover, in all of our experiments where TBZ or CBZ were added, including those repeated and not shown, cut cells quickly amassed and the viability is lost prematurely compared to wild type in the same conditions.

Conversely, upon overproduction of TOG domains in a wild type background ($pTOG^+$ - chapter 4, section 4.2), cells arrest in metaphase without spindle damage or chromosome missegregation. In overexpressed condition, $pTOG^+$ cells quickly lose their viability and fail to grow. This lethal phenotype is abolished upon deletion of spindle checkpoint proteins, suggesting that overproduction of TOG domains hyper-activates the spindle assembly checkpoint. Overall, although artificial conditions were often used in the studies of both $\Delta TOG1$ and $pTOG^+$, results consistently implicate TOG1 to function in the spindle checkpoint cascade.

It is of note that this thesis also suggests that the TOG1 domain specificity functions in the spindle assembly checkpoint cascade. We have made this deduction from the lack of cell polarity, microtubule or chromosome segregation defects at any temperature in $\Delta TOG1$. In addition, $\Delta TOG1 \Delta klp5$ was viable and did not show additive phenotype.

Moreover, the number of cells showing Mad2, Mad3 and Bub1 dots were observed in $\Delta TOG1$ only when microtubule drugs were added. Despite the evidence, however, we acknowledge that it is challenging to confirm the specificity of TOG1 function, due to the overlapping requirements of the spindle- and checkpoint- functions of Alp14.

6.3.1 Involvement of TOG1 in the spindle checkpoint through kinetochore proteins

Investigation to elucidate the role of TOG1 in the spindle checkpoint in our study reveals interesting findings. Firstly, in $\Delta TOG1$, visualisation of Mad2-GFP, Mad3-GFP and Bub1-GFP in synchronised mitotic cells indicate that they are able to localise to kinetochores in the presence of CBZ (chapter 3, section 3.2). From existing knowledge of localisation dependencies, we were able to assume from our results that all spindle checkpoint proteins were able to localise to kinetochores in $\Delta TOG1$. Intriguingly, the percentage of cells containing strong Mad2-GFP and Mad3-GFP dots hyper-accumulated, while the number of cells displaying Bub1-GFP dots appear to be similar to that of wild type. To ensure accuracy and verity, these experiments have been repeated several times, with the results of each showing specific hyper-accumulation of Mad2 and Mad3, but not Bub1.

The hyper-accumulation of Mad2 and Mad3, without Bub1 in our study is significant because Mad2 and Mad3 are thought turnover from the kinetochore to rearrange into a complex with Slp1 (Chung and Chen 1999, Sudakin *et al.* 2001; Hardwick *et al.* 2000; Millband and Hardwick 2002; Sudakin and Yen 2004; Di Antoni *et al.* 2005). To date, structural studies of Mad2 show that the protein exists in two structural conformations through the position of its C-terminal tail. It is thought that ‘free’ Mad2 cannot readily bind to Slp1. Instead, Mad2-Slp1 complex forms when a free Mad2 is modified at the kinetochore by another Mad1-bound Mad2. This modification is thought to allow its rearrangement into anaphase-inhibiting MCC complex (containing Slp1-Mad2-Mad3-Bub3 – Sudakin *et al.* 2001; Hardwick *et al.* 2000; Millband and Hardwick 2002; Sudakin and Yen 2004; Di Antoni *et al.* 2005). Although the structure of Mad3 has yet to be studied, Mad3 is also thought to be required to rearrange into the MCC complex, using the kinetochore as a catalytic site for its modification (Sironi *et al.* 2002; Musacchio and Hardwick 2002), while Bub1 is not required to be rearranged into the APC-inhibiting MCC complex with Slp1. Put together, we postulate that specific hyper-

accumulation of Mad2 and Mad3 in $\Delta TOG1$ may be caused by their inability to turnover from the kinetochore in the absence of TOG1.

One fundamental question is how the spindle assembly checkpoint could be activated in $\Delta TOG1$ if Mad2 and Mad3 were unable to turnover in this condition? One possibility is that mechanisms of spindle checkpoint activation and maintenance are different. Some studies have shown that anaphase delay can occur without localisation of Mad2 to the kinetochore (DeLuca *et al.* 2003; MerRajagopalan *et al.* 2004; Meraldi *et al.* 2004; Gillett *et al.* 2004), which suggests that there may be a population of ‘already-modified’ free Mad2 that may be able to directly bind to Slp1. The cell’s initial response to spindle damage may be directly activating Mad2-Slp1 interaction rather than localising Mad2 to the kinetochore for modification, as the latter would result in a more delayed response. However, as the population of ‘modified’ Mad2 becomes depleted, free (unmodified) Mad2 needs to localise to the kinetochore to allow for binding to Slp1, thereby maintaining the spindle checkpoint. It is important to note that free Mad2 is thought to require modification because its conformation requires high energy to drive Mad2-Slp1 binding (Chung and Chen 1999, Sudakin *et al.* 2001; Hardwick *et al.* 2000; Millband and Hardwick 2002; Sudakin and Yen 2004; Di Antoni *et al.* 2005). In this case, it is also possible that upon spindle damage, the cells preferably drive the high-energy Mad2-Slp1 binding as an initial response.

Given that the kinetochore acts as catalytic site for the turnover of Mad2 and Mad3, we also analysed localisation of outer kinetochore proteins in $\Delta TOG1$. To our surprise, the result from this experiment shows that in the absence of TOG1, outer kinetochore proteins Nuf2 and Ndc80 were delocalised from the kinetochore in spindle damaged conditions. This data fittingly links in with previous findings that unlike other kinetochore complexes, the Nuf2-Ndc80 complex (consists of Nuf2, Ndc80/Hec1, Spc24 and Spc25) also functions as a component of the spindle assembly checkpoint (Janke *et al.* 2001; McClelland *et al.* 2004). Moreover, like $\Delta TOG1$, some *nuf2* mutants or depletion of Nuf2/Hec1 affected the localisation of only some checkpoint proteins. For example, chicken Hec1 or Nuf2 depletion caused mitotic arrest with only BubR1 but not Mad2 localisation (Hori *et al.* 2003). Similarly, depletion of hSpc25 showed a loss of Hec1 and hMad1, while hBub1 and hBubR1 recruitment were retained (Bharadwaj *et al.* 2004). Conjointly, it is possible that TOG1 may maintain the spindle assembly

checkpoint by localising or stabilising the Nuf2/Ndc80 complex at the kinetochore in conditions where the spindle is compromised. Consistently, further investigation into Alp14 and Nuf2 found the proteins to form a complex. Because TOG1 localises Nuf2 and Ndc80, we speculate that the TOG domain is required for Nuf2-Alp14 interaction or that Nuf2 directly interacts with the TOG domain.

It is interesting that the delocalisation of Nuf2 in $\Delta TOG1$ only occurs in spindle-damaged condition. An explanation for this could be that Nuf2 becomes delocalised in $\Delta TOG1$ only when the spindle assembly checkpoint is activated due to a high level of activity at the kinetochore during checkpoint activation/maintenance. This implies that Alp14 stabilises Nuf2 during spindle checkpoint maintenance, suggesting that Alp14 may be able to localise to the kinetochore in a microtubule-independent fashion. Another possibility is that Alp14 interacts with Nuf2 in early mitosis, during which both proteins are localised to the SPB-centromere cluster. By binding to Nuf2, Alp14 localises Nuf2 to the kinetochore, thereby stabilises the kinetochore structure. Note that Nuf2 has been shown to localise to SPBs prior to being transferred onto the kinetochore (Nabetani *et al.* 2001; Appelgren *et al.* 2003). When the inner or central kinetochore is disrupted, for example in *mis12* mutant, the SPB-centromere cluster is abolished, with Nuf2 observed with the SPBs (Asakawa *et al.* 2005).

From analysis of $\Delta TOG1$, we propose that TOG1 is required to stabilise Nuf2 at the kinetochore when spindle is damaged to maintain the spindle assembly checkpoint. In this model, Alp14 is required for the recruitment or stabilisation of Nuf2 at the kinetochore, which in turn ensures spindle assembly checkpoint proteins to be stably retained at this site. In the absence of TOG1, the outer kinetochore is destabilised, causing unstable localisation of spindle checkpoint proteins and inhibition of APC via Mad2 and Mad3 cannot be maintained.

Recall that consistent to findings from $\Delta TOG1$ experiments, overexpression of TOG domains ($pTOG^+$) resulted in hyper-activation of the spindle assembly checkpoint. In this condition, the number of cells displaying Bub1-GFP was intriguingly observed even though Mad2-GFP accumulation was not detected. Although this phenomenon appears surprising at first glance, it ties in with our speculation that TOG1 maintains the spindle checkpoint via the Nuf2/Ndc80 complex. As discussed earlier, components of the

Nuf2/Ndc80 complex have been shown to be required for localisation of only some spindle checkpoint components (Martin-Lluesma *et al.* 2002; DeLuca *et al.* 2003; Hori *et al.* 2003; Gillett *et al.* 2004; Meraldi *et al.* 2004; Bharadwaj *et al.* 2004). Loss of hHec1 localisation at the kinetochore by RNAi or antibody depletion in HeLa cells causes kinetochore-localisation of Mps1, Mad2, and Mad3 to be lost (Martin-Lluesma *et al.* 2002; Meraldi *et al.* 2004). In these studies, the recruitment of Bub1 or BubR1 were intriguingly unaffected, suggesting that the Nuf2/Ndc80 complex may regulate the spindle assembly checkpoint specifically via Mph1, Mad1 and Mad2. In addition, in *nuf2* mutants or Nuf2/Ndc80/Hec1 depletion, the spindle assembly checkpoint is activated even though Mad2 is not recruited to the kinetochore (Martin-Lluesma *et al.* 2002; Meraldi *et al.* 2004; Gillett *et al.* 2004). However, despite lack of Mad2 at the kinetochore, the spindle checkpoint component is required for the viability of the cell when hHec1 is depleted as simultaneous depletion of hHec1 and hMad2 resulted in lethality (Martin-Lluesma *et al.* 2002). This also supports earlier findings that the spindle checkpoint cascade is probably not linear and may contain branches (Waters *et al.* 1998; Hoffman *et al.* 2001; Tang *et al.* 2001; Rajagopalan *et al.* 2004; Tournier *et al.* 2004). Although the Nuf2/Ndc80 localisation intensity appears as wild type in *pTOG*⁺ in our study, we cannot exclude the possibility that Nuf2/Ndc80 function is compromised in this condition.

Finally, to further support our data we can suggest experiments that may confirm our findings and speculations. Firstly, co-immunoprecipitation of the Slp1-Mad2 and Slp1-Mad3 complex (for example during a time course in the presence of CBZ) could provide a concrete evidence for the turnover of Mad2 and Mad3. This experiment was attempted in this thesis, but due to technical difficulties with the specificity of Slp1 anti-bodies, we were unable to further investigate this line of experiments. Note that we also attempted to tag Slp1 with 13myc for the co-immunoprecipitation assay. However, C-terminal tagging of Slp1 resulted in cut cells in the presence of microtubule drugs, showing that Slp1-13myc could not fully function in the spindle assembly checkpoint. To verify our Nuf2 data, it may be possible to visualise localisation of checkpoint proteins in *nuf2* mutants. In addition, synchronous mutations of *nuf2*⁺ and TOG1 or *alp14*⁺ may also offer persuasive and conclusive data. Lastly, to clarify the protein-binding properties of TOG1, a binding assay between TOG1 and Nuf2 would need to be carried out. An effort to finding TOG binding partners, for example by TAP-tagging TOG1 and TOG2 or two-

hybrid screens, could lead to interesting results which would further elucidate the role of TOG domains.

6.3.2 The importance of kinetochore stability in spindle assembly checkpoint and maintenance.

Why would the spindle checkpoint require Alp14 to localise/stabilise Nuf2 only during maintenance? The kinetochore is a structure that is built upon by complexes of proteins that need to endure several mechanical stresses. These include spindle attachment, and in the case of mono-orientation or lack of bipolarity, detachment and reattachment, which require phosphorylation of kinetochore proteins by aurora kinase (Tanaka *et al.* 2002; Ohi *et al.* 2003; Andrews *et al.* 2004; DeWar *et al.* 2004). Moreover, upon detection of unattached or tensionless kinetochores, spindle checkpoint proteins are recruited, which additionally requires Mad2 and Mad3 turnover. In wild type, errors arising from unattached or tensionless kinetochores are often rapidly corrected once the spindle checkpoint is activated. However, in conditions where spindles are severely damaged such as mutants, these errors cannot be rectified as rapidly and the spindle assembly checkpoint needs to be maintained. It is compelling to speculate that as the spindle checkpoint is maintained, kinetochores continuously endure the mechanical stress of Mad2 and Mad3 turnover or possibly drive the turnover as a catalytic site, and therefore requires additional maintenance.

In this scenario, we propose that upon spindle damage, an intact kinetochore is able to activate the spindle assembly checkpoint. However, as the damage persists and the checkpoint is maintained, the kinetochore structure needs to be stabilised to cope with a constant activity of Mad2 and Mad3 turnover. From our results, we contemplate that Alp14 localises or stabilises the Nuf2 complex at the kinetochore during spindle checkpoint maintenance, thereby cohering the kinetochore structure during this process.

If this were the case, it may seem surprising that cells would regulate spindle checkpoint maintenance via a plus-end microtubule protein. In the circumstances where spindles are unattached, this explanation appears illogical, as proteins bound to microtubule plus-ends cannot not interact with the kinetochore. However, it is important to note that in wild type cells, particularly in higher eukaryotes, a single kinetochore is captured by several spindles. Unattachment by a single spindle could render the kinetochore tensionless,

resulting in the spindle checkpoint is activated. In our experiments, microtubule drugs TBZ and CBZ were often used. In these drugs, microtubules appear not to be completely depolymerised (our observation - unpublished), which in turn might allow for Alp14 localisation. Alternatively, Alp14 may be recruited to kinetochores in a microtubule-independent manner.

Lastly, it should also be mentioned that although the *alp14-1270* and $\Delta TOG1$ are viable in a $\Delta mad2$ background double deletion of *alp14*⁺ and *mad2*⁺ results in synthetic lethality. At this point it is unclear what causes the lethality, though it is possible that severe microtubule defects together with the absence of spindle checkpoint control led to the loss of viability. This possibility is supported by the fact that larger deletions of Alp14 are lethal with $\Delta mad2$, (ie. while $\Delta TOG1$ and $\Delta TOG2$ are viable with $\Delta mad2$, $\Delta N-MT$ and $\Delta N-C$ are lethal in this condition).

6.3.3 The conservation of the TOG1 in spindle assembly checkpoint maintenance.

Despite sequence and functional conservation of the TOG family of proteins, the role of TOG domains in the spindle assembly checkpoint has never been reported previously. The role of TOG proteins in the spindle checkpoint may be masked by their functions in microtubule-stabilisation in other organisms. It is of note that like TOG homologues in budding yeast and higher eukaryotes, the spindle checkpoint is also activated in *alp14* mutants at the restrictive temperature, where the lack of functional Alp14 causes weak spindles and spindle-kinetochore interaction. It is only when spindle damage is induced at the permissive temperature in *alp14* temperature-sensitive mutants that Alp14's role in spindle checkpoint becomes evident. By systematic truncations of Alp14, we have been able to separate the spindle checkpoint function from the microtubule-stabilising function, facilitating the study of the protein's involvement in the spindle assembly checkpoint.

6.4 Alp14 and Dis1

In addition to Alp14, fission yeast also contains another TOG protein, Dis1. Analysis of Alp14 and Dis1 sequence shows high conservation, with two TOG domains at the N-

terminus and diverged C-terminal regions which carry microtubule-binding and coiled-coil domains. In our study, *alp14⁺* and *dis1⁺* was shown have some overlapping functions (chapter 2 and chapter 5). Deletion of both *alp14⁺* and *dis1⁺* leads to lethality at any temperature, indicating that *alp14* or *dis1* mutants were kept viable only by the other's functions. Consistently, when one of the TOG proteins were deleted, their growth defects at respective temperatures were rescued by introduction of multicopy plasmids containing either gene. However, incomplete suppression of Δ *dis1* by the *palp14⁺* was detected and raised the possibility that the two proteins may not show a complete overlap in their roles. Indeed, studies of *dis1* and *alp14* mutants show that both proteins are required for the formation of bipolar spindle in mitosis (Nabeshima *et al.* 1995 and 1998; Nakaseko *et al.* 1996 and 2001; Garcia *et al.* 2001). However, while cell polarity defects caused by compromised cytoplasmic microtubules are detected in the absence of Alp14, cells lacking Dis1 are not bent or branched at the restrictive temperature (Nabeshima *et al.* 1995; Nakaseko *et al.* 1996 and 2001; Garcia *et al.* 2001). In addition, Dis1 has not been found to function in the spindle checkpoint maintenance. Also note that our results are also suggestive of some competition between Dis1 and Alp14. Partial deletions of Alp14 appear to be more sensitive to microtubule drugs than Δ *alp14* (chapter 3), which suggests that Dis1 is able to compromise for Alp14 function in Δ *alp14*. In *alp14* partial deletions, on the other hand, Dis1 may be unable to do so due to competition.

6.5 Concluding Remarks

In this thesis, we report a study of a microtubule stabiliser, Alp14, by domain analysis. Our results consistently show that despite high structural conservation, the two TOG domains in Alp14 are required for distinct mechanisms, namely the first TOG domain is required for the spindle assembly checkpoint and the second TOG domain is essential for microtubule stabilisation. Upon deletion of the first TOG domain, cells lose the ability to maintain the spindle checkpoint in spindle damaged conditions, and upon overproduction the checkpoint is hyper-activated without apparent spindle damage. From analyses of the role of Alp14 in the spindle checkpoint, our data suggest that Alp14 may maintain the checkpoint via the outer kinetochore Nuf2/Ndc80 complex as Alp14 is found to bind to Nuf2, while deletion of the first TOG motif causes Nuf2 and Ndc80 to be delocalised from kinetochore in spindle damaged conditions. Thus Alp14-TOG is a multi-functional

protein. It plays both structural and regulatory roles in microtubule and mitotic spindle functions in a domain-dependent manner. As the TOG family is well-conserved, roles for Alp14-TOG may be retained throughout evolution. This notion awaits future studies in various systems.

CHAPTER 7

Materials and Methods

7.1 Laboratory stocks and solutions

All media, pipette tips, autoclaved glassware and other commonly used solutions were provided by the Cancer Research UK Central Services.

Solutions, buffers and media

The recipes for buffers and solutions described in this chapter are listed below.

Culture Media	
L-Broth (LB, for bacterium)	170mM NaCl, 0.5% (w/v) yeast extract, 1% (w/v) bacto-tryptone.
YE5S (rich media, for fission yeast)	0.5% Difco yeast extract (yeast nitrogen base – amino acids not yet added), 3% dextrose +250 mg/ml, histidine, leucine, uracil, adenine, and lysine.
EMM (selective or minimal media, for fission yeast)	14.7 mM KH phthalate, 15.5 mM Na ₂ HPO ₄ , 93.5 mM NH ₄ Cl, 111 mM dextrose, salt and vitamin stocks.
N. Starvation media	EMM–NH ₄ Cl.
YE (rich media, for fission yeast)	0.5% Difco yeast extract, 3% dextrose
YFM (freezing media, for storage of fission yeast)	YE5S with approximately 15% glycerol
YPD (rich media, for budding yeast)	2% peptone, 1% yeast extract, 2% dextrose
SD (selective media, for budding yeast)	0.67% Difco yeast extract 2% dextrose
DNA reagents	
TBE	0.02M Tris borate, 0.4 mM Na ₂ EDTA

TAE	0.08M Tris acetate, 2 mM Na ₂ EDTA
TE	10 mM Tris-HCl, pH 7.0, 0.1 M EDTA.
10X loading buffer (DNA agarose gel)	60% (w/v) sucrose, 0.1% (w/v) bromophenol blue.
Protein reagents	
HB Buffer	0.5 M MOPS, pH 7.2, 0.6 M β-glycerophosphate, 1 M MgCl ₂ , 0.5 M EGTA, 50 mM sodium orthovanadate, 0.5 % Triton X-100, 5 M NaCl, added just prior to use: protease inhibitor cocktail (containing 20 μg/ml leupeptin, 20 μg/ml aprotinin, 20 μg/ml pepstatin A), 15mM P-nitrophenyl-phosphate (PNPP), 1 mM dithiothreitol (DTT), 1 mM phenyl-methyl-sulfonyl-fluoride (PMSF).
RIPA buffer	50 mM Tris. Cl. PH7.5, 150mM NaCl, 1% Nonidet P-40, 0.5% sodium deoxyxholate, 0.1% SDS.
SDS acrylamide gel	Cambrex 4-20% PAGE [®] precast gels and Biorad 10% precast gels.
5X loading buffer (PAGE)	60 mM Tris-Hcl (pH 6.8), 25% Glycerol, 2% SDS, 14.4 mM 2-mercaptoethanol, 1% bromophenol blue.
SDS PAGE buffer	25 mM Tris, 250 mM glycine pH 8.3, 0.1% SDS.
Transfer buffer	39 mM glycine, 48 mM Tris base, 0.037% SDS, 20% methanol.
Reagents for immunofluorescence	
PBS	170 mM sodium chloride, 3 mM KCl, 10 mM Na ₂ HPO ₄ , 2 mM KH ₂ PO ₄ .
PEM (pH 6.9)	100 mM PIPES, 1 mM EGTA, 1 mM MgSO ₄ .
PEMS	PEM + 1.2 M Sorbitol.
PEMBAL (pH 6.9)	PEM +1%BSA, 0.1% NaN ₃ , 100 mM lysine hydrochloride. Filter sterilised.

Commercial Kits:

- TaKaRa LA Taq[™] – Polymerase chain reaction (PCR) kit, adapted for amplification of long fragments (5-17kb).
- Promega Wizard[®] DNA Clean-up system – DNA purification system for linear and circular DNA of sizes 200-50000bp, used in the study to purify DNA from PCR reactions.

- Promega Gene Clean[®] system– DNA purification system for linear DNA of sizes 200-50000bp from agarose gels.
- Amersham –ECL, antibody detection system.

7.2 Yeast physiology

7.2.1 Fission yeast nomenclature

The commonly used nomenclature in fission yeast used in this thesis is as follows. *cis*-elements such as gene names are represented by italics *e.g. alp14*. The wild type allele is represented by a superscript plus, *e.g. alp14⁺*. If a mutant allele of the gene is being referred to, its allele number will follow the gene name, *e.g. alp14-1270*. When a gene has been deleted with a specific marker gene this is written as the gene name followed by the name of the gene that is replacing it, separated by a ‘::’ *e.g. alp14::kan^r*. Deleted genes are also referred to with a ‘Δ’ before the gene name *e.g. Δalp14*. A gene that has been tagged is denoted by the gene name followed by the name of the tag with its specific marker, *eg. alp14⁺-GFP-kan^r*.

In this thesis, existing markers are often swapped (deleted and replaced) with another marker to facilitate construction of further strains. When this is the case, the name of the specific marker follows one it is replacing, separated by a ‘::’, *eg. alp14⁺-GFP-kan::ura4⁺*. Constructions of partial deletions in this thesis are denoted by ‘Δ’ followed by the region deleted or the region deleted followed by the specific marker replacing it, *eg. Δ1-240-alp14 or 639-809::ura4⁺*. Trans-elements are not italicised in fission yeast, and gene products are given the same name as the gene name with the first letter is in upper-case *e.g. Alp14*. Tagged gene products are written with the protein name followed by the name of the tag, *e.g. Alp14-GFP*.

Strain growth and maintenance

Fission yeast strains were stored, revived from frozen cultures, grown and maintained according to well-established methods (Moreno *et al.*, 1991; MacNeill and Fantes, 1993). Specifics of individual experiments are as described in the results chapters 2-5. Overall, fission and budding yeast cells were grown either on solid agar plates or in liquid media,

whose recipes for listed above in section 7.1. Stocks of yeast strains were stored in YFP media at -70°C .

7.2.2 Transformation of DNA into fission yeast cells

Transformation of fission yeast cells were carried out to either introduce a plasmid or integrate a PCR fragment into the genome. The transformation protocol, based on the method of Keeny and Boeke (1994), uses Lithium acetate (10x LiAc: 1M lithium acetate, pH 7.5; 10x TE:0.1 M Tris-HCl, 0.01 M EDTA, pH 7.5) and fresh 40% PEG. Calf thymus DNA sodium salt was also used as a carrier for transformation of PCR fragments. Transformations of DNA fragments and plasmids used approximately 3-10 and 1.0 μg of DNA respectively. In all cases, cells grown to log phase were used at the concentration of 1×10^7 cells/plate. Selection is allowed by transformation of DNA containing a wild type copy of the marker gene into auxotrophic yeast strains. Selective markers used include, *LEU2*, *ura4⁺*, *his7⁺*, and *kan^r* (kanamycin resistance). A list of DNA plasmids and oligonucleotides used to amplify PCR fragments for transformations in this study is listed in sections 7.2.8 and 7.2.9. Note that only oligomers used in individual experiments are listed, and most of the strains created and studies in the thesis were obtained by mating and random spore analyses of existing strains.

7.2.3 Tetrad dissection and random spore analysis

The majority of strains used in our study were constructed by tetrad dissection or random spore analysis. Cells carrying different genotypes and markers were mated on plates containing minimal media in absence of nitrogen and left to sporulate. Once mated and asci observed, they are treated with 0.5% helicase. In tetrad dissection, all four spores of each ascus are separated on plates by a micromanipulator to give a line of four isolated spores, separated by about 3-5mm. Random spore analysis, however, allows daughter cells to grow unassorted. Desired strains are then obtained by marker selection. Both methods rely on genetic recombinations and probabilities. Resulting strains from transformation and tetrad/random spore analyses are listed in section 7.2.10, together with strains obtained externally which were used in this study,

7.2.4 Production of synchronous cultures

To synchronise cells for observation in G₂ and M phases, experiments using hydroxy-urea (HU) block and release were carried out. HU is a drug that grossly disturbs DNA

replication, causing cell cycle arrest in early S-phase following activation of S-phase checkpoint. Addition of HU allows cells to accumulate in early S phase and once cells are released into HU-free media, they are able to resume the cell cycle at late S-phase / early G₂. For our experiments, 10 mM HU was added to exponentially growing cultures and incubated for three hours at 30°C or four hours at 27°C. Cells were then filtered, washed and resuspended in HU-free medium. In the case of HU release into media containing microtubule drug CBZ in $\Delta TOG1$ cells, we added HU directly to the cells grown in selective liquid media in the absence of thiamine (to express the *P81nmt* promoter). After wash out, we resuspended the cells in selective media lacking thiamine but with added CBZ at 50µg/ml. Wild type cells were subjected to the same conditions to ensure the accuracy of the experiments. Note that HU synchronisation was chosen for these experiments to allow microtubule drugs to take effect, as well as time for observation of mitotic progression.

Unlike HU, *cdc25-22* block arrests cells in late G₂. As discussed in chapter 5, Cdc25 is a phosphatase whose activity is absolutely required for mitotic entry. When the function of Cdc25 is compromised in the *cdc25-22* mutant, cells fail to progress from G₂ at restrictive temperatures. To induce arrest, cells carrying a *cdc25-22* mutation were shifted up to 36°C. After four hours, the cultures were shifted down to 26°C for release into mitosis. Samples were taken every 15 minutes after G₂ release and stained with calcofluor, a fluorescent reagent that stains the septa, to follow cell cycle progression and thereby allowing the degree of synchronisation to be measured.

Although cell cycle synchronisation is also possible by nitrogen starvation and release, we did not carry these experiments out. Instead we used nitrogen starvation and refeeding to induce plasmid loss to study defects of simultaneous *alp14⁺/dis1⁺/klp5/6⁺* deletions (chapter 5). In these experiments, cells were starved of nitrogen for 12 hours, washed and resuspended in rich media at 30°C. Mid log phase cells were filtered and washed in MM without nitrogen and then resuspended in the same nitrogen free media, starvation was for 12 hours at 30°C. Cells were then filtered and grown in rich YE5S media at 30°C. Samples were collected at different time points for immuno-staining with anti α -tubulin.

7.2.5 Microtubule drug treatment

Sensitivity to microtubule drugs were carried out using thiabendazole (TBZ). On plates, TBZ was added to plates at concentrations of 10 to 30 $\mu\text{g/ml}$, and to liquid YE5S at a concentration of 50 $\mu\text{g/ml}$. Stock solutions of TBZ were stored at 20mg/ml concentrations in DMSO at -20°C . To visual cells in microtubule drugs, however, we used carbendazole (CBZ) at a concentration of 50 $\mu\text{g/ml}$ as previously described in Hardwick *et al.* (2000). Stock solutions of CBZ were stored at 5mg/ml in DMSO at -20°C .

7.2.6 Chromosome loss assay

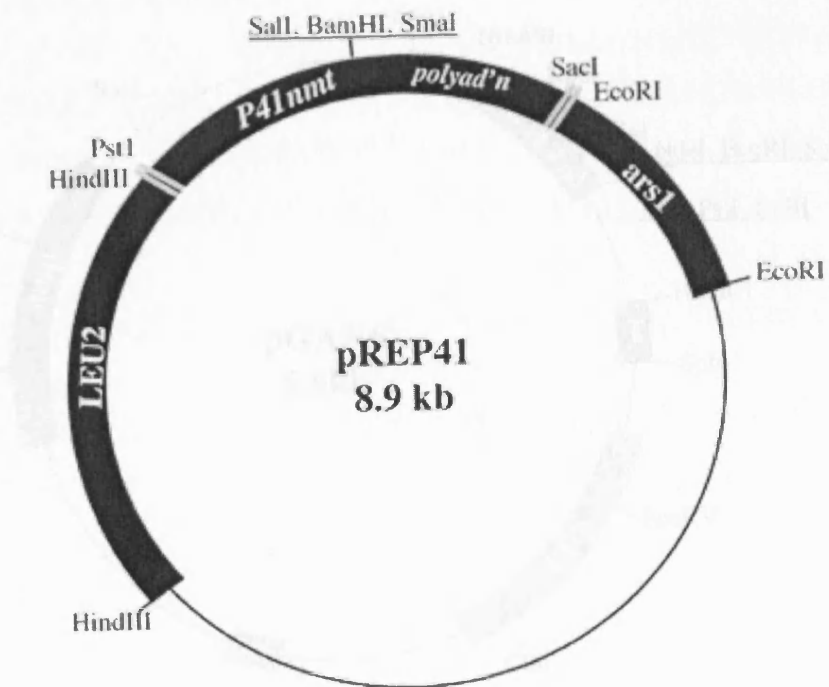
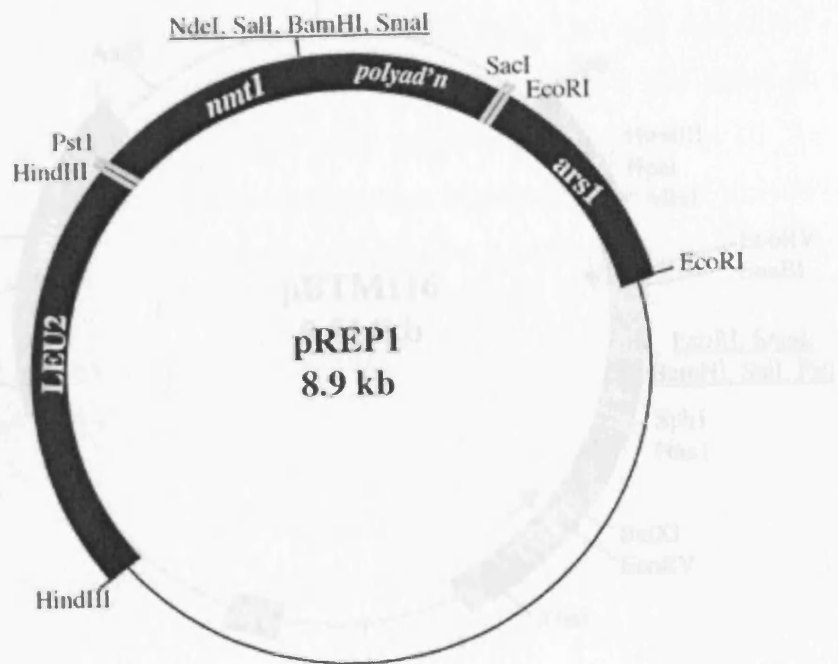
The chromosome loss experiment was carried out to test the fidelity of chromosome segregation in $\Delta klp5/6$, $\Delta mad2$ and $\Delta klp5\Delta mad2$ mutants in comparison to wild type. For the assays, we used methods according to Niwa *et al.* (1989). Cells carrying non-essential linear minichromosome 16 (ch.16) grown on selective media lacking adenine (to retain mini-chromosome) were plated on rich YE media and incubated at 30°C for four days. The ch.16, derived from the centromeric region of chromosome 3, contains the *M216* allele that is able to compensate for the *M210* mutation, which is carried endogenously in the genome. The minichromosome is stably maintained in normal mitosis but when DNA replication or segregation defects occur, the minichromosomes are lost and can be observed as red auxotrophs. The percentage of chromosome loss per one cell division is calculated by counting the number of colonies showing red half-sectors (indicate chromosome loss in the first cell division) against the total number of colonies.

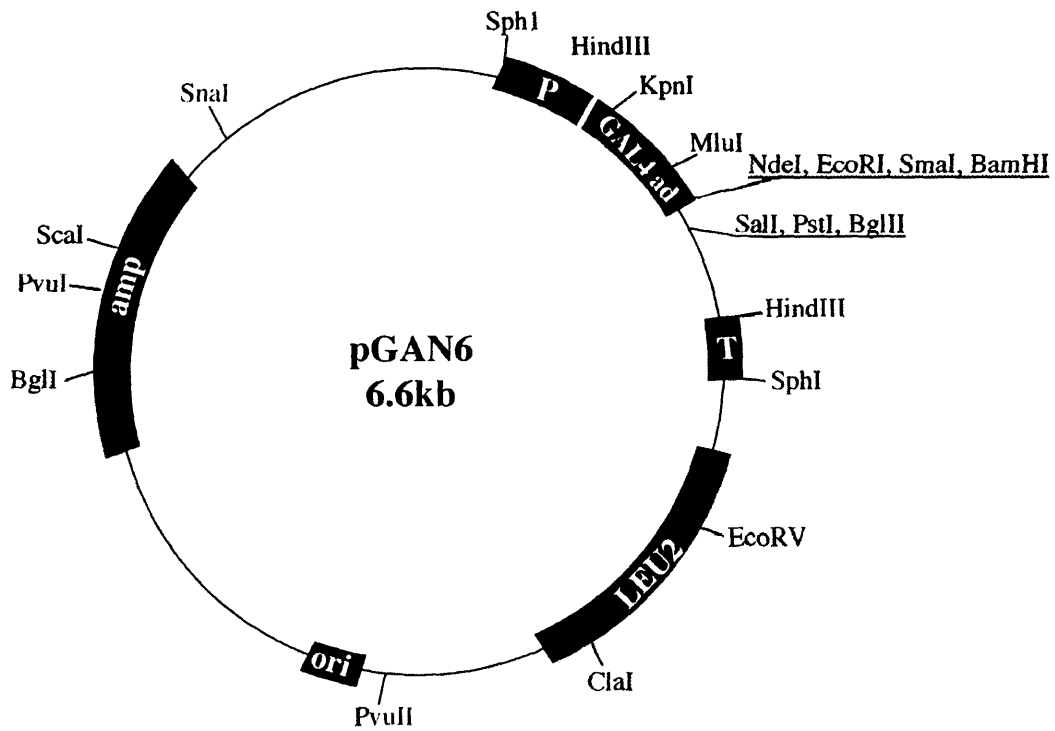
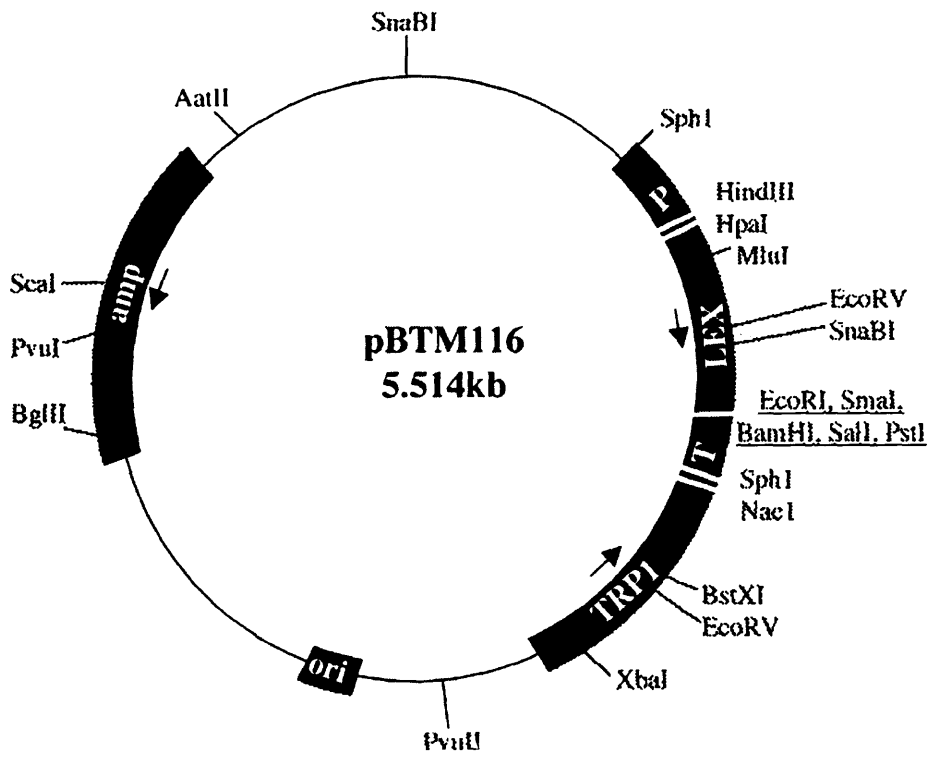
7.2.7 Two hybrid Assay

The two-hybrid assays were carried out using budding yeast as described in Luban and Goff (1995). Two different proteins, or partially deleted protein, are expressed in complementary plasmids that contain distinct parts of markers. The assay functions on the basis that protein expression from each plasmid is not selected as the markers are not fully expressed. However, if the two proteins interact, the markers are fully expressed, allowing for positive selection. In this study, plasmids used are pGAN6 and pBMT116 (see section 7.2.8) which, when interaction occurs, expresses β -galactosidase and His1⁺.

Both plasmids are transformed into the L40 budding yeast strain carrying a mutation at the *his1* locus, to test for interaction. Detection of interaction is by streaking cells onto rich media, allowing them to grow, then replica onto minimal media in the absence of histidine. Colonies that grow in this condition indicate interaction. Protein binding can also be detected by a β -galactosidase assay on filters. In this assay, streaked cells on rich media can be directly replicated onto filter paper (Whatmann 3MM or Hi-bond filter). The filter is then immersed in liquid nitrogen for one min then placed on top of another filter paper that had been previously submerged in 2 ml of Z-buffer (contains β -mercaptoethanol) and 50 μ l of X-gal. The reaction was incubated at 30 °C for 2 hours until the colour is developed. The reaction can be stopped by placing the replica onto a filter paper immersed with 1M Na₂CO₃.

7.2.8 Plasmids





7.2.9 Oligonucleotides

Designs of oligomers were based on methods and plasmids from Bahler *et al.* (1998). *Italics* signify DNA sequence designed to bind to plasmids from Bahler *et al.*, while capitalised letters are genome-binding sequences and additional restriction sites. The plasmid-binding sequences allow amplification of the marker on the plasmids, while the genome-binding sequences provide insertion the DNA fragment by homologous recombination. For example, in genes disruption experiments, the *kan^r* gene flanked with sequences corresponding to the 5' and 3' ends of the relevant genes were transformed into wild type strains (also see section 7.3 for details). Note when *Alp14* were partially deleted or overexpressed, special care is taken when ordering the oligonucleotides to ensure that the resulting deletions would be in-frame.

Δalp14 (kan^r)

- Fw:TTTAGAATTGGAGTTTTGGGAGAGCATTGCTGTTTATTTATCTTATAC
GCTCCTTTAATTTTTGGCACCCCGGAGGAACCGGATCCCCGGGTAAATTA
- Rv:GATATTATCATTATTCTAAAACATTAATAAATAAGAAAGGGAAGGGACA
TTGGAATGTAAACGAAAGAATTTAAAAGAATTTCGAGCTCGTTTAAAC

Alp14-tag (at the C-terminus)

- Fw:CCATTGATTTAGCTGCCAAACTAAAACAAAAAATTACTGAGATGAAA
CAAACAGACCAAAGACATCAGGGATTGATTCACCGGATCCCCGGGTAAATTA
- Rv:GTTACCATTTGACTCCATCTTTAACCTATAGTTAAATCTGATTTTAAAGA
AATTTGGTATAAACGAGAATACGTATTTGTGATTTCGAGCTCGTTTAAAC

Systematic deletion from the C-terminus and endogenous overexpression from the N-terminus:

- Rv: CATTAAAAAATAGAAAGGGAAGTAAGGGACATTGGAATGTAAACGA
AAGAATTTAAAAACTAGTGAATCAATCCCTGATGGAATTCGAGCTCGTTTAA
AC
- *Δ696-809alp14 (ΔTail-GFP)* Fw: ATGAAGAGAATATTTCTATGCAAAAACAAC
TCAGTGAATTGAAAGGTGAATTAATACCTTACGCAGTGCCAGGAAAGCCTA
ATAGCGGATCCCCGGGTAAATTA
- *Δ639-809alp14 (ΔMT-GFP and ov-TOG2-C)* Fw: TGCAAAATTTGAAGAACATGG

AGTTGGACGATCCGGCTCCTCAACCGGCTAAGCATTACAGAGTTGATCGTTA
TGAACACTAATAGCGGATCCCCGGGTTAATTAA

- *Δ420-809alp14 (ΔC-GFP and ov-TOG2)* Fw: CTGTTTTGGCTACATCCAGTTTGG
ATGACTTAGCCGAGCTCATTGCTAGCTTTGCCGGGAACAAAAATCCTCAAAT
CAAATAATAGCGGATCCCCGGGTTAATTAA

Systematic deletion from the N-terminus and endogenous overexpression from the C-terminus:

- Fw: GTAAAGTTTGACAGTGTTGTATTTGCCTACAGGCTTAACGAGTAATTA
CTTATTATTTATTCAAAAAAGGGAGAAAAGGTGAATTCGAGCTCGTTTAAAC

- *P3nmt-*alp14* (ov-*alp14* FL) and P81nmt-*alp14* (FL and FL-GFP)* Rv: AGACGCACT
TTCCATACTTTATGTACTATTCTTGATTCTAGAGGAAGTTTGGAGTAGTCTTC
TTCTTGATCTTGGCTCATCATGATTTAACAAAGCGACTATA

- *Δ1-240alp14 (ΔTOG1 / ΔTOG1-GFP and ov-C-TOG1)* Rv: TCACTTTTTTATTCTC
GAGAGCAGGTTGCTCTTCTACCTGTGTTTCAACATTCGGCTCTGATGTAGGTT
GCTGACTTTTCATGATTTAACAAAGCGACTATA

- *Δ1-430alp14 (ΔTOG2-GFP)* Rv: GTATCAGAAACACCAGGAACGCATGCTTTA
GCACAGGTATCAACTGTAAACTTAGATGGTAAGGATGTCATATTACTGAACA
TGATTTAACAAAGCGACTATA

- *Δ1-696alp14 (ΔN-M-GFP and ov-tail2)* Rv: AATGAGGGACTCGTAGAGAGCTCT
AAAAAGTCAGTATTAGCTCTTCGCATAAATGCAGGTTTTCTGTCTCCTATTGG
TGACATGATTTAACAAAGCGACTATA

- *Δ1-710alp14 (ΔN-C-GFP and ov-tail1)* Rv: AGTTTAGGTCTAGTAGGTTCAAATT
CCCTCACTGAACGTTGAAATGAGGGACTCGTAGAGAGCTCTAAAAAGTCAGT
ATTCATGATTTAACAAAGCGACTATA

- *Δ1-150alp14 (ov-C-TOG2)* Rv: GAGATATGTGGAATAATCATTTTTGAAGGAA
TAACTTTAGCACCAAAGTCTCAACTAGACTAGCAATGGCAGCGACATTCAT
GATTTAACAAAGCGACTATA

Klp5-tag (at the C-terminus)

- Fw: CTAATCTTTCATCTTTCAAATCCAGCTAACATTATTAGGAAATCTTTAAG
CATGGCTGAAAACGAAGAAGAGAAAGCCACCCGGATCCCCGGGTTAATTAA

- Rv: ACATATATGTACGCTTGTATTTGATAGTGCATTACGAACGAATTGTGC
AAGTTTACTAAGAGAATTTTAGGGTTTATAAAGAATTCGAGCTCGTTTAAAC

Mph1-tag (at the C-terminus)

- Fw:GCACAAGCGATTAAATAAGGAACTTATTGATAGCATGGCTTATGATTG
CGTTAGCAATTTACGAAAAATGCCAGAACGGATCCCCGGGTAAATTA
- Rv:GTATCAAAGTATAGATATCAGGGGCCATATAATATGTGGTTCATTAATT
CAAGGTCATAATTACCTTCTTTTAAAAGAGCGGAATTCGAGCTCGTTTAAAC

Mad3-tag (at the C-terminus)

- Fw:GCCTTTGAAATCTCCAAGAAAATTGGACCCTCTTGGGAAATTTCAAGT
TCATTGTGATGAGGAAGTATCGAAAGAACGGATCCCCGGGTAAATTA
- Rv:CCTATTTCTTATTCCGGGAGTCATGATGTACAATAGTTGTTAATCTAAT
AACGCCAATACTTTAAATCTTTTCTTTATCGGAATTCGAGCTCGTTTAAAC

Bub3-tag (at the C-terminus)

- Fw:GTGCTCAAGAAGAAGCCGCTGGTAATATCTATGTTCATGCTTTGGAAT
CCAACCTTGCAGCTCCAAAGTTAAAGTCACGGATCCCCGGGTAAATTA
- Rv:GCTTCAAATAATATAAATTTTCATATGTATGCAGTAAAAGAATCTGCAT
AAGATTTTACATGGATGAAGCTTTTTGATGAGCGAATTCGAGCTCGTTTAAAC

Mad1-tag (at the C-terminus)

- Fw:TACGATTTTGGTGTGATGAACGCAAACAATACCAGGCATGTTAGCGG
CTCTAACGTTAGACTTCTTGACAAAAATGATCGGATCCCCGGGTAAATTA
- Rv:GACTAGTTTGTAATGGTGAATATATTTAGCGCTTAGGCCAGTACAAA
CTGTTTACAGTTTCATTGTATCGACATTGAAGGGAATTCGAGCTCGTTTAAAC

Slp1-tag (at the C-terminus)

- Fw:TTTGGCGAGTTTATGATGGGGACCACGTTAAAAGGCCCATTTCCAATTA
CCAAAACCCCGTCCAGCAGCATAACAATCCGTCGGATCCCCGGGTAAATTA
- Rv:AATAAAATAAAARAGTGAGTAACTGATGCAACATAGTGATTTCGACGAG
CTAAACGTTGAAATCTAAAAGAACTGGTGTGTGAATTCGAGCTCGTTTAAAC

pREP1-TOG⁺ (alp14-1-420) construction:

- Fw (NdeI):GGAATTCCATATGAGCCAAGATCAAGAAGAAGACTACTCC
- Rv (SmaI):AGGCCCGGGCTATTAGATCTCGAGAACAACAACTAAAGCAGGAGC

Plasmid construction for two-hybrid assay:

- mad2 (EcoR1) Fw: CCGGAATTCATGTCTAGCGTTCCTCCATAAGAACGAATTTT TCAC
- mad2 (BamH1) rv: CGCGGATCCCTAAGGATTCCTCGATATGCAACTTGACA
- Slp1 (Nde1) Fw: GGAATTCCATATGGAGATAGCAGGTAATTCTTCAACCATA
- Slp1 (BamH1) Rv: CGCGGATCCTCAACGGATTGTTATGCTGCTGGACGGGGT
- Mad3 (SmaI) Fw: TCCCCGGGATGGAACCATTAGATGCTGGCAAGAAGCTGG
- Mad3 (BglII) rv: GGAAGATCTTTATTCTTTTCGATACTTCCTCATCACAATG

7.2.10 Strain List**Fission Yeast Strains**

Name	Genotype	Derivation
513	<i>h⁻ leulura4</i>	lab stock
TP108-3D	<i>h⁺ leulura4his2</i>	lab stock
CHP428	<i>h⁺ leul ura4 his7ade6-210</i>	Dr Hoffman
CHP429	<i>h⁻ leulura4 his7ade6-216</i>	Dr Hoffman
HM248	<i>h⁺ his2ade6-210 containing ch.16</i>	Dr Niwa
143	<i>h⁻ leul-cdc13-GFP-LEU2⁺</i>	Dr. Yanagida
cut7-446	<i>h⁻ leul cut7-446</i>	Dr. Hagen
MA218	<i>h⁻ leulura4 nuf2⁺-CFP-kan^r</i>	lab stock
MA613	<i>h⁻ leulura4 ndc80⁺-GFP-kan^r</i>	lab stock
Cdc25-22	<i>h⁻ leulcdc25-22</i>	Dr Nurse
KM311-110	<i>h⁻ leulnda3-311</i>	Lab stock
NK001	<i>h⁺ leulura4-kan^r-GFP-P3nmt-atb2⁺</i>	lab stock
AE148	<i>h⁻ leulura4mad2::ura4⁺</i>	Dr Matsumoto
AE307	<i>h⁺ leul ura4 mad2⁺-GFP-LEU2⁺</i>	Dr Matsumoto
AE310	<i>h⁻ leulnda3-311-mad2⁺-GFP-LEU2⁺</i>	Dr Matsumoto
	<i>h⁻ leulura4-mad2⁺-GFP-kan::ura4⁺</i>	lab stock
	<i>h⁻ leulura4-bub1⁺-GFP-kan::ura4⁺</i>	lab stock
DMSP059	<i>h⁺ leulhis3ura4ade6-m210-mad3⁺-GFP::his3⁺</i>	Dr. Hardwick
NK129	<i>h⁻ leulura4-mad3⁺-GFP-kan^r</i>	this study
AE249	<i>h⁻ leulura4-mad1::ura4⁺</i>	Dr Matsumoto
1-K7	<i>h⁻ leulura4-mad2::LEU2⁺</i>	lab stock

SS560	<i>h⁻ leu1ura4ade6-m216-mph1::ura4⁺</i>	Dr. Sazer
SS562	<i>h⁺ leu1ura4ade6-m210-mph1::ura4⁺</i>	Dr. Sazer
NK113	<i>h⁺ leu1his2ura4-mad3::ura4⁺</i>	this study
NK116	<i>h⁻ leu1ura4-bub3::ura4⁺</i>	this study
464	<i>h⁺ leu1ura4his1ade6-m210-bub1::LEU2⁺</i>	Dr. Javerzat
393	<i>h⁻ leu1ura4his1ade6-m216-bub1::ura4⁺</i>	Dr. Javerzat
NK023	<i>h⁻ leu1ura4-klp5⁺-3HA-kan^r</i>	this study
NK017	<i>h⁻ leu1ura4-klp5⁺-13myc-kan^r</i>	this study
NK032	<i>h⁻ leu1ura4-klp5-13myc--kan^r -cdc25-22</i>	this study
FH178	<i>h⁻ leu1-cut2⁺-3HA-LEU2⁺</i>	Dr. Yanagida
NK024	<i>h⁻ leu1ura4-klp6⁺-3HA-kan^r</i>	this study
NK006	<i>h⁺ leu1his7ura4-kan^r -GFP-atb2⁺-klp5::ura4⁺</i>	this study
NK007	<i>h⁺ leu1his7ura4-kan^r -GFP-atb2⁺-klp6::ura4⁺</i>	this study
MA060	<i>h⁹⁰ leu1ura4his7ade6-m216-klp5::ura4⁺</i>	lab stock
MA061	<i>h⁻ leu1ura4his7ade6-m210-klp6::ura4⁺</i>	lab stock
MA081	<i>h⁻ leu1ura4-klp5::ura4⁺-klp6::ura4⁺</i>	lab stock
NK028-1B	<i>h⁻ leu1ura4his2-klp6::ura4 -mad2::ura4⁺</i>	this study
NK029-1B	<i>h⁻ leu1ura4kan^r-klp5:: kan^r -mad2::ura4⁺</i>	this study
NK038	<i>h⁻ ura4-ade6-210-klp5::ura4 containing mini-ch.16</i>	this study
NK059	<i>h⁻ leu1ura4ade6-210-mad2:: kan^r containing mini-ch.16</i>	this study
NK061	<i>h⁻ leu1ura4ade6-210-mad2:: kan^r -klp5::ura4⁺ containing mini-ch.16</i>	this study
NK019	<i>h⁻ leu1ura4-kan^r -P3nmt-klp6⁺</i>	this study
NK025	<i>h⁻ leu1ura4-kan^r ^R-P3nmt-klp5⁺</i>	this study
NK066	<i>h⁻ leu1ura4-kan^r-P3nmt-klp5⁺-P3nmt-klp6⁺</i>	this study
NK036	<i>h⁻ leu1ura4-kan^r-P3nmt-klp5⁺-mad2::ura4⁺</i>	this study
NK034	<i>h⁻ leu1ura4-klp5:: kan^r-dis1::ura4⁺ containing pdis1⁺</i>	this study
NK039	<i>h⁻ leu1ura4-alp14:: kan^r-klp5::ura4⁺-klp6⁺::ura4-palp14⁺</i>	this study
NK040	<i>h⁻ leu1ura4-alp14:: kan^r-klp5::ura4⁺ containing palp14⁺</i>	this study
alp14-1270	<i>h⁻ leu1ura4-alp14-1270</i>	lab stock
NK054	<i>h⁻ leu1ura4-klp5:: kan^r-alp14-1270 containing palp14⁺</i>	this study
NK056	<i>h⁻ leu1ura4-klp5::kan^r-dis1-203 containing pdis1⁺</i>	this study
NK074	<i>h⁻ leu1ura4-mad2::ura4-klp5:: kan^r-alp14-1270 containing palp14⁺</i>	this study

NK075	<i>h⁻ leulura4-mad2::ura4-klp5:: kan^r-dis1-203</i> <i>containing pdis1⁺</i>	this study
NK092	<i>h⁻ leul-klp5⁺-GFP- kan^r-alp14:kan^r</i>	this study
NK072	<i>h⁺ leulura4his2 dis1::ura4⁺-alp14:: kan^r containing pdis1⁺</i>	this study
NK004	<i>h⁺ leulura4-alp14:: kan^r</i>	this study
NK162	<i>h⁻ leulura4 alp14::kan::ura4⁺</i>	this study
NK008	<i>h⁺ leulhis7-alp14⁺-GFP-kan^r</i>	this study
NK010	<i>h⁺ leulura4-alp14:: kan^r containing pREP1⁺</i>	this study
NK011	<i>h⁺ leulura4-Alp14:: kan^r containing pdis1⁺</i>	this study
NK012	<i>h⁺ leulura4-Alp14:: kan^r containing palp14⁺</i>	this study
NK014	<i>h⁻ leul-dis1::ura4⁺ containing pREP1⁺</i>	this study
NK015	<i>h⁻ leulura4-dis::ura4⁺ containing pdis1⁺</i>	this study
NK016	<i>h⁻ leulura4-dis1::ura4⁺ containing palp14⁺</i>	this study
NK041	<i>h⁻ leul-alp14-1270 containing palp14⁺</i>	this study
NK043	<i>h⁻ leul-dis1-203 containing pdis1⁺</i>	this study
NK063	<i>h⁻ leulhis7-alp14-GFP-kan::ura4⁺</i>	this study
MA015	<i>h⁻ leulura4 alp14⁺-13myc- kan^r</i>	lab stock
NK013	<i>h⁻ leulura4- kan^r-P81nmt-GFP-alp14⁺ (FL)</i>	this study
NK067	<i>h⁻ leulhis7- kan^r-P81nmt-</i> <i>alp14⁺-GFP-kan::ura4⁺ (FL-GFP)</i>	this study
NK093	<i>h⁻ leulura4- kan^r-P81nmt-Δ1-240-alp14 (ΔTOG1)</i>	this study
NK095	<i>h⁺ leulura4his2- kan^r-P81nmt-Δ1-240-alp14(ΔTOG1)</i>	this study
NK073	<i>h⁻ leulura4his7- kan^r-P81nmt-Δ1-240-</i> <i>alp14-GFP-kan::ura4⁺ (ΔTOG1-GFP)</i>	this study
NK085	<i>h⁻ leulura4his7- kan^r-P81nmt-Δ1-430-alp14-</i> <i>GFP-kan::ura4⁺ (ΔTOG2-GFP)</i>	this study
NK080	<i>h⁻ leulura4his7-kan^r -P81nmt-Δ1-696-alp14-</i> <i>GFP-kan::ura4⁺ (ΔN-M-GFP)</i>	this study
NK076	<i>h⁺ leulura4his2- kan^r-P81nmt-Δ1-240-alp14-</i> <i>GFP-kan::ura4⁺ (ΔTOG1-GFP) -dis1::LEU⁺</i>	this study
NK081	<i>h⁻ leulura4 his7- kan^r-P81nmt-Δ1-240-alp14-</i> <i>GFP-kan::ura4⁺ (ΔTOG1-GFP) containing palp14⁺</i>	this study
NK083	<i>h⁻ leulura4 his7- kan^r-P81nmt-Δ1-696-alp14-</i> <i>GFP-kan::ura4⁺ (ΔN-M-GFP) containing palp14⁺</i>	this study

NK146	<i>h⁻ leulura4 his7- kan^r -P81nmt-Δ1-710- alp14- GFP-kan::ura4⁺ (ΔN-C-GFP) containing palp14⁺</i>	this study
NK096	<i>h⁻ leulura4 kan^r-P81nmt -alp14⁺-GFP-kan::ura4⁺-(FL) -mad2::LEU2⁺</i>	this study
NK097	<i>h⁻ leulura4- kan^r-P81nmt-Δ1-240- alp14- GFP-kan::ura4⁺ (ΔTOG1-GFP) -mad2::LEU2⁺</i>	this study
NK099	<i>h⁻ leulura4- kan^r-P81nmt-Δ1-430- alp14- GFP-kan::ura4⁺ (ΔTOG2-GFP) -mad2::LEU2⁺</i>	this study
NK101	<i>h⁻ leulura4- kan^r-P81nmt-Δ1-696- alp14- GFP-kan::ura4⁺ (ΔN-M-GFP) -mad2::LEU2⁺</i>	this study
NK102	<i>h⁻ leulura4- kan^r-P81nmt-Δ1-710- alp14- GFP-kan::ura4⁺ (ΔN-C-GFP) -mad2::LEU2⁺</i>	this study
NK107	<i>h⁻ leulura4- kan^r -P81nmt-Δ1-240- alp14(ΔTOG1) -bub1::LEU2⁺</i>	this study
NK109	<i>h⁻ leulura4- kan^r-P81nmt-Δ1-240- alp14(ΔTOG1) -mad1::ura4⁺</i>	this study
NK111	<i>h⁻ leulura4- kan^r -P81nmt-Δ1-240- alp14 (ΔTOG1) -mph1::ura4⁺</i>	this study
NK112	<i>h⁻ leulura4- kan^r -P81nmt-1-Δ240- alp14 (ΔTOG1) -mad3::ura4⁺</i>	this study
NK110	<i>h⁻ leulura4- kan^r -P81nmt-Δ1-240- alp14 (ΔTOG1) -mad2::ura4⁺</i>	this study
NK120	<i>h⁻ leulura4- kan^r -P81nmt-Δ1-240- alp14 (ΔTOG1) -bub3::ura4⁺</i>	this study
NK125	<i>h⁻ leulura4 containing pREP3x-mph1⁺</i>	this study
NK126	<i>h⁻ leulura4 containing pREP41x-mad2⁺</i>	this study
NK127A	<i>h⁻ leulura4- kan^r -P81nmt-Δ1-240- alp14 (ΔTOG1) containing pREP3x-mph1⁺</i>	this study
NK127B	<i>h⁻ leulura4- kan^r -P81nmt-Δ1-240- alp14 (ΔTOG1) containing pREP41x-mad2⁺</i>	this study
NK104	<i>h⁻ leulura4- kan^r -P81nmt-Δ1-240- alp14 (ΔTOG1) -mad2⁺-GFP-LEU2⁺</i>	this study
NK105	<i>h⁻ leulura4- kan^r -P81nmt-Δ1-240- alp14 (ΔTOG1) -bub1⁺-GFP-ura4⁺</i>	this study

NK148	<i>h⁻ leu1his3ura4ade6-210-Mad3⁺-GFP::his3-kan^r -P81nmt-Δ1-210-<i>alp14</i> (ΔTOG1)</i>	this study
NK137	<i>h⁻ leu1ura4- kan^r -P81nmt-<i>alp14</i>-Δ1-240 (ΔTOG1) -<i>alp11-924</i></i>	this study
NK198	<i>h⁺ leu1ura4his2- kan^r -P81nmt-Δ1-240-<i>alp14</i> (ΔTOG1) -<i>klp5::ura4⁺</i></i>	this study
NK199	<i>h⁺ leu1ura4his2- kan^r -P81nmt-Δ1-240-<i>alp14</i> (ΔTOG1) -<i>klp6::ura4⁺</i></i>	this study
NK185	<i>h⁻ leu1ura4- kan^r -P81nmt-Δ1-240-<i>alp14</i> (ΔTOG1) -<i>cdc13-GFP-LEU2⁺</i></i>	this study
NK186	<i>h⁻ leu1ura4 cdc13⁺-GFP-LEU2⁺-<i>bub1::ura⁺</i></i>	this study
NK187	<i>h⁻ leu1ura4-<i>mad2::ura4⁺-cdc13⁺-GFP-LEU2⁺</i></i>	this study
NK188	<i>h⁻ leu1ura4-<i>mad3::ura4⁺-cdc13⁺-GFP-LEU2⁺</i></i>	this study
NK195	<i>h⁻ leu1ura4 kan^r -P81nmt-Δ1-240-<i>alp14</i>-GFP-<i>kan::ura4⁺</i> (ΔTOG1-GFP)-<i>cut7-446</i></i>	this study
NK189	<i>h⁺ leu1ura4his2-<i>slp1⁺-13myc- kan^r</i></i>	this study
NK211	<i>h⁻ leu1ura4 kan^r -P81nmt-Δ1-240-<i>alp14</i> (ΔTOG1) -<i>slp1-myc- kan^r</i></i>	this study
NK236	<i>h⁻ leu1ura4 <i>mad2⁺-GFP-ura4⁺-nuf2⁺-CFP- kan^r</i></i>	this study
NK238	<i>h⁻ leu1ura4 <i>bub1⁺-GFP- kan^r -nuf2⁺-CFP- kan^r</i></i>	this study
NK239	<i>h⁻ leu1ura4 kan^r -P81nmt-Δ1-240-<i>alp14</i> (ΔTOG1) -<i>bub1⁺-GFP- kan^r -nuf2⁺-CFP- kan^r</i></i>	this study
NK240	<i>h⁻ leu1ura4 kan^r -P81nmt-Δ1-240-<i>alp14</i>- (ΔTOG1) <i>mad2⁺-GFP- kan^r -nuf2⁺-CFP- kan^r</i></i>	this study
NK243	<i>h⁺ leu1ura4his2-<i>alp14⁺-13myc- kan^r -nuf2⁺-CFP- kan^r</i></i>	this study
NK241	<i>h⁻ leu1ura4 kan^r -P81nmt-Δ1-240-<i>alp14</i> (ΔTOG1) -<i>ndc80⁺-GFP- kan^r</i></i>	this study
NK247	<i>h⁻ leu1ura4 kan^r -P81nmt-Δ1-240-<i>alp14</i> (ΔTOG1) -<i>mis6⁺-GFP- kan^r</i></i>	this study
NK226	<i>h⁻ leu1ura4-<i>alp14⁺-13myc- kan^r -mad2⁺-GFP- kan^r ::ura4⁺</i></i>	this study
NK228	<i>h⁺ leu1ura4his3ade6- kan^r -P81nmt-Δ1-240-<i>alp14</i>- (ΔTOG1) <i>Mad3⁺-GFP-HIS3⁺-Mad2⁺-13myc- kan^r</i></i>	this study
ov- <i>alp14</i>	<i>h⁻ leu1ura4-P3nmt- kan^r -<i>alp14</i></i>	this study
NK123	<i>h⁺ leu1his2ura4-P3nmt- kan^r -<i>alp14</i>-</i>	

	<i>421-809::ura4⁺ (ov-TOG2)</i>	this study
NK124	<i>h⁺ leu1his2ura4-P3nmt- kan^r -alp14-639-809::ura4⁺ (ov-TOG2-C)</i>	this study
NK142	<i>h⁺ leu1his2ura4-P3nmt- kan^r -alp14-421-809::ura4⁺ (ov-TOG2) containing palp14⁺</i>	this study
NK144	<i>h⁺ leu1his2ura4-P3nmt- kan^r -alp14-639-809::ura4⁺ (ov-TOG2-C) containing palp14⁺</i>	this study
NK138	<i>h⁹⁰ leu1ura4-P3nmt- kan^r -alp14-421-809::ura4⁺ (ov-TOG2) -mad2::LEU2⁺</i>	this study
NK139	<i>h⁹⁰ leu1ura4-P3nmt- kan^r -alp14-639-809::ura4⁺ (ov-TOG2-C) -mad2::LEU2⁺</i>	this study
NK196	<i>h⁺ leu1ura4his7ade6-216-P3nmt- kan^r -alp14-421-809::ura4⁺ (ov-TOG2)-bub1::LEU2⁺</i>	this study
NK197	<i>h⁺ leu1ura4his7ade6-216-P3nmt- kan^r -alp14-639-809::ura4⁺ (ov-TOG2-C) -bub1::LEU2⁺</i>	this study
NK216	<i>h⁺ leu1ura4his7- kan^r -P3nmt-alp14-421-809::ura4⁺::LEU2⁺ (ov-TOG2) -mph1::ura4⁺</i>	this study
NK217	<i>h⁺ leu1ura4his7- kan^r -P3nmt-alp14-421-809::ura4⁺::LEU2⁺ (ov-TOG2) -bub3::ura4⁺</i>	this study
NK218	<i>h⁺ leu1ura4his7- kan^r -P3nmt-alp14-421-809::ura4⁺::LEU2⁺ (ov-TOG2) -mad3::ura4⁺</i>	this study
NK219	<i>h⁺ leu1ura4his7- kan^r -P3nmt-alp14-639-809::ura4⁺::LEU2⁺ (ov-TOG2-C) -mph1::ura4⁺</i>	this study
NK220	<i>h⁺ leu1ura4his7- kan^r -P3nmt-alp14-639-809::ura4⁺::LEU2⁺ (ov-TOG2-C) -mad1::ura4⁺</i>	this study
NK221	<i>h⁺ leu1ura4his7- kan^r -P3nmt-alp14-639-809::ura4⁺::LEU2⁺ (ov-TOG2-C) -mad3::ura4⁺</i>	this study
NK131	<i>h⁻ leu1ura4-kan^r -P3nmt-alp14-mad2::ura4⁺</i>	this study
NK231	<i>h⁺ leu1ura4- kan^r -P3nmt-alp14-bub1⁺-GFP-ura4⁺</i>	this study
NK135	<i>h⁻ leu1ura4- kan^r -P3nmt-alp14-639-809::ura4(ov-TOG2-C)-mad2⁺-GFP-LEU2⁺</i>	this study
NK230	<i>h⁺ leu1ura4his7 kan^r -P3nmt-alp14-421-809::ura4⁺ (ov-TOG2) bub1⁺-GFP-ura4⁺</i>	this study
NK237	<i>h⁺ leu1ura4his7 kan^r -P3nmt-alp14-421-809::ura4(ov-TOG2-C)</i>	

	<i>-bub1⁺-GFP-ura4⁺-nuf2-CFP- kan^r</i>	this study
NK202	<i>h⁻ leulura4his7- kan^r -P3nmt-Δ1-150-<i>alp14</i>- GFP-kan::<i>ura4</i> (ov-C-TOG2-GFP)</i>	this study
NK203	<i>h⁻ leulura4his7- kan^r -P3nmt-Δ1-696-<i>alp14</i>- GFP-kan::<i>ura4</i> (ov-tail2-GFP)</i>	this study
NK204	<i>h⁻ leulura4his7 kan^r -P3nmt-Δ1-710-<i>alp14</i>- GFP-kan::<i>ura4</i>(ov-tail1-GFP)</i>	this study
NK229	<i>h⁺ leulura4his7 kan^r -P3nmt-Δ1-240-<i>alp14</i>-GFP- kan::<i>ura4</i>+(ov-c-TOG1) mad2⁺-GFP-LEU2⁺</i>	this study
NK242	<i>h⁻ leulura4 containing pREP1-1-430-<i>alp14</i> (pTOG⁺)</i>	this study
NK245	<i>h⁻ leulura4his7-mad2::<i>ura4</i>⁺ containing pREP1-1-430-<i>alp14</i> (pTOG⁺)</i>	this study
NK246	<i>h⁻ leulura4his1ade6-bub1::<i>ura4</i>⁺ containing pREP1-1-430-<i>alp14</i> (pTOG⁺)</i>	this study
NK248	<i>h⁺ his2leulura4 nuf2⁺-CFP- kan^r containing pREP1-1-430-<i>alp14</i> (pTOG⁺)</i>	this study
NK249	<i>h⁻ leulura4 ndc80⁺-GFP- kan^r containing pREP1-1-430-<i>alp14</i> (pTOG⁺)</i>	this study
NK250	<i>h⁻ leulura4 bub1⁺-GFP- kan^r ::<i>ura4</i>⁺ containing pREP1-1-430-<i>alp14</i> (pTOG⁺)</i>	this study
NK251	<i>h⁻ leulura4 mad2⁺-GFP- kan^r ::<i>ura4</i>⁺ containing pREP1-1-430-<i>alp14</i> (pTOG⁺)</i>	this study
NK252	<i>h⁻ leulura4 mad2⁺-13myc- kan^r containing pREP1-1-430-<i>alp14</i> (pTOG⁺)</i>	this study
Slp1-myc	<i>h⁻ leulura4 slp1⁺-13myc- kan^r</i>	lab stock
NK214	<i>h⁻ leulura4 slp1⁺-13myc- kan^r - mad2⁺-GFP-LEU2⁺</i>	this study

Budding Yeast Strains (for two-hybrid assay and controls)

Name	Genotype	Derivation
L40	<u>Mata his3-D200 trp1-901 leu2-3 ade2 LYS2::(lexAop)4-HIS3</u> <u>URA3::(lexAop)8-lacZi</u>	Dr Cooper
NK150	L40 containing <i>pGAN6-slp1⁺</i> and <i>pBMT116-<i>alp14</i>⁺</i>	this study
NK151	L40 containing <i>pGAN6-slp1⁺</i> and <i>pBMT116-<i>alp14</i>-Δ420-809 (ΔC)</i>	this study

NK152	L40 containing <i>pGAN6-slp1⁺</i> and <i>pBMT116-<i>alp14</i>-Δ1-430 (ΔTOG2)</i>	this study
NK154	L40 containing <i>pGAN6-slp1⁺</i> and <i>pBMT116-<i>alp14</i>-Δ1-696 (ΔN-M)</i>	this study
NK155	L40 containing <i>pGAN6-slp1⁺</i> and <i>pBMT116-<i>alp14</i>⁺</i>	this study
NK156	L40 containing <i>pGAN6-<i>mad2</i>⁺</i> and <i>pBMT116-<i>alp14</i>-Δ420-809 (ΔC)</i>	this study
NK158	L40 containing <i>pGAN6-<i>mad2</i>⁺</i> and <i>pBMT116-<i>alp14</i>-Δ1-430 (ΔTOG2)</i>	this study
NK160	L40 containing <i>pGAN6-<i>mad2</i>⁺</i> and <i>pBMT116-<i>alp14</i>-Δ1-696 (ΔN-M)</i>	this study
MS-L40raf/ras	L40 containing <i>pGAN6-<i>raf</i>⁺</i> and <i>pBMT116-<i>ras</i>⁺</i>	lab stock
NK167	L40 containing <i>pGAN6-<i>raf</i>⁺</i> and <i>pBMT116-<i>alp14</i>⁺</i>	this study
NK169	L40 containing <i>pGAN6-<i>mad3</i>⁺</i> and <i>pBMT116-<i>alp14</i>⁺</i>	this study
NK172	L40 containing <i>pGAN6-<i>mad3</i>⁺</i> and <i>pBMT116-<i>alp14</i>-Δ1-430 (ΔTOG2)</i>	this study
NK175	L40 containing <i>pGAN6-<i>mad3</i>⁺</i> and <i>pBMT116-<i>alp14</i>-Δ1-430 (ΔTOG2)</i>	this study
NK177	L40 containing <i>pGAN6-<i>mad3</i>⁺</i> and <i>pBMT116-<i>alp14</i>-Δ1-696 (ΔN-M)</i>	this study

7.3 Molecular Biological techniques

Molecular Biological techniques were used as described (Maniatis *et al.*, 1982) including preparation of competent bacteria, growth and transformation of bacterial cells, gel electrophoresis of DNA in TBE buffer, restriction enzyme digests and minipreps.

Nucleic Acid preparation and manipulation

Standard molecular biological techniques were followed as described (Sambrook *et al.*, 1989). Enzymes were used as recommended by the suppliers (New England Biolabs), digestion was performed at 37°C for 2-4 hours for plasmid DNA. For ligation, DNA fragment, ligase and buffer were mixed and incubated at 16°C for 3-12 hours. DNA

fragments from digestion and ligations were examined on a 1% (w/v) agarose gels in 1X TBE buffer which was electrophoreses at 100V in 1X TBE buffer.

Polymerase Chain Reaction

PCR reactions were performed with Taq polymerase when the product was to be used for transformations and with Vent polymerase for colony PCRs. PCR reactions for yeast transformations were performed in 100 μ l volumes with 1 mM MgSO₄, 1 μ M of each primer, 10 ng of template DNA and 200 mM dNTPs and 2.5 units of enzyme. Colony PCRs were performed in a similar manner except that yeast cells were added to the reaction before boiling. Following this the enzyme was added and the PCR started. All PCRs were performed on a Peiliter Thermal Cycler-200. 5 μ l of PCR product was run on a 1% DNA agarose gel. Products were purified using the using the *Promega wizard^R DNA clean up system* (also see section 7.1).

Deletion, overexpression and C-terminal epitope tagging of genes by chromosomal integration

Deletion of genes were carried out by insertion of *kan'* genes into wild type strains. Truncation of Alp14 from the C-terminus was carried out by replacement of the target DNA sequence with a *GFP-kan'* encoding sequence, allowing selection by kanacymin resistance and visualisation of the protein localisation by GFP. In experiments where the N-terminal of Alp14 were deleted, the promoter and target sequence were replaced by weak *P8Inmt* or strong *P3nmt* promoters. The thiamine repressible *nmt* promoters were integrated in the genome in front of the initiator ATG genes by a PCR-based gene targeting method (Bahler *et al.*, 1998). In order to activate the promoter and over-produce proteins, cultures were grown in rich media until mid log phase and then filtered, washed and resuspended in minimal media without thiamine. Cultures were then followed for 20 hours, which is about 4-5 generations. On plates, strains carrying *nmt*-expressed genes were streaked on media lacking thiamine and grown overnight to induce expression (MacNeill and Fantes, 1993). Note for partial deletions or overexpressions, special care is taken to ensure production of in-frame sequences. Alp14 mutant proteins were often subjected to Western Blotting analyses to detect presence of correctly truncated strains.

C-terminal tagging with GFP, 13myc or 3HA epitopes was also performed insertion of PCR-generated fragments in the same manner as described above and in Bahler *et al.*, (1998). In these experiments, sequences encoding the epitopes were inserted at the 3' end of the gene, but before the stop codon to allow epitope expression.

Subcloning genes and partially deleted genes into plasmids

For ectopic expression of genes or partially deleted genes, the target DNA were amplified by PCR with oligomer sequences corresponding to the 5' and 3' of the target DNA plus additional restriction enzyme sites. After amplification and purification, the DNA and plasmid are subjected to digestion with appropriate restriction enzymes, purified and ligated. The resulting plasmid containing target DNA is identified by its size in electrophoresis agarose gels. Plasmids were then transformed into competent *E. coli* strain HB101. To do this, competent *E. coli*, previously stored at -70°C, were thawed on ice and incubated for 10 minutes with 10 µg of plasmid DNA. After heat shocking at 42°C for 90 seconds, 1 ml of LB media was added and they were kept at 37°C for 30 minutes. Finally, they were plated out onto LB plates containing ampicillin and left to grow overnight at 37°C.

20 colonies were selected from each of the LB plates containing ampicillin. They were then grown in selective LB media and minipreps were performed to re-isolate the plasmid. Note that minipreps carried out in this study were mostly performed by an in-house service. However, methods of DNA preparation from *E. Coli* is briefly described below (see section entitled Isolation of plasmid DNA from *E. coli*).

Once purified, the plasmid DNA were then run on a DNA gel to check the presence of DNA. Digestion patterns were then compared between the original plasmid and the plasmid containing target sequence. In order to check if plasmid construction was successful, the plasmids were transformed into wild type cells or relevant mutants. Those exerting a defect in wild type cells or suppressing phenotypes in mutant cells were then selected. Note that pREP3-*mad2*⁺, pREP41-*mad2*⁺ and pREP41-*mph1*⁺ were provided by the Dr. Sazer's laboratory. *palp14*⁺ (pAL plasmid - *LEU2*⁺ marker; Alp14 is expressed by its natural promoter) was taken from the lab stock and had not been constructed in this study.

Isolation of plasmid DNA from *E. coli*

400 ml of transformed *E. coli* were grown overnight in LB + 100 µg/ml ampicillin at 37°C. Cells were harvested by centrifugation at 5000 rpm for 5 minutes and the pellet was resuspended in 10 ml of plasmid preparation solution 1 (QIAGEN - P1 - 50 mM glucose, 25 mM Tris-pH 8.0, 10 mM EDTA) containing 100 µg/ml RNase A. 10ml of P2 (200 mM sodium hydroxide, 1% (w/v) SDS) was added and cells were left to lyse for 10 minutes on ice. The addition of 10ml of P3 (3 M potassium Acetate) precipitated the bacterial and plasmid DNA. DNA was separated from the cell debris by filtering it through a QIAGEN syringe. Plasmid DNA was collected in a column (QIAGEN tip 500) that had been equilibrated with equilibration buffer (750 mM NaCl₂, 50 mM MOPS pH7.0, 15%(v/v) 50 mM MOPS pH7.0, 15% (v/v) Ethanol). Degraded RNA and cellular debris pass through the column, while plasmid DNA is retained. The QIAGEN tip was then washed twice in 60 ml Wash buffer (50 mM MOPS pH7.0, 15% (v/v) Ethanol) and the plasmid DNA eluted with 15 ml elution buffer (1.25 M NaCl, 50 mM Tris-HCl pH 8.5, 15% (v/v) Ethanol). Plasmid DNA was then recovered by isopropanol precipitation.

7.4 Protein biochemistry

Fission yeast cell extract and Western blotting

Fission yeast whole cell extracts were prepared by lysing 10-50 ml of mid log-phase cells with glass beads in HB buffer (Moreno *et al.*, 1991). Protein concentration was determined using a Bradford assay (BioRad). Extracts were boiled in sample buffer for five minutes and 30 µg of extract was run on a 10% SDS-polyacrylamide gel (BioRad). For western blots, the protein was blotted onto ImmobilonTM-P (Millipore) transfer membrane. Horseradish peroxidase-conjugated goat anti-rabbit IgG, goat anti-mouse IgG (BioRad) and chemiluminescence system (ECL, Amersham) were used to detect bound antibodies.

Immunoprecipitations

For immunoprecipitation analysis, 4-10 mg of soluble cell extract was prepared in the same way as for western blot analysis described above. However, high salt HB buffer or RIPA buffer were preferably used to reduce non-specific anti-body binding in our IP

experiments. Added directly to freshly extracted proteins were 2.5 μg of mono- or polyclonal anti-GFP or anti-myc antibody. The mixture was incubated at 4°C for two hours, after which 30 μl of Protein A-Sepharose beads (Pharmacia Biotech. Co. – prewashed 4 times in the same buffer used for extraction) were added and incubation continued for another two hours. The protein A beads (now conjugated with the antibody and specific protein bound to it) were then washed eight times in buffer followed by the addition of 10 μl sample buffer. Samples were run on a 10% SDS-PAGE gel and candidate proteins were detected as described above. Note that an anti-myc antibody that has been pre-conjugated with beads were most often used in our experiments.

Antibodies for Immunoprecipitation and Western analysis

HA(16B12)	BabCO (MMS-101R)	monoclonal	1/500
GFP	Boeringer (clone 7.1&13.1)	monoclonal	1/200
Myc	Babco (9E10)	monoclonal	1/800
α -tubulin	Sigma (T5168)	monoclonal	1/5,000
myc-beads/ affinity matrix	covance (9E10)	monoclonal	1/20

7.5 Microscopic analysis

Analysis of DNA and septa

Analysis of the DNA and septa were performed by fixing 1 ml of cell culture in 1/10 volume of formaldehyde for 10 minutes. After washing in PBSA, cells were visualised with the addition of DAPI or calcofluor and viewed under a fluorescence microscope. Cells were pelleted and re-suspended in YE.

Indirect immunofluorescent microscopy

Immunofluorescence procedures were used as described in Hagan and Hyams (1988) to stain α -tubulin and SPB component, Sad-1. Asynchronous or synchronous 5×10^7 cells in mid-log phase were filtered and fixed in methanol at -70°C for 10 minutes. After 3 washes in PEM the cell wall was digested with 0.6 mg/ml zymolyase 20T in PEMS for 70 minutes (37°C, shaking). After digestion, cells were pelleted and resuspended in 1% TritonX in PEMS for 5 minutes at room temperature. After 3 further washes in PEM,

cells were incubated in PEMBAL for 30 minutes and primary antibody was added in 50 μ l of PEMBAL and left overnight. The primary antibody was washed out with PEMBAL, and the secondary antibody added in 200 μ l PEMBAL and incubated in the dark for 2 hours. Finally, after washing the secondary antibody out with PEMBAL, cells were resuspended in PBSA + 0.2 μ g/ml NaN₃. Images were viewed by fluorescent microscopy.

Primary antibodies

Sad1	Dr. Iain Hagan	polyclonal	1:25
α -tubulin (TAT-1)	Dr.Keith Gull	monoclonal	1:40

Secondary antibodies

Cy3-conjugated goat	anti-rabbit IgG (Sigma C2306)	1:500
Cy3-conjugated sheep	anti-mouse IgG (Sigma C2128)	1:500
Fluorescein-linked sheep	anti-rabbit IgG (Amersham F0208)	1:40
Fluorescein-linked sheep	anti-mouse IgG (Amersham F0261)	1:40

Florescent microscopy imaging of fixed and live cells

Live imaging was performed as described in Brunner and Nurse (2000), using a thin layer of agar or lectin to prevent cell movements. For imaging, pictures of live and fixed cells, including those previously subjected to immuno-staining, were taken by chilled cameras connected to a computer and microscope. Imaging programmes used in this study include Kinetics Imaging (Zeiss), Improvion Velocity (Zeiss) and Delta Vision (Olympics). In all studies, Z-stacks (200-400 nm steps) were taken. For visualisation and quantification of Nuf2 and Ndc80 dots, images were deconvolved to subtract calculated haze (spread of light). Velocity and Delta Vision programme were the used to calculate the maximum intensity of the dots against the light intensity in the background. All images were processed by Adobe® Photoshop.

References

- Abrieu A, Magnaghi-Jaulin L, Kahana JA, Peter M, Castro A, Vigneron S, Lorca T, Cleveland DW, Labbe JC**, *Mps1 is a kinetochore-associated kinase essential for the vertebrate mitotic checkpoint.*, Cell. 2001 Jul 13;106(1):83-93.
- Adachi Y, Toda T, Niwa O, Yanagida M**, *Differential expressions of essential and nonessential alpha-tubulin genes in Schizosaccharomyces pombe.*, Mol Cell Biol. 1986 Jun;6(6):2168-78.
- Aizawa H, Sekine Y, Takemura R, Zhang Z, Nangaku M, Hirokawa N.**, *Kinesin family in murine central nervous system.*, J Cell Biol. 1992 Dec;119(5):1287-96.
- Alberts B, Bray D, Lewis J, Raff M, Roberts K, Watson JD**, *Molecular biology of the cell.*, New York, Garland publishing, Inc. 1994
- Alfa CE, Booher R, Beach D, Hyams JS**, *Fission yeast cyclin: subcellular localisation and cell cycle regulation.*, J Cell Sci Suppl. 1989;12:9-19.
- Amor DJ, Kalitsis P, Sumer H, Choo KH**, *Building the centromere: from foundation proteins to 3D organization.*, Trends Cell Biol. 2004 Jul;14(7):359-68.
- Andrews PD, Ovechkina Y, Morrice N, Wagenbach M, Duncan K, Wordeman L, Swedlow JR**, *Aurora B regulates MCAK at the mitotic centromere.*, Dev Cell. 2004 Feb;6(2):253-68.
- Appelgren H, Kniola B, Ekwall K**, *Distinct centromere domain structures with separate functions demonstrated in live fission yeast cells.*, J Cell Sci. 2003 Oct 1;116(Pt 19):4035-42.
- Asakawa H, Hayashi A, Haraguchi T, Hiraoka Y**, *Dissociation of the Nuf2-Ndc80 Complex Releases Centromeres from the Spindle-Pole Body during Meiotic Prophase in Fission Yeast.*, Mol Biol Cell. 2005 Feb 23.
- Bahler J, Wu JQ, Longtine MS, Shah NG, McKenzie A, Steever A, Wach A, Philippsen A and Pringle JR**, *Heterologous modules for efficient and versatile PCR-based gene targeting in Schizosaccharomyces pombe.*, Yeast 1998; 14(10): 943-51.
- Barton NR and Goldstein LS**, *Going mobile: microtubule motors and chromosome segregation.*, Proc Natl Acad Sci U S A. 1996 Mar 5;93(5):1735-42.
- Bernard P, Hardwick K, Javerzat JP**, *Fission yeast bub1 is a mitotic centromere protein essential for the spindle checkpoint and the preservation of correct ploidy through mitosis.*, J Cell Biol. 1998 Dec 28;143(7):1775-87.
- Bernard P, Maure JF, Partridge JF, Genier S, Javerzat JP, Allshire RC**, *Requirement of heterochromatin for cohesion at centromeres.*, Science. 2001 Dec 21;294(5551):2539-42.
- Bernard P and Allshire R**, *Centromeres become unstuck without heterochromatin.*, Trends Cell Biol. 2002 Sep;12(9):419-24.

- Bharadwaj R, Qi W, Yu H**, *Identification of two novel components of the human NDC80 kinetochore complex.*, J Biol Chem. 2004 Mar 26;279(13):13076-85
- Binder LI, Guillozet-Bongaarts AL, Garcia-Sierra F, Berry RW**, *Tau, tangles, and Alzheimer's disease.*, Biochim Biophys Acta. 2005 Jan 3;1739(2-3):216-23.
- Booher RN, Alfa CE, Hyams JS, Beach DH**, *The fission yeast cdc2/cdc13/suc1 protein kinase: regulation of catalytic activity and nuclear localization.*, Cell. 1989 Aug 11;58(3):485-97.
- Brinkley BR and Stubblefield E**, *The fine structure of the kinetochore of a mammalian cell in vitro.*, Chromosoma. 1966;19(1):28-43.
- Brunner D and Nurse P**, *CLIP170-like tip1p spatially organizes microtubular dynamics in fission yeast.*, Cell 2000; 102(5): 695-704.
- Cassimeris L, Gard D, Tran PT, Erickson HP**, *XMAP215 is a long thin molecule that does not increase microtubule stiffness.*, J Cell Sci. 2001 Aug;114(Pt 16):3025-33
- Charrasse S, Mazel M, Taviaux S, Berta P, Chow T, Larroque C**, *Characterization of the cDNA and pattern of expression of a new gene over-expressed in human hepatomas and colonic tumors.*, Eur J Biochem. 1995 Dec 1;234(2):406-13.
- Charrasse S, Coubes P, Arrancibia S, Larroque C**, *Expression of the tumor over-expressed ch-TOG gene in human and baboon brain.*, Neurosci Lett. 1996 Jul 12;212(2):119-22.
- Charrasse S, Schroeder M, Gauthier-Rouviere C, Ango F, Cassimeris L, Gard DL, Larroque C**, *The TOGp protein is a new human microtubule-associated protein homologous to the Xenopus XMAP215.*, J Cell Sci. 1998 May;111 (Pt 10):1371-83.
- Chen RH, Waters JC, Salmon ED, Murray AW**, *Association of spindle assembly checkpoint component XMAD2 with unattached kinetochores.*, Science. 1996 Oct 11;274(5285):242-6.
- Chen RH, Brady DM, Smith D, Murray AW, Hardwick KG**, *The spindle checkpoint of budding yeast depends on a tight complex between the Mad1 and Mad2 proteins.*, Mol Biol Cell. 1999 Aug;10(8):2607-18.
- Cheeseman IM, Enquist-Newman M, Muller-Reichert T, Drubin DG, Barnes G**, *Mitotic spindle integrity and kinetochore function linked by the Duo1p/Dam1p complex.*, J Cell Biol. 2001 Jan 8;152(1):197-212.
- Chung E and Chen RH**, *Spindle checkpoint requires Mad1-bound and Mad1-free Mad2.*, Mol Biol Cell. 2002 May;13(5):1501-11.
- Cottingham FR, Gheber L, Miller DL, Hoyt MA**, *Novel roles for saccharomyces cerevisiae mitotic spindle motors.*, J Cell Biol. 1999 Oct 18;147(2):335-50.
- Cullen CF, Deak P, Glover DM, Ohkura H**, *mini spindles: A gene encoding a conserved microtubule-associated protein required for the integrity of the mitotic spindle in Drosophila.*, J Cell Biol. 1999 Sep 6;146(5):1005-18.

- De Antoni A, Pearson CG, Cimini D, Canman JC, Sala V, Nezi L, Mapelli M, Sironi L, Faretta M, Salmon ED, Musacchio A**, *The Mad1/Mad2 complex as a template for Mad2 activation in the spindle assembly checkpoint.*, *Curr Biol.* 2005 Feb 8;15(3):214-25.
- DeLuca JG, Howell BJ, Canman JC, Hickey JM, Fang G, Salmon ED**, *Nuf2 and Hec1 are required for retention of the checkpoint proteins Mad1 and Mad2 to kinetochores.*, *Curr Biol.* 2003 Dec 2;13(23):2103-9.
- DeLuca JG, Dong Y, Hergert P, Strauss J, Hickey JM, Salmon ED, McEwen BF**, *Hec1 and nuf2 are core components of the kinetochore outer plate essential for organizing microtubule attachment sites.*, *Mol Biol Cell.* 2005 Feb;16(2):519-31.
- Desai A, Verma S, Mitchison TJ, Walczak CE**, *Kin I kinesins are microtubule-destabilizing enzymes.*, *Cell.* 1999 Jan 8;96(1):69-78.
- Dewar H, Tanaka K, Nasmyth K, Tanaka TU**, *Tension between two kinetochores suffices for their bi-orientation on the mitotic spindle.*, *Nature.* 2004 Mar 4;428(6978):93-7.
- De Wulf P, McAinsh AD, Sorger PK**, *Hierarchical assembly of the budding yeast kinetochore from multiple subcomplexes.*, *Genes Dev.* 2003 Dec 1;17(23):2902-21.
- DeZwaan TM, Ellingson E, Pellman D, Roof DM**, *Kinesin-related KIP3 of Saccharomyces cerevisiae is required for a distinct step in nuclear migration.*, *J Cell Biol.* 1997 Sep 8;138(5):1023-40.
- Drummond DR and Hagan IM**, *Mutations in the bimC box of Cut7 indicate divergence of regulation within the bimC family of kinesin related proteins.*, *J Cell Sci.* 1998 Apr;111 (Pt 7):853-65.
- Egel R, Kohli J, Thuriaux P, Wolf K**, *Genetics of the fission yeast Schizosaccharomyces pombe.* *Annu Rev Genet.* 1980;14:77-108.
- Enquist-Newman M, Cheeseman IM, Van Goor D, Drubin DG, Meluh PB, Barnes G**, *Dad1p, third component of the Duo1p/Dam1p complex involved in kinetochore function and mitotic spindle integrity.*, *Mol Biol Cell.* 2001 Sep;12(9):2601-13.
- Euskirchen GM.**, *Nnf1p, Dsn1p, Mtw1p, and Nsl1p: a new group of proteins important for chromosome segregation in Saccharomyces cerevisiae.*, *Eukaryot Cell.* 2002 Apr;1(2):229-40.
- Fang G, Yu H, Kirschner MW**, *Direct binding of CDC20 protein family members activates the anaphase-promoting complex in mitosis and G1.*, *Mol Cell.* 1998 Aug;2(2):163-71.
- Farr KA and Hoyt MA**, *Bub1p kinase activates the Saccharomyces cerevisiae spindle assembly checkpoint.*, *Mol Cell Biol.* 1998 May;18(5):2738-47.
- Fraschini R, Beretta A, Sironi L, Musacchio A, Lucchini G, Piatti S**, *Bub3 interaction with Mad2, Mad3 and Cdc20 is mediated by WD40 repeats and does not require intact kinetochores.*, *EMBO J.* 2001 Dec 3;20(23):6648-59.

- Fujita A, Vardy L, Garcia MA, Toda T**, *A fourth component of the fission yeast gamma-tubulin complex, Alp16, is required for cytoplasmic microtubule integrity and becomes indispensable when gamma-tubulin function is compromised.*, Mol Biol Cell. 2002 Jul;13(7):2360-73.
- Fukagawa T and Brown WR**, *Efficient conditional mutation of the vertebrate CENP-C gene.*, Hum Mol Genet. 1997 Dec;6(13):2301-8.
- Funabiki H, Yamano H, Kumada K, Nagao K, Hunt T, Yanagida M**, *Cut2 proteolysis required for sister-chromatid separation in fission yeast.*, Nature. 1996 May 30;381(6581):438-41.
- Funabiki H, Kumada K, Yanagida M**, *Fission yeast Cut1 and Cut2 are essential for sister chromatid separation, concentrate along the metaphase spindle and form large complexes.*, EMBO J. 1996 Dec 2;15(23):6617-28.
- Gachet Y, Tournier S, Millar JB, Hyams JS**, *A MAP kinase-dependent actin checkpoint ensures proper spindle orientation in fission yeast.*, Nature. 2001 Jul 19;412(6844):352-5.
- Gachet Y, Tournier S, Millar JB, Hyams JS**, *Mechanism controlling perpendicular alignment of the spindle to the axis of cell division in fission yeast.*, EMBO J. 2004 Mar 24;23(6):1289-300.
- Garcia MA, Vardy L, Koonruga N, Toda T**, *Fission yeast ch-TOG/XMAP215 homologue Alp14 connects mitotic spindles with the kinetochore and is a component of the Mad2-dependent spindle checkpoint.*, EMBO J. 2001 Jul 2;20(13):3389-401.
- Garcia MA, Koonruga N, Toda T**, *Two kinesin-like Kin I family proteins in fission yeast regulate the establishment of metaphase and the onset of anaphase A.*, Curr Biol. 2002 Apr 16;12(8):610-21.
- Garcia MA, Koonruga N, Toda T**, *Spindle-kinetochore attachment requires the combined action of Kin I-like Klp5/6 and Alp14/Dis1-MAPs in fission yeast.*, EMBO J. 2002 Nov 15;21(22):6015-24.
- Gard DL and Kirschner MW**, *A microtubule-associated protein from Xenopus eggs that specifically promotes assembly at the plus-end.*, J Cell Biol. 1987 Nov;105(5):2203-15.
- Gard DL and Kirschner MW**, *Microtubule assembly in cytoplasmic extracts of Xenopus oocytes and eggs.*, J Cell Biol. 1987 Nov;105(5):2191-201.
- Gard DL, Becker BE, Josh Romney S**, *MAPPING the eukaryotic tree of life: structure, function, and evolution of the MAP215/Dis1 family of microtubule-associated proteins.*, Int Rev Cytol. 2004;239:179-272.
- Gaudet A and Fitzgerald-Hayes M**, *Alterations in the adenine-plus-thymine-rich region of CEN3 affect centromere function in Saccharomyces cerevisiae.*, Mol Cell Biol. 1987 Jan;7(1):68-75.
- Gergely F, Kidd D, Jeffers K, Wakefield JG, Raff JW**, *D-TACC: a novel centrosomal*

- protein required for normal spindle function in the early Drosophila embryo.* EMBO J. 19, 241-252 (2000).
- Gergely F, Draviam VM, Raff JW,** *The ch-TOG/XMAP215 protein is essential for spindle pole organization in human somatic cells.*, Genes Dev. 2003 Feb 1;17(3):336-41.
- Ghosh and Paweletz N,** *Centrosome-kinetochore interaction in multinucleate cells.*, Chromosoma. 1987;95(2):136-43.
- Gillett ES, Espelin CW, Sorger PK,** *Spindle checkpoint proteins and chromosome-microtubule attachment in budding yeast.*, J Cell Biol. 2004 Feb 16;164(4):535-46.
- Gonczy P, Schnabel H, Kaletta T, Amores AD, Hyman T, Schnabel R,** *Dissection of cell division processes in the one cell stage Caenorhabditis elegans embryo by mutational analysis.*, J Cell Biol. 1999 Mar 8;144(5):927-46.
- Graf R, Euteneuer U, Ho TH, Rehberg M,** *Regulated expression of the centrosomal protein DdCP224 affects microtubule dynamics and reveals mechanisms for the control of supernumerary centrosome number.*, Mol Biol Cell. 2003 Oct;14(10):4067-74.
- Grewal SI and Moazed D,** *Heterochromatin and epigenetic control of gene expression.*, Science. 2003 Aug 8;301(5634):798-802.
- Hagan IM and Hyams JS,** *The use of cell division cycle mutants to investigate the control of microtubule distribution in the fission yeast Schizosaccharomyces pombe.* J Cell Sci 1988; 89(Pt 3): 343-57.
- Hagan I, Hayles J, Nurse P,** *Cloning and sequencing of the cyclin-related cdc13+ gene and a cytological study of its role in fission yeast mitosis.*, J Cell Sci. 1988 Dec;91 (Pt 4):587-95.
- Hagan I and Yanagida M,** *Novel potential mitotic motor protein encoded by the fission yeast cut7+ gene.*, Nature. 1990 Oct 11;347(6293):563-6.
- Hagan I and Yanagida M,** *Kinesin-related cut7 protein associates with mitotic and meiotic spindles in fission yeast.*, Nature. 1992 Mar 5;356(6364):74-6.
- Hardwick KG, Li R, Mistrot C, Chen RH, Dann P, Rudner A, Murray AW,** *Lesions in many different spindle components activate the spindle checkpoint in the budding yeast Saccharomyces cerevisiae.*, Genetics. 1999 Jun;152(2):509-18.
- Hardwick KG, Johnston RC, Smith DL, Murray AW,** *MAD3 encodes a novel component of the spindle checkpoint which interacts with Bub3p, Cdc20p, and Mad2p.*, J Cell Biol. 2000 Mar 6;148(5):871-82.
- He X, Patterson TE, Sazer S,** *The Schizosaccharomyces pombe spindle checkpoint protein mad2p blocks anaphase and genetically interacts with the anaphase-promoting complex.*, Proc Natl Acad Sci U S A. 1997 Jul 22;94(15):7965-70.
- He X, Jones MH, Winey M, Sazer S,** *Mph1, a member of the Mps1-like family of dual specificity protein kinases, is required for the spindle checkpoint in S. pombe.*, J Cell

- Sci. 1998 Jun;111 (Pt 12):1635-47.
- Hirokawa N and Takemura R**, *Kinesin superfamily proteins and their various functions and dynamics.*, Exp Cell Res. 2004 Nov 15;301(1):50-9.
- Hiraoka Y, Toda T, Yanagida M**, *The NDA3 gene of fission yeast encodes beta-tubulin: a cold-sensitive nda3 mutation reversibly blocks spindle formation and chromosome movement in mitosis.*, Cell. 1984 Dec;39(2 Pt 1):349-58.
- Hirata D, Masuda H, Eddison M, Toda T**, *Essential role of tubulin-folding cofactor D in microtubule assembly and its association with microtubules in fission yeast.*, EMBO J. 1998 Feb 2;17(3):658-66.
- Hirsh D and Vanderslice R**, *Temperature-sensitive developmental mutants of Caenorhabditis elegans.*, Dev Biol. 1976 Mar;49(1):220-35.
- Hoffman DB, Pearson CG, Yen TJ, Howell BJ, Salmon ED**, *Microtubule-dependent changes in assembly of microtubule motor proteins and mitotic spindle checkpoint proteins at PtK1 kinetochores.*, Mol Biol Cell. 2001 Jul;12(7):1995-2009.
- Hori T, Haraguchi T, Hiraoka Y, Kimura H, Fukagawa T**, *Dynamic behavior of Nuf2-Hec1 complex that localizes to the centrosome and centromere and is essential for mitotic progression in vertebrate cells.*, J Cell Sci. 2003 Aug 15;116(Pt 16):3347-62.
- Howell BJ, Hoffman DB, Fang G, Murray AW, Salmon ED**, *Visualization of Mad2 dynamics at kinetochores, along spindle fibers, and at spindle poles in living cells.*, J Cell Biol. 2000 Sep 18;150(6):1233-50.
- Hunter AW, Caplow M, Coy DL, Hancock WO, Diez S, Wordeman L, Howard J**, *The kinesin-related protein MCAK is a microtubule depolymerase that forms an ATP-hydrolyzing complex at microtubule ends.*, Mol Cell. 2003 Feb;11(2):445-57.
- Hwang LH, Lau LF, Smith DL, Mistrot CA, Hardwick KG, Hwang ES, Amon A, Murray AW**, *Budding yeast Cdc20: a target of the spindle checkpoint.*, Science. 1998 Feb 13;279(5353):1041-4.
- Ikui AE, Furuya K, Yanagida M, Matsumoto T**, *Control of localization of a spindle checkpoint protein, Mad2, in fission yeast.*, J Cell Sci. 2002 Apr 15;115(Pt 8):1603-10.
- Iouk T, Kerscher O, Scott RJ, Basrai MA, Wozniak RW**, *The yeast nuclear pore complex functionally interacts with components of the spindle assembly checkpoint.*, J Cell Biol. 2002 Dec 9;159(5):807-19.
- Janke C, Ortiz J, Lechner J, Shevchenko A, Shevchenko A, Magiera MM, Schramm C, Schiebel E**, *The budding yeast proteins Spc24p and Spc25p interact with Ndc80p and Nuf2p at the kinetochore and are important for kinetochore clustering and checkpoint control.*, EMBO J. 2001 Feb 15;20(4):777-91.
- Janke C, Ortiz J, Tanaka TU, Lechner J, Schiebel E**, *Four new subunits of the Dam1-Duo1 complex reveal novel functions in sister kinetochore biorientation.*, EMBO J. 2002 Jan 15;21(1-2):181-93.

- Jaspersen SL and Winey M**, *The budding yeast spindle pole body: structure, duplication, and function.*, Annu Rev Cell Dev Biol. 2004;20:1-28.
- Jin QW, Pidoux AL, Decker C, Allshire RC, Fleig U**, *The Mal2p protein is an essential component of the fission yeast centromere.*, Mol Cell Biol. 2002 Oct;22(20):7168-83
- Jones MH, Bachant JB, Castillo AR, Giddings TH Jr, Winey M**, *Yeast Dam1p is required to maintain spindle integrity during mitosis and interacts with the Mps1p kinase.*, Mol Biol Cell. 1999 Jul;10(7):2377-91.
- Levesque AA and Compton DA**, *The chromokinesin Kid is necessary for chromosome arm orientation and oscillation, but not congression, on mitotic spindles.*, J Cell Biol. 2001 Sep 17;154(6):1135-46.
- Li R and Murray AW**, *Feedback control of mitosis in budding yeast.*, Cell. 1991 Aug 9;66(3):519-31.
- Li Y and Benezra R**, *Identification of a human mitotic checkpoint gene: hsMAD2.*, Science. 1996 Oct 11;274(5285):246-8.
- Li Y, Bachant J, Alcasabas AA, Wang Y, Qin J, Elledge SJ**, *The mitotic spindle is required for loading of the DASH complex onto the kinetochore.*, Genes Dev. 2002 Jan 15;16(2):183-97.
- Li X and Nicklas RB**, *Mitotic forces control a cell-cycle checkpoint.*, Nature. 1995 Feb 16;373(6515):630-2
- Liao H, Li G, Yen TJ.**, *Mitotic regulation of microtubule cross-linking activity of CENP-E kinetochore protein.*, Science. 1994 Jul 15;265(5170):394-8
- Liu ST, Hittle JC, Jablonski SA, Campbell MS, Yoda K, Yen TJ**, *Human CENP-I specifies localization of CENP-F, MAD1 and MAD2 to kinetochores and is essential for mitosis.*, Nat Cell Biol. 2003 Apr;5(4):341-5.
- Logarinho E, Bousbaa H, Dias JM, Lopes C, Amorim I, Antunes-Martins A, Sunkel CE**, *Different spindle checkpoint proteins monitor microtubule attachment and tension at kinetochores in Drosophila cells.*, J Cell Sci. 2004 Apr 1;117(Pt 9):1757-71.
- Luban J and Goff SP**, *The yeast two-hybrid system for studying protein-protein interactions.*, Curr Opin Biotechnol. 1995 Feb;6(1):59-64. Review.
- Luo X, Tang Z, Rizo J, Yu H**, *The Mad2 spindle checkpoint protein undergoes similar major conformational changes upon binding to either Mad1 or Cdc20.*, Mol Cell. 2002 Jan;9(1):59-71.
- Kashina AS, Baskin RJ, Cole DG, Wedaman KP, Saxton WM, Scholey JM**, *A bipolar kinesin.*, Nature. 1996 Jan 18;379(6562):270-2.
- Keeney JB and Boeke JD**, *Efficient targeted integration at leu1-32 and ura4-294 in Schizosaccharomyces pombe.*, Genetics. 1994 Mar;136(3):849-56.

- Kinoshita K, Arnal I, Desai A, Drechsel DN, Hyman AA**, *Reconstitution of physiological microtubule dynamics using purified components.*, Science. 2001 Nov 9;294(5545):1340-3.
- Kinoshita K, Habermann B, Hyman AA**, *XMAP215: a key component of the dynamic microtubule cytoskeleton.*, Trends Cell Biol. 2002 Jun;12(6):267-73.
- Kitagawa K, Abdulle R, Bansal PK, Cagney G, Fields S, Hieter P.**, *Requirement of Skp1-Bub1 interaction for kinetochore-mediated activation of the spindle checkpoint.*, Mol Cell. 2003 May;11(5):1201-13.
- Kim SH, Lin DP, Matsumoto S, Kitazono A, Matsumoto T**, *Fission yeast Slp1: an effector of the Mad2-dependent spindle checkpoint.*, Science. 1998 Feb 13;279(5353):1045-7.
- Kline-Smith SL and Walczak CE**, *The microtubule-destabilizing kinesin XKCM1 regulates microtubule dynamic instability in cells.*, Mol Biol Cell. 2002 Aug;13(8):2718-31.
- Kline-Smith SL, Khodjakov A, Hergert P, Walczak CE**, *Depletion of centromeric MCAK leads to chromosome congression and segregation defects due to improper kinetochore attachments.*, Mol Biol Cell. 2004 Mar;15(3):1146-59
- Kniola B, O'Toole E, McIntosh JR, Mellone B, Allshire R, Mengarelli S, Hultenby K, Ekwall K**, *The domain structure of centromeres is conserved from fission yeast to humans.*, Mol Biol Cell. 2001 Sep;12(9):2767-75.
- Kops GJ, Kim Y, Weaver BA, Mao Y, McLeod I, Yates JR 3rd, Tagaya M, Cleveland DW**, *ZW10 links mitotic checkpoint signaling to the structural kinetochore.*, J Cell Biol. 2005 Apr 11;169(1):49-60.
- Kosco KA, Pearson CG, Maddox PS, Wang PJ, Adams IR, Salmon ED, Bloom K, Huffaker TC**, *Control of microtubule dynamics by Stu2p is essential for spindle orientation and metaphase chromosome alignment in yeast.*, Mol Biol Cell. 2001 Sep;12(9):2870-80
- Kotani S, Tanaka H, Yasuda H, Todokoro K**, *Regulation of APC activity by phosphorylation and regulatory factors.*, Cell Biol. 1999 Aug 23;146(4):791-800.
- MacNeill SA and Fantes P**, *Methods for analysis of the fission yeast cell cycle*, *The Cell Cycle*, Practical Approach Series, IRL Press at Oxford University Press 1993, : 93-125.
- Maddox P, Straight A, Coughlin P, Mitchison TJ, Salmon ED**, *Direct observation of microtubule dynamics at kinetochores in Xenopus extract spindles: implications for spindle mechanics.*, J Cell Biol. 2003 Aug 4;162(3):377-82.
- Maney T, Wagenbach M, Wordeman L**, *Molecular dissection of the microtubule depolymerizing activity of mitotic centromere-associated kinesin.*, J Biol Chem. 2001 Sep 14; 276(37): 34753-8
- Maniatis T, Fritsch E and Sambrook J**, *Molecular cloning: a laboratory manual.*, Cold Spring Harbour Laboratory press (1982).

- Martin-Lluesma S, Stucke VM, Nigg EA**, *Role of Hec1 in spindle checkpoint signaling and kinetochore recruitment of Mad1/Mad2.*, Science. 2002 Sep 27;297(5590):2267-70.
- McAinsh AD, Tytell JD, Sorger PK**, *Structure, function, and regulation of budding yeast kinetochores.*, Annu Rev Cell Dev Biol. 2003;19:519-39.
- McClelland ML, Gardner RD, Kallio MJ, Daum JR, Gorbsky GJ, Burke DJ, Stukenberg PT**, *The highly conserved Ndc80 complex is required for kinetochore assembly, chromosome congression, and spindle checkpoint activity.*, Genes Dev. 2003 Jan 1;17(1):101-14.
- McClelland ML, Kallio MJ, Barrett-Wilt GA, Kestner CA, Shabanowitz J, Hunt DF, Gorbsky GJ, Stukenberg PT**, *The vertebrate Ndc80 complex contains Spc24 and Spc25 homologs, which are required to establish and maintain kinetochore-microtubule attachment.*, Curr Biol. 2004 Jan 20;14(2):131-7.
- Meeks-Wagner D, Wood JS, Garvik B, Hartwell LH**, *Isolation of two genes that affect mitotic chromosome transmission in S. cerevisiae.*, Cell. 1986 Jan 17;44(1):53-63.
- Meraldi P, Draviam VM, Sorger PK**, *Timing and checkpoints in the regulation of mitotic progression.*, Dev Cell. 2004 Jul;7(1):45-60.
- Millband DN and Hardwick KG**, *Fission yeast Mad3p is required for Mad2p to inhibit the anaphase-promoting complex and localizes to kinetochores in a Bub1p-, Bub3p-, and Mph1p-dependent manner.*, Mol Cell Biol. 2002 Apr;22(8):2728-42. 200
- Millband DN, Campbell L, Hardwick KG.**, *The awesome power of multiple model systems: interpreting the complex nature of spindle checkpoint signaling.*, Trends Cell Biol. 2002 May;12(5):205-9.
- Miller RK, Heller KK, Frisen L, Wallack DL, Loayza D, Gammie AE, Rose MD**, *The kinesin-related proteins, Kip2p and Kip3p, function differently in nuclear migration in yeast.*, Mol Biol Cell. 1998 Aug;9(8):2051-68.
- Miranda JJ, De Wulf P, Sorger PK, Harrison SC.***The yeast DASH complex forms closed rings on microtubules.*, Nat Struct Mol Biol. 2005 Feb;12(2):138-43.
- Moreno S, Klar A, Nurse P**, *Molecular genetic analysis of fission yeast Schizosaccharomyces pombe.*, Methods Enzymol. 1991;194:795-823.
- Musacchio A and Hardwick KG**, *The spindle checkpoint: structural insights into dynamic signaling.*, Nat Rev Mol Cell Biol. 2002 Oct;3(10):731-41. 2002
- Nabeshima K, Kurooka H, Takeuchi M, Kinoshita K, Nakaseko Y, Yanagida M**, *p93dis1, which is required for sister chromatid separation, is a novel microtubule and spindle pole body-associating protein phosphorylated at the Cdc2 target sites.*, Genes Dev. 1995 Jul 1;9(13):1572-85.
- Nabeshima K, Nakagawa T, Straight AF, Murray A, Chikashige Y, Yamashita YM, Hiraoka Y, Yanagida M**, *Dynamics of centromeres during metaphase-anaphase transition in fission yeast: Dis1 is implicated in force balance in metaphase bipolar*

- spindle.*, Mol Biol Cell. 1998 Nov;9(11):3211-25.
- Nabetani A, Koujin T, Tsutsumi C, Haraguchi T, Hiraoka Y**, *A conserved protein, Nuf2, is implicated in connecting the centromere to the spindle during chromosome segregation: a link between the kinetochore function and the spindle checkpoint.*, Chromosoma. 2001 Sep;110(5):322-34.
- Nakaseko Y, Nabeshima K, Kinoshita K, Yanagida M**, *Dissection of fission yeast microtubule associating protein p93Dis1: regions implicated in regulated localization and microtubule interaction.*, Genes Cells. 1996 Jul;1(7):633-44.
- Nakaseko Y, Goshima G, Morishita J, Yanagida M**, *M phase-specific kinetochore proteins in fission yeast: microtubule-associating Dis1 and Mtc1 display rapid separation and segregation during anaphase.*, Curr Biol. 2001 Apr 17;11(8):537-49.
- Nagasaki K, Maass N, Manabe T, Hanzawa H, Tsukada T, Kikuchi K, Yamaguchi K**, *Identification of a novel gene, DAM1, amplified at chromosome 1p13.3-21 region in human breast cancer cell lines.*, Cancer Lett. 1999 Jun 1;140(1-2):219-26.
- Neuwald AF and Hirano T**, *HEAT repeats associated with condensins, cohesins, and other complexes involved in chromosome-related functions.*, Genome Res. 2000 Oct;10(10):1445-52.
- Niwa O, Matsumoto T, Chikashige Y, Yanagida M**, *Characterization of Schizosaccharomyces pombe minichromosome deletion derivatives and a functional allocation of their centromere.*, EMBO J. 1989 Oct;8(10):3045-52.
- Noda Y, Sato-Yoshitake R, Kondo S, Nangaku M, Hirokawa N**, *KIF2 is a new microtubule-based anterograde motor that transports membranous organelles distinct from those carried by kinesin heavy chain or KIF3A/B.*, J Cell Biol. 1995 Apr;129(1):157-67.
- Nogales E, Wang HW, Niederstrasser H**, *Tubulin rings: which way do they curve?*, Curr Opin Struct Biol. 2003 Apr;13(2):256-61.
- Noma K, Sugiyama T, Cam H, Verdel A, Zofall M, Jia S, Moazed D, Grewal SI**, *RITS acts in cis to promote RNA interference-mediated transcriptional and post-transcriptional silencing.*, Nat Genet. 2004 Nov;36(11):1174-80.
- Obuse C, Iwasaki O, Kiyomitsu T, Goshima G, Toyoda Y, Yanagida M**, *A conserved Mis12 centromere complex is linked to heterochromatic HP1 and outer kinetochore protein Zwint-1.*, Nat Cell Biol. 2004 Nov;6(11):1135-4
- Pardo M and Nurse P**, *Equatorial retention of the contractile actin ring by microtubules during cytokinesis.*, Science. 2003 Jun 6;300(5625):1569-74.
- Petersen J and Hagan IM**, *S. pombe aurora kinase/survivin is required for chromosome condensation and the spindle checkpoint attachment response.*, Curr Biol. 2003 Apr 1;13(7):590-7.
- Pidoux AL and Allshire RC**, *Kinetochore and heterochromatin domains of the fission yeast centromere.*, Chromosome Res. 2004;12(6):521-34.

- Pidoux AL, Richardson W, Allshire RC**, *Sim4: a novel fission yeast kinetochore protein required for centromeric silencing and chromosome segregation.*, J Cell Biol. 2003 Apr 28;161(2):295-307.
- Pinsky BA, Tatsutani SY, Collins KA, Biggins S**, *An Mtw1 complex promotes kinetochore biorientation that is monitored by the Ipl1/Aurora protein kinase.*, Dev Cell. 2003 Nov;5(5):735-45.
- Popov AV, Pozniakovskiy A, Arnal I, Antony C, Ashford AJ, Kinoshita K, Tournebize R, Hyman AA, Karsenti E**, *XMAP215 regulates microtubule dynamics through two distinct domains.*, EMBO J. 2001 Feb 1;20(3):397-410.
- Ohi R, Coughlin ML, Lane WS, Mitchison TJ**, *An inner centromere protein that stimulates the microtubule depolymerizing activity of a KinI kinesin.*, Dev Cell. 2003 Aug;5(2):309-21
- Ohkura H, Adachi Y, Kinoshita N, Niwa O, Toda T, Yanagida M**, *Cold-sensitive and caffeine-supersensitive mutants of the Schizosaccharomyces pombe dis genes implicated in sister chromatid separation during mitosis.*, EMBO J. 1988 May;7(5):1465-73.
- Ohkura H, Garcia MA, Toda T**, *Dis1/TOG universal microtubule adaptors - one MAP for all?*, J Cell Sci. 2001 Nov;114(Pt 21):3805-12.
- Oliferenko S and Balasubramanian MK**, *Astral microtubules monitor metaphase spindle alignment in fission yeast.*, Nat Cell Biol. 2002 Oct;4(10):816-20.
- Ovechkina Y, Wagenbach M, Wordeman L**, *K-loop insertion restores microtubule depolymerizing activity of a "neckless" MCAK mutant.*, Cell Biol. 2002 Nov 25;159(4):557-62.
- Radcliffe P, Hirata D, Childs D, Vardy L, Toda T**, *Identification of novel temperature-sensitive lethal alleles in essential beta-tubulin and nonessential alpha 2-tubulin genes as fission yeast polarity mutants.*, Mol Biol Cell. 1998 Jul;9(7):1757-71.
- Rajagopalan S, Bimbo A, Balasubramanian MK, Oliferenko S**, *A potential tension-sensing mechanism that ensures timely anaphase onset upon metaphase spindle orientation.*, Curr Biol. 2004 Jan 6;14(1):69-74.
- Rieder CL, Schultz A, Cole R, Sluder G**, *Anaphase onset in vertebrate somatic cells is controlled by a checkpoint that monitors sister kinetochore attachment to the spindle.*, J Cell Biol. 1994 Dec;127(5):1301-10.
- Ris H and Witt PL**, *Structure of the mammalian kinetochore.*, Chromosoma. 1981;82(2):153-70.
- Sambrook J, Fritsch E, Sambrook J**, *Molecular cloning: a laboratory manual*, Cold Spring Harbour Laboratory press (1989).
- Sato M, Koonrugsu N, Toda T, Vardy L, Tournier S, Millar JB**, *Deletion of Mia1/Alp7 activates Mad2-dependent spindle assembly checkpoint in fission yeast.*, Nat Cell Biol. 2003 Sep;5(9):764-6;

- Sato M, Vardy L, Angel Garcia M, Koonrugsu N, Toda T**, *Interdependency of fission yeast Alp14/TOG and coiled coil protein Alp7 in microtubule localization and bipolar spindle formation.*, Mol Biol Cell. 2004 Apr;15(4):1609-22.
- Sawin KE, LeGuellec K, Philippe M, Mitchison TJ**, *Mitotic spindle organization by a plus-end-directed microtubule motor.*, Nature. 1992 Oct 8;359(6395):540-3.
- Sawin KE and Nurse P**, *Regulation of cell polarity by microtubules in fission yeast.*, J Cell Biol. 1998 Jul 27;142(2):457-71.
- Schaar BT, Chan GK, Maddox P, Salmon ED, Yen TJ**, *CENP-E function at kinetochores is essential for chromosome alignment.*, J Cell Biol. 1997 Dec 15;139(6):1373-82.
- Severin F, Habermann B, Huffaker T, Hyman T**, *Stu2 promotes mitotic spindle elongation in anaphase.*, Cell Biol. 2001 Apr 16;153(2):435-42.
- Shannon KB, Canman JC, Salmon ED**, *Mad2 and BubR1 function in a single checkpoint pathway that responds to a loss of tension.*, Mol Biol Cell. 2002 Oct;13(10):3706-19.
- Shiroguchi K, Ohsugi M, Edamatsu M, Yamamoto T, Toyoshima Y**, *The second microtubule-binding site of monomeric kid enhances the microtubule affinity.*, J Biol Chem. 2003 Jun 20;278(25):22460-5
- Shteinberg M, Protopopov Y, Listovsky T, Brandeis M, Hershko A**, *Phosphorylation of the cyclosome is required for its stimulation by Fizzy/cdc20.*, Biochem Biophys Res Commun. 1999 Jun 24;260(1):193-8.
- Sironi L, Melixetian M, Faretta M, Prosperini E, Helin K, Musacchio A**, *Mad2 binding to Mad1 and Cdc20, rather than oligomerization, is required for the spindle checkpoint.*, EMBO J. 2001 Nov 15;20(22):6371-82.
- Sironi L, Mapelli M, Knapp S, De Antoni A, Jeang KT, Musacchio A**, *Crystal structure of the tetrameric Mad1-Mad2 core complex: implications of a 'safety belt' binding mechanism for the spindle checkpoint.*, EMBO J. 2002 May 15;21(10):2496-506.
- Skoufias DA, Andreassen PR, Lacroix FB, Wilson L, Margolis RL**, *Mammalian mad2 and bub1/bubR1 recognize distinct spindle-attachment and kinetochore-tension checkpoints.*, Proc Natl Acad Sci U S A. 2001 Apr 10;98(8):4492-7
- Spittle C, Charrasse S, Larroque C, Cassimeris L**, *The interaction of TOGp with microtubules and tubulin.*, J Biol Chem. 2000 Jul 7;275(27):20748-53.
- Straight AF, Sedat JW, Murray AW**, *Time-lapse microscopy reveals unique roles for kinesins during anaphase in budding yeast.*, J Cell Biol. 1998 Nov 2;143(3):687-94.
- Sudakin V, Chan GK, Yen TJ**, *Checkpoint inhibition of the APC/C in HeLa cells is mediated by a complex of BUBR1, BUB3, CDC20, and MAD2.*, J Cell Biol. 2001 Sep 3;154(5):925-36.
- Sudakin V and Yen TJ**, *Purification of the mitotic checkpoint complex, an inhibitor of the*

- APC/C from HeLa cells.*, *Methods Mol Biol.* 2004;281:199-2
- Stoyan T, Gloeckner G, Diekmann S, Carbon J**, *Multifunctional centromere binding factor 1 is essential for chromosome segregation in the human pathogenic yeast *Candida glabrata*.*, *Mol Cell Biol.* 2001 Aug;21(15):4875-88.
- Takahashi K, Yamada H, Yanagida M**, *Fission yeast minichromosome loss mutants mis cause lethal aneuploidy and replication abnormality.*, *Mol Biol Cell.* 1994 Oct;5(10):1145-58.
- Takahashi K, Chen ES, Yanagida M**, *Requirement of Mis6 centromere connector for localizing a CENP-A-like protein in fission yeast.*, *Science.* 2000 Jun 23;288(5474):2215-9.
- Tanaka TU, Rachidi N, Janke C, Pereira G, Galova M, Schiebel E, Stark MJ, Nasmyth K**, *Evidence that the Ipl1-Sli15 (Aurora kinase-INCENP) complex promotes chromosome bi-orientation by altering kinetochore-spindle pole connections.*, *Cell.* 2002 Feb 8;108(3):317-29.
- Tang Z, Bharadwaj R, Li B, Yu H**, *Mad2-Independent inhibition of APCCdc20 by the mitotic checkpoint protein BubR1.*, *Dev Cell.* 2001 Aug;1(2):227-37
- Tang Z, Shu H, Oncel D, Chen S, Yu H**, *Phosphorylation of Cdc20 by Bub1 provides a catalytic mechanism for APC/C inhibition by the spindle checkpoint.*, *Mol Cell.* 2004 Nov 5;16(3):387-97.
- Toda T, Umesono K, Hirata A, Yanagida M**, *Cold-sensitive nuclear division arrest mutants of the fission yeast *Schizosaccharomyces pombe*.*, *J Mol Biol.* 1983 Aug 5;168(2):251-70.
- Tomkiel J, Cooke CA, Saitoh H, Bernat RL, Earnshaw WC**, *CENP-C is required for maintaining proper kinetochore size and for a timely transition to anaphase.*, *J Cell Biol.* 1994 May;125(3):531-45.
- Tournebize R, Popov A, Kinoshita K, Ashford AJ, Rybina S, Pozniakovskiy A, Mayer TU, Walczak CE, Karsenti E, Hyman AA**, *Control of microtubule dynamics by the antagonistic activities of XMAP215 and XKCM1 in *Xenopus* egg extracts.*, *Nat Cell Biol.* 2000 Jan;2(1):13-9.
- Tournier S, Gachet Y, Buck V, Hyams JS, Millar JB**, *Disruption of astral microtubule contact with the cell cortex activates a Bub1, Bub3, and Mad3-dependent checkpoint in fission yeast.*, *Mol Biol Cell.* 2004 Jul;15(7):3345-56.
- Uhlmann F, Wernic D, Poupart MA, Koonin EV, Nasmyth K**, *Cleavage of cohesin by the CD clan protease separin triggers anaphase in yeast.*, *Cell.* 2000 Oct 27;103(3):375-86.
- Uhlmann F**, *Secured cutting: controlling separase at the metaphase to anaphase transition.*, *EMBO Rep.* 2001 Jun;2(6):487-92.
- Vale RD, Reese TS, Sheetz MP**, *Identification of a novel force-generating protein, kinesin, involved in microtubule-based motility.*, *Cell.* 1985 Aug;42(1):39-50.

- Van Breugel M, Drechsel D, Hyman A**, *Stu2p, the budding yeast member of the conserved Dis1/XMAP215 family of microtubule-associated proteins is a plus end-binding microtubule destabilizer.*, J Cell Biol. 2003 Apr 28;161(2):359-69.
- Vanoosthuysse V and Hardwick KG**, *The complexity of Bub1 regulation-- phosphorylation, phosphorylation, phosphorylation.*, Cell Cycle. 2003 Mar-Apr;2(2):118-9.
- Vasquez RJ, Gard DL, Cassimeris L**, *XMAP from Xenopus eggs promotes rapid plus end assembly of microtubules and rapid microtubule polymer turnover.*, J Cell Biol. 1994 Nov;127(4):985-93.
- Vigneron S, Prieto S, Bernis C, Labbe JC, Castro A, Lorca T**, *Kinetochore localization of spindle checkpoint proteins: who controls whom?*, Mol Biol Cell. 2004 Oct;15(10):4584-96. Epub 2004 Jul 21.
- Walczak CE, Mitchison TJ, Desai A**, *XKCM1: a Xenopus kinesin-related protein that regulates microtubule dynamics during mitotic spindle assembly.*, Cell. 1996 Jan 12;84(1):37-47.
- Walczak CE, Gan EC, Desai A, Mitchison TJ, Kline-Smith SL**, *The microtubule-destabilizing kinesin XKCM1 is required for chromosome positioning during spindle assembly.*, Curr Biol. 2002 Oct 29;12(21):1885-9.
- Wang PJ and Huffaker TC**, *Stu2p: A microtubule-binding protein that is an essential component of the yeast spindle pole body.*, J Cell Biol. 1997 Dec 1;139(5):1271-80.
- Wandall A, Tranebjaerg L, Tommerup N**, *A neocentromere on human chromosome 3 without detectable alpha-satellite DNA forms morphologically normal kinetochores.*, Chromosoma. 1998 Dec;107(6-7):359-65.
- Wang Y and Burke DJ**, *Checkpoint genes required to delay cell division in response to nocodazole respond to impaired kinetochore function in the yeast Saccharomyces cerevisiae.*, Mol Cell Biol. 1995 Dec;15(12):6838-44.
- Wassmann K, Liberal V, Benzra R**, *Mad2 phosphorylation regulates its association with Mad1 and the APC/C.*, EMBO J. 2003 Feb 17;22(4):797-806.
- Waters JC, Chen RH, Murray AW, Salmon ED**, *Localization of Mad2 to kinetochores depends on microtubule attachment, not tension.*, J Cell Biol. 1998 Jun 1;141(5):1181-91.
- Weiss E and Winey M**, *The Saccharomyces cerevisiae spindle pole body duplication gene MPS1 is part of a mitotic checkpoint.*, J Cell Biol. 1996 Jan;132(1-2):111-23.
- West AG and Fraser P**, *Remote control of gene transcription.*, Hum Mol Genet. 2005 Apr 15;14 Suppl 1:R101-11.
- West RR, Malmstrom T, Troxell CL, McIntosh JR**, *Two related kinesins, klp5+ and klp6+, foster microtubule disassembly and are required for meiosis in fission yeast.*, Mol Biol Cell. 2001 Dec;12(12):3919-32.
- West RR, Malmstrom T, McIntosh JR**, *Kinesins klp5(+) and klp6(+) are required for*

- normal chromosome movement in mitosis.*, J Cell Sci. 2002 Mar 1;115(Pt 5):931-40.
- Westermann S, Avila-Sakar A, Wang HW, Niederstrasser H, Wong J, Drubin DG, Nogales E, Barnes G**, *Formation of a dynamic kinetochore- microtubule interface through assembly of the Dam1 ring complex.*, Mol Cell. 2005 Jan 21;17(2):277-90.
- Wigge PA and Kilmartin JV**, *The Ndc80p complex from Saccharomyces cerevisiae contains conserved centromere components and has a function in chromosome segregation.*, J Cell Biol. 2001 Jan 22;152(2):349-60.
- Winey M, Goetsch L, Baum P, Byers B**, *MPS1 and MPS2: novel yeast genes defining distinct steps of spindle pole body duplication.*, J Cell Biol. 1991 Aug;114(4):745-54.
- Whittington AT, Vugrek O, Wei KJ, Hasenbein NG, Sugimoto K, Rashbrooke MC, Wasteneys GO**, *MOR1 is essential for organizing cortical microtubules in plants.*, Nature. 2001 May 31;411(6837):610-3.
- Wordeman L, Mitchison TJ**, *Identification and partial characterization of mitotic centromere-associated kinesin, a kinesin-related protein that associates with centromeres during mitosis.*, J Cell Biol. 1995 Jan;128(1-2):95-104.
- Wordeman L, Wagenbach M, Maney T**, *Mutations in the ATP-binding domain affect the subcellular distribution of mitotic centromere-associated kinesin (MCAK).*, Cell Biol Int. 1999;23(4):275-86.
- Yamaguchi S, Decottignies A, Nurse P**, *Function of Cdc2p-dependent Bub1p phosphorylation and Bub1p kinase activity in the mitotic and meiotic spindle checkpoint.*, EMBO J. 2003 Mar 3;22(5):1075-87.
- Yamamoto M and Miklos GL**, *Genetic studies on heterochromatin in Drosophila melanogaster and their implications for the functions of satellite DNA.*, Chromosoma. 1978 Mar 22;66(1):71-98.
- Zhang Y and Lees E**, *Identification of an overlapping binding domain on Cdc20 for Mad2 and anaphase-promoting complex: model for spindle checkpoint regulation.*, Mol Cell Biol. 2001 Aug;21(15):5190-9.
- Zimmerman S, Daga RR, Chang F**, *Intra-nuclear microtubules and a mitotic spindle orientation checkpoint.*, Cell Biol. 2004 Dec;6(12):1245-6.
- Zhou J, Panda D, Landen JW, Wilson L, Joshi HC**, *Minor alteration of microtubule dynamics causes loss of tension across kinetochore pairs and activates the spindle checkpoint.*, J Biol Chem. 2002 May 10;277(19):17200-8.

- Baum M and Clarke L.**, *Fission yeast homologs of human CENP-B have redundant functions affecting cell growth and chromosome segregation.*, Mol Cell Biol. 2000 Apr;20(8):2852-64.
- Biggins S, Murray AW.** *The budding yeast protein kinase Ipl1/Aurora allows the absence of tension to activate the spindle checkpoint.*, Genes Dev. 2001 Dec 1;15(23):3118-29.
- Blower MD and Karpen GH.**, *The role of Drosophila CID in kinetochore formation, cell-cycle progression and heterochromatin interactions.*, Nat Cell Biol. 2001 Aug;3(8):730-9.
- Ciosk R, Zachariae W, Michaelis C, Shevchenko A, Mann M, Nasmyth K.**, *An ESP1/PDS1 complex regulates loss of sister chromatid cohesion at the metaphase to anaphase transition in yeast.*, Cell. 1998 Jun 12;93(6):1067-76.
- Draviam VM, Xie S, Sorger PK.**, *Chromosome segregation and genomic stability.*, Curr Opin Genet Dev. 2004 Apr;14(2):120-5.
- Fukagawa T, Mikami Y, Nishihashi A, Regnier V, Haraguchi T, Hiraoka Y, Sugata N, Todokoro K, Brown W, Ikemura T.**, *CENP-H, a constitutive centromere component, is required for centromere targeting of CENP-C in vertebrate cells.*, EMBO J. 2001 Aug 15;20(16):4603-17.
- Hardwick KG, Weiss E, Luca FC, Winey M, Murray AW.**, *Activation of the budding yeast spindle assembly checkpoint without mitotic spindle disruption.*, Science. 1996 Aug 16;273(5277):953-6.
- Hardwick KG.**, *Checkpoint signalling: Mad2 conformers and signal propagation.*, Curr Biol. 2005 Feb 22;15(4):R122-4.
- Howman EV, Fowler KJ, Newson AJ, Redward S, MacDonald AC, Kalitsis P, Choo KH.**, *Early disruption of centromeric chromatin organization in centromere protein A (Cenpa) null mice.*, Proc Natl Acad Sci U S A. 2000 Feb 1;97(3):1148-53
- Hudson DF, Fowler KJ, Earle E, Saffery R, Kalitsis P, Trowell H, Hill J, Wreford NG, de Kretser DM, Cancilla MR, Howman E, Hii L, Cutts SM, Irvine DV, Choo KH.**, *Centromere protein B null mice are mitotically and meiotically normal but have lower body and testis weights.*, J Cell Biol. 1998 Apr 20;141(2):309-19.
- Indjeian VB, Stern BM, Murray AW.**, *The centromeric protein Sgo1 is required to sense lack of tension on mitotic chromosomes.*, Science. 2005 Jan 7;307(5706):130-3.
- Kadura S, He X, Vanoosthuyse V, Hardwick KG, Sazer S.**, *The A78V mutation in the Mad3-like domain of Schizosaccharomyces pombe Bub1p perturbs nuclear accumulation and kinetochore targeting of Bub1p, Bub3p, and Mad3p and spindle assembly checkpoint function.*, Mol Biol Cell. 2005 Jan;16(1):385-95.
- Kouprina N, Ebersole T, Koriabine M, Pak E, Rogozin IB, Katoh M, Oshimura M, Ogi K, Peredelchuk M, Solomon G, Brown W, Barrett JC, Larionov V.**, *Cloning of human centromeres by transformation-associated recombination in yeast and generation of functional human artificial chromosomes.*, Nucleic Acids Res. 2003 Feb 1;31(3):922-34.
- Nishihashi A, Haraguchi T, Hiraoka Y, Ikemura T, Regnier V, Dodson H, Earnshaw WC, Fukagawa T.**, *CENP-I is essential for centromere function in vertebrate cells.*, Dev Cell. 2002 Apr;2(4):463-76.
- Rancati G, Crispo V, Lucchini G, Piatti S.**, *Mad3/BubR1 Phosphorylation During Spindle Checkpoint Activation Depends on both Polo and Aurora Kinases in Budding Yeast.*, Cell Cycle. 2005 Jul 9;4(7)
- Salmon ED, Cimini D, Cameron LA, DeLuca JG.**, *Merotelic kinetochores in mammalian tissue cells.*, Philos Trans R Soc Lond B Biol Sci. 2005 Mar 29;360(1455):553-68.
- Tanaka TU.**, *Chromosome bi-orientation on the mitotic spindle.*, Philos Trans R Soc Lond B Biol Sci. 2005 Mar 29;360(1455):581-9.